

Towards site-specific functional analysis of RNA N6-methyladenosine and 5- methylcytosine in *Arabidopsis thaliana*

Huong Thi Thuy Ta

A thesis submitted for the degree of Doctor of Philosophy (Bioscience)



THE UNIVERSITY
of ADELAIDE

The University of Adelaide

Faculty of Sciences

School of Biological Sciences

January 2022

Table of contents

Table of contents	ii
Abstract	iv
Declaration	vi
Acknowledgements	vii
Abbreviations	ix
List of Figures	xii
Chapter I: Introduction	1
Overview	2
Insights into the “epitranscriptome”	2
More than random “decorations” - RNA modifications as an emerging layer of gene regulation	2
Conceptualizing “epitranscriptomics”- functional insight is key	5
RNA m⁶A and m⁵C - Two models of the “epitranscriptome”	6
High-throughput profiling of RNA m ⁶ A and m ⁵ C	7
The most abundant and well-studied internal mRNA modification - m ⁶ A.....	9
The sibling of epigenetic DNA methylation – RNA m ⁵ C coming of age	11
Using m ⁶ A and m ⁵ C for modelling the “epitranscriptome”	14
Synthetic systems for functional studies of RNA modifications	14
Synthetic platforms for RNA study	14
Embracing the RNA wonder – Can a special RNA structure prevent RNA methylation?	15
CRISPR-Cas13 for active alterations of RNA modifications	17
Summary	21
References	22
Chapter II: Towards targeted RNA N6-methyladenosine demethylation in plants	36
Abstract	37
Introduction	37
Materials and Methods	40
Results	43
Design and construction of dCas13b-ALKBH10B.....	43
Selection of targets for testing dCas13b-ALKBH10B in <i>A. thaliana</i>	46
Targeting dCas13b-ALKBH10B to m ⁶ A sites on TTG1 altered trichome morphology	47
Targeting dCas13b-ALKBH10B to <i>FT</i> did not cause late or early flowering	54
Discussion	57
References	67
Chapter III: Towards targeted RNA 5-methylcytosine demethylation in plants 71	

Abstract	72
Introduction	72
Materials and methods	78
Results	82
Design and construction of dCas13-TET1	82
Characterization of dCas13-TET1 by transient expression in <i>N. benthamiana</i> .	85
m ⁵ C at C3349 on <i>MAIGO5</i> (<i>MAG5</i>) as a potential endogenous target for testing of targeted m ⁵ C demethylation systems	87
Efficacy of dCas13b-TET1 on <i>MAG5</i> C3349 determined by Bisulfite-amplicon- sequencing.....	88
Mutated STTM may cause degradation of non-m ⁵ C modified mRNA.....	90
Discussion	93
Supplementary data	95
References	101
Chapter IV: Deciphering RNA 5-methylcytosine in <i>Arabidopsis thaliana</i>'s root development	106
Abstract	107
Introduction	107
Materials and methods	111
Results	115
<i>SHY2/IAA3</i> and <i>IAA16</i> are not key factors in m ⁵ C regulation of root development	115
Dynamics of RNA m ⁵ C methylation on <i>SHY2/IAA3</i> and <i>IAA16</i> in root tissue ..	117
Conservation of C348 on <i>IAA3</i> mRNAs	118
Interference to C348 on <i>SHY2/IAA3</i> does not cause detectable effect on root growth <i>in planta</i>	121
Discussion	123
Supplementary Data	126
References	134
Chapter V: General discussion and Conclusion	154
General discussion	155
Targeted manipulations for functional studies of RNA methylations.....	155
Multi-approach functional studies of a modified site – Appreciating discrepancies	157
Concluding remark	159
Appendix	160

Abstract

Phenotype prediction from DNA or RNA sequence in eukaryotes is difficult as a result of the multiple layers of gene expression regulation. One of these regulatory layers is RNA modification which occurs either co-transcriptionally or post-transcriptionally to RNA and affects many aspects of RNA biology. Recent transcriptome-wide insights of RNA modifications have begun to elucidate the extent of this landscape, leading to the proposition of the “epitranscriptome”. However, understanding the “epitranscriptome” and its consequences to RNA metabolism, functional relevance and mechanism of action remains an enormous undertaking. The lack of tools to specifically manipulate an RNA modification has hampered the un-biased evaluation of their importance as well as understanding of the mechanism underlying their activities in a site-specific manner.

During my research, I investigated the RNA-guided RNA targeting system CRISPR-dCas13 and the RNA-based technique Short Tandem Target Mimic (STTM) regarding their potential to develop programmable systems for targeted demethylation of two RNA modifications N6-methyladenosine (m^6A) and 5-methylcytosine (m^5C) in *Arabidopsis thaliana*. Initial results indicated unsuccessful interference to m^5C deposition using the STTM approach. In contrast, fusion of dCas13 to RNA modifying domains ALKBH10B or human TEN-ELEVEN TRANSLOCATION1 (hTET1) respectively enabled alterations of m^6A - or m^5C -bearing reporter or endogenous transcripts in either *Nicotiana benthamiana* or *A. thaliana*. However, further investigation is required to understand the robustness of both approaches. Possible improvements are discussed for targeted RNA demethylation tools using CRISPR-dCas13.

In addition, the functional relevance of RNA m^5C in root development in *A. thaliana* was also extensively investigated with regards to previously proposed involvement of two transcripts *SHORT HYPOCOTYL 2* (*SHY2/IAA3*) and *INDOLEACETIC ACID-INDUCED PROTEIN 16* (*IAA16*). Phenotypic and mRNA quantification analyses of m^5C -deficient and *SHY2/IAA3* loss-of-function mutants refuted a key role for *SHY2/IAA3* and *IAA16* in m^5C regulation of root development. Although I identified an m^5C site C348 on *SHY2/IAA3* using bisulfite RNA amplicon sequencing and initial nucleotide conservation analysis suggested that this site is more

conserved than other non-methylated cytosines within *SHY2/IAA3* mRNA, functional analysis using dCas13-hTET1 conjugate did not support the importance of this C348 *in planta*. In summary, RNA-guided CRISPR-dCas13 and multi-strategy approaches for site-specific functional study offers potential to significantly improve our understanding of RNA modifications.

Declaration

I certify that this work contains no material which has been accepted for the award of any other degree or diploma in my name in any university or other tertiary institution and, to the best of my knowledge and belief, contains no material previously published or written by another person, except where due reference has been made in the text. In addition, I certify that no part of this work will, in the future, be used in a submission in my name for any other degree or diploma in any university or other tertiary institution without the prior approval of the University of Adelaide and where applicable.

I give permission for the digital version of my thesis to be made available on the web, via the University's digital research repository, the Library Search and also through web search engines, unless permission has been granted by the University to restrict access for a period of time.

Huong Thi Thuy Ta

30 January 2022

Acknowledgements

One of my dear teachers at Vietnam National University once told me that the most important thing about a PhD is how one grows in research, and in life.

I would like to firstly thank my PhD supervisor, Assoc. Prof Iain Searle. I am not sure if I had been given a second chance, I would have still chosen to become your student. Nevertheless, thank you for the experience and I am truly grateful for what I have learned in the lab. Your sharp and innovative mind is what I'll remember.

My thanks also go to my two co-supervisors, Dr. Simon Baxter and Dr. Nathan Watson-Haigh, and my two Postgraduate Co-ordinators, Prof David Adelson and Assoc Prof Keith Shearwin. I know the past several years have not been particularly pleasant to say the least. I really appreciate all your support which kept me going. I also hope you had something to remember about me rather than just my being in conflict with Iain. And thanks Dave and Keith, for always being there for me.

I thank my friends from Searle lab and Baxter lab for the help over the years. I'm especially thankful to now Dr. Christopher Ward for the discussions of bioinformatic analyses in this study, and the friendship that got me through some difficult times. And I'm still looking forward to discussing "The Republic" with you Chris, maybe over a matcha somewhere in JP.

I thank the School of Biological Sciences and its extended community for not only the support in the form of experimental facilities, but more importantly, the chance to learn about various scientific topics and interesting discoveries.

I am in debt to all my former teachers and mentors at Vietnam National University, Japan National Institute of Genetics and Okinawa Institute of Science and Technology, for the knowledge I was imparted, for the passion and inspiration that led to this PhD and will continue to follow me as long as I do science.

Lastly, to my mom, Trieu Thi Hoa, my sister and dad, I have probably become someone whose character and career are out of your ability to comprehend, but your

great love and support are what made them all possible. I have lived and loved as how you showed me to, and even above my career, I wish you the happiness and peace you deserve. And to our little angel, π , as well as my own future child(ren), may you learn to embrace every moment of life.

Adelaide, Jan 2022

Abbreviations

Ψ Pseudouridine

A

ALKBH α -ketoglutarate-dependent dioxygenase alkB homolog

B

bp Base pairs

BS-amp-seq Bisulfite amplicon sequencing

BS-RNA-seq Bisulfite RNA sequencing

C

Cas13 CRISPR-associated protein 13

cDNA Complementary DNA

CDS Coding sequence

CLIP Crosslinking and immunoprecipitation

CRISPR Clustered Regularly Interspaced Short Palindromic Repeat

D

dCas13 (Catalytically) dead Cas13

dLwaCas13a dCas13a from *Leptotrichia wadei*

dPspCas13b dCas13b from *Prevotella* sp. P5-125

dRfxCas13d dCas13d from *Ruminococcus flavefaciens* XPD3002

dsDNA Double stranded DNA

DNA Deoxyribonucleic acid

DNMT DNA methyltransferase

F

⁵C 5-formylcytosine

FT FLOWERING LOCUS T

FTO Fat mass and obesity associated protein

H

HEK293T	Human embryonic kidney 293 cells
HeLa	Human cervical cancer cell line
hm ⁵ C	5-hydroxymethylcytosine
HNRNPC	Heterogeneous nuclear ribonucleoprotein C

I

iCLIP	individual nucleotide resolution crosslinking and immunoprecipitation
-------	---

M

m ¹ A	N1-methyladenosine
m ⁵ C	5-methylcytosine
m ⁶ A	N6-methyladenosine
METTTL3	Methyltransferase like 3
METTTL14	Methyltransferase like 14
miRNA	MicroRNA
mRNA	Messenger RNA
MTA	Adenosine methyltransferase (m ⁶ A methyltransferase in <i>A. thaliana</i>)

N

NSUN	NOP2/Sun domain family, member
------	--------------------------------

P

Poly(A)	Polyadenylation
---------	-----------------

R

RNA	Ribonucleic acid
RIP	RNA Immunoprecipitation
rRNA	Ribosomal RNA

S

siRNA	Small interfering RNA
STTM	Short Tandem Target Mimic

T

TET	TEN-ELEVEN TRANSLOCATION protein
TM	Target Mimic
TRDMT1	tRNA aspartic acid methyltransferase 1
TRM4B	tRNA-specific methyltransferase 4b
tRNA	transfer RNA
TTG1	TRANSPARENT TESTA GLABRA 1

U

UTR	untranslated region
-----	---------------------

W

WTAP	Wilms tumor 1 associated protein
------	----------------------------------

Y

YTDHF	YTH domain family
-------	-------------------

List of Figures

Figure I-1: Prevalent modifications on eukaryotic mRNA.....	4
Figure I-2: Functional relevance accounts for a small portion of our current understanding of RNA modifications.....	6
Figure I-3: RNA sequestration or destruction by TM and/or STTM.....	16
Figure I-4: Applications of active CRISPR-Cas13 and derivatives.....	19
Figure II-1: Harnessing Arabidopsis ALKBH10B and catalytically deactivated enzyme dCas13 for targeted RNA m ⁵ C demethylation.....	39
Figure II-2: Design and construction of dCas13b-(m)ALKBH10B.	46
Figure II-3: Trichome characterization of transgenic plants expressing dCas13b-ALKBH10 targeting m ⁶ A sites on <i>TTG1</i> mRNA.....	48
Figure II-4: Molecular characterization of transgenic plants expressing dCas13b-ALKBH10 to target m ⁶ A sites on <i>TTG1</i> mRNA.	51
Figure II-5: <i>TTG1</i> mRNA abundance in transgenic plants expressing <i>TTG1</i> -targeting dCas13b-ALKBH10.	53
Figure II-6: Targeting dCas13b-ALKBH10B to DRACH motifs on <i>FT</i> mRNA.	56
Figure III-1: Harnessing the human DNA dioxygenase TET1 (hTET1) and catalytically deactivated enzyme dCas13 for targeted RNA m ⁵ C demethylation.	75
Figure III-2: Adopting STTM for preventing methylation on mRNA nucleobases.....	77
Figure III-3: Design and construction of dCas13-(m)TET1.	84
Figure III-4: Characterization of dCas13-TET1 in <i>N. benthamiana</i>	86
Figure III-5: Impact of stably expressed dCas13b-TET1 targeting <i>MAG5</i> C3349.....	89
Figure III-6: Testing STTM for targeted prevention of RNA methylation.	92
Figure IV-1: Auxin signaling pathway.....	108
Figure IV-2: Assessing the role of <i>SHY2/IAA3</i> and <i>IAA16</i> in m ⁵ C regulation of root development.....	116
Figure IV-3: Detection of m ⁵ C sites on <i>SHY2/IAA3</i> mRNA using BS-amp-seq (library I).	118
Figure IV-4: Conservation of C348 on <i>SHY2/IAA3</i>	121

Figure IV-5: Interference of dCas13-TET1 to C348 on *SHY2/IAA3* does not alter root growth in *Arabidopsis*. 122

Chapter I: Introduction

Overview

The regulation of gene expression in eukaryotes is a well-orchestrated process of many regulatory layers. During and post synthesis, RNA transcripts undergo various processing steps in which they are tailored with different modifications, editing and splicing events. The occurrence of chemical modifications on RNA was reported as early as 1951 (Cohn & Volkin 1951). Advancements in high-throughput sequencing techniques in recent years have brought an unprecedented chance to profile various RNA modifications in a transcriptome-wide manner in several plants and animals, paving the way for investigation of their biological relevance. Once thought to be random and insignificant “decorations”, many of the modifications have emerged as a new component of gene expression, namely the “epitranscriptome”. Despite the recent explosion in research and discoveries of new RNA modifications, their dynamics and putative functions, a majority of these matters remains perplexing and is awaiting validation or further elucidation. Establishing “epitranscriptomics” will require functional studies and elucidation of molecular mechanism at single nucleotide resolution, perhaps firstly through the “model” RNA modifications such as N6-methyladenosine or 5-methylcytosine.

Insights into the “epitranscriptome”

More than random “decorations” - RNA modifications as an emerging layer of gene regulation

Chemical modifications on RNA range from small scale covalent addition of single or multiple chemical groups onto the sugar ring (eg. 2'-O-methyladenosine) or nucleobases (eg. N1-methyladenosine (m¹A), N6-methyladenosine (m⁶A), 3-methylcytidine (m³C), 5-methylcytosine (m⁵C), 1-methylguanosine (m¹G), and N7-methylguanosine (m⁷G)), to deamination events which convert one nucleotide (nt) into another (eg. A-to-I editing). Detection of non-canonical RNA residues (other than A, U, G, C) was documented as early as 1951 (Cohn & Volkin 1951) despite their identification being elusive until years later (Cohn 1960). Among the first to be discovered was pseudouridine (ψ), the most abundant modified residue and sometimes considered the “fifth nucleotide” in RNA (Cohn 1960; Holley et al. 1965) (Figure I-1). Improvement in detecting methods over five decades, especially mass spectrometry, has revealed more than 150 RNA modifications in virtually all types of

RNA throughout the three domains of life (Ma, J et al. 2021). Of all RNA species, RNA modifications studies have been largely focused on abundant ones such as tRNA and rRNA with the early realization that they are highly modified (Holley et al. 1965). Other non-coding RNA such as small nuclear RNA also contains a wide range of modifications including ψ , ribose and base methylations (Bohnsack & Sloan 2018).

5'-cap and poly(A) tail are important terminal modifications on mRNA known since the 1970s (Furuichi, LaFiandra & Shatkin 1977; Shatkin 1976; Wei, CM, Gershowitz & Moss 1976). These modifications facilitate pre-mRNA processing, stability, nuclear export as well as translation, owing to their interactions with cap- or poly(A)-binding proteins (Flaherty et al. 1997; Furuichi, LaFiandra & Shatkin 1977; Gallie 1991; Izaurralde et al. 1994). Although their functions were much less known, documentation of internal modifications on mRNAs, including N^6 -methyladenosine (m^6A), 1-methyladenosine (m^1A), N^6 -2'-*O*-dimethyladenosine (m^6Am), 5-methylcytidine (m^5C) and 5-hydroxymethylcytidine (hm^5C) (Figure I-1) dated back around the same time (Desrosiers, Friderici & Rottman 1974; Dubin & Taylor 1975; Dunn 1961; Lavi, Fernandez-Mufioz & Darnell 1977; Schibler & Perry 1977; Wei, C-M & Moss 1977). The role of m^6A in pre-mRNA processing/transport and its importance in mammalian cells were also noted early (Rottman et al. 1986), yet the difficulties in getting a comprehensive view of the modification's landscape and the ignorance of an active demethylation activity that can occur on it had obscured further interpretation into the possible regulatory role of this modification.

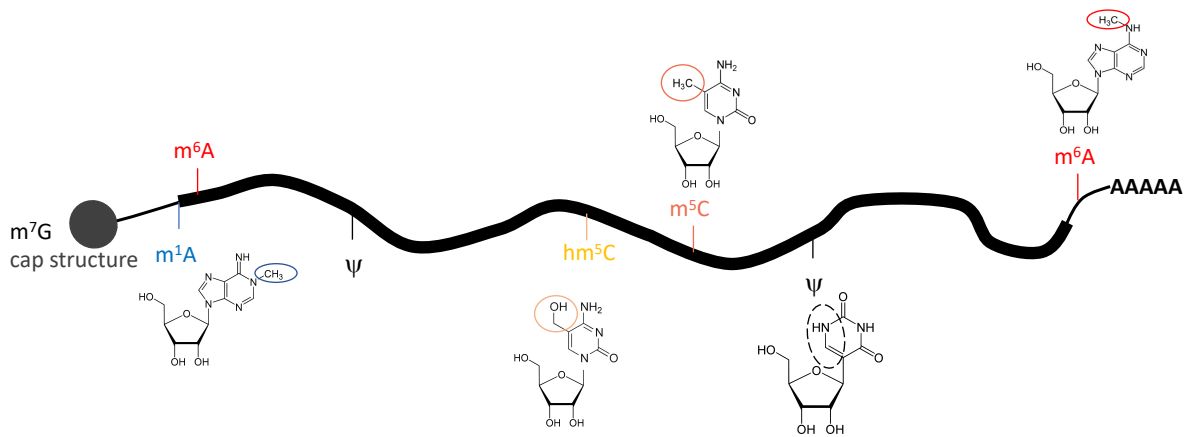


Figure I-1: Prevalent modifications on eukaryotic mRNA. Beside 5' cap and poly(A) tail, mRNAs can be “decorated” with a number of internal modifications. Pseudouridine (ψ) is the first discovered and most abundant RNA modification. Other prevalent modifications include many types of methylation to the nucleobases such as N⁶-methyladenosine (m⁶A), 1-methyladenosine (m¹A), 5-methylcytidine (m⁵C) and 5-hydroxymethylcytidine (hm⁵C).

The discovery of proteins that remove RNA m⁶A brought a new wave of interest in m⁶A and RNA modifications alike (Jia et al. 2011; Zheng et al. 2013), as the reversibility is reminiscent of that of epigenetic controls on DNA. Later, a few other RNA methylations such as m¹A and m⁶Am were also shown to be reversible (Jia et al. 2011; Li, X et al. 2016; Liu, F et al. 2016; Mauer et al. 2017). These findings strongly pointed towards a regulatory role of RNA modifications similar to that of the epigenome, supporting the previous postulation of the “epitranscriptome” (He, C. 2010). Alongside, the advancement in mapping and quantifying methods especially high-throughput sequencing enabled detailed and transcriptome-wide profiling of many RNA modifications including m⁵C, m⁶A, m⁶Am, ψ , m¹A, hm⁵C (Carlile et al. 2014; Delatte, B. et al. 2016; Dominissini et al. 2012; Dominissini et al. 2016). These studies highlighted the great diversity and pervasiveness of RNA modifications, paving the way for establishment of certain links between these “epitranscriptomic” marks, RNA metabolism and subsequent phenotypical consequences. It also came to light that a number of modified sites on RNA are conserved amongst closely related species or even across the three domains of life (Jackman & Alfonzo 2013; Li, S &

Mason 2014; Schwartz et al. 2013), suggesting their conserved functions and evolutionary importance. As a result, RNA modification has been transformed from insignificant “decorations” into a field of its own.

Conceptualizing “epitranscriptomics”- functional insight is key

The exponential numbers of RNA modifications and modified RNA sequences identified in various mapping attempts over the years, while being important and providing critical information such as depositing motifs and plausible factors involved, are inadequate when it comes to consolidating the regulatory role of these modifications: If the modifications do no jobs, whether they are present or absent makes no difference. In addition, a majority of modified sites, especially those on mRNAs, has low occurrence (less than 20% of identical RNA sequences are modified) (David et al. 2017; Huang, T et al. 2019; Legrand et al. 2017), and different studies can report variable modification levels at the same site. Therefore, identifying the impact and mode of action of such lowly modified sites with potentially changing stoichiometry is important in both understanding of their regulatory role and verification of mapping data. In these senses, functional studies of RNA modifications should be aimed to unbiasedly detail biological impacts of RNA modifications at specific sites, on particular RNA sequences (Figure 1-2). Currently, such studies are largely missing for internal modifications on mRNAs. Functional relevance of RNA modifications has mostly been inferred from mutations of proteins involving their deposition, recognition and removal (usually referred to as “writers”, “readers” and “erasers”, respectively). The indirect evidence sometimes leads to misinterpretation of RNA modification’s functions as the proteins can have functions unrelated to RNA modifications. Besides, knockout of the proteins leads to global change in the RNA modification landscape which does not allow identification of specific modified sites/cellular activities leading to morphological changes, especially for the proteins that use more than one RNA species as substrates. The highlights and shortcomings in functional studies of RNA modifications will be discussed in detail below through two important RNA methylations m⁶A and m⁵C.

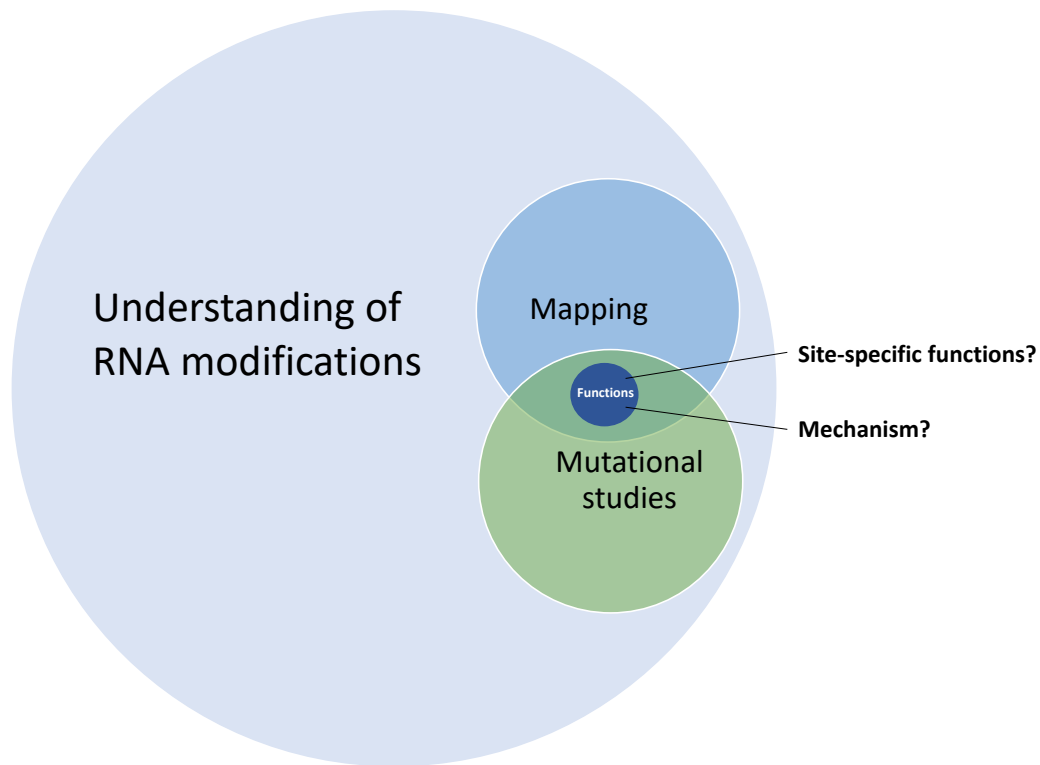


Figure I-2: Functional relevance accounts for a small portion of our current understanding of RNA modifications. Efforts in mapping and studies of RNA modifications’s “writer”, “reader” and “eraser” mutants have suggested certain biological functions of these modifications. However, site-specific functional analyses and underlying mechanism are underrepresented in the field, leaving uncertainties regarding the relevance of an “epitranscriptome”.

RNA m⁶A and m⁵C - Two models of the “epitranscriptome”

m⁶A and m⁵C are uniquely two shared modifications between RNA and DNA (apart from the oxidized products of m⁵C such as hm⁵C, f⁵C and ca⁵C). The similarity of these RNA and DNA methylations with respect to their relatively small scale (covalent modification instead of base-alteration), chemical properties and reversibility makes RNA m⁶A and m⁵C stand out as key modifications for solidifying the regulatory role of RNA modifications. Methods for detection of RNA m⁶A and m⁵C are also amongst the most used and well-investigated, some benefited from the nearly 80-year legacy of DNA methylation studies.

High-throughput profiling of RNA m⁶A and m⁵C

Advent of next generation sequencing (NGS) and more recently third generation sequencing with Nanopore technologies have fuelled RNA m⁶A and m⁵C studies with exponential transcriptome-wide mapping data. Unlike some other RNA modifications that can arrest reverse transcription and be tracked by following sequencing (Ebhardt et al. 2009; Ryvkin et al. 2013), m⁶A and m⁵C do not alter Watson-Crick base-pairing conferred by reverse transcriptases. RNA immunoprecipitation with respective antibodies coupled with NGS (RIP-seq) has become the method of choice for a number of studies and provided valuable whole transcriptome mappings for m⁶A and m⁵C modifications (Dominissini et al. 2012; Meyer, K. D. et al. 2012). This immunoprecipitation approach however relies heavily on the specificity of the antibody, often requires large amounts of biological samples, has relatively poor reproducibility and gives approximate (peaks of several hundred bases) instead of precise locations of modified sites. Cross-linking strategies have been adopted for more stable bonding between modification-bearing RNA fragments and antibody or binding proteins, and subsequent identification of the modifications to a greater precision (Chen, K et al. 2015; Hussain et al. 2013; Khoddami & Cairns 2014; Linder et al. 2015).

Besides immunoprecipitation approach, RNA m⁶A can be mapped transcriptome-wide with the use of enzymatic treatments that alter the methylation status or adjacent sequence for detection with downstream sequencing in methods named DART-seq (deamination adjacent to RNA modification targets) or m⁶A-SEAL (Meyer, Kate D. 2019; Wang, Ye et al. 2020). To map m⁶A to single-nucleotide resolution in an antibody-independent manner, m⁶A-sensitive ribonuclease MazF is a promising approach (Garcia-Campos et al. 2019). The enzyme recognizes and cleaves upstream of an m⁶ACA motif, which can then be detected as truncated reads in sequencing. While this method is currently not applicable ubiquitously due to the limited recognition motif of MazF, similar approach with evolved MazF or m⁶A-sensitive DNazymes (Sednev et al. 2018; Yu et al. 2021) with expanded recognition motifs is predicted to out-perform the antibody-based methods in a near future. It is worth noting that other methods for mapping of m⁶A that take advantages of m⁶A's chemical characteristics such as hindering of splinted DNA elongation and ligation are available (Liu, Nian et

al. 2013; Wang, Y. et al. 2021). These methods can be complex and have poor high-throughput potential but are powerful in validating methylation status of specific sites. Regarding m⁵C, apart from immunoprecipitation, the chemical-based approach widely used in DNA, Bisulfite sequencing, has also been adapted for mapping of RNA m⁵C (BS-RNA-seq) (Edelheit et al. 2013; Schaefer et al. 2009; Squires et al. 2012). Compared to antibody-based approaches, BS-RNA-seq offer base-specific profiling of m⁵C with a simpler library preparation procedure but does suffer from biases especially conversion efficiency due to distinct features of RNA compared to DNA in Bisulfite treatment (Helm & Motorin 2017). Another limitation of BS-RNA-seq is the inability to discriminate m⁵C and its oxidized product hm⁵C (and potentially other similar methylations such as 4-methylcytosine). Nevertheless, BS-RNA-seq has contributed substantially to our knowledge of the m⁵C landscape in different RNA types in many animal and plant species (Amort et al. 2013; David et al. 2017; Edelheit et al. 2013; Militello et al. 2014; Squires et al. 2012).

Recently, the direct RNA sequencing offered by Nanopore technologies has opened an unprecedented opportunity to overcome the shortcomings in aforementioned methods to profile RNA modifications at single nucleotide resolution with high efficiency and in an unbiased manner. Direct RNA sequencing also has the potential to enable simultaneous identification of different RNA modifications on the same RNA molecules, which is critical in uncovering the interplay between RNA modifications. Algorithms have been developed mostly for detection of m⁶A from direct RNA sequencing data with 80-90% accuracy (Liu, H et al. 2019; Lorenz et al. 2020; Parker et al. 2020; Pratanwanich et al. 2021), while methods for determining other modifications including m⁵C and hm⁵C have also begun to be explored (Begik et al. 2021). With accuracy improved, direct RNA sequencing with Nanopore technologies will be a resourceful tool to expand our understanding of not only m⁶A and m⁵C but also other RNA modifications.

RNA m⁶A and m⁵C's high throughput sequencing data has been documented in different databases (Ma, J et al. 2021), facilitating investigations of various aspects of RNA modifications including their functions and regulatory mechanism.

The most abundant and well-studied internal mRNA modification - m⁶A

The presence, abundance and even motif of m⁶A on mRNA was actively investigated as early as 1970s (Desrosiers, Friderici & Rottman 1974; Lavi, Fernandez-Mufioz & Darnell 1977; Perry & Kelley 1974; Wei, C-M & Moss 1977; Wei, CM, Gershowitz & Moss 1976). These early studies, mostly in cultured animal cells, revealed the occurrence of this modification on mRNAs around one or two per 1000 nucleotides compared to an average of one per 1800-3000 in other non-ribosomal RNAs. The great improvement in m⁶A-profiling methods has offered for the first time the transcriptome-wide view of this modification (Dominissini et al. 2012; Meyer, K. D. et al. 2012). These studies showed that while accounting for a large fraction of m⁶A, the coding region of mRNA is less methylated when normalized by length, whereas the 3'UTR and especially the proximal sequence upstream of stop codon are highly enriched with this methylation. In plants, beside 3'UTR and stop codon, start codon is also a hotspot for m⁶A methylation (Li, Y et al. 2014; Luo et al. 2014).

m⁶A is deposited to RNA sequence by a complex of “writer” proteins with Methyltransferase like 3 (METTL3) and Methyltransferase like 14 (METTL14) (or MTA and MTB in plants (Bujnicki et al. 2002; Zhong et al. 2008), respectively) playing the key roles (Bokar et al. 1994; Liu, J et al. 2014). Besides, a number of proteins help fine-tune the methylation activity of the m⁶A “writer” including Wilm's tumor 1 associating protein (WTAP), VIRMA/KIAA1429 and zinc finger CCCH domain-containing protein 13 (ZC3H13) (Knuckles et al. 2018; Ping et al. 2014; Schwartz et al. 2014). In *A. thaliana*, MTA/MTB heterodimer is joined by FKBP12 interacting protein 37 KD (FIP37), VIRILIZER and HAKAI (Ruzicka et al. 2017). Recent sequencing techniques have also better informed the motif of m⁶A deposition on mRNA which is conservely RRACH (R = A/G, H = not G) in mouse, human cell lines (Dominissini et al. 2012; Meyer, K. D. et al. 2012) and plants (Luo et al. 2014; Wan et al. 2015). This A-rich motif might partly explain the enrichment of m⁶A near stop codon and 3'UTR where A bases occur with higher frequency. The preference of m⁶A deposition in mRNA 3'UTR was further demonstrated to be mediated by VIRMA/KIAA1429 in a region-specific manner (Yue et al. 2018). m⁶As were also found to cluster in the hairpin structures in *METHIONINE ADENOSYLTRANSFERASE 2A* 3'UTR, suggesting a role for mRNA secondary structure in methylation deposition (Shima et al. 2017). In line with this, Chen, T et al. (2015) gave evidence that binding

of micro RNAs to mRNA can guide m⁶A installation through recruiting METTL3 to the binding site.

m⁶A motifs are also important for the activities of m⁶A “readers”. However, they appear to diverge from m⁶A consensus motif RRACH to some extent. While the binding motif of YTHDC1, a member of the large YTH domain m⁶A “reader” family in mammals, is GGACH, corresponding well to the m⁶A consensus, SRSF3 and SRSF10 of the serine/arginine-rich (SR) protein family favour UGGAC and AGGACMG (M = A or C), respectively (Xiao, W et al. 2016). In plants, members of the YTH domain family known as EVOLUTIONARILY CONSERVED C TERMINAL, ECT2, ECT3 and ECT4 have also been experimentally demonstrated as m⁶A “readers” (Arribas-Hernández, L. et al. 2020; Scutenaire et al. 2018; Wei, L-H et al. 2018; Wu, Peled-Zehavi & Galili 2020) and are likely to have different binding motifs from the animal counterparts, for example URUAW (R = G/A; W = U/A) for ECT2 (Wei, L-H et al. 2018). The third group of m⁶A “readers” heterogeneous nuclear ribonucleoproteins (hnRNPs) contains HNRNPA2B1 which in human cells also binds to RGAC.

The metabolism of m⁶A was complete with the discovery of m⁶A “erasers” Fat mass and obesity associated protein (FTO) and Alkylation repair homologue protein 5 (ALKBH5) (Jia et al. 2011; Zheng et al. 2013) which remove RNA m⁶A in mammals. Recently, the plant counterpart of these m⁶A “erasers”, ALKBH9B and ALKBH10B, have also been revealed (Duan et al. 2017; Martínez-Pérez et al. 2017).

m⁶A has a wide range of effects on mRNA metabolism which include but not limited to RNA stability, RNA secondary structure, alternative splicing, and translation (Liu, N. et al. 2015; Liu, N. et al. 2017; Wang, X. et al. 2015). In both plants and animals, m⁶A can either enhance (Huang, H et al. 2018; Wei, L-H et al. 2018) or reduce (Duan et al. 2017; Wang, Xiao et al. 2014) the stability of mRNA transcripts. The different effects are potentially a result of different m⁶A “reader” proteins recognizing the particular targets, and differences in environmental and physiological cues (Huang, H et al. 2018). In a similar manner, other aforementioned functions of m⁶A such as in RNA splicing and translation are conferred by and dependent on associated m⁶A “readers”. As a result of these various molecular impact, m⁶A is vital for both plant and animal development. Null or knockdown mutants of many of the m⁶A “writer” complex

components are embryonically lethal, while others have severe growth defects or disorders (Hongay & Orr-Weaver 2011; Ruzicka et al. 2017; Zhong et al. 2008). In *A. thaliana*, a mutational study on single, double and triple mutants of the “reader” proteins ECT2/ECT3/ECT4 demonstrated a recurrent requirement for these proteins in normal development of many plant organs such as root, leaf, flower and fruit (Arribas-Hernández, L. et al. 2020). m⁶A was also linked to floral transition in *A. thaliana*, with mutant of the “eraser” *alkbh10b* exhibits a late flowering phenotype (Duan et al. 2017). In mice, the loss of FTO or ALKBH5 results in adipogenesis defects or male infertility, respectively. However, it is worth noting that expression of not FTO but a connected homeobox gene IRX3 was shown to directly regulate body weight in mice (Smemo et al. 2014), suggesting that this enzyme can play role other than m⁶A-related and inferring m⁶A function in adipose metabolism from its knockout could have been biased. Despite certain biases, an increasing number of studies have successfully narrowed down a set of transcripts might be playing roles in m⁶A regulation of observed phenotypes, paving the way for validation and follow-up studies to detail the underlying mechanism from modification to phenotype of this modification (Duan et al. 2017; Gao, Y et al. 2020; Mendel et al. 2021; Shima et al. 2017; Su et al. 2018; Wei, L-H et al. 2018).

The sibling of epigenetic DNA methylation – RNA m⁵C coming of age

Studies have reported variable pervasiveness of RNA m⁵C in different species. In human HeLa cells, Squires et al. (2012) reported more than ten thousand m⁵C sites in both mRNA and non-coding RNAs, using Bisulfite sequencing (BS-RNA-seq). The same technique, when applied to mouse embryonic stem cells with stringent computational analyses, found mRNAs were sparsely or not even methylated (Legrand et al. 2017). In *A. thaliana*, transcriptome-wide BS-RNA-seq detected less than 1500 m⁵C sites in three tissue types shoots, siliques and roots, with 1% threshold set for methylation calling (David et al. 2017), while a study utilized an RNA immunoprecipitation approach documented more than six thousand m⁵C peaks in seedlings (Cui et al. 2017). Within mRNAs, although greater numbers of m⁵C sites were detected in the coding sequence, when normalized for length and read coverage, the distribution of m⁵C is enriched in untranslated regions, especially the 3'UTR (David et al. 2017; Squires et al. 2012).

Two RNA m⁵C “writers” identified to date are tRNA specific methyltransferase 4 (TRM4) also known as NOP2/Sun domain protein 2 (NSUN2) (Khoddami & Cairns 2013) and Transfer RNA aspartic acid methyltransferase 1 (TRDMT1) or DNA methyltransferase 2 (DNMT2) (Goll et al. 2006). The methyltransferases are S-adenosylmethionine (SAM)-dependent, although how they recognize targets remains elusive. The motifs for m⁵C methylation deposition have been suggested in several studies. In plants, Cui et al. (2017) reported two consensus motifs for m⁵C HACCR and CUYCUYC with occurrence being around 50% and 42% of methylated peak identified in an m⁵C-RIP approach. These motifs are distinct from the motif identified in archaea AUCGANGU (Edelheit et al. 2013). No such motifs have been identified in animals (Hussain et al. 2013; Squires et al. 2012) although at least two studies have demonstrated a CG-rich region proximal to m⁵C sites (Squires et al. 2012; Yang, X et al. 2017). In addition, David et al. (2017) demonstrated the importance of 50-nt surrounding an m⁵C site for its deposition, suggesting the involvement of RNA secondary structure. The observation that m⁵C site is enriched near binding sites of Argonaute proteins (Squires et al. 2012) might also suggest a correlation between local RNA structure and m⁵C deposition.

The mRNA export adaptor ALYREF is the only m⁵C “reader” known to date (Yang, X et al. 2017). RNA m⁵C demethylase(s) has not been uncovered in both plant and animal, although in animals, the DNA dioxygenase TEN-ELEVEN TRANSLOCATION (TET) protein family is speculated as a key factor. It has been hypothesized that RNA m⁵C demethylation may occur through a serial oxidation from m⁵C to hm⁵C, f⁵C (5-formylcytosine), ca⁵C (5-carbonylcytosine) and finally C in a similar manner with the DNA demethylation in animals which is performed by the TET family, although the DNA m⁵C demethylation itself is not fully understood. Supporting this hypothesis, three members of the TET family were shown to catalyze m⁵C-to-hm⁵C conversion *in vitro* and in human cell cultures (Fu et al. 2014; Shen, Q et al. 2018). Moreover, the *Drosophila melanogaster* TET protein which first known to catalyze DNA m⁶A demethylation was also evidenced to convert RNA m⁵C into hm⁵C in this species (Delatte, Benjamin et al. 2016). Even less is known about a putative RNA m⁵C demethylase in plants, however, ortholog(s) of TET proteins or member(s) of the other common dioxygenase family AlkB (Mielecki et al. 2012) could be the enzyme in quest.

Huong, Ngoc and Kang (2020) proposed *A. thaliana* ALKBH6 as a potential m⁵C/m⁶A “eraser” due to its observed binding to m⁵C- and m⁶A-bearing RNAs in an electrophoretic mobility shift assay. However, there appeared no difference in binding affinity of this protein to modified and non-modified RNAs used, and the authors did not evidence the demethylase activity of the protein.

Similar to m⁵C “eraser”, the biological importance of m⁵C on mRNA remains largely elusive. Being recognized by ALYREF suggested a role for m⁵C in nuclear export of mRNAs in mammals (Yang, X et al. 2017). m⁵C was also linked to RNA movement across graft junction in plants via the double mutant of m⁵C “writers” TRDMT1 and TRM4B (Yang, L et al. 2019). The impact of RNA m⁵C on RNA metabolism appears to be context-dependent. While this modification enhances stability of both synthetic and cellular mRNA (Cui et al. 2017; Warren et al. 2010), no pronounced correlation between global changes in m⁵C level and shifted gross transcript abundance has been reported (David et al. 2017; Hussain et al. 2013; Tuorto et al. 2012). At the translational level, globally, m⁵C can negatively affect protein translation in NSUN2-knockout mouse skin and HeLa cells (Huang, T et al. 2019), which was shown through computational analysis of ribosome profiling data. However, m⁵C can also enhance translation of a Luciferase reporter *in vitro* (Li, Q et al. 2017). These suggested impacts at the molecular level might have resulted in defects in mutations of m⁵C “writers”. For example, NSUN2 and TRM4B take part in oxidative stress responses in animals and plants, perhaps via regulation of tRNA cleavage in the absence of m⁵C (Blanco, S. et al. 2014; David et al. 2017). Depletion of NSUN2 in both mouse and human causes hair defect and decreased body size and weight (Blanco, Sandra et al. 2011; Fahiminiya et al. 2014), which could be roughly attributed to perturbed stem cell homeostasis. In line with this, mutants of TRM4B in *A. thaliana* exhibits aberrant root meristem proliferation and subsequent shorter primary roots (David et al. 2017). However, given that NSUN2 and TRM4B use both tRNAs and mRNAs as substrates, the exact mechanism and modified RNA sequences underlying respective phenotypes will need further elucidation.

Using m⁶A and m⁵C for modelling the “epitranscriptome”

Our current understanding of m⁶A and m⁵C not only supports the regulatory role that RNA modifications might serve, but can also push forward new discoveries to fortify the “epitranscriptome” proposition. The huge numbers of m⁶A and m⁵C sites mapped lay foundation for functional analyses to confirm the relevance of the modified sites and investigation of underlying mechanism, while the various and relatively well-developed detection techniques facilitate functional assays. There are a number of approaches that could be taken to harness m⁶A and m⁵C for conceptualizing “epitranscriptomics”, I propose two following investigations: (i) Site-specifically study the function of m⁶A and m⁵C sites/regions mapped. (ii) Develop tools to specifically remove, or alter a modified site for evaluation of its importance.

Synthetic systems for functional studies of RNA modifications

Synthetic platforms for RNA study

The ability to bind and modify RNA of synthetic systems which come in both RNA and protein forms has made valuable contributions to our understanding of RNA biology. RNA-based systems, such as the various RNA interference (RNAi)-based techniques that utilizes short double-stranded RNA sequence for binding to mRNA and inhibition of gene expression (Caplen et al. 2001; Elbashir et al. 2001), or Target Mimic (Ivashuta et al. 2011; Todesco et al. 2010) and Short Tandem Target Mimic (Tang, G. et al. 2012) which can be used to block the function of small RNAs that regulates gene expression by post-transcriptional gene silencing, have proven the versatility of RNA in uncovering their own interplay. However, these RNA-based techniques mostly allow modulation of target level but not more complicated tasks such as actively altering their sequence or chemical modifications. On the other hand, engineered proteins with RNA binding factors such as Pumilio and FBF (Wang, M et al. 2018) or Pentatricopeptide repeat (Manna 2015) and an effector module of choice enable binding and more flexible manipulations to RNA targets. Generating these proteins however is generally laborious and also limited by the presence of binding motifs on

target RNA. The flexibility and programmability of RNA-guided RNA-binding proteins offer superior solution over both RNA-based techniques and conventional RNA binding motifs in efficient searching and modifying of RNA. Clustered Regularly Interspaced Short Palindromic Repeats (CRISPR) together with CRISPR-associated (Cas) protein 13 (CRISPR-Cas13) is one such system that has revolutionized RNA research since its recent discovery (Abudayyeh, Omar O. et al. 2016). Either it is utilizing new promising systems or expanding the limited use of a less-expected system, successful new ideas will benefit RNA studies as a whole.

Embracing the RNA wonder – Can a special RNA structure prevent RNA methylation?

Inhibition of gene expression by RNAi mechanism could be a result of either mRNA degradation or translation inhibition, depending on the degree of complementarity between the interfering RNAs (hereby referred to as iRNA) and targets (van den Berg, Mols & Han 2008). If mismatches occur, translation inhibition tends to be observed. The phenomenon was further linked to altered structural/functional conformation of translating ribosomes binding to iRNA-bound mRNA (Ma, X et al. 2013).

It is interesting that the negative regulatory effect of iRNA on mRNA can be reversed by upstream negative regulators Target Mimics (TM) and Short Tandem Target Mimic (STTM) (Figure I-3). TM was adopted from the naturally occurring phenomenon in plant in which a non-coding RNA *INDUCED BY PHOSPHATE STARVATION 1 (IPS1)* mimicking the mRNA target *PHOSPHATE 2 (PHO2)* of the microRNA miR399 can prevent the degradation of *PHO2* (Franco-Zorrilla et al. 2007). It was hypothesized that *IPS1* (TM) competes with mRNA target for binding to microRNA, thus protects the mRNA from RNA-induced silencing. TM binds to microRNA imperfectly, with a 3-nt bulge between nucleotide 10 and 11 of microRNA and additional single-nt mismatches (Figure I-3). Despite the plausible assumption that the TM-microRNA duplex can get cleaved by the RNA-induced silencing complex, the abundance of neither of the entities is affected upon binding, pointing towards rather an underlying mechanism of RNA sequestration (Franco-Zorrilla et al. 2007).

works an order of magnitude more effectively than TM in blocking the function of microRNAs. Surprisingly, in contrast to TM, STTM triggers drastic reduction of microRNA targets, partially via small RNA degrading nucleases (Yan et al. 2012). The significantly enhancement in the performance of STTM compared to TM is deemed to the loosely self-complementary linker that helps stabilize the STTM structure while not being attacked by components of RNA-induced Silencing Complex (Tang, Guiliang & Tang 2013).

Collectively from these studies, I asked the question whether a similar structure to TM or STTM can bind to mRNA in a similar manner to iRNAs and sequester the binding site or alter binding proteins in such a way that these proteins fail to confer its impact to the site or proximal regions. Such a system can interfere with deposition of RNA modification, revealing the importance of the modified site in its absence.

CRISPR-Cas13 for active alterations of RNA modifications

CRISPR-Cas (Clustered Regularly Interspaced Short Palindromic Repeats – CRISPR associated protein) is naturally a defense system in prokaryotes, which has inspired an exceptional generation of genome engineering tools. The detection, elucidation and adoption of CRISPR-Cas have spanned several decades since the presence of short direct repeats interspersing varied sequences in bacterial genomes was first reported in 1987 (Ishino et al. 1987). It is now relatively well-understood that the interspacing sequences (spacers) are derived from foreign genetic materials and that CRISPR-Cas is an adaptive immune mechanism utilizing these spacers as the guides for its action. Essentially, immune response by CRISPR-Cas takes three main steps: (i) insertion of foreign DNA into between two direct repeats of a special past-invasion storage genomic region known as CRISPR array, (ii) transcription of CRISPR array into single precursor CRISPR mRNA (pre-crRNAs) which is then processed into individual mature CRISPR RNAs (crRNAs), or usually referred to as guide RNAs (gRNAs), and (iii) Cas-induced cleavage of foreign nucleic acid bound by a gRNA. The mode of action of CRISPR-Cas provides excellent specificity and programmability required for a pair of molecular scissors with slight engineering (Cong et al. 2013; Jinek et al. 2012). In addition, the ability to separate the cleaving activity of most CRISPR-Cas systems from their binding activity allows utilization of catalytically inactivated

CRISPR-dCas as nucleic acid binding platforms, vastly expanding the manipulations that could be performed on target.

Amongst CRISPR-Cas systems, CRISPR-Cas13 is a natural and exclusive RNA-guided RNA-targeting platform. Its endoribonuclease activity has been harnessed for multiple applications ranging from specific knockdown of RNA targets to programmable cell death due to promiscuous degradation of cellular RNAs (Abudayyeh, Omar O. et al. 2017; Wang, Q et al. 2019) (Figure I-4A). Meanwhile, mutations of single or multiple catalytic residues in either of the two endoribonuclease HEPN (higher eukaryotes and prokaryotes nucleotide-binding) domains on Cas13s abolished their cleaving activity while retaining their high affinity to target (Abudayyeh, Omar O. et al. 2016; Konermann et al. 2018; Smargon et al. 2017). These catalytically dead Cas13s (dCas13s) became a competitive RNA binding platform and can provide utilities on their own (Figure I-4B) or be tethered to customizable effector domains to confer new applications (Figure I-4C).

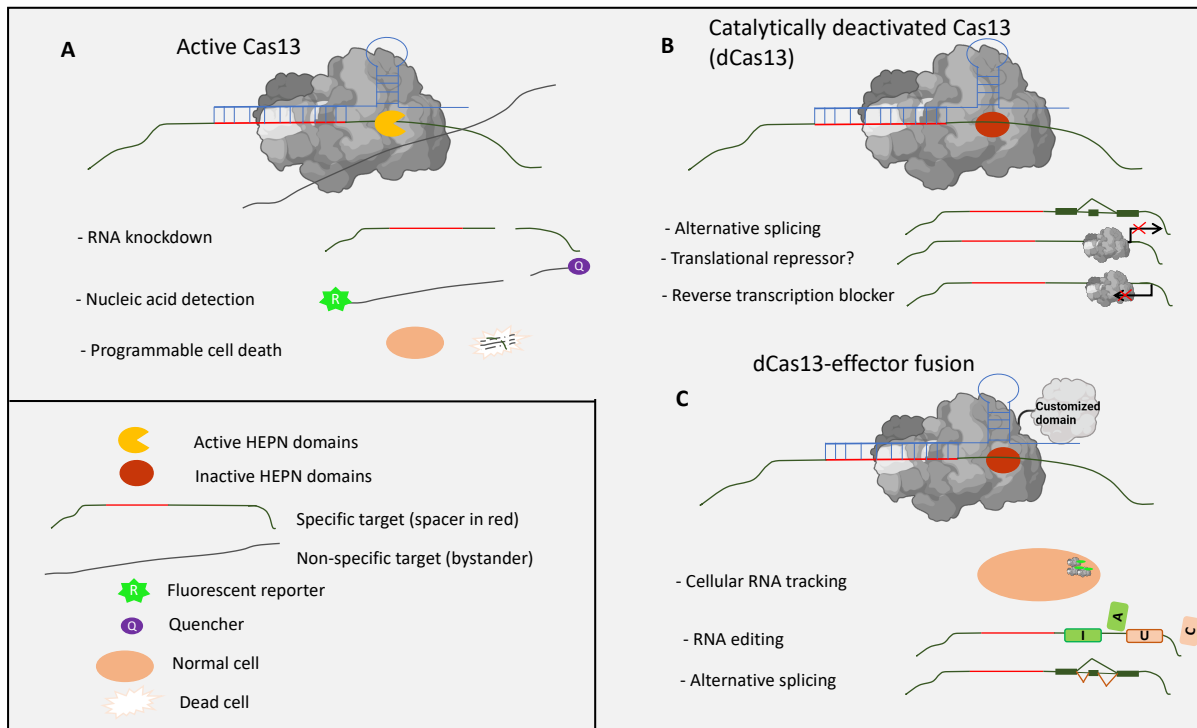


Figure I-4: Applications of active CRISPR-Cas13 and derivatives. A, Important applications of active Cas13 include targeting for cleaving of various RNA species such as mRNA, circular RNA, and long-noncoding RNA (i); in vitro detection of nucleic acid based on promiscuous activity of Cas13 which cleaves quencher off a fluorescent reporter upon binding specific target (ii); and programmable cell death triggered by promiscuous degradation of cellular RNAs (iii). B, A catalytically inactive Cas13 system (dCas13) can be used to regulate exon exclusion, block in vitro reverse transcription and, potentially, translation thanks to specific binding of the system to different locations on RNA transcripts. C, dCas13 can be tethered with an effector domain of choice to enable cellular tracking of specific RNAs, RNA modifications such as A-to-I and C-to-U editing, and more alternative splicing activities such as exon inclusion.

dCas13-effector fusions were successfully applied to RNA tracking, identifying of RNA interacting partners and RNA targeted manipulations. Han et al. (2020) developed a dCas13-APEX system which specifically binds to RNA and biotinylates interacting

proteins which then can be pulled down and identified by mass spectrometry. With this system, the authors demonstrated a functional interaction between the human m⁶A demethylase ALKBH5 and telomerase. Tethering dCas13 with RNA deaminase ADAR2 enabled A to I and C to U editing in mammalian RNA, in the systems named as REPAIR (RNA Editing for Programmable A to I Replacement) and RESCUE (RNA Editing for Specific C-to-U Exchange), respectively (Abudayyeh, O. O. et al. 2019; Cox et al. 2017). Targeted RNA m⁶A methylation (TRM) was the first tool based on dCas13 developed to aid functional studies of RNA m⁶A methylation. Wilson et al. (2020) showed that fusion of dCas13 and m⁶A methyltransferase METTL3/METTL14 enabled targeted RNA m⁶A methylation in bacterial and mammalian cells. Compared to a similar system using modified RNA-guided DNA endonuclease Cas9 (Liu, X-M et al. 2019), TRM editor with METTL3 showed similar efficiency with considerably higher specificity and simpler programmability. Similar systems with dCas13 from different bacterial species fused to ALKBH5 have also been developed, enabling targeted m⁶A demethylation in human cell lines (Li, Jiexin et al. 2020; Xia et al. 2021). Together, these examples highlight the potential of using dCas13-based systems in uncovering different aspects of RNA modifications. It could be expected that fusing dCas13 with other RNA modifying domains will allow expanded manipulations such as changing the effects of RNA modifications through “reader” domains, or installation/removal of other RNA modifications. It is also not known if the binding of dCas13 itself to RNA sequences would interfere with endogenous RNA methylation machinery and functionality. Such effect might result in disturbed methylation status and allow study of their function.

Summary

RNA modifications have emerged as non-random and critical alterations to RNA that ensure normal plant and animal development. However, their regulatory role, as of an “epitranscriptome”, is currently not clear. Functional studies of RNA modifications are lagging far behind the remarkable number of modified sites mapped transcriptome-wide. Site-specific studies of RNA modifications’ function, and tools to manipulate modified sites with high precision are needed. Meanwhile, the chemistry and available resources make m⁵C and m⁶A two exceptional models to uncover the functional landscape of RNA modifications in greater detail. In the following chapters, I describe the development of synthetic tools aimed for targeted demethylation of RNA m⁵C and m⁶A in plants, as well as substantial effort in deciphering the role of m⁵C in *A. thaliana*’s root development in a site-specific manner. In particular, three research chapters are presented before a general discussion chapter:

Chapter II: Towards targeted RNA N6-methyladenosine demethylation in plants

Chapter III: Towards targeted RNA 5-methylcytosine demethylation in plants

Chapter IV: Deciphering RNA 5-methylcytosine in *Arabidopsis thaliana*’s root development

References

Abudayyeh, OO, Gootenberg, JS, Essletzbichler, P, Han, S, Joung, J, Belanto, JJ, Verdine, V, Cox, DBT, Kellner, MJ, Regev, A, Lander, ES, Voytas, DF, Ting, AY & Zhang, F 2017, 'RNA targeting with CRISPR–Cas13', *Nature*, vol. 550, no. 7675, 2017/10/01, pp. 280-284.

Abudayyeh, OO, Gootenberg, JS, Franklin, B, Koob, J, Kellner, MJ, Ladha, A, Joung, J, Kirchgatterer, P, Cox, DBT & Zhang, F 2019, 'A cytosine deaminase for programmable single-base RNA editing', *Science*, vol. 365, no. 6451, Jul 26, pp. 382-386.

Abudayyeh, OO, Gootenberg, JS, Konermann, S, Joung, J, Slaymaker, IM, Cox, DBT, Shmakov, S, Makarova, KS, Semenova, E, Minakhin, L, Severinov, K, Regev, A, Lander, ES, Koonin, EV & Zhang, F 2016, 'C2c2 is a single-component programmable RNA-guided RNA-targeting CRISPR effector', *Science*, vol. 353, no. 6299, p. aaf5573.

Amort, T, Soulière, MF, Wille, A, Jia, X-Y, Fiegl, H, Wörle, H, Micura, R & Lusser, A 2013, 'Long non-coding RNAs as targets for cytosine methylation', *RNA Biology*, vol. 10, no. 6, 2013/06/01, pp. 1002-1008.

Arribas-Hernández, L, Simonini, S, Hansen, MH, Paredes, EB, Bressendorff, S, Dong, Y, Østergaard, L & Brodersen, P 2020, 'Recurrent requirement for the m(6)A-ECT2/ECT3/ECT4 axis in the control of cell proliferation during plant organogenesis', *Development*, vol. 147, no. 14, Jul 24.

Begik, O, Lucas, MC, Prysycz, LP, Ramirez, JM, Medina, R, Milenkovic, I, Cruciani, S, Liu, H, Vieira, HGS, Sas-Chen, A, Mattick, JS, Schwartz, S & Novoa, EM 2021, 'Quantitative profiling of native RNA modifications and their dynamics using nanopore sequencing', *bioRxiv*, p. 2020.2007.2006.189969.

Blanco, S, Dietmann, S, Flores, JV, Hussain, S, Kutter, C, Humphreys, P, Lukk, M, Lombard, P, Treps, L, Popis, M, Kellner, S, Hölter, SM, Garrett, L, Wurst, W, Becker, L, Klopstock, T, Fuchs, H, Gailus-Durner, V, Hrabě de Angelis, M, Káradóttir, RT, Helm, M, Ule, J, Gleeson, JG, Odom, DT & Frye, M 2014, 'Aberrant methylation of tRNAs links cellular stress to neuro-developmental disorders', *Embo j*, vol. 33, no. 18, Sep 17, pp. 2020-2039.

Blanco, S, Kurowski, A, Nichols, J, Watt, FM, Benitah, SA & Frye, M 2011, 'The RNA–Methyltransferase Misu (NSun2) Poises Epidermal Stem Cells to Differentiate', *PLOS Genetics*, vol. 7, no. 12, p. e1002403.

Bohnsack, MT & Sloan, KE 2018, 'Modifications in small nuclear RNAs and their roles in spliceosome assembly and function', *Biol Chem*, vol. 399, no. 11, Oct 25, pp. 1265-1276.

Bokar, JA, Rath-Shambaugh, ME, Ludwiczak, R, Narayan, P & Rottman, F 1994, 'Characterization and partial purification of mRNA N6-adenosine methyltransferase from HeLa cell nuclei. Internal mRNA methylation requires a multisubunit complex', *J Biol Chem*, vol. 269, no. 26, Jul 1, pp. 17697-17704.

Bujnicki, JM, Feder, M, Radlinska, M & Blumenthal, RM 2002, 'Structure prediction and phylogenetic analysis of a functionally diverse family of proteins homologous to the MT-A70 subunit of the human mRNA:m(6)A methyltransferase', *J Mol Evol*, vol. 55, no. 4, Oct, pp. 431-444.

Caplen, NJ, Parrish, S, Imani, F, Fire, A & Morgan, RA 2001, 'Specific inhibition of gene expression by small double-stranded RNAs in invertebrate and vertebrate systems', *Proc Natl Acad Sci U S A*, vol. 98, no. 17, Aug 14, pp. 9742-9747.

Carlile, TM, Rojas-Duran, MF, Zinshteyn, B, Shin, H, Bartoli, KM & Gilbert, WV 2014, 'Pseudouridine profiling reveals regulated mRNA pseudouridylation in yeast and human cells', *Nature*, vol. 515, no. 7525, Nov 6, pp. 143-146.

Chen, K, Lu, Z, Wang, X, Fu, Y, Luo, G-Z, Liu, N, Han, D, Dominissini, D, Dai, Q, Pan, T & He, C 2015, 'High-Resolution N6-Methyladenosine (m⁶A) Map Using Photo-Crosslinking-Assisted m⁶A Sequencing', *Angewandte Chemie International Edition*, vol. 54, no. 5, pp. 1587-1590.

Chen, T, Hao, Y-J, Zhang, Y, Li, M-M, Wang, M, Han, W, Wu, Y, Lv, Y, Hao, J, Wang, L, Li, A, Yang, Y, Jin, K-X, Zhao, X, Li, Y, Ping, X-L, Lai, W-Y, Wu, L-G, Jiang, G, Wang, H-L, Sang, L, Wang, X-J, Yang, Y-G & Zhou, Q 2015, 'm⁶A RNA Methylation Is Regulated by MicroRNAs and Promotes Reprogramming to Pluripotency', *Cell Stem Cell*, vol. 16, no. 3, pp. 289-301.

Cohn, WE 1960, 'Pseudouridine, a Carbon-Carbon Linked Ribonucleoside in Ribonucleic Acids: Isolation, Structure, and Chemical Characteristics', *Journal of Biological Chemistry*, vol. 235, no. 5, 1960/05/01/, pp. 1488-1498.

Cohn, WE & Volkin, E 1951, 'Nucleoside-5'-Phosphates from Ribonucleic Acid', *Nature*, vol. 167, no. 4247, 1951/03/01, pp. 483-484.

Cong, L, Ran, FA, Cox, D, Lin, S, Barretto, R, Habib, N, Hsu, PD, Wu, X, Jiang, W, Marraffini, LA & Zhang, F 2013, 'Multiplex genome engineering using CRISPR/Cas systems', *Science*, vol. 339, no. 6121, Feb 15, pp. 819-823.

Cox, DBT, Gootenberg, JS, Abudayyeh, OO, Franklin, B, Kellner, MJ, Joung, J & Zhang, F 2017, 'RNA editing with CRISPR-Cas13', *Science*, vol. 358, no. 6366, Nov 24, pp. 1019-1027.

Cui, X, Liang, Z, Shen, L, Zhang, Q, Bao, S, Geng, Y, Zhang, B, Leo, V, Vardy, LA, Lu, T, Gu, X & Yu, H 2017, '5-Methylcytosine RNA Methylation in *Arabidopsis Thaliana*', *Molecular Plant*, vol. 10, no. 11, pp. 1387-1399.

David, R, Burgess, A, Parker, B, Li, J, Pulsford, K, Sibbritt, T, Preiss, T & Searle, IR 2017, 'Transcriptome-Wide Mapping of RNA 5-Methylcytosine in *Arabidopsis* mRNAs and Noncoding RNAs', *Plant Cell*, vol. 29, no. 3, Mar, pp. 445-460.

Delatte, B, Wang, F, Ngoc, LV, Collignon, E, Bonvin, E, Deplus, R, Calonne, E, Hassabi, B, Putmans, P, Awe, S, Wetzel, C, Kreher, J, Soin, R, Creppe, C, Limbach, PA, Gueydan, C, Kruys, V, Brehm, A, Minakhina, S, Defrance, M, Steward, R & Fuks, F 2016, 'RNA biochemistry. Transcriptome-wide distribution and function of RNA hydroxymethylcytosine', *Science*, vol. 351, no. 6270, Jan 15, pp. 282-285.

Delatte, B, Wang, F, Ngoc, LV, Collignon, E, Bonvin, E, Deplus, R, Calonne, E, Hassabi, B, Putmans, P, Awe, S, Wetzel, C, Kreher, J, Soin, R, Creppe, C, Limbach, PA, Gueydan, C, Kruys, V, Brehm, A, Minakhina, S, Defrance, M, Steward, R & Fuks, F 2016, 'Transcriptome-wide distribution and function of RNA hydroxymethylcytosine', *Science*, vol. 351, no. 6270, pp. 282-285.

Desrosiers, R, Friderici, K & Rottman, F 1974, 'Identification of Methylated Nucleosides in Messenger RNA from Novikoff Hepatoma Cells', *Proceedings of the National Academy of Sciences*, vol. 71, no. 10, p. 3971.

Dominissini, D, Moshitch-Moshkovitz, S, Schwartz, S, Salmon-Divon, M, Ungar, L, Osenberg, S, Cesarkas, K, Jacob-Hirsch, J, Amariglio, N, Kupiec, M, Sorek, R & Rechavi, G 2012, 'Topology of the human and mouse m⁶A RNA methylomes revealed by m⁶A-seq', *Nature*, vol. 485, no. 7397, Apr 29, pp. 201-206.

Dominissini, D, Nachtergaele, S, Moshitch-Moshkovitz, S, Peer, E, Kol, N, Ben-Haim, MS, Dai, Q, Di Segni, A, Salmon-Divon, M, Clark, WC, Zheng, G, Pan, T, Solomon, O, Eyal, E, Hershkovitz, V, Han, D, Doré, LC, Amariglio, N, Rechavi, G & He, C 2016, 'The dynamic N(1)-methyladenosine methylome in eukaryotic messenger RNA', *Nature*, vol. 530, no. 7591, Feb 25, pp. 441-446.

Duan, H-C, Wei, L-H, Zhang, C, Wang, Y, Chen, L, Lu, Z, Chen, PR, He, C & Jia, G 2017, 'ALKBH10B Is an RNA N⁶-Methyladenosine Demethylase Affecting *Arabidopsis* Floral Transition', *The Plant Cell*, vol. 29, no. 12, pp. 2995-3011.

Dubin, DT & Taylor, RH 1975, 'The methylation state of poly A-containing messenger RNA from cultured hamster cells', *Nucleic Acids Res*, vol. 2, no. 10, Oct, pp. 1653-1668.

Dunn, DB 1961, 'The occurrence of 1-methyladenine in ribonucleic acid', *Biochimica et biophysica acta*, vol. 46, no. 1, 1961/01/01/, pp. 198-200.

Ebhardt, HA, Tsang, HH, Dai, DC, Liu, Y, Bostan, B & Fahlman, RP 2009, 'Meta-analysis of small RNA-sequencing errors reveals ubiquitous post-transcriptional RNA modifications', *Nucleic Acids Res*, vol. 37, no. 8, May, pp. 2461-2470.

Edelheit, S, Schwartz, S, Mumbach, MR, Wurtzel, O & Sorek, R 2013, 'Transcriptome-wide mapping of 5-methylcytidine RNA modifications in bacteria, archaea, and yeast reveals m⁵C within archaeal mRNAs', *PLoS Genet*, vol. 9, no. 6, Jun, p. e1003602.

Elbashir, SM, Harborth, J, Lendeckel, W, Yalcin, A, Weber, K & Tuschl, T 2001, 'Duplexes of 21-nucleotide RNAs mediate RNA interference in cultured mammalian cells', *Nature*, vol. 411, no. 6836, May 24, pp. 494-498.

Fahiminiya, S, Almuriekhi, M, Nawaz, Z, Staffa, A, Lepage, P, Ali, R, Hashim, L, Schwartzentruber, J, Abu Khadija, K, Zaineddin, S, Gamal, H, Majewski, J & Ben-Omran, T 2014, 'Whole exome sequencing unravels disease-causing genes in consanguineous families in Qatar', *Clinical Genetics*, vol. 86, no. 2, pp. 134-141.

Flaherty, SM, Fortes, P, Izaurralde, E, Mattaj, JW & Gilmartin, GM 1997, 'Participation of the nuclear cap binding complex in pre-mRNA 3' processing', *Proc Natl Acad Sci U S A*, vol. 94, no. 22, Oct 28, pp. 11893-11898.

Franco-Zorrilla, JM, Valli, A, Todesco, M, Mateos, I, Puga, MI, Rubio-Somoza, I, Leyva, A, Weigel, D, García, JA & Paz-Ares, J 2007, 'Target mimicry provides a new mechanism for regulation of microRNA activity', *Nature Genetics*, vol. 39, no. 8, 2007/08/01, pp. 1033-1037.

Fu, L, Guerrero, CR, Zhong, N, Amato, NJ, Liu, Y, Liu, S, Cai, Q, Ji, D, Jin, S-G, Niedernhofer, LJ, Pfeifer, GP, Xu, G-L & Wang, Y 2014, 'Tet-Mediated Formation of 5-Hydroxymethylcytosine in RNA', *Journal of the American Chemical Society*, vol. 136, no. 33, 2014/08/20, pp. 11582-11585.

Furuichi, Y, LaFiandra, A & Shatkin, AJ 1977, '5'-Terminal structure and mRNA stability', *Nature*, vol. 266, no. 5599, Mar 17, pp. 235-239.

Gallie, DR 1991, 'The cap and poly(A) tail function synergistically to regulate mRNA translational efficiency', *Genes Dev*, vol. 5, no. 11, Nov, pp. 2108-2116.

Gao, Y, Vasic, R, Song, Y, Teng, R, Liu, C, Gbyli, R, Biancon, G, Nelakanti, R, Lobben, K, Kudo, E, Liu, W, Ardasheva, A, Fu, X, Wang, X, Joshi, P, Lee, V, Dura, B, Viero, G, Iwasaki, A, Fan, R, Xiao, A, Flavell, RA, Li, H-B, Tebaldi, T & Halene, S 2020, 'm⁶A Modification Prevents Formation of Endogenous Double-Stranded

RNAs and Deleterious Innate Immune Responses during Hematopoietic Development', *Immunity*, vol. 52, no. 6, pp. 1007-1021.e1008.

Garcia-Campos, MA, Edelheit, S, Toth, U, Safra, M, Shachar, R, Viukov, S, Winkler, R, Nir, R, Lasman, L, Brandis, A, Hanna, JH, Rossmanith, W & Schwartz, S 2019, 'Deciphering the "m⁶A Code" via Antibody-Independent Quantitative Profiling', *Cell*, vol. 178, no. 3, 2019/07/25/, pp. 731-747.e716.

Goll, MG, Kirpekar, F, Maggert, KA, Yoder, JA, Hsieh, C-L, Zhang, X, Golic, KG, Jacobsen, SE & Bestor, TH 2006, 'Methylation of tRNA^{Asp} by the DNA Methyltransferase Homolog Dnmt2', *Science*, vol. 311, no. 5759, pp. 395-398.

Han, S, Zhao, BS, Myers, SA, Carr, SA, He, C & Ting, AY 2020, 'RNA–protein interaction mapping via MS2- or Cas13-based APEX targeting', *Proceedings of the National Academy of Sciences*, vol. 117, no. 36, p. 22068.

He, C 2010, 'Grand challenge commentary: RNA epigenetics?', *Nat Chem Biol*, vol. 6, no. 12, Dec, pp. 863-865.

Helm, M & Motorin, Y 2017, 'Detecting RNA modifications in the epitranscriptome: predict and validate', *Nature Reviews Genetics*, vol. 18, no. 5, 2017/05/01, pp. 275-291.

Holley, RW, Everett, GA, Madison, JT & Zamir, A 1965, 'NUCLEOTIDE SEQUENCES IN THE YEAST ALANINE TRANSFER RIBONUCLEIC ACID', *J Biol Chem*, vol. 240, May, pp. 2122-2128.

Huang, H, Weng, H, Sun, W, Qin, X, Shi, H, Wu, H, Zhao, BS, Mesquita, A, Liu, C, Yuan, CL, Hu, Y-C, Hüttelmaier, S, Skibbe, JR, Su, R, Deng, X, Dong, L, Sun, M, Li, C, Nachtergaele, S, Wang, Y, Hu, C, Ferchen, K, Greis, KD, Jiang, X, Wei, M, Qu, L, Guan, J-L, He, C, Yang, J & Chen, J 2018, 'Recognition of RNA N(6)-methyladenosine by IGF2BP proteins enhances mRNA stability and translation', *Nature cell biology*, vol. 20, no. 3, pp. 285-295.

Huang, T, Chen, W, Liu, J, Gu, N & Zhang, R 2019, 'Genome-wide identification of mRNA 5-methylcytosine in mammals', *Nature Structural & Molecular Biology*, vol. 26, no. 5, 2019/05/01, pp. 380-388.

Huong, TT, Ngoc, LNT & Kang, H 2020, 'Functional Characterization of a Putative RNA Demethylase ALKBH6 in Arabidopsis Growth and Abiotic Stress Responses', *International journal of molecular sciences*, vol. 21, no. 18, p. 6707.

Hussain, S, Sajini, AA, Blanco, S, Dietmann, S, Lombard, P, Sugimoto, Y, Paramor, M, Gleeson, JG, Odom, DT, Ule, J & Frye, M 2013, 'NSun2-mediated cytosine-5

methylation of vault noncoding RNA determines its processing into regulatory small RNAs', *Cell Rep*, vol. 4, no. 2, Jul 25, pp. 255-261.

Ishino, Y, Shinagawa, H, Makino, K, Amemura, M & Nakata, A 1987, 'Nucleotide sequence of the *iap* gene, responsible for alkaline phosphatase isozyme conversion in *Escherichia coli*, and identification of the gene product', *Journal of bacteriology*, vol. 169, no. 12, pp. 5429-5433.

Ivashuta, S, Banks, IR, Wiggins, BE, Zhang, Y, Ziegler, TE, Roberts, JK & Heck, GR 2011, 'Regulation of gene expression in plants through miRNA inactivation', *PLOS ONE*, vol. 6, no. 6, p. e21330.

Izaurralde, E, Lewis, J, McGuigan, C, Jankowska, M, Darzynkiewicz, E & Mattaj, JW 1994, 'A nuclear cap binding protein complex involved in pre-mRNA splicing', *Cell*, vol. 78, no. 4, Aug 26, pp. 657-668.

Jackman, JE & Alfonzo, JD 2013, 'Transfer RNA modifications: nature's combinatorial chemistry playground', *Wiley Interdiscip Rev RNA*, vol. 4, no. 1, Jan-Feb, pp. 35-48.

Jia, G, Fu, Y, Zhao, X, Dai, Q, Zheng, G, Yang, Y, Yi, C, Lindahl, T, Pan, T, Yang, YG & He, C 2011, 'N⁶-methyladenosine in nuclear RNA is a major substrate of the obesity-associated FTO', *Nat Chem Biol*, vol. 7, no. 12, Oct 16, pp. 885-887.

Jinek, M, Chylinski, K, Fonfara, I, Hauer, M, Doudna, JA & Charpentier, E 2012, 'A programmable dual-RNA-guided DNA endonuclease in adaptive bacterial immunity', *Science*, vol. 337, no. 6096, Aug 17, pp. 816-821.

Khoddami, V & Cairns, BR 2013, 'Identification of direct targets and modified bases of RNA cytosine methyltransferases', *Nature Biotechnology*, vol. 31, no. 5, 2013/05/01, pp. 458-464.

Khoddami, V & Cairns, BR 2014, 'Transcriptome-wide target profiling of RNA cytosine methyltransferases using the mechanism-based enrichment procedure Aza-IP', *Nature Protocols*, vol. 9, no. 2, 2014/02/01, pp. 337-361.

Knuckles, P, Lence, T, Haussmann, IU, Jacob, D, Kreim, N, Carl, SH, Masiello, I, Hares, T, Villaseñor, R, Hess, D, Andrade-Navarro, MA, Biggiogera, M, Helm, M, Soller, M, Bühler, M & Roignant, JY 2018, 'Zc3h13/Flacc is required for adenosine methylation by bridging the mRNA-binding factor Rbm15/Spenito to the m(6)A machinery component Wtap/FI(2)d', *Genes Dev*, vol. 32, no. 5-6, Mar 1, pp. 415-429.

Lavi, U, Fernandez-Mufioz, R & Darnell, JE, Jr. 1977, 'Content of N-6 methyl adenylic acid in heterogeneous nuclear and messenger RNA of HeLa cells', *Nucleic Acids Research*, vol. 4, no. 1, pp. 63-69.

Legrand, C, Tuorto, F, Hartmann, M, Liebers, R, Jacob, D, Helm, M & Lyko, F 2017, 'Statistically robust methylation calling for whole-transcriptome bisulfite sequencing reveals distinct methylation patterns for mouse RNAs', *Genome research*, vol. 27, no. 9, pp. 1589-1596.

Li, J, Chen, Z, Chen, F, Xie, G, Ling, Y, Peng, Y, Lin, Y, Luo, N, Chiang, C-M & Wang, H 2020, 'Targeted mRNA demethylation using an engineered dCas13b-ALKBH5 fusion protein', *Nucleic Acids Research*, vol. 48, no. 10, pp. 5684-5694.

Li, Q, Li, X, Tang, H, Jiang, B, Dou, Y, Gorospe, M & Wang, W 2017, 'NSUN2-Mediated m⁵C Methylation and METTL3/METTL14-Mediated m⁶A Methylation Cooperatively Enhance p21 Translation', *Journal of Cellular Biochemistry*, vol. 118, no. 9, pp. 2587-2598.

Li, S & Mason, CE 2014, 'The pivotal regulatory landscape of RNA modifications', *Annu Rev Genomics Hum Genet*, vol. 15, pp. 127-150.

Li, X, Xiong, X, Wang, K, Wang, L, Shu, X, Ma, S & Yi, C 2016, 'Transcriptome-wide mapping reveals reversible and dynamic N1-methyladenosine methylome', *Nature Chemical Biology*, vol. 12, no. 5, 2016/05/01, pp. 311-316.

Li, Y, Wang, X, Li, C, Hu, S, Yu, J & Song, S 2014, 'Transcriptome-wide N6-methyladenosine profiling of rice callus and leaf reveals the presence of tissue-specific competitors involved in selective mRNA modification', *RNA Biology*, vol. 11, no. 9, 2014/09/02, pp. 1180-1188.

Linder, B, Grozhik, AV, Olarerin-George, AO, Meydan, C, Mason, CE & Jaffrey, SR 2015, 'Single-nucleotide-resolution mapping of m⁶A and m⁶Am throughout the transcriptome', *Nat Methods*, vol. 12, no. 8, Aug, pp. 767-772.

Liu, F, Clark, W, Luo, G, Wang, X, Fu, Y, Wei, J, Wang, X, Hao, Z, Dai, Q, Zheng, G, Ma, H, Han, D, Evans, M, Klungland, A, Pan, T & He, C 2016, 'ALKBH1-Mediated tRNA Demethylation Regulates Translation', *Cell*, vol. 167, no. 7, Dec 15, p. 1897.

Liu, H, Begik, O, Lucas, MC, Ramirez, JM, Mason, CE, Wiener, D, Schwartz, S, Mattick, JS, Smith, MA & Novoa, EM 2019, 'Accurate detection of m⁶A RNA modifications in native RNA sequences', *Nature Communications*, vol. 10, no. 1, 2019/09/09, p. 4079.

Liu, J, Yue, Y, Han, D, Wang, X, Fu, Y, Zhang, L, Jia, G, Yu, M, Lu, Z, Deng, X, Dai, Q, Chen, W & He, C 2014, 'A METTL3-METTL14 complex mediates mammalian nuclear RNA N6-adenosine methylation', *Nat Chem Biol*, vol. 10, no. 2, Feb, pp. 93-95.

Liu, N, Dai, Q, Zheng, G, He, C, Parisien, M & Pan, T 2015, 'N(6)-methyladenosine-dependent RNA structural switches regulate RNA-protein interactions', *Nature*, vol. 518, no. 7540, Feb 26, pp. 560-564.

Liu, N, Parisien, M, Dai, Q, Zheng, G, He, C & Pan, T 2013, 'Probing N6-methyladenosine RNA modification status at single nucleotide resolution in mRNA and long noncoding RNA', *RNA (New York, N.Y.)*, vol. 19, no. 12, pp. 1848-1856.

Liu, N, Zhou, KI, Parisien, M, Dai, Q, Diatchenko, L & Pan, T 2017, 'N6-methyladenosine alters RNA structure to regulate binding of a low-complexity protein', *Nucleic Acids Res*, vol. 45, no. 10, Jun 2, pp. 6051-6063.

Liu, X-M, Zhou, J, Mao, Y, Ji, Q & Qian, S-B 2019, 'Programmable RNA N6-methyladenosine editing by CRISPR-Cas9 conjugates', *Nature Chemical Biology*, vol. 15, no. 9, 2019/09/01, pp. 865-871.

Lorenz, DA, Sathe, S, Einstein, JM & Yeo, GW 2020, 'Direct RNA sequencing enables m(6)A detection in endogenous transcript isoforms at base-specific resolution', *RNA (New York, N.Y.)*, vol. 26, no. 1, pp. 19-28.

Luo, G-Z, MacQueen, A, Zheng, G, Duan, H, Dore, LC, Lu, Z, Liu, J, Chen, K, Jia, G, Bergelson, J & He, C 2014, 'Unique features of the m⁶A methylome in *Arabidopsis thaliana*', *Nature Communications*, vol. 5, no. 1, 2014/11/28, p. 5630.

Ma, J, Zhang, L, Chen, S & Liu, H 2021, 'A brief review of RNA modification related database resources', *Methods*, 2021/03/08/.

Ma, X, Kim, E-J, Kook, I, Ma, F, Voshall, A, Moriyama, E & Cerutti, H 2013, 'Small interfering RNA-mediated translation repression alters ribosome sensitivity to inhibition by cycloheximide in *Chlamydomonas reinhardtii*', *The Plant Cell*, vol. 25, no. 3, pp. 985-998.

Manna, S 2015, 'An overview of pentatricopeptide repeat proteins and their applications', *Biochimie*, vol. 113, 2015/06/01/, pp. 93-99.

Martínez-Pérez, M, Aparicio, F, López-Gresa, MP, Bellés, JM, Sánchez-Navarro, JA & Pallás, V 2017, 'Arabidopsis m⁶A demethylase activity modulates viral infection of a plant virus and the m⁶A abundance in its genomic RNAs', *Proceedings of the National Academy of Sciences*, vol. 114, no. 40, p. 10755.

Mauer, J, Luo, X, Blanjoie, A, Jiao, X, Grozhik, AV, Patil, DP, Linder, B, Pickering, BF, Vasseur, J-J, Chen, Q, Gross, SS, Elemento, O, Debart, F, Kiledjian, M & Jaffrey, SR

2017, 'Reversible methylation of m⁶Am in the 5' cap controls mRNA stability', *Nature*, vol. 541, no. 7637, 2017/01/01, pp. 371-375.

Mendel, M, Delaney, K, Pandey, RR, Chen, K-M, Wenda, JM, Vågbø, CB, Steiner, FA, Homolka, D & Pillai, RS 2021, 'Splice site m⁶A methylation prevents binding of U2AF35 to inhibit RNA splicing', *Cell*, vol. 184, no. 12, 2021/06/10/, pp. 3125-3142.e3125.

Meyer, KD 2019, 'DART-seq: an antibody-free method for global m⁶A detection', *Nature Methods*, vol. 16, no. 12, 2019/12/01, pp. 1275-1280.

Meyer, KD, Saletore, Y, Zumbo, P, Elemento, O, Mason, CE & Jaffrey, SR 2012, 'Comprehensive analysis of mRNA methylation reveals enrichment in 3' UTRs and near stop codons', *Cell*, vol. 149, no. 7, Jun 22, pp. 1635-1646.

Mielecki, D, Zugaj, DŁ, Muszewska, A, Piwowarski, J, Chojnacka, A, Mielecki, M, Nieminuszczy, J, Grynberg, M & Grzesiuk, E 2012, 'Novel AlkB Dioxygenases—Alternative Models for In Silico and In Vivo Studies', *PLOS ONE*, vol. 7, no. 1, p. e30588.

Militello, KT, Chen, LM, Ackerman, SE, Mandarano, AH & Valentine, EL 2014, 'A map of 5-methylcytosine residues in *Trypanosoma brucei* tRNA revealed by sodium bisulfite sequencing', *Molecular and Biochemical Parasitology*, vol. 193, no. 2, 2014/02/01/, pp. 122-126.

Parker, MT, Knop, K, Sherwood, AV, Schurch, NJ, Mackinnon, K, Gould, PD, Hall, AJW, Barton, GJ & Simpson, GG 2020, 'Nanopore direct RNA sequencing maps the complexity of *Arabidopsis* mRNA processing and m⁶A modification', *eLife*, vol. 9, 2020/01/14, p. e49658.

Perry, RP & Kelley, DE 1974, 'Existence of methylated messenger RNA in mouse L cells', *Cell*, vol. 1, no. 1, pp. 37-42.

Ping, XL, Sun, BF, Wang, L, Xiao, W, Yang, X, Wang, WJ, Adhikari, S, Shi, Y, Lv, Y, Chen, YS, Zhao, X, Li, A, Yang, Y, Dahal, U, Lou, XM, Liu, X, Huang, J, Yuan, WP, Zhu, XF, Cheng, T, Zhao, YL, Wang, X, Rendtlew Danielsen, JM, Liu, F & Yang, YG 2014, 'Mammalian WTAP is a regulatory subunit of the RNA N⁶-methyladenosine methyltransferase', *Cell Res*, vol. 24, no. 2, Feb, pp. 177-189.

Pratanwanich, PN, Yao, F, Chen, Y, Koh, CWQ, Wan, YK, Hendra, C, Poon, P, Goh, YT, Yap, PML, Chooi, JY, Chng, WJ, Ng, SB, Thiery, A, Goh, WSS & Göke, J 2021, 'Identification of differential RNA modifications from nanopore direct RNA sequencing with xPore', *Nature Biotechnology*, 2021/07/19.

Rottman, F, Narayan, P, Goodwin, R, Camper, S, Yao, Y, Horowitz, S, Albers, R, Ayers, D, Maroney, P & Nilsen, T 1986, 'Distribution of m⁶A in mRNA and its Possible Biological Role', in RT Borchardt, CR Creveling & PM Ueland (eds), *Biological Methylation and Drug Design: Experimental and Clinical Role of S-Adenosylmethionine*, Humana Press, Totowa, NJ, pp. 189-200.

Ruzicka, K, Zhang, M, Campilho, A, Bodi, Z, Kashif, M, Saleh, M, Eeckhout, D, El-Showk, S, Li, H, Zhong, S, De Jaeger, G, Mongan, NP, Hejatko, J, Helariutta, Y & Fray, RG 2017, 'Identification of factors required for m(6) A mRNA methylation in Arabidopsis reveals a role for the conserved E3 ubiquitin ligase HAKAI', *New Phytol*, vol. 215, no. 1, Jul, pp. 157-172.

Ryvkin, P, Leung, YY, Silverman, IM, Childress, M, Valladares, O, Dragomir, I, Gregory, BD & Wang, LS 2013, 'HAMR: high-throughput annotation of modified ribonucleotides', *Rna*, vol. 19, no. 12, Dec, pp. 1684-1692.

Schaefer, M, Pollex, T, Hanna, K & Lyko, F 2009, 'RNA cytosine methylation analysis by bisulfite sequencing', *Nucleic Acids Res*, vol. 37, no. 2, Feb, p. e12.

Schibler, U & Perry, RP 1977, 'The 5'-termini of heterogeneous nuclear RNA: a comparison among molecules of different sizes and ages', *Nucleic Acids Res*, vol. 4, no. 12, Dec, pp. 4133-4149.

Schwartz, S, Agarwala, SD, Mumbach, MR, Jovanovic, M, Mertins, P, Shishkin, A, Tabach, Y, Mikkelsen, TS, Satija, R, Ruvkun, G, Carr, SA, Lander, ES, Fink, GR & Regev, A 2013, 'High-resolution mapping reveals a conserved, widespread, dynamic mRNA methylation program in yeast meiosis', *Cell*, vol. 155, no. 6, Dec 5, pp. 1409-1421.

Schwartz, S, Mumbach, MR, Jovanovic, M, Wang, T, Maciag, K, Bushkin, GG, Mertins, P, Ter-Ovanesyan, D, Habib, N, Cacchiarelli, D, Sanjana, NE, Freinkman, E, Pacold, ME, Satija, R, Mikkelsen, TS, Hacohen, N, Zhang, F, Carr, SA, Lander, ES & Regev, A 2014, 'Perturbation of m⁶A writers reveals two distinct classes of mRNA methylation at internal and 5' sites', *Cell Rep*, vol. 8, no. 1, Jul 10, pp. 284-296.

Scutenaire, J, Deragon, JM, Jean, V, Benhamed, M, Raynaud, C, Favory, JJ, Merret, R & Bousquet-Antonelli, C 2018, 'The YTH Domain Protein ECT2 Is an m(6)A Reader Required for Normal Trichome Branching in Arabidopsis', *Plant Cell*, vol. 30, no. 5, May, pp. 986-1005.

Sednev, MV, Mykhailiuk, V, Choudhury, P, Halang, J, Sloan, KE, Bohnsack, MT & Höbartner, C 2018, 'N(6) -Methyladenosine-Sensitive RNA-Cleaving Deoxyribozymes', *Angew Chem Int Ed Engl*, vol. 57, no. 46, Nov 12, pp. 15117-15121.

Shatkin, AJ 1976, 'Capping of eucaryotic mRNAs', *Cell*, vol. 9, no. 4 pt 2, Dec, pp. 645-653.

Shen, Q, Zhang, Q, Shi, Y, Shi, Q, Jiang, Y, Gu, Y, Li, Z, Li, X, Zhao, K, Wang, C, Li, N & Cao, X 2018, 'Tet2 promotes pathogen infection-induced myelopoiesis through mRNA oxidation', *Nature*, vol. 554, no. 7690, 2018/02/01, pp. 123-127.

Shima, H, Matsumoto, M, Ishigami, Y, Ebina, M, Muto, A, Sato, Y, Kumagai, S, Ochiai, K, Suzuki, T & Igarashi, K 2017, 'S-Adenosylmethionine Synthesis Is Regulated by Selective N(6)-Adenosine Methylation and mRNA Degradation Involving METTL16 and YTHDC1', *Cell Rep*, vol. 21, no. 12, Dec 19, pp. 3354-3363.

Smemo, S, Tena, JJ, Kim, K-H, Gamazon, ER, Sakabe, NJ, Gómez-Marín, C, Aneas, I, Credidio, FL, Sobreira, DR, Wasserman, NF, Lee, JH, Puviindran, V, Tam, D, Shen, M, Son, JE, Vakili, NA, Sung, H-K, Naranjo, S, Acemel, RD, Manzanares, M, Nagy, A, Cox, NJ, Hui, C-C, Gomez-Skarmeta, JL & Nóbrega, MA 2014, 'Obesity-associated variants within FTO form long-range functional connections with IRX3', *Nature*, vol. 507, no. 7492, 2014/03/01, pp. 371-375.

Squires, JE, Patel, HR, Nusch, M, Sibbritt, T, Humphreys, DT, Parker, BJ, Suter, CM & Preiss, T 2012, 'Widespread occurrence of 5-methylcytosine in human coding and non-coding RNA', *Nucleic Acids Res*, vol. 40, no. 11, Jun, pp. 5023-5033.

Su, R, Dong, L, Li, C, Nachtergaele, S, Wunderlich, M, Qing, Y, Deng, X, Wang, Y, Weng, X, Hu, C, Yu, M, Skibbe, J, Dai, Q, Zou, D, Wu, T, Yu, K, Weng, H, Huang, H, Ferchen, K, Qin, X, Zhang, B, Qi, J, Sasaki, AT, Plas, DR, Bradner, JE, Wei, M, Marcucci, G, Jiang, X, Mulloy, JC, Jin, J, He, C & Chen, J 2018, 'R-2HG Exhibits Anti-tumor Activity by Targeting FTO/m⁶A/MYC/CEBPA Signaling', *Cell*, vol. 172, no. 1, pp. 90-105.e123.

Tang, G & Tang, X 2013, 'Short Tandem Target Mimic: A Long Journey to the Engineered Molecular Landmine for Selective Destruction/Blockage of MicroRNAs in Plants and Animals', *Journal of Genetics and Genomics*, vol. 40, no. 6, 2013/06/20/, pp. 291-296.

Tang, G, Yan, J, Gu, Y, Qiao, M, Fan, R, Mao, Y & Tang, X 2012, 'Construction of short tandem target mimic (STTM) to block the functions of plant and animal microRNAs', *Methods*, vol. 58, no. 2, Oct, pp. 118-125.

Todesco, M, Rubio-Somoza, I, Paz-Ares, J & Weigel, D 2010, 'A collection of target mimics for comprehensive analysis of microRNA function in *Arabidopsis thaliana*', *PLoS Genet*, vol. 6, no. 7, Jul 22, p. e1001031.

Tuorto, F, Liebers, R, Musch, T, Schaefer, M, Hofmann, S, Kellner, S, Frye, M, Helm, M, Stoecklin, G & Lyko, F 2012, 'RNA cytosine methylation by Dnmt2 and NSun2

promotes tRNA stability and protein synthesis', *Nature Structural & Molecular Biology*, vol. 19, no. 9, 2012/09/01, pp. 900-905.

van den Berg, A, Mols, J & Han, J 2008, 'RISC-target interaction: cleavage and translational suppression', *Biochimica et biophysica acta*, vol. 1779, no. 11, pp. 668-677.

Wan, Y, Tang, K, Zhang, D, Xie, S, Zhu, X, Wang, Z & Lang, Z 2015, 'Transcriptome-wide high-throughput deep m⁶A-seq reveals unique differential m⁶A methylation patterns between three organs in *Arabidopsis thaliana*', *Genome Biology*, vol. 16, no. 1, 2015/12/14, p. 272.

Wang, M, Ogé, L, Perez-Garcia, M-D, Hamama, L & Sakr, S 2018, 'The PUF Protein Family: Overview on PUF RNA Targets, Biological Functions, and Post Transcriptional Regulation', *International journal of molecular sciences*, vol. 19, no. 2, p. 410.

Wang, Q, Liu, X, Zhou, J, Yang, C, Wang, G, Tan, Y, Wu, Y, Zhang, S, Yi, K & Kang, C 2019, 'The CRISPR-Cas13a Gene-Editing System Induces Collateral Cleavage of RNA in Glioma Cells', *Advanced Science*, vol. 6, no. 20, p. 1901299.

Wang, X, Lu, Z, Gomez, A, Hon, GC, Yue, Y, Han, D, Fu, Y, Parisien, M, Dai, Q, Jia, G, Ren, B, Pan, T & He, C 2014, 'N⁶-methyladenosine-dependent regulation of messenger RNA stability', *Nature*, vol. 505, no. 7481, 2014/01/01, pp. 117-120.

Wang, X, Zhao, BS, Roundtree, IA, Lu, Z, Han, D, Ma, H, Weng, X, Chen, K, Shi, H & He, C 2015, 'N(6)-methyladenosine Modulates Messenger RNA Translation Efficiency', *Cell*, vol. 161, no. 6, Jun 4, pp. 1388-1399.

Wang, Y, Xiao, Y, Dong, S, Yu, Q & Jia, G 2020, 'Antibody-free enzyme-assisted chemical approach for detection of N⁶-methyladenosine', *Nature Chemical Biology*, vol. 16, no. 8, 2020/08/01, pp. 896-903.

Wang, Y, Zhang, Z, Sepich-Poore, C, Zhang, L, Xiao, Y & He, C 2021, 'LEAD-m(6) A-seq for Locus-Specific Detection of N(6) -Methyladenosine and Quantification of Differential Methylation', *Angew Chem Int Ed Engl*, vol. 60, no. 2, Jan 11, pp. 873-880.

Warren, L, Manos, PD, Ahfeldt, T, Loh, YH, Li, H, Lau, F, Ebina, W, Mandal, PK, Smith, ZD, Meissner, A, Daley, GQ, Brack, AS, Collins, JJ, Cowan, C, Schlaeger, TM & Rossi, DJ 2010, 'Highly efficient reprogramming to pluripotency and directed differentiation of human cells with synthetic modified mRNA', *Cell Stem Cell*, vol. 7, no. 5, Nov 5, pp. 618-630.

Wei, C-M & Moss, B 1977, 'Nucleotide sequences at the N6-methyladenosine sites of HeLa cell messenger ribonucleic acid', *Biochemistry*, vol. 16, no. 8, 1977/04/19, pp. 1672-1676.

Wei, CM, Gershowitz, A & Moss, B 1976, '5'-Terminal and internal methylated nucleotide sequences in HeLa cell mRNA', *Biochemistry*, vol. 15, no. 2, 1976/01/01, pp. 397-401.

Wei, L-H, Song, P, Wang, Y, Lu, Z, Tang, Q, Yu, Q, Xiao, Y, Zhang, X, Duan, H-C & Jia, G 2018, 'The m⁶A Reader ECT2 Controls Trichome Morphology by Affecting mRNA Stability in Arabidopsis', *The Plant Cell*, vol. 30, no. 5, pp. 968-985.

Wilson, C, Chen, PJ, Miao, Z & Liu, DR 2020, 'Programmable m⁶A modification of cellular RNAs with a Cas13-directed methyltransferase', *Nature Biotechnology*, vol. 38, no. 12, 2020/12/01, pp. 1431-1440.

Wu, J, Peled-Zehavi, H & Galili, G 2020, 'The m⁶A reader ECT2 post-transcriptionally regulates proteasome activity in Arabidopsis', *New Phytologist*, vol. 228, no. 1, 2020/10/01, pp. 151-162.

Xia, Z, Tang, M, Ma, J, Zhang, H, Gimple, RC, Prager, BC, Tang, H, Sun, C, Liu, F, Lin, P, Mei, Y, Du, R, Rich, JN & Xie, Q 2021, 'Epitranscriptomic editing of the RNA N6-methyladenosine modification by dCasRx conjugated methyltransferase and demethylase', *Nucleic Acids Research*, vol. 49, no. 13, pp. 7361-7374.

Xiao, W, Adhikari, S, Dahal, U, Chen, Y-S, Hao, Y-J, Sun, B-F, Sun, H-Y, Li, A, Ping, X-L, Lai, W-Y, Wang, X, Ma, H-L, Huang, C-M, Yang, Y, Huang, N, Jiang, G-B, Wang, H-L, Zhou, Q, Wang, X-J, Zhao, Y-L & Yang, Y-G 2016, 'Nuclear m⁶A Reader YTHDC1 Regulates mRNA Splicing', *Molecular Cell*, vol. 61, no. 4, 2016/02/18/, pp. 507-519.

Yan, J, Gu, Y, Jia, X, Kang, W, Pan, S, Tang, X, Chen, X & Tang, G 2012, 'Effective Small RNA Destruction by the Expression of a Short Tandem Target Mimic in Arabidopsis', *The Plant Cell*, vol. 24, no. 2, pp. 415-427.

Yang, L, Perrera, V, Saplaoura, E, Apelt, F, Bahin, M, Kramdi, A, Olas, J, Mueller-Roeber, B, Sokolowska, E, Zhang, W, Li, R, Pitzalis, N, Heinlein, M, Zhang, S, Genovesio, A, Colot, V & Kragler, F 2019, 'm⁵C Methylation Guides Systemic Transport of Messenger RNA over Graft Junctions in Plants', *Current Biology*, vol. 29, no. 15, 2019/08/05/, pp. 2465-2476.e2465.

Yang, X, Yang, Y, Sun, B-F, Chen, Y-S, Xu, J-W, Lai, W-Y, Li, A, Wang, X, Bhattarai, DP, Xiao, W, Sun, H-Y, Zhu, Q, Ma, H-L, Adhikari, S, Sun, M, Hao, Y-J, Zhang, B, Huang, C-M, Huang, N, Jiang, G-B, Zhao, Y-L, Wang, H-L, Sun, Y-P & Yang, Y-G 2017, '5-methylcytosine promotes mRNA export — NSUN2 as the methyltransferase

and ALYREF as an m⁵C reader', *Cell Research*, vol. 27, no. 5, 2017/05/01, pp. 606-625.

Yu, H, Pu, Q, Weng, Z, Zhou, X, Li, J, Yang, Y, Luo, W, Guo, Y, Chen, H, Wang, D & Xie, G 2021, 'DNAzyme based three-way junction assay for antibody-free detection of locus-specific N6-methyladenosine modifications', *Biosensors and Bioelectronics*, vol. 194, 2021/12/15/, p. 113625.

Yue, Y, Liu, J, Cui, X, Cao, J, Luo, G, Zhang, Z, Cheng, T, Gao, M, Shu, X, Ma, H, Wang, F, Wang, X, Shen, B, Wang, Y, Feng, X, He, C & Liu, J 2018, 'VIRMA mediates preferential m⁶A mRNA methylation in 3'UTR and near stop codon and associates with alternative polyadenylation', *Cell Discovery*, vol. 4, no. 1, 2018/02/27, p. 10.

Zheng, G, Dahl, JA, Niu, Y, Fedorcsak, P, Huang, CM, Li, CJ, Vågbø, CB, Shi, Y, Wang, WL, Song, SH, Lu, Z, Bosmans, RP, Dai, Q, Hao, YJ, Yang, X, Zhao, WM, Tong, WM, Wang, XJ, Bogdan, F, Furu, K, Fu, Y, Jia, G, Zhao, X, Liu, J, Krokan, HE, Klungland, A, Yang, YG & He, C 2013, 'ALKBH5 is a mammalian RNA demethylase that impacts RNA metabolism and mouse fertility', *Mol Cell*, vol. 49, no. 1, Jan 10, pp. 18-29.

Zhong, S, Li, H, Bodi, Z, Button, J, Vespa, L, Herzog, M & Fray, RG 2008, 'MTA is an Arabidopsis messenger RNA adenosine methylase and interacts with a homolog of a sex-specific splicing factor', *The Plant Cell*, vol. 20, no. 5, pp. 1278-1288.

Chapter II: Towards targeted RNA N6-methyladenosine demethylation in plants

Abstract

Representing the most prevalent RNA modifications on eukaryotic mRNA, N⁶-methyladenosine has been of interest for decades. Despite major progresses in the field, a detailed picture of how specific m⁶A-modified sites impact gene expression and phenotypes has been obscured by the inability to manipulate this modification with high precision. In this chapter, I adopted the RNA-guided RNA targeting system CRISPR-Cas13 for specific binding and removal of m⁶A methylation in *A. thaliana*. Catalytically dead Cas13 (dCas13) tethered to the *A. thaliana* m⁶A demethylase ALKBH10B caused phenotypical alterations when targeted to m⁶A-bearing mRNA *TRANSPARENT TESTA GLABRA 1 (TTG1)*, which correlated with a change in m⁶A abundance of the transcript. Study of the phenotype and molecular analysis for the *TTG1*-targeting dCas13-ALKBH10B transgenic plants revealed additional information about the mechanism underlying the m⁶A sites' activities. Together with recently developed tools based on CRISPR-dCas13 for targeted m⁶A manipulations in animal, dCas13-ALKBH10B described in this study offers the opportunity to obtain unbiased and specific understanding of RNA m⁶A's function and mechanism.

Introduction

N⁶-methyladenosine (m⁶A) is the most prevalent and highly conserved internal RNA modification on eukaryotic mRNA. In both plants and mammals, m⁶A is reversible and requires a number of enzymes for its activities. A complex of proteins, known as “writers”, is responsible for deposition of m⁶A to RNA, with key components being Methyltransferase like3 (METTL3), METTL14 and Wilms' tumor 1-associating protein (WTAP) in mammals (Bokar et al. 1994; Liu, J et al. 2014; Ping et al. 2014), or respective orthologs MTA, MTB and FKBP12 interacting protein 37 KD (FIP37) in plants (Bujnicki et al. 2002; Ruzicka et al. 2017; Zhong et al. 2008). Fat-mass and obesity associated protein (FTO) and AlkB homolog 5 (ALKBH5) actively demethylate m⁶A in mammals (Jia et al. 2011; Zheng et al. 2013), while ALKBH10B and ALKBH9B plays the role in plants (Duan et al. 2017; Martínez-Pérez et al. 2017). These proteins are known as “erasers”. In addition, m⁶A is recognized by three major classes of

“reader” proteins, YTH-domain protein family, serine/arginine-rich (SR) protein family, and heterogeneous nuclear ribonucleoproteins (hnRNPs). Several YTH-domain “reader” proteins were reported in *A. thaliana* as EVOLUTIONARILY CONSERVED C TERMINAL (ECT) proteins. These “readers” allow translation of m⁶A into downstream effects, such as RNA stability, subcellular localization and splicing.

To date, most of the knowledge about the function and molecular mechanism of RNA m⁶A is derived from studies on mutations of enzymes involving its deposition, removal or recognition. Null mutants of a number of the core m⁶A “writer” complex are embryonically lethal in *A. thaliana*, fly, and mouse (Geula et al. 2015; Hongay & Orr-Weaver 2011; Ruzicka et al. 2017; Shen, L et al. 2016; Zhong et al. 2008), which underscores the critical importance of m⁶A in embryonic development. FIP37 was shown to affect shoot apical meristem (SAM) cell differentiation in *A. thaliana*, with *fip37* mutants exhibiting SAM over-proliferation and subsequent lack of aerial organs (Ruzicka et al. 2017). Combining a number of molecular and genetic approaches, the authors further linked the overproliferated SAM phenotype to increased stability in two SAM-regulated transcripts *SHOOT MERISTEMLESS (STM)* and *WUSCHEL (WUS)* upon the loss of m⁶A. In line with the report, several transcripts regulating floral transition such as *FLOWERING LOCUS T (FT)*, *SQUAMOSA PROMOTER BINDING PROTEIN-LIKE 3 (SPL3)* and *SPL9* were shown to be destabilized upon accumulation of m⁶A in the m⁶A “eraser” mutant *alkbh10b*, leading to the late flowering phenotype in this mutant. In contrast, failure to recognize m⁶A in the “reader” mutant *ect2-1* was demonstrated to correlate with destabilization of transcripts including *TRANSPARENT TESTA GLABRA 1 (TTG1)*, *IRREGULAR TRICHOME BRANCH1 (ITB1)* and *DISTORTED TRICHOMES 2 (DIS2)*, which in turn correlate with an over-branching phenotype of leaf trichome in *A. thaliana*. Together with ECT2, other m⁶A “readers” such as ECT3 and ECT4 were shown to be essential for normal growth and development of a number of organs throughout a plant life, such as root length and gravitropism, leaf and flower patterning, and silique morphology. While these findings derived from mutants of m⁶A-related enzymes are valuable, there is a lack of specificity and solid connection between the phenotypes, causal transcripts, modified site(s) and the underlying mechanism.

To support unbiased evaluation of m⁶A's biological role, tools that allow manipulations to specific modified sites in mammalian cells have been developed. Among the first developed are the tools based on the RNA-guided DNA targeting system CRISPR-Cas9. In these tools, catalytically inactive dCas9 was heavily engineered to bind to RNA and fused to METTL3-METTL14 or ALKBH5/FTO to deposit or remove m⁶A, respectively (Liu, X-M et al. 2019). Recently, similar systems utilizing the RNA-guided RNA targeting system CRISPR-Cas13 and METTL3/METTL14 or ALKBH5 which offer higher specificity and simpler programmability than the dCas9 fusions have also been reported (Li, Jiexin et al. 2020; Wilson et al. 2020; Xia et al. 2021). Despite the successes in animal studies, such systems in plants are absent.

Here, I developed a targeted m⁶A demethylase system by fusing catalytically inactive dCas13b from *Prevotella* sp. P5-125 to ALKBH10B to form dCas13-ALKBH10B (Figure III-1) for specific binding and altering m⁶A methylation status of mRNA in *A. thaliana*. I used the system to elucidate the connection between m⁶A on *TTG1* and *FT* mRNAs with trichome morphology and flowering time, respectively.

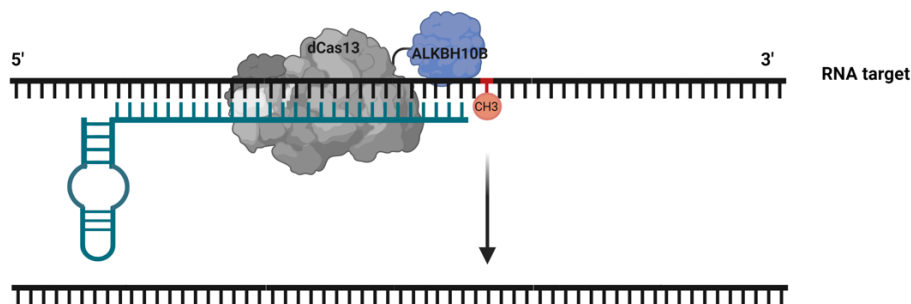


Figure II-1: Harnessing Arabidopsis ALKBH10B and catalytically deactivated enzyme dCas13 for targeted RNA m⁶A demethylation. The *Arabidopsis* ALKBH10B tethered to RNA-guided RNA binding protein dCas13 potentially can be directed to specific nucleotide(s) and enable targeted removal of RNA m⁶A.

Materials and Methods

Plasmid construction

dCas13-(m)ALKBH10B: dPspCas13b gene fragment (3.3 kb) was PCR amplified from plasmids pC0054 (Addgene, Plasmids #103870) and cloned into pMDC32 backbone by Gateway cloning to generate pCas13b. (m)ALKBH10B were ordered as geneBlocks from Integrated DNA Technologies (IDT) and inserted at the 3' of dCas13b gene by Gibson Assembly (Gibson et al. 2009). For expression of gRNA (including both inherent direct repeat (DR) and spacer which base-pairs with target), gene fragments of *AtU6-Bsalx2* were ordered as geneBlocks (IDT) and inserted into the pCas13-(m)ALKBH10B plasmids. *AtU6-1-Bsalx2* allows integration of new spacers to be expressed by *AtU6* by one step Golden gate cloning (Engler, Kandzia & Marillonnet 2008). An optimized protocol for Golden gate cloning including overnight incubation at 37°C and exclusion of the final 50°C incubation enabled highly reliable insertion of spacers to dCas13-(m)ALKBH10B, which was confirmed by PCR of the insert, Sanger sequencing and additional enzyme digest and PCR of sequence flanking *Bsal* sites for a subset of constructs.

No-ALK: Gene fragment of a 5-methylcytosine dioxygenase, *TET1*, was cloned into pCas13b plasmid instead of (m)ALKBH10B. This plasmid is described in detail in Chapter III.

pEmpty: empty vector pEmpty which contains neither of dCas13-ALKBH10B nor gRNA cassette was generated by *HindIII* and *SpeI* double digest of pCas13b plasmid followed by T4 DNA ligation with a 24-nt filler sequence to replace the dCas13 fragment.

Design of gRNA spacer for dCas13-(m)ALKBH10B (exclusively referred to as “spacer” hereby)

Due to the presence of clustered targeted sites as well as the frequent occurrence of adenosine nucleotides in the 3'UTRs which would correspond to long T-stretches in gRNA, spacers were designed to: (i) locate 2-6nt 5' to a single targeted site, (ii) avoid overlap with sites targeted by another spacer, (iii) avoid four consecutive adenosines. Spacers were 28-nt long which is optimal length used by PspCas13b (Cox et al. 2017), except for one spacer targeting the first m⁶A motif near start codon of FT which was 24-nt long. Details of spacer sequence can be found in Supplementary Table II-S2.

Arabidopsis transformation and transgenic plant generation

Constructs were transformed into *Agrobacterium* USDA cells by electroporation for subsequent plant transformation by floral dipping (Clough & Bent 1998). Transformants were selected on 15ug/mL HygromycinB ½ MS medium. 3:1 segregation ratio was used to determine single-insertion event. Heterozygous plants with single insert were carried to the next generations for generation to identify a homozygous line. Plants were grown in long day conditions (16-hour light/8-hour darkness) at 21°C.

Naming of transgenic plants

T₁ generation plants were labelled with single numbers, for example #1, #2, #3. T₂ and T₃ plants carried their parent's names as prefixes, followed by their own labels, with a dot “.” being the separator. For example, #1.1 indicates a T₂ plant that derived from the T₁ plant #1. Similarly, #1.1.1 indicates a T₃ plant that derived from the T₂ plant #1.1. Note that to simplify some figures, the hash sign “#” might be removed.

Phenotype characterization

Trichome branching: For T₁, T₂ plants, seeds were plated on selection medium (½ MS, no sucrose, 15 ug/mL HygromycinB), grown for 7-10 days before being transferred to soil. The third and fourth true leaves of three-week old plants were taken for analysis. All trichomes on each leaf were examined for the number of branches under a light microscope (Leica).

Flowering time: T₂ seeds were placed on ½ MS medium for identification of single-copy lines and then seeds of these lines were sown directly on soil. The numbers of rosette and cauline leaves were counted for each plant at anthesis.

RT-qPCR

Total RNA was extracted and purified from 14-day old shoot tissues of wild-type and transgenic plants using Spectrum Plant Total RNA extraction kit (Sigma). cDNA was synthesized with Superscript III Reverse transcriptase (Invitrogen) and used as input for quantification with FastStart SYBR Green Master Mix (Roche) on a QuantStudio 7 Flex System (Applied Biosystems). Biological duplicates and technical triplicates were assayed. *TUBULIN 2 (TUB2)* was used as internal control for normalization of transcripts.

SELECT-qPCR

SELECT reaction was carried out as previously described (Xiao, Y et al. 2018). Briefly, 1-1.5 ug total RNA was mixed with 40 nM each of UP and DOWN probe, 5 uM dNTP and 1X Cutsmart Buffer (NEB) in a 17 uL reaction. The mixture was incubated in temperature gradient as follows: 90°C/1 min, 80°C/1 min, 70°C/1 min, 60°C/1 min, 50°C/1 min, 40°C/6 min. 3 uL of (0.01 U BSt 2.0 DNA polymerase, 0.5 U SplintR Ligase and 1 uM ATP) was added to make a 20 uL final volume and mixture was incubated at 40°C/20 min and 80°C/20 min and kept at 4°C. 2 uL of reaction was used as template for qPCR with 2X Faststart Universal SYBR Green Master Mix (Roche) and 200uM each of SELECT forward and reverse primer. Probes and Primers are listed in Supplementary Table II-S2.

Results

Design and construction of dCas13b-ALKBH10B

Tethering two or more functional domains to obtain a translational fusion with a novel function is now common. Recently, dCas13 was fused to a number of domains or proteins such as the RNA deaminase ADAR2, m⁶A “writer” METTL3/METTL14 or m⁶A “eraser” ALKBH5, allowing specific modifications to RNA molecules in mammalian systems (Abudayyeh, O. O. et al. 2019; Cox et al. 2017; Li, Jiexin et al. 2020; Wilson et al. 2020; Xia et al. 2021). These examples highlight the potential use of dCas13 in a novel fusion for targeted manipulations of m⁶A in other organisms. Of several tested dCas13 orthologs, dPspCas13b from *Prevotella* sp. P5-125 was reported to have high targeting efficiency, a relatively small size and no reported toxicity compared to other orthologs (Buchman et al. 2020; Zhang et al. 2020). I therefore used dPspCas13b to develop a targeted m⁶A demethylation system in *A. thaliana*.

dPspCas13b offers specific binding to RNA and m⁶A demethylase catalytic activity can be performed by *Arabidopsis* ALKBH10B. In order to enhance the specificity of dCas13b-ALKBH10B translational fusion, I removed the RNA binding domain from ALKBH10B and tethered only the catalytic domain (Figure III-2A) to the C-terminus of dCas13b. Similarly, a second fusion of dCas13b and catalytically inactive ALKBH10B domain (mALKBH10B) was generated as a control (Figure III-2B). To facilitate protein folding, a three-amino acid Glycine-Serine-Glycine (GSG) linker was inserted between the two domains in each construct (van Rosmalen, Krom & Merx 2017). To promote localization of the dCas13b-(m)ALKBH10B fusions to the nucleus, a SV40 nuclear localization signal (NLS) was added to the N-terminus.

The gRNAs comprising of both Cas13 intrinsic direct repeats (DRs) and spacers matching RNA target sequences for the dCas13-(m)ALKBH10B system were expressed under the Pol III *AtU6* promoter. The recognition motif known as the Protospacer Adjacent Motif (PAM) or Protospacer Flanking Site (PFS) is not required in most Cas13 orthologs including dPspCas13b when used in eukaryotes (Cox et al. 2017), which facilitates flexible targeting. In this study, spacers for each m⁶A target nucleotide were placed 2-6 nucleotides 5' of the target site. Depending on a particular

target, slightly different gRNA design was adopted, which is detailed in the following sections.

Both components, fusion protein and gRNA, of dCas13b-(m)ALKBH10 were combined on a single vector (Figure II-2C). To construct dCas13b-(m)ALKBH10B, several cloning steps were required (Figure II-2C). Final dCas13b-(m)ALKBH10B constructs utilized Type IIS restriction enzyme BsaI and Golden Gate cloning (Engler, Kandzia & Marillonnet 2008) for integration of new spacers (Figure II-2C).

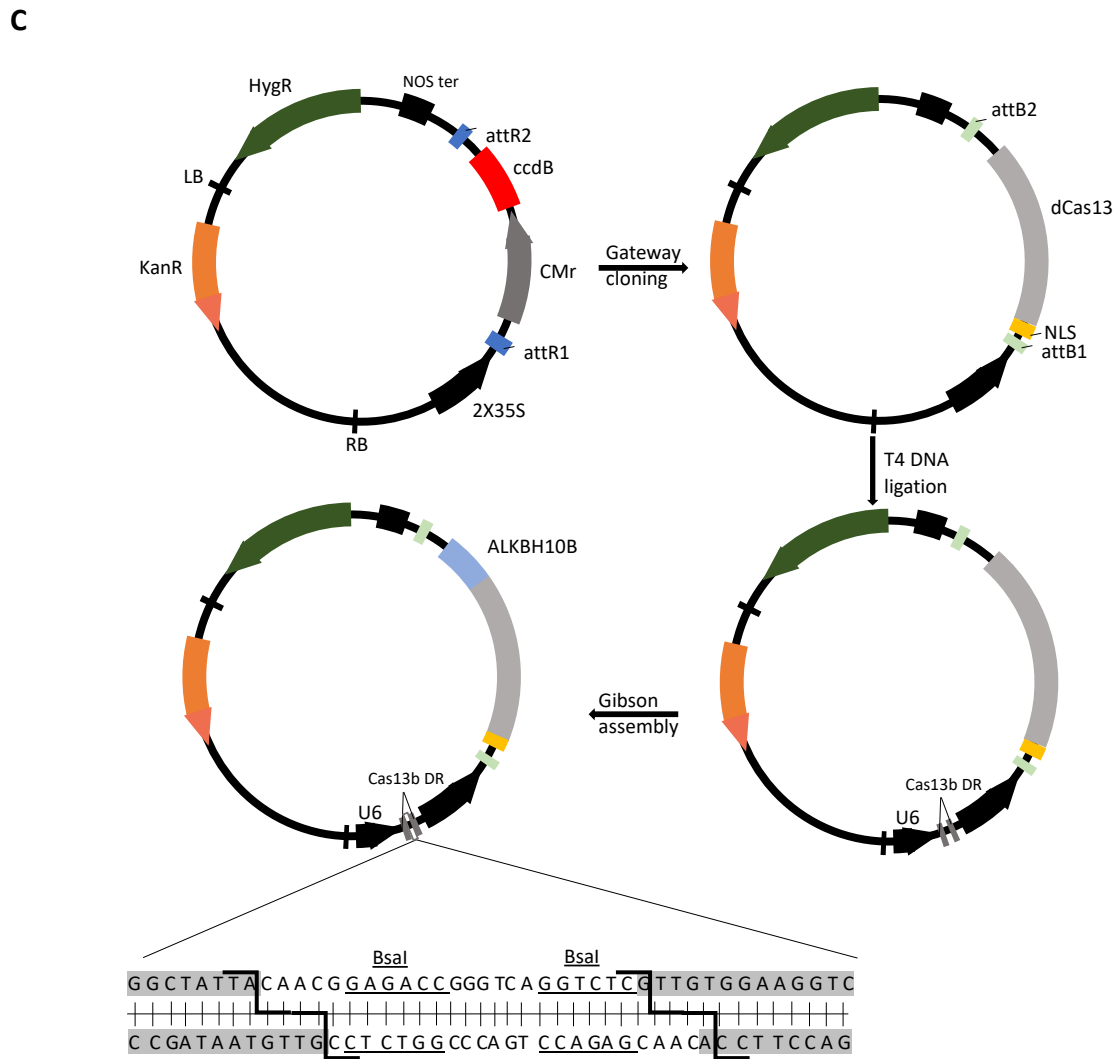
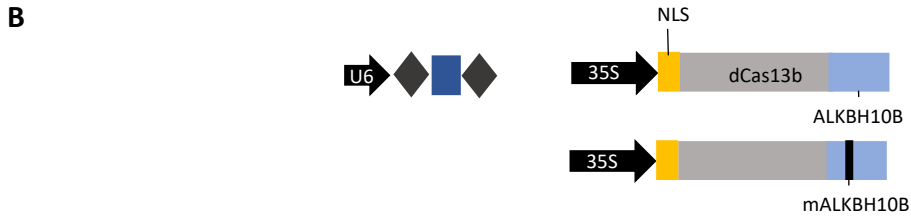
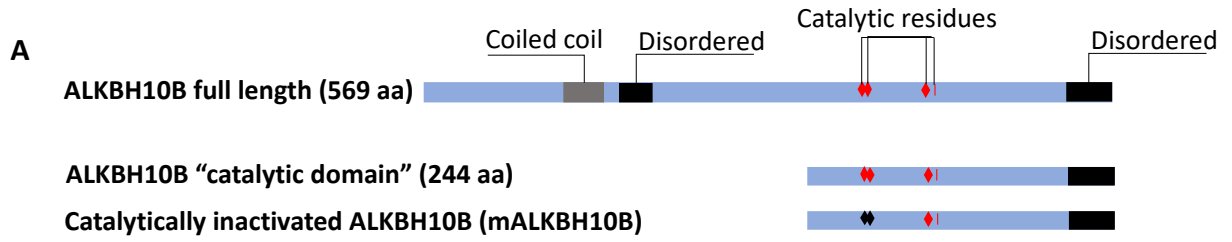


Figure II-2: Design and construction of dCas13b-(m)ALKBH10B. A, Catalytic domain of ALKBH10B used in dCas13b-ALKBH10B fusion covers amino acid 325-569 of the full-length protein. Catalytically inactive mALKBH10B has mutations in two conserved iron-binding residues H366A and E368A (Duan et al. 2017) (small black diamonds). B, Two components of dCas13b-(m)ALKBH10B are gRNA (including both DRs, charcoal diamonds and spacer, navy rectangle) driven by an *AfU6* promoter, and dCas13-(m)ALKBH10B fusion with a SV40 NLS sequence at the N-terminus. C, Flow diagram of dCas13b-ALKBH10B construction. New spacers can be cloned into the *Bsa*I sites (underlined) by Golden gate cloning.

Selection of targets for testing dCas13b-ALKBH10B in *A. thaliana*

Often, observed *in vitro* efficiencies do not reflect the cellular activity and therefore dCas13b-ALKBH10B constructs were directly tested *in vivo* in *A. thaliana*. To this end, *TRANSPARENT TESTA GLABRA 1 (TTG1)* and *Flowering locus T (FT)* were two endogenous mRNA transcripts that were selected for my experiments.

In an early transcriptome-wide profiling of m⁶A in two *A. thaliana* accessions Can-0 and Hen-16, *TTG1* was found to contain two m⁶A peaks near the start and stop codons (Luo et al. 2014). Later, two separate studies utilizing m⁶A-RNA immunoprecipitation (m⁶A-RIP) confirmed the m⁶A peaks on *TTG1*, with the peak near stop codon-3'UTR region being consistently more pronounced than the start codon peak (Duan et al. 2017; Wei, L-H et al. 2018). Wei, L-H et al. (2018) further proposed that these m⁶A sites were bound by the m⁶A “reader” ECT2 and reduced transcript abundance of *TTG1* was observed in the *ect2-1* mutant. Reduced *TTG1* mRNA correlated with over-branched trichome phenotype in *ect2-1*. Using computational approaches, putative m⁶A nucleotides on *TTG1* mRNA were predicted and documented in the RNA modification database RMbase 2.0 (Xuan et al. 2017). According to this database, *TTG1* has four m⁶A sites clustered in the 3'UTR and two single m⁶A sites in either the 5'UTR or CDS. The m⁶A on *TTG1* is among the most well-supported m⁶A sites from all m⁶A studies in *A. thaliana* to date. Therefore, I tested the efficacy of the dCas13b-ALKBH10B to remove the methyl group from m⁶A sites on *TTG1* mRNA.

To comprehensively examine the efficacy of dCas13b-ALKBH10B, *FT* was chosen as a second target mRNA. *FT* is a major regulator of flowering time in *Arabidopsis* under long-day photoperiods (Qin, Bai & Wu 2017). Although being less well-documented compared to m⁶A on *TTG1* mRNA, *FT* was reported with a strong m⁶A peak near the start codon and a second peak near the stop codon whose accumulation was linked to the decreased stability of *FT* mRNA in *alkbh10b*, leading to a late-flowering phenotype in the mutant (Duan et al. 2017). Directing dCas13b-ALKBH10B to the m⁶A sites of *FT* mRNA to remove the methyl groups was expected to produce early-flowering plants, giving an easy phenotypic indicator of the fusion protein's efficacy.

Below, I detail the work that have been accomplished for each target.

Targeting dCas13b-ALKBH10B to m⁶A sites on *TTG1* altered trichome morphology

To efficiently target the putative m⁶A cluster in the 3'UTR of *TTG1* mRNA, a gRNA array named "3'UTR array" of four gRNA spacers was designed (Figure II-3A). Each spacer was 4-6 nt 5' to each putative m⁶A site. An additional array containing all four 3'UTR spacers and two spacers targeting m⁶A sites on the CDS and 5'UTR of *TTG1*, named "all-gRNA array", was also generated and introduced into both constructs with active ALKBH10B and catalytically inactivated mALKBH10B. The expression of dCas13-(m)ALKBH10B mRNA in transgenic plants was confirmed by RT-qPCR (Supplementary Figure II-S1).

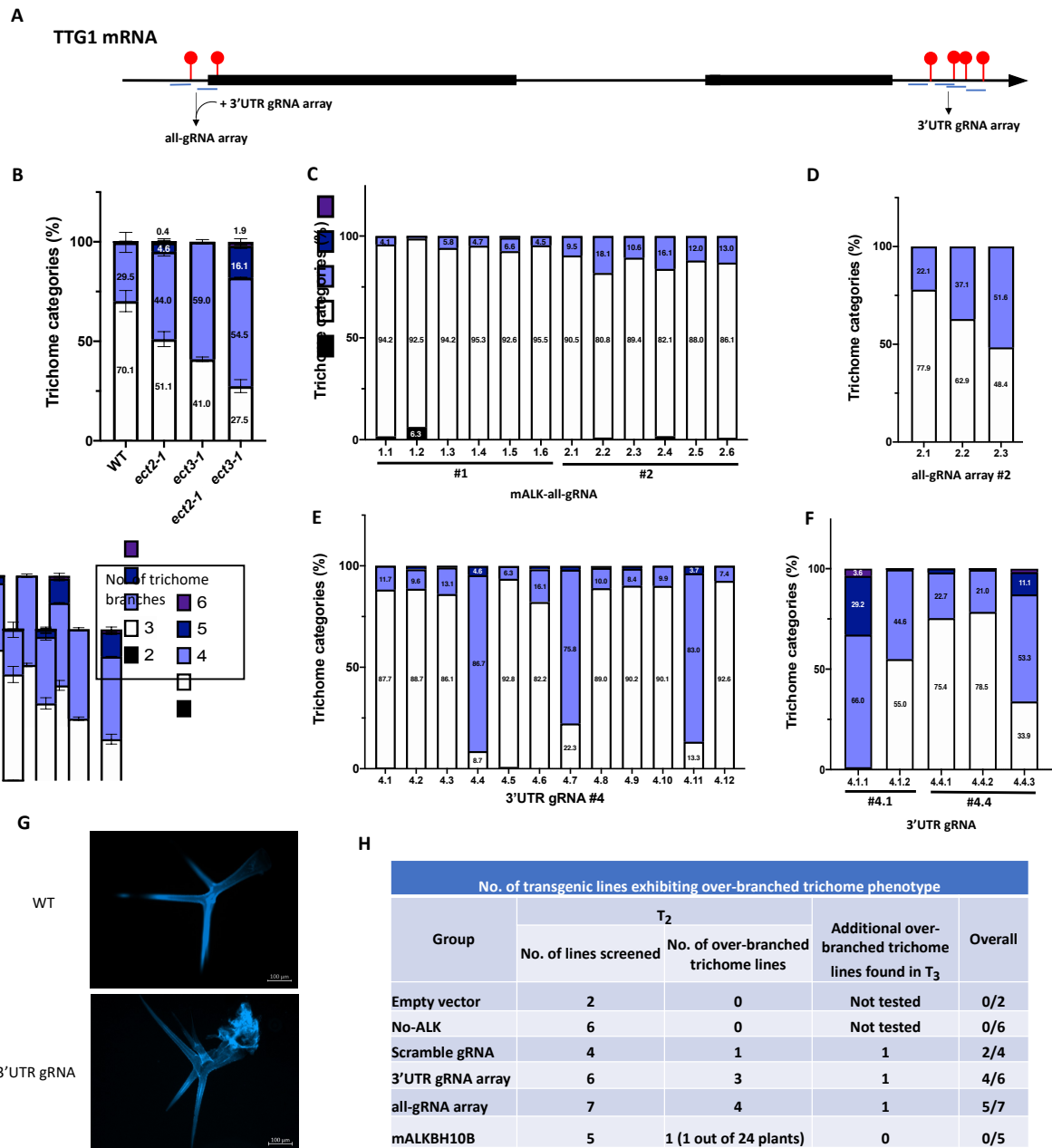


Figure II-3: Trichome characterization of transgenic plants expressing dCas13b-ALKBH10 targeting m⁶A sites on *TTG1* mRNA. Constructs containing active dCas13b-ALKBH10B with 3'UTR gRNA array (3'UTR gRNA array), active dCas13b-ALKBH10B with gRNAs targeting all putative m⁶A sites on *TTG1* (all-gRNA array), or catalytically inactive dCas13b-mALKBH10B with all-gRNA array (mALK-all-gRNA) were introduced into *A. thaliana*. Control constructs include empty vector, Scramble gRNA (random sequence) and a plasmid with dCas13b but neither ALKBH10B or mALKBH10B (No-ALK). T₂ (C, D, E) and T₃ (F) generations were examined for

trichome distribution on the third and fourth true leaves at three-week old. A, Schematic of gRNA spacer design to target m⁶A sites on *TTG1*. B, Trichome distribution in wild-type, single mutant of each of the m⁶A “readers” ECT2 (*ect2-1*) and ECT3 (*ect3-1*), and *ect2-1 ect3-1* double mutant. C, D, E, Trichome distribution in T₂ transgenic plants expressing “mALK-all-gRNA”, “all-gRNA array” or “3’UTR gRNA array”, respectively. “#” denotes independent transgenic lines. F, Trichome distribution of progenies of two plants in (E). Note that “4.1” or “4.4” prefix indicates the respective parent as shown in (E). G, Trichomes of wild-type and a “3UTR gRNA array” transgenic plant over-stained with DAPI for observation under an epifluorescence microscope. H, Summary of over-branched trichome phenotype in each group of transgenic plants. 40% or more of 4-, 5-, and 6-branch trichomes was considered “over-branched trichome phenotype”. “Additional over-branched trichome lines found in T₃” are lines that were not found to have the phenotype in T₂ but in T₃ generation. In one line of mALKBH10B, one out of 24 T₂ plants screened exhibited over-branched trichome phenotype, compared to ratios of or above one in six in other lines with the phenotype (Supplementary Figure II-S2, Panel E of this figure), thus this line was not considered an over-branched trichome line. The phenomenon could be explained by residual activity of mALKBH10B (Duan et al. 2017).

Given the vital role of *TTG1* in trichome morphology regulation (Zhao et al. 2008) and the observation that mutants of ECT m⁶A “readers” such as ECT2 and ECT3 had slight to severely over-branched trichome phenotypes (Arribas-Hernández et al. 2018; Scutenaire et al. 2018; Wei, L-H et al. 2018), to examine the effect of dCas13b-ALKBH10B when targeting m⁶A sites on *TTG1* mRNA, I first screened for trichome phenotypes of T₂ transgenic plants. The third and fourth true leaves of three-week old T₂ plants were analyzed. Indeed, I observed mild to highly over-branched trichome in a number of independent transgenic lines expressing either the “3’UTR gRNA array” (four out of six lines) or the “all-gRNA array” (five out of seven lines) (Figure II-3D,E), but not the lines with inactive mALKBH10B, empty vector or without ALKBH10B (No-ALK) (Figure II-3C,H, Supplementary Figure II-S2). Eight out of nine over-branched trichome lines showed a similar level of over-branching when compared to either *ect2-1* or *ect3-1* (Figure II-3B,D). In one unique line of “3’UTR gRNA array”, line #4, the over-branching phenotype was similar or more severe than the highly branched *ect2-*

1 *ect3-1* double mutant (Figure II-3E). A clear trend observed was that dependent transgenic plants, that are within a line, can show high levels of trichome morphology variation (Figure II-3D-F). The variation did not correlate with transgene zygosity (Supplementary Table II-S1). However, both the highly over-branching phenotype and the variation within a line was inherited to the next generations (Figure II-3E,F, Supplementary Figure II-S3). Unexpectedly, plants containing a dCas13b-ALKBH10B with a scrambled gRNA had a mild over-branched trichome phenotype, suggesting off-target effect of the dCas13-ALKBH10B fusion (Supplementary Figure II-S2C). Nonetheless, collectively, these results strongly pointed toward molecular perturbation of trichome morphology regulatory network when targeting dCas13-ALKBH10B to m⁶A sites on *TTG1*.

Next, I aimed to measure the level of m⁶A on *TTG1* mRNAs in the transgenic plants, by two methods: m⁶A-RIP-qPCR and SELECT-qPCR (Xiao, Y et al. 2018). m⁶A-RIP utilizes m⁶A antibody to capture m⁶A-bearing RNA fragments which is then quantified by qPCR. On the other hand, SELECT harnesses the ability of m⁶A to hinder both DNA polymerization and ligation of DNA probes when splinted by an RNA template, allowing determination of m⁶A level at a nucleotide via the threshold cycles (C_t values) in downstream qPCR (Figure II-4A). Unfortunately, due to the technical difficulties of each method and the time constraints, results for both methods were largely not achieved. For m⁶A-RIP-qPCR, the main limitation was the substantial amount of input RNA, 200-300 ug RNA, required for each biological sample, making assaying all groups of transgenic plants laborious. Therefore, only a test with smaller amounts of input RNA, 10-40 ug, was done. However, these small input amounts after going through m⁶A-RIP did not give reliable quantitation of the 3'UTR region of *TTG1* mRNA (expected to contain m⁶A sites) in wild-type plants (C_t values ~30 or undetermined, data not shown). Due to the time constraints, optimization and amendments to this approach could not be performed. For SELECT-qPCR, two out of four targeted m⁶A nucleotides in the 3'UTR, "3'UTR site 2" and "3'UTR site 3", and the m⁶A nucleotide in CDS were assayed along with a non-m⁶A site residing in the 3'UTR, named "N-site", which serve as a negative control (Supplementary Figure II-S4A). However, three sites: 3'UTR site 3, CDS and N-site showed signs of non-specific amplification (Supplementary Figure II-S4B) and will require optimization of reaction components. Nevertheless, I found two T₂ transgenic lines targeting m⁶A cluster in 3'UTR, line #3.5

and #4.3, exhibited reduction in m⁶A levels at 3'UTR site 2 compared to wild-type, pEmpty and Scramble gRNA lines in two independent experiments (Figure II-4C, Supplementary Figure II-4C). An additional line with the “all-gRNA array”, line #1.3, that did not show over-branched trichome phenotype also had slight reduction in the m⁶A level at the site (Figure II-4C). However, a “mALK-all gRNA” line, #2.4, exhibited variable results in the two experiments (Figure II-4C, Supplementary Figure II-4C). Therefore, the m⁶A level in *TTG1*-targeting dCas13b-ALKBH10B remain to be confirmed.

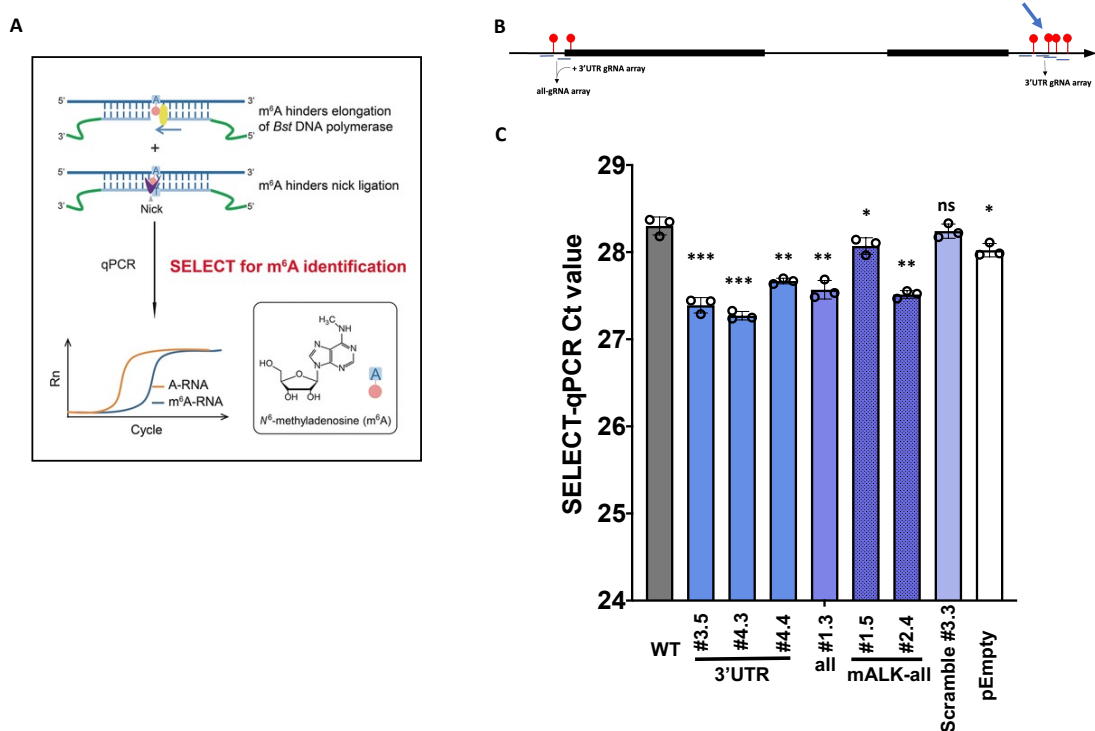


Figure II-4: Molecular characterization of transgenic plants expressing dCas13b-ALKBH10 to target m⁶A sites on *TTG1* mRNA. A, Principle of SELECT-qPCR for site-specific determination of m⁶A abundance (Xiao, Y et al. 2018). Two DNA probes matching sequences flanking the nucleotide of interest on an mRNA are incubated with the RNA template, DNA polymerase such as *Bst* v2.0 and a splint ligase. m⁶A hinders both the DNA polymerization and ligation while a non-m⁶A nucleotide allows the reactions to occur. Successful elongation and ligation of DNA splinted by a non-m⁶A template results in the strand being amplified with low C_t value in subsequent

qPCR, which is in contrast to an m⁶A-template. B, m⁶A site 2 (arrowed) in the 3'UTR of *TTG1* was assayed with SELECT-qPCR and results (C_t values) are shown in (C). C, SELECT-qPCR results of 14-day old shoot tissues of T₃ transgenic plants depicted in (B). Note that bulked tissues were used, thus samples are shown with their parents' names. Technical triplicates were performed. Asterisks indicate statistical significance of the difference between each transgenic line and wild-type by Welch's t test. *: p value <0.05; **: p value < 0.01; ***: p value < 0.001; ns: not significant. 3'UTR, "3'UTR gRNA array" plants; all, "all-gRNA array" plants.

Along with assessing m⁶A abundance on *TTG1* mRNA, I examined the steady-state *TTG1* mRNA transcript abundance in the dCas13b-ALKBH10B transgenic lines and controls by RT-qPCR. Two "3'UTR gRNA array" transgenic lines showing strong over-branched trichome phenotype, two "all-gRNA array" homozygous lines which did not show over-branching of trichome, two lines of mALK-all-gRNA, one line of the scrambled gRNA, along with wild-type and *ect2-1* mutant were assayed (Figure II-5). Interestingly, *TTG1* transcript abundance was not significantly (p value >0.1) reduced in *ect2-1* compared to wild-type. This result was different from the results obtained by a similar RT-qPCR experiment for wild-type and *ect2-1* reported previously (Wei, L-H et al. 2018), however was consistent with the RNA-seq data provided in the same study. Both "3'UTR gRNA array" lines that showed a strong over-branched trichome phenotype had the same *TTG1* mRNA abundance compared to wild-type. Together, these results suggest that m⁶A on *TTG1* mRNA does not regulate trichome morphology through *TTG1* mRNA abundance but through a different mechanism. In addition, three out of four transgenic lines expressing "all-gRNA array", two lines with active ALKBH10B and two lines with mALKBH10B, exhibited increased *TTG1* mRNA abundance, suggesting that dCas13b-(m)ALKBH10 binding to 5'UTR or CDS of *TTG1* mRNA can interfere with mRNA turnover rates.

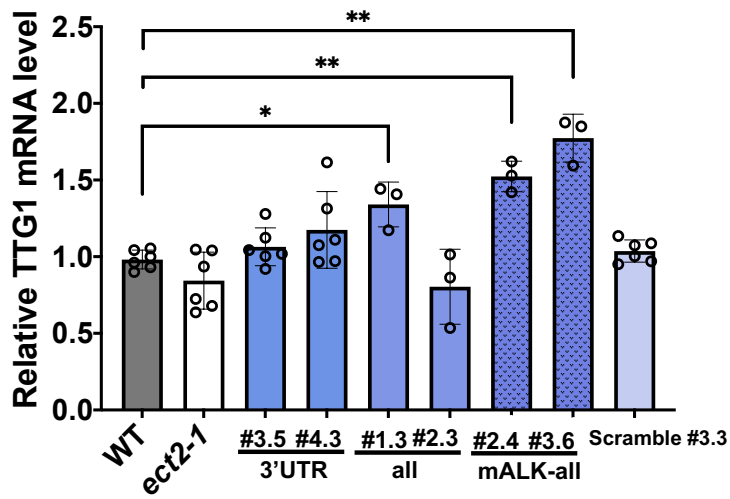


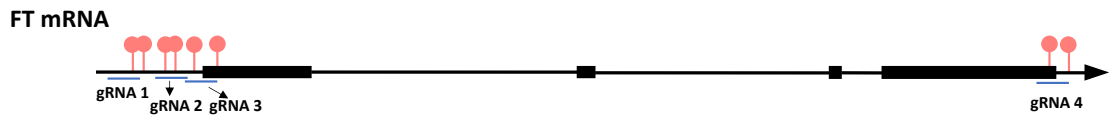
Figure II-5: *TTG1* mRNA abundance in transgenic plants expressing *TTG1*-targeting dCas13b-ALKBH10. RT-qPCR was performed for total RNA extracted from 14-day old shoot tissues. Biological duplicates and technical triplicates were performed. *ACT2* was an internal control. Error bars represent standard deviation of mean. Welch's t test. *: p value <0.05; **: p value < 0.01.

Targeting dCas13b-ALKBH10B to *FT* did not cause late or early flowering

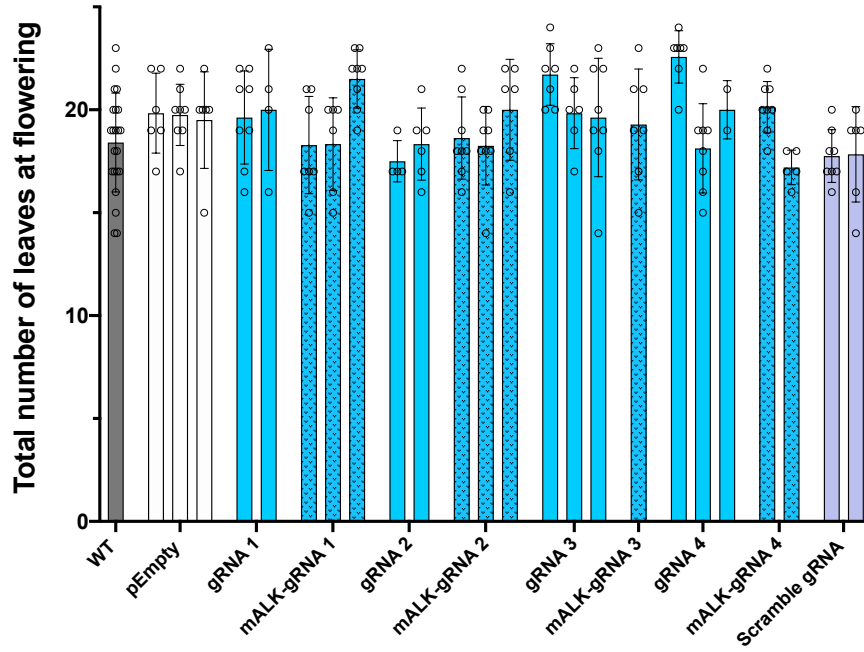
For the second target, *FT*, due to the unavailability of single nucleotide resolution m⁶A data, I searched for the m⁶A consensus motif DRACH (D = not C, R = A or G, H = not G) in 75-nt regions flanking the m⁶A RIP peaks near the start or stop codons identified in Duan et al. (2017). The search gained six and two DRACH sites near *FT*'s start and stop codons, respectively (Figure II-6A, Supplementary Information).

Four different single spacers were designed to direct dCas13b-ALKBH10B to the DRACH sites on *FT* mRNA. Due to the close distribution of the six DRACH sites near the start codon, three spacers were designed to cover all these DRACH sites but do not overlap each other (Figure II-6A). Each spacer was 2-3 nt 5' of a DRACH site. All spacer sequences can be found in Supplementary Table II-S2. Each of the four spacers were cloned into both constructs with dCas13-ALKBH10B and dCas13-mALKBH10B. The resulting eight constructs were transformed into wild-type *A. thaliana* and twelve T₁ plants were isolated for each construct. One to three T₁ plants with single transgene insert of each construct were selected and their seeds, that is T₂ generation, were subject to a flowering time assay. The flowering time of the dCas13-ALKBH10B T₂ plants and controls including wild-type, two homozygous scramble gRNA and three homozygous empty vector lines was measured under long day photoperiods. However, none of the transgenic lines exhibited a significantly earlier or later flowering time than wild-type (Figure II-6B,C).

A



B



C

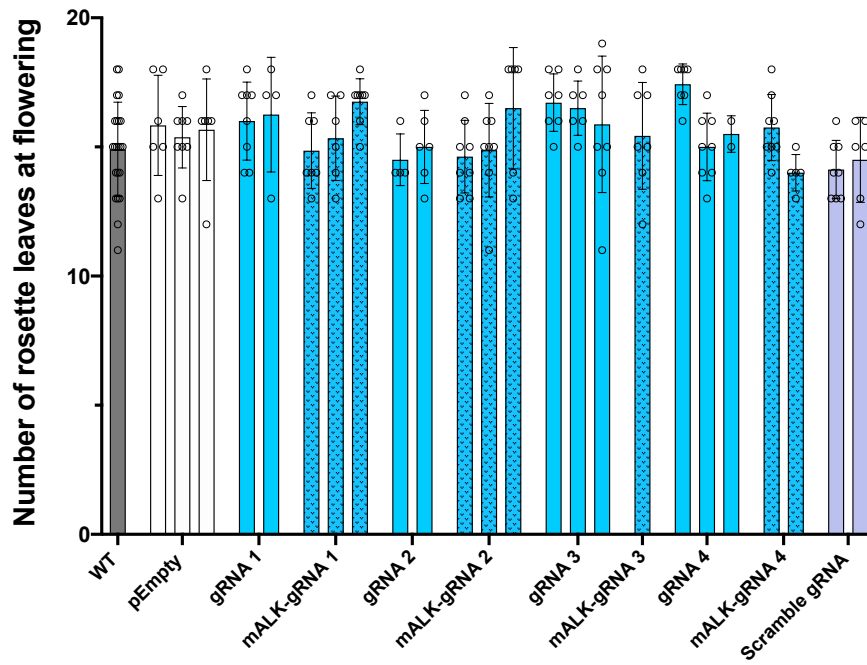


Figure II-6: Targeting dCas13b-ALKBH10B to DRACH motifs on *FT* mRNA. m⁶A consensus motif DRACH was used to design spacers to direct dCas13b-ALKBH10B to m⁶A on *FT*. Full *FT*-targeting dCas13b-ALKBH10B constructs were introduced into *A. thaliana* and T₂ transgenic plants were monitored for their numbers of leaves at flowering under long day photoperiods. A, Positioning of spacers for dCas13b-ALKBH10B to target DRACH sites on *FT*. *FT* genomic structure is depicted as black boxes (exons) and black lines (introns and UTRs). Orange lollipop shapes represent m⁶A consensus DRACH motifs near *FT*'s start and stop codon. Small navy bars underneath are spacers for gRNAs of dCas13b-ALKBH10B. DRACH sites and spacers are not to scale. B-C, Total number of leaves (rosette + cauline) (B) or number of rosette leaf only (C) at flowering of *FT*-targeting dCas13b-ALKBH10B T₂ plants. Each bar represents an independent transgenic line. Error bars represent standard deviation of mean.

Discussion

Functional studies of RNA m⁶A in plants are restricted by the lack of tools to manipulate the modification specifically. Here, I developed a dCas13b-ALKBH10B fusion and tested its demethylation effect on two mRNA targets *TTG1* and *FT* in *A. thaliana*. Targeting of the translational fusion to m⁶A sites on *TTG1* mRNA increased the trichome branching as expected, with slight reduction in m⁶A level at one targeted site detected. Meanwhile, targeting the fusion to *FT* mRNA did not change the flowering time.

The trichome phenotype of transgenic dCas13-ALKBH10B *TTG1* targeted plants

While m⁶A level in *TTG1*-targeting dCas13b-ALKBH10B plants remains an importance investigation to be done, the altered trichome phenotype in the plants has delivered interesting messages: Firstly, no effect of ALKBH10B over-expression on vegetative growth has been reported. The over-branched trichome phenotype in most of the transgenic lines with either “3’UTR gRNA array” or “all-gRNA array”, and some of the Scramble gRNA lines, is in line with the similar phenotypes observed in the mutants of m⁶A “readers” as demonstrated in this study, or of the m⁶A deficient mutants *mta* and *fip37* (Ruzicka et al. 2017). This data points toward effective removal of m⁶A on *TTG1* by dCas13-ALKBH10B, and supports a link between m⁶A regulation of trichome morphology and *TTG1* mRNA as previously reported (Wei, L-H et al. 2018). However, the m⁶A regulation of trichome morphology is not via *TTG1* mRNA abundance, as shown in RT-qPCR results in this study. Secondly, the trichome phenotype observed in transgenic plants are highly variable and inheritable. While the differential expression of dCas13b-ALKBH10B (Supplementary Figure II-S1) and the dynamic of RNA turnover and metabolism partially explain the variations, the drastically different phenotypes within dependent plants of the same transgenic line might point toward a dosage-dependent or threshold mechanism of a key factor in the regulation of the phenotype. In fact, *TTG1* and other components of the core trichome initiation complex were postulated to function in a dosage manner (Pesch et al. 2015). Alternatively, the high-level variations might be a result of dCas13-ALKBH10B-mediated disruption of phenotypic variation buffering (Queitsch, Sangster & Lindquist 2002). In addition, the

absence of over-branched trichome phenotype in one generation and its return in the next suggested that the effect might be reprogrammed during meiosis.

No flowering time effect when *FT* mRNA was targeted

There are several explanations for no detection of early-flowering in *FT* m⁶A targeted transgenic plants: (i) One spacer might not be enough to remove the m⁶A cluster and to have a detectable effect; (ii) Targeting *FT* mRNA might not be the key to altering the floral transition, either due to the insignificance of the m⁶A on the *FT* transcript or other regulators such as *SQUAMOSA PROMOTER-BINDING PROTEIN-LIKE3 (SL3)* and *SL9* (Duan et al. 2017) are important m⁶A targets. Further molecular characterization of the transgenic plants will be required to clarify the demethylation efficiency of dCas13b-ALKBH10B at m⁶A sites on *FT*.

Design of dCas13b-ALKBH10B

m⁶As largely cluster to 3'UTR and 5'UTR sequences in which adenosine bases occur frequently. One limitation for the current design of the dCas13-ALKBH10B system is the promoter driving gRNA expression – U6 – utilizes T-stretch as transcriptional terminators, which might result in lower production of gRNA bearing a 4-T stretch. In human, a 4-T stretch can cause 75% reduction in transcription using U6 (Gao, Z, Herrera-Carrillo & Berkhout 2018). It is important to also note that direct repeat sequence of PspCas13b used in this study contain a T4 stretch, yet U6 was successfully used in the pioneering paper of A to I editing with dCas13-ADAR2 in human cells (Cox et al 2017).

While it is theoretically feasible to calculate, or predict, optimal binding site for gRNA of a dCas13 fusion, this could be a great challenge in practice, especially to target RNAs which have largely unpredictable and dynamic secondary structures. In line with this argument, study with dCas13-ALKBH5 (Li, Jiexin et al. 2020) reported successful removal of m⁶A in human cell line with gRNA distancing up to three kilobases (3kb) from targeted sites. Wilson et al. (2020) reported gRNA binding 8-15 nt 5' of targeted sites having most efficient methylation activity, which varies amongst targets. Study by Xia et al. (2021) on the other hand demonstrated that the 10-nucleotide window around targeted sites are most efficient for either dCasRx-ALKBH5 or dCasRx-

METLL3 and used spacers overlapping targeted sites for their study. This is somewhat surprising however, as ALKBH5 and METLL3 are single-stranded RNA enzymes and are expected to be less active on paired nucleotides.

ALKBH5 contains an RNA binding domain, which could be expected to give non-specific binding and therefore off-target effect when fused to a dCas13. All of the published dCas13-ALKBH5 studies however reported a minimal such effect in mammalian cells. In contrast, having remove the putative RNA binding domain from ALKBH10B fused to dCas13b, I still detected plants with over-branched trichome phenotype in Scramble gRNA transgenic plants. This poses the question of whether previous studies were not able to detect off-target effect comprehensively, or this effect is specific in plants. However, I cannot exclude the possibility that the Scramble gRNA sequence may bind non-specifically to multiple transcripts or genomic regions, causing unexpected effects, despite the unlikelihood of hits to the *A. thaliana* genome when predicted informatically using NCBI BLAST (data not shown). Further investigations will be required to clarify the observation.

Supplementary Data

Supplementary Table:

Supplementary Table II-S1: Example of poor correlation between transgene zygosity and trichome phenotype of *TTG1*-targeting dCas13b-ALKBH10B transgenic plants. Four independent transgenic lines, #1 to #4, of “3’UTR gRNA array” are shown. Three-week old plants heterozygous or homozygous for the transgene were examined for trichome distribution. $\geq 40\%$ of trichome with four or more than four branches (4+ branch trichome) is considered over-branched trichome phenotype, with the over-branching levels colour-coded as in the right panel. +/-: homozygous line, shaded in light green.

	T1	T2	% of 4+ branch trichome
TTG1-3'UTR-gRNA array	#1	#1.1	24.6
		#1.2	13.0
		#1.3	46.4
		#1.4	34.9
	#2	#2.6	35.7
		#2.5	23.3
		#2.3	34.0
	#3	#3.5	39.8
		#3.6	47.8
	#4	#4.1	11.7
		#4.2	11.3
		#4.3	13.9
		#4.4	91.3
		#4.7	77.7
		#4.11	86.7

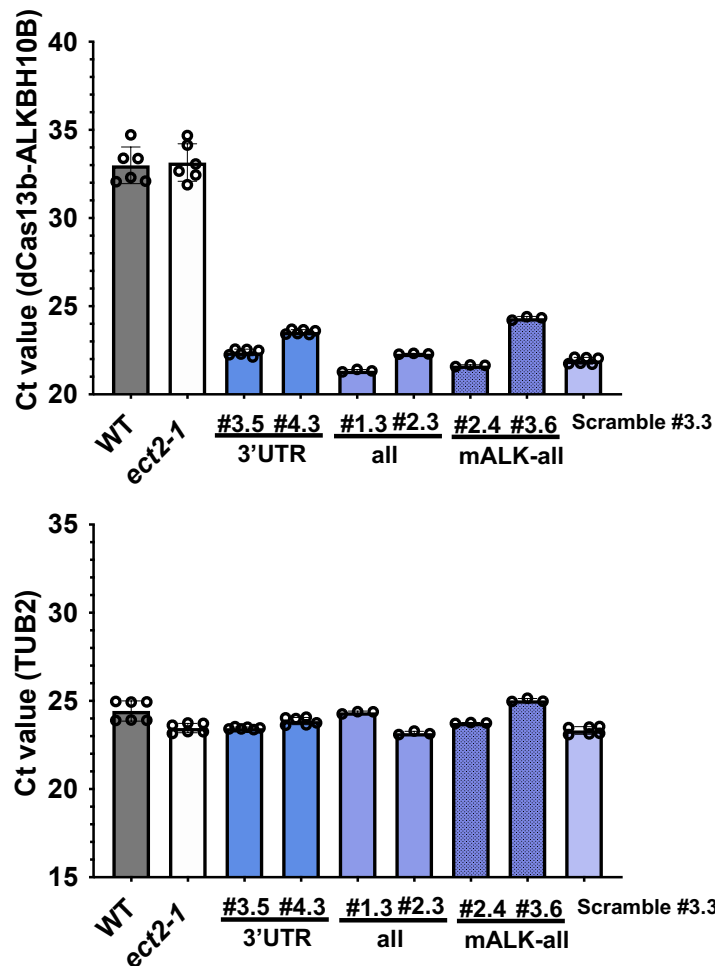
35 <x<40
40 <x<55
>55

+/+

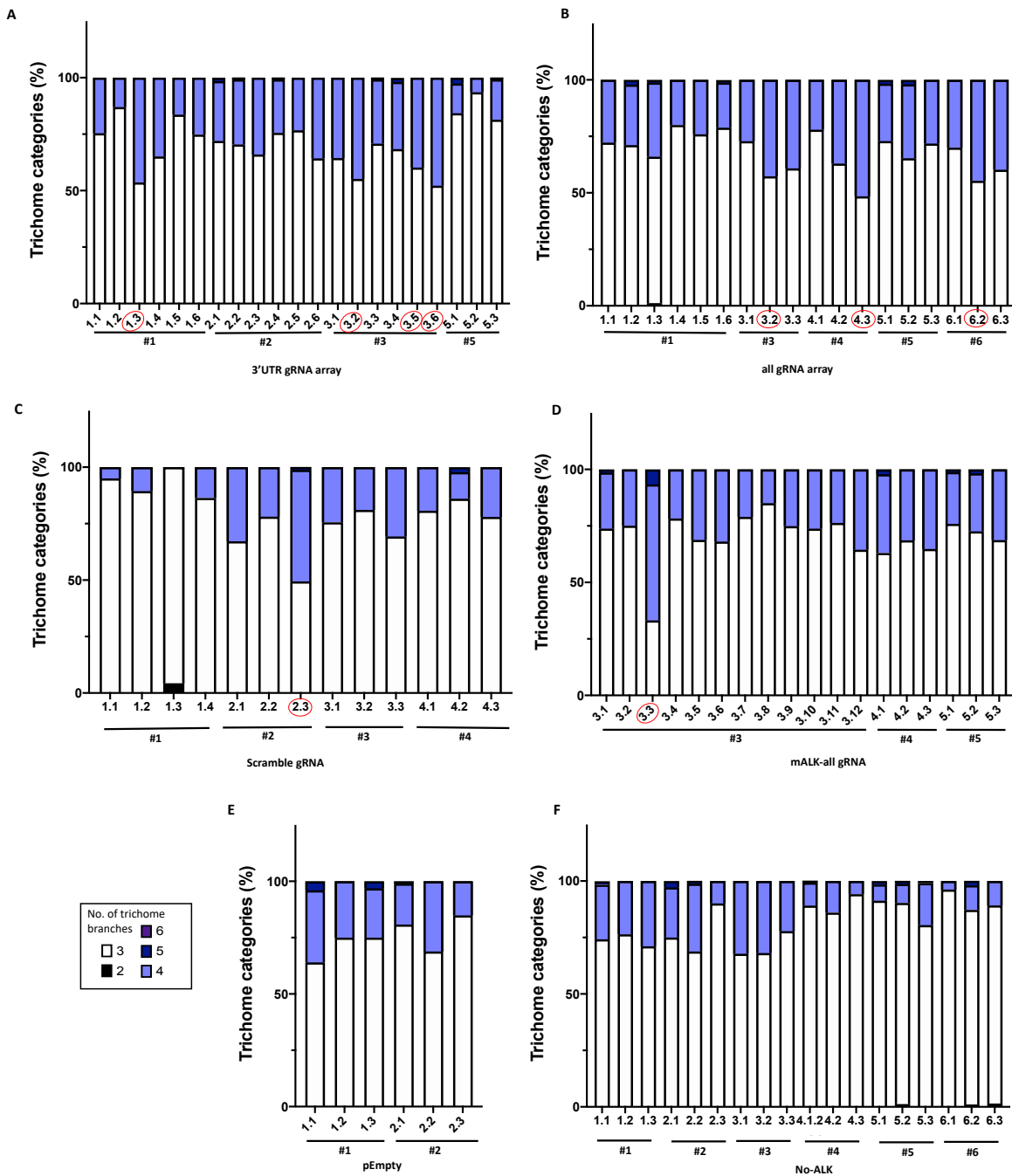
Supplementary Table II-S2: DNA sequences used in this chapter

RT-qPCR primers to check expression of dCas13b-ALKBH10B mRNA	
Cas13_ALK_qF	GCCGTTAGGTCTCTTGTATTCTGG
Cas13_ALK_qR	GGGGAGTACGCCATCATGA
Spacer sequences	
TTG1-g6-UTR3/1-F	CAAC CTAAAATCCTTATTGATCACTTCACATC G
TTG1-g6-UTR3/1-R	ACAAC GATGTGAAGTGATCAATAAGGATTTTAG
TTG1-g6-UTR3/2-F	CAAC TTACAATCAGATAGATACAGAGTCATTG G
TTG1-g6-UTR3/2-R	ACAAC CAATGACTCTGTATCTATCTGATTGTAA
TTG1-g6-UTR3/3-F	CAAC AAATGAATTCAGTTTTAGTTACAATCAG G
TTG1-g6-UTR3/3-R	ACAAC CTGATTGTAATAAACTGAATTCATTT
TTG1-g6-UTR3/4-F	CAAC ACACAACATAAGATAATAGTATCATTTG G
TTG1-g6-UTR3/4-R	ACAAC CAAATGATACTATTATCTTATGTTGTGT
TTG1-g6-CDS-F	CAAC ATCTGGATAACGAATCTGGAGCTGAATT G
TTG1-g6-CDS-R	ACAAC AATTCAGCTCCAGATTCGTTATCCAGAT
TTG1-g6-UTR5-F	CAAC GGTCAGTGTGAGTCGGATTTTTCAAGAG G
TTG1-g6-UTR5-R	ACAAC CTCTTGAAAAATCCGACTGACACTGACC
FT-gRNA1-F	CAAC TTTGTTTCTGCTTCTTTAATTTGT G
FT-gRNA1-R	ACAAC ACAAAATTAAGAAGCAGAAACAAA
FT-gRNA2-F	CAAC CTCTGTGTTGATTGTTTCTGTTTACTT G
FT-gRNA2-R	ACAAC AAGTAAAACAGAAACAATCAACACAGAG
FT-gRNA3-F	CAAC CTTATATTTATAGACATCTTTGATCTTG G
FT-gRNA3-R	ACAAC CAAGATCAAAGATGTCTATAAATAAAG
FT-gRNA4-F	CAAC TCTTCCTCCGAGCCACTCTCCCTCTGA G
FT-gRNA4-R	ACAAC TCAGAGGGAGAGTGGCTGCGGAGGAAGA
Scramble_F	CAACGCTAGCTAGCGGCATCATTGACCATACTG
Scramble_R	ACAACAGTATGGTCAATGATGCCGCTAGCTAGC
SELECT-qPCR primers and probes	
SELECT-qF	ATGCAGCGACTCAGCCTCTG
SELECT-qR	TAGCCAGTACCGTAGTGCGTG
TTG1-3UTR-2-X-UP	TAGCCAGTACCGTAGTGCGTG TGGTTCATCAAATGAATTCAG
TTG1-3UTR-2-X-DOWN	TTTAGTTACAATCAGATAGATACA CAGAGGCTGAGTCGCTGCAT
TTG1-3UTR-3-X-UP	TAGCCAGTACCGTAGTGCGTGCAACATAAGATAATAGTATCATTTGG
TTG1-3UTR-3-X-DOWN	TCATCAAATGAATTCAGTTTTAG CAGAGGCTGAGTCGCTGCAT
TTG1-3UTR-N-UP	TAGCCAGTACCGTAGTGCGTGTTTAGTTACAATCAGATAGATACAG
TTG1-3UTR-N-DOWN	GTCATTGCGGACCTAAAA CAGAGGCTGAGTCGCTGCAT
TTG1-CDS-X-UP	TAGCCAGTACCGTAGTGCGTG CGTATGTGACGGCGG
TTG1-CDS-X-DOWN	TTCCGATCTGGATAACGA CAGAGGCTGAGTCGCTGCAT

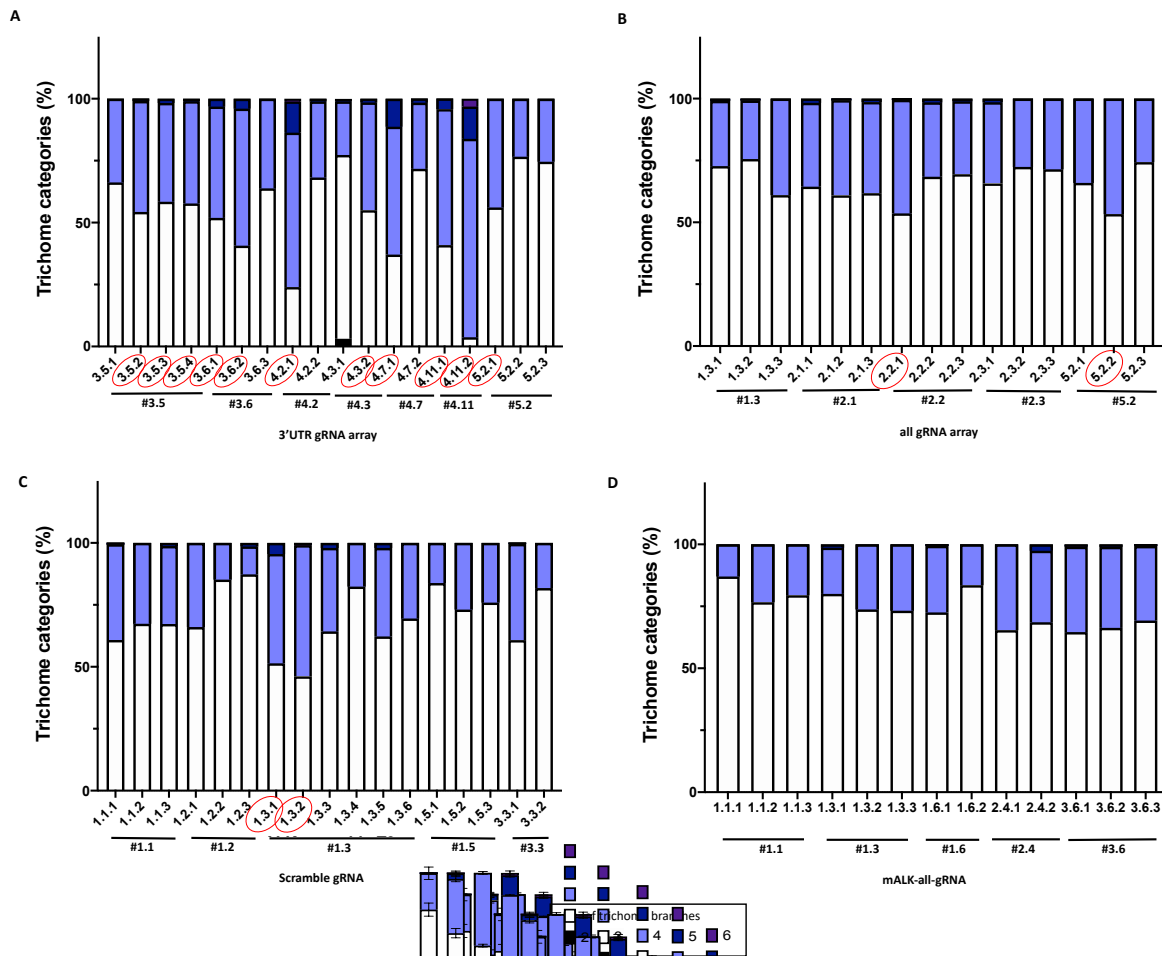
Supplementary Figure:



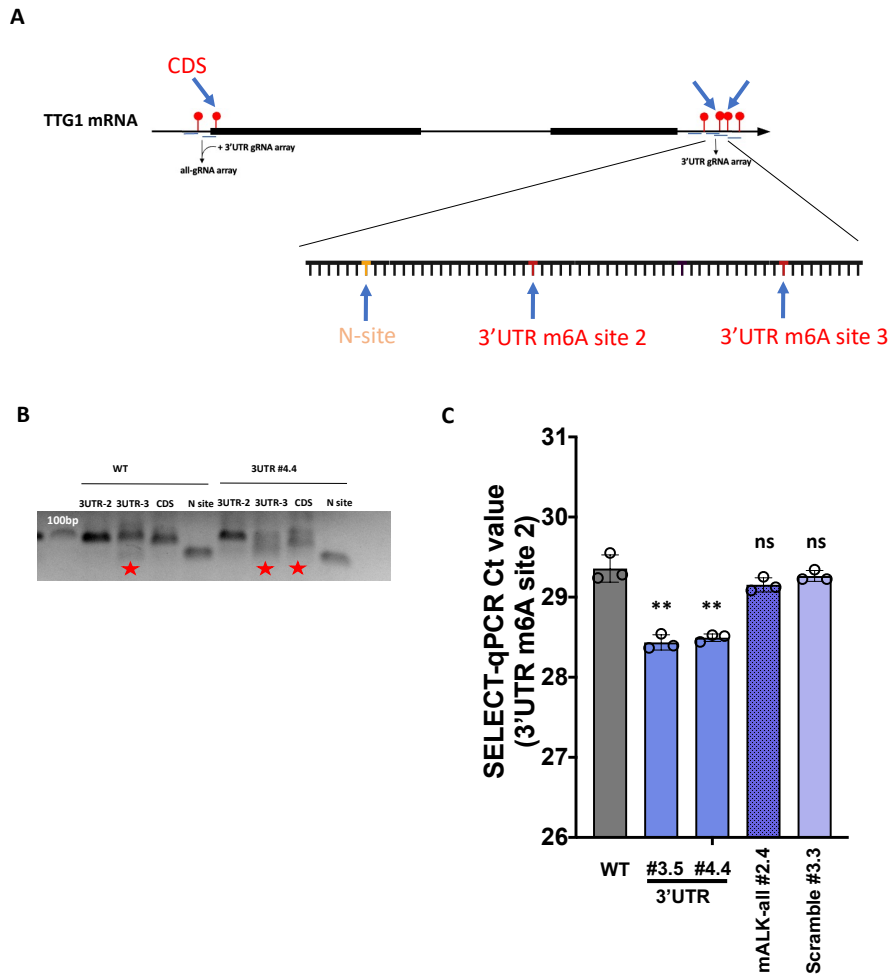
Supplementary Figure II-S1: Expression of dCas13b-ALKBH10B mRNA in *A. thaliana* determined by RT-qPCR. Primers binding to the dCas13b-ALKBH10 junction (Supplementary Table II-S2) were used to detect the transcript in RT-qPCR (Upper). Detection of C_t values above 30 likely indicate false signals. *TUB2* was shown as a control (Lower). Biological duplicates and technical triplicates were performed. 3'UTR, "3'UTR gRNA array" plants. all, "all-gRNA array" plants. "#" denotes transgenic line used.



Supplementary Figure II-S2: Trichome phenotype of *TTG1*-targeting dCas13b-*ALKBH10B* and control vector T_2 transgenic plants. The third and fourth true leaves of 3-week old T_2 plants were analyzed. A, 3'UTR gRNA array. B, all-gRNA array. C, Scramble gRNA. D, mALK-all gRNA. E, pEmpty. F, No-ALK. Plants showing over-branched trichome phenotype ($\geq 40\%$ of 4-, 5- and 6-branch trichomes) are circled in red. One line (T_1) of "3'UTR-gRNA array", one line of "all-gRNA array", and twelve plants (T_2) of "mALK-all gRNA #3" that did not exhibit over-branched trichome phenotype are not shown but summarized in Figure II-3.



Supplementary Figure II-S3: Trichome phenotype of *TTG1*-targeting dCas13b-*ALKBH10B* and control vector T_3 transgenic plants. The third and fourth true leaves of 3-week old T_3 plants were analyzed. A, 3'UTR gRNA array. B, all-gRNA array. C, Scramble gRNA. D, mALK-all-gRNA. Plants showing over-branched trichome phenotype ($\geq 40\%$ of 4-, 5- and 6-branch trichomes) are circled in red.



Supplementary Figure II-S4: SELECT-qPCR for site-specific m6A quantification of *TTG1*-targeting dCas13b-ALKBH10B plants. A, Target sites on *TTG1* mRNA planned for SELECT-qPCR. m6A site 2 and site 3 in 3'UTR of *TTG1*, the m6A on CDS, a non-m6A site (N site) residing in between m6A site 2 and site 1 in 3'UTR of *TTG1* were subject to SELECT incubation with DNA probes, DNA polymerase and ligase, and subsequent qPCR. B, End-point qPCR products on 1.5% agarose gel showed non-specific amplification with probes for 3'UTR site 3, CDS (red stars) and N-site (all products are expected ~95bp long). Consistent with this, qPCR melt curve plots for 3'UTR site 3 and CDS showed subtle shoulder, although Sanger sequencing largely confirmed the main products were correct (data not shown). C, SELECT-qPCR results (Ct values) for wild-type and dCas13b-ALKBH10B transgenic plants. Bulked 14-day old shoot tissues of T₃ plants were used. Technical triplicates were performed. Asterisks indicate statistical significance of the difference between each transgenic line and wild-type by Welch's t test. **: p value < 0.01; ns: not significant. 3'UTR, "3'UTR gRNA array".

Supplementary Information:

Sequence of FT full-length CDS. DRACH motifs in <75 nt distance from either start or stop codon (underlined) are highlighted in red.

acaataaagaagcagaaacaaaaacaagtaaaacagaacaatcaacacagagaaaccacctgtttgttcaa
gatcaaagATGTCTATAAATATAAGAGACCCTCTTATAGTAAGCAGAGTTGTTGGAG
ACGTTCTTGATCCGTTTAATAGATCAATCACTCTAAAGGTTACTTATGGCCAAAG
AGAGGTGACTAATGGCTTGGATCTAAGGCCTTCTCAGGTTCAAACAAGCCAAG
AGTTGAGATTGGTGGAGAAGACCTCAGGAACCTTCTATACTTTGGTTATGGTGGG
TCCAGATGTTCCAAGTCCTAGCAACCCTCACCTCCGAGAATATCTCCATTGGTT
GGTGACTGATATCCCTGCTACAACCTGGAACAACCTTTGGCAATGAGATTGTGTG
TTACGAAAATCCAAGTCCCCTGCAGGAATTCATCGTGTCGTGTTTATATTGTTT
CGACAGCTTGGCAGGCAAACAGTGTATGCACCAGGGTGGCGCCAGAACTTCAA
CACTCGCGAGTTTGCTGAGATCTACAATCTCGGCCTTCCCGTGGCCGCAGTTTT
CTACAATTGTCAGAGGGAGAGTGGCTGCGGAGGAAGAAGACTTTAGatggcttctcc
ttataaccaattgatattgcatactctgatgagattatgcatctatagtatttaatttaataaccatttatgatacgagtaa
cgaacggtgatgatgcctatagtagttcaatatataagtggtgtaataaaaatgagagggggaggaaaatgagagtggt
ttacttatatagtggtgatgataattatattaatctacatgaaatgaagtgttatattatactta

References

Abudayyeh, OO, Gootenberg, JS, Franklin, B, Koob, J, Kellner, MJ, Ladha, A, Joung, J, Kirchgatterer, P, Cox, DBT & Zhang, F 2019, 'A cytosine deaminase for programmable single-base RNA editing', *Science*, vol. 365, no. 6451, Jul 26, pp. 382-386.

Arribas-Hernández, L, Bressendorff, S, Hansen, MH, Poulsen, C, Erdmann, S & Brodersen, P 2018, 'An m(6)A-YTH Module Controls Developmental Timing and Morphogenesis in Arabidopsis', *Plant Cell*, vol. 30, no. 5, May, pp. 952-967.

Bokar, JA, Rath-Shambaugh, ME, Ludwiczak, R, Narayan, P & Rottman, F 1994, 'Characterization and partial purification of mRNA N6-adenosine methyltransferase from HeLa cell nuclei. Internal mRNA methylation requires a multisubunit complex', *J Biol Chem*, vol. 269, no. 26, Jul 1, pp. 17697-17704.

Buchman, AB, Brogan, DJ, Sun, R, Yang, T, Hsu, PD & Akbari, OS 2020, 'Programmable RNA Targeting Using CasRx in Flies', *The CRISPR journal*, vol. 3, no. 3, pp. 164-176.

Bujnicki, JM, Feder, M, Radlinska, M & Blumenthal, RM 2002, 'Structure prediction and phylogenetic analysis of a functionally diverse family of proteins homologous to the MT-A70 subunit of the human mRNA:m(6)A methyltransferase', *J Mol Evol*, vol. 55, no. 4, Oct, pp. 431-444.

Clough, SJ & Bent, AF 1998, 'Floral dip: a simplified method for Agrobacterium-mediated transformation of Arabidopsis thaliana', *Plant J*, vol. 16, no. 6, Dec, pp. 735-743.

Cox, DBT, Gootenberg, JS, Abudayyeh, OO, Franklin, B, Kellner, MJ, Joung, J & Zhang, F 2017, 'RNA editing with CRISPR-Cas13', *Science*, vol. 358, no. 6366, Nov 24, pp. 1019-1027.

Duan, H-C, Wei, L-H, Zhang, C, Wang, Y, Chen, L, Lu, Z, Chen, PR, He, C & Jia, G 2017, 'ALKBH10B Is an RNA N⁶-Methyladenosine Demethylase Affecting Arabidopsis Floral Transition', *The Plant Cell*, vol. 29, no. 12, pp. 2995-3011.

Geula, S, Moshitch-Moshkovitz, S, Dominissini, D, Mansour, AA, Kol, N, Salmon-Divon, M, Hershkovitz, V, Peer, E, Mor, N, Manor, YS, Ben-Haim, MS, Eyal, E, Yunger, S, Pinto, Y, Jaitin, DA, Viukov, S, Rais, Y, Krupalnik, V, Chomsky, E, Zerbib, M, Maza, I, Rechavi, Y, Massarwa, R, Hanna, S, Amit, I, Levanon, EY, Amariglio, N, Stern-Ginossar, N, Novershtern, N, Rechavi, G & Hanna, JH 2015, 'Stem cells. m⁶A mRNA methylation facilitates resolution of naïve pluripotency toward differentiation', *Science*, vol. 347, no. 6225, Feb 27, pp. 1002-1006.

Hongay, CF & Orr-Weaver, TL 2011, 'Drosophila Inducer of MEiosis 4 (IME4) is required for Notch signaling during oogenesis', *Proceedings of the National Academy of Sciences*, vol. 108, no. 36, p. 14855.

Jia, G, Fu, Y, Zhao, X, Dai, Q, Zheng, G, Yang, Y, Yi, C, Lindahl, T, Pan, T, Yang, YG & He, C 2011, 'N6-methyladenosine in nuclear RNA is a major substrate of the obesity-associated FTO', *Nat Chem Biol*, vol. 7, no. 12, Oct 16, pp. 885-887.

Li, J, Chen, Z, Chen, F, Xie, G, Ling, Y, Peng, Y, Lin, Y, Luo, N, Chiang, C-M & Wang, H 2020, 'Targeted mRNA demethylation using an engineered dCas13b-ALKBH5 fusion protein', *Nucleic Acids Research*, vol. 48, no. 10, pp. 5684-5694.

Liu, J, Yue, Y, Han, D, Wang, X, Fu, Y, Zhang, L, Jia, G, Yu, M, Lu, Z, Deng, X, Dai, Q, Chen, W & He, C 2014, 'A METTL3-METTL14 complex mediates mammalian nuclear RNA N6-adenosine methylation', *Nat Chem Biol*, vol. 10, no. 2, Feb, pp. 93-95.

Liu, X-M, Zhou, J, Mao, Y, Ji, Q & Qian, S-B 2019, 'Programmable RNA N6-methyladenosine editing by CRISPR-Cas9 conjugates', *Nature Chemical Biology*, vol. 15, no. 9, 2019/09/01, pp. 865-871.

Luo, G-Z, MacQueen, A, Zheng, G, Duan, H, Dore, LC, Lu, Z, Liu, J, Chen, K, Jia, G, Bergelson, J & He, C 2014, 'Unique features of the m⁶A methylome in *Arabidopsis thaliana*', *Nature Communications*, vol. 5, no. 1, 2014/11/28, p. 5630.

Martínez-Pérez, M, Aparicio, F, López-Gresa, MP, Bellés, JM, Sánchez-Navarro, JA & Pallás, V 2017, 'Arabidopsis m⁶A demethylase activity modulates viral infection of a plant virus and the m⁶A abundance in its genomic RNAs', *Proceedings of the National Academy of Sciences*, vol. 114, no. 40, p. 10755.

Ping, XL, Sun, BF, Wang, L, Xiao, W, Yang, X, Wang, WJ, Adhikari, S, Shi, Y, Lv, Y, Chen, YS, Zhao, X, Li, A, Yang, Y, Dahal, U, Lou, XM, Liu, X, Huang, J, Yuan, WP, Zhu, XF, Cheng, T, Zhao, YL, Wang, X, Rendtlew Danielsen, JM, Liu, F & Yang, YG 2014, 'Mammalian WTAP is a regulatory subunit of the RNA N6-methyladenosine methyltransferase', *Cell Res*, vol. 24, no. 2, Feb, pp. 177-189.

Ruzicka, K, Zhang, M, Campilho, A, Bodi, Z, Kashif, M, Saleh, M, Eeckhout, D, El-Showk, S, Li, H, Zhong, S, De Jaeger, G, Mongan, NP, Hejatko, J, Helariutta, Y & Fray, RG 2017, 'Identification of factors required for m(6) A mRNA methylation in *Arabidopsis* reveals a role for the conserved E3 ubiquitin ligase HAKAI', *New Phytol*, vol. 215, no. 1, Jul, pp. 157-172.

Scutenaire, J, Deragon, JM, Jean, V, Benhamed, M, Raynaud, C, Favory, JJ, Merret, R & Bousquet-Antonelli, C 2018, 'The YTH Domain Protein ECT2 Is an m⁶A Reader Required for Normal Trichome Branching in Arabidopsis', *Plant Cell*, vol. 30, no. 5, May, pp. 986-1005.

Shen, L, Liang, Z, Gu, X, Chen, Y, Teo, Zhi Wei N, Hou, X, Cai, Weiling M, Dedon, Peter C, Liu, L & Yu, H 2016, 'N⁶-Methyladenosine RNA Modification Regulates Shoot Stem Cell Fate in Arabidopsis', *Developmental Cell*, vol. 38, no. 2, pp. 186-200.

van Rosmalen, M, Krom, M & Merkx, M 2017, 'Tuning the Flexibility of Glycine-Serine Linkers To Allow Rational Design of Multidomain Proteins', *Biochemistry*, vol. 56, no. 50, 2017/12/19, pp. 6565-6574.

Wei, L-H, Song, P, Wang, Y, Lu, Z, Tang, Q, Yu, Q, Xiao, Y, Zhang, X, Duan, H-C & Jia, G 2018, 'The m⁶A Reader ECT2 Controls Trichome Morphology by Affecting mRNA Stability in Arabidopsis', *The Plant Cell*, vol. 30, no. 5, pp. 968-985.

Wilson, C, Chen, PJ, Miao, Z & Liu, DR 2020, 'Programmable m⁶A modification of cellular RNAs with a Cas13-directed methyltransferase', *Nature Biotechnology*, vol. 38, no. 12, 2020/12/01, pp. 1431-1440.

Xia, Z, Tang, M, Ma, J, Zhang, H, Gimple, RC, Prager, BC, Tang, H, Sun, C, Liu, F, Lin, P, Mei, Y, Du, R, Rich, JN & Xie, Q 2021, 'Epitranscriptomic editing of the RNA N⁶-methyladenosine modification by dCasRx conjugated methyltransferase and demethylase', *Nucleic Acids Research*, vol. 49, no. 13, pp. 7361-7374.

Xiao, Y, Wang, Y, Tang, Q, Wei, L, Zhang, X & Jia, G 2018, 'An Elongation- and Ligation-Based qPCR Amplification Method for the Radiolabeling-Free Detection of Locus-Specific N⁶-Methyladenosine Modification', *Angew Chem Int Ed Engl*, vol. 57, no. 49, Dec 3, pp. 15995-16000.

Xuan, J-J, Sun, W-J, Lin, P-H, Zhou, K-R, Liu, S, Zheng, L-L, Qu, L-H & Yang, J-H 2017, 'RMBase v2.0: deciphering the map of RNA modifications from epitranscriptome sequencing data', *Nucleic Acids Research*, vol. 46, no. D1, pp. D327-D334.

Zhang, K, Zhang, Z, Kang, J, Chen, J, Liu, J, Gao, N, Fan, L, Zheng, P, Wang, Y & Sun, J 2020, 'CRISPR/Cas13d-Mediated Microbial RNA Knockdown', *Frontiers in bioengineering and biotechnology*, vol. 8, pp. 856-856.

Zhao, M, Morohashi, K, Hatlestad, G, Grotewold, E & Lloyd, A 2008, 'The TTG1-bHLH-MYB complex controls trichome cell fate and patterning through direct targeting of regulatory loci', *Development*, vol. 135, no. 11, Jun, pp. 1991-1999.

Zheng, G, Dahl, JA, Niu, Y, Fedorcsak, P, Huang, CM, Li, CJ, Vågbø, CB, Shi, Y, Wang, WL, Song, SH, Lu, Z, Bosmans, RP, Dai, Q, Hao, YJ, Yang, X, Zhao, WM, Tong, WM, Wang, XJ, Bogdan, F, Furu, K, Fu, Y, Jia, G, Zhao, X, Liu, J, Krokan, HE, Klungland, A, Yang, YG & He, C 2013, 'ALKBH5 is a mammalian RNA demethylase that impacts RNA metabolism and mouse fertility', *Mol Cell*, vol. 49, no. 1, Jan 10, pp. 18-29.

Zhong, S, Li, H, Bodi, Z, Button, J, Vespa, L, Herzog, M & Fray, RG 2008, 'MTA is an Arabidopsis messenger RNA adenosine methylase and interacts with a homolog of a sex-specific splicing factor', *The Plant Cell*, vol. 20, no. 5, pp. 1278-1288.

Chapter III: Towards targeted RNA 5-methylcytosine demethylation in plants

Abstract

Methylation at the fifth carbon on cytosine (5-methylcytosine, m⁵C) in DNA is well established as an important epigenetic regulator of gene expression. In contrast, the role and mechanism of this modification on RNA remains largely elusive, partly due to the lack of molecular tools to manipulate it with high specificity. Here, I report the utilization of two RNA binding platforms CRISPR-dCas13 and Short Tandem Target Mimic (STTM) for specific binding and altering m⁵C methylation status of mRNA targets in plants. Fusion of dCas13 to the human dioxygenase TET1 (hTET1) allowed removal of m⁵C on a sensor sequence detected via expression of conjugated Luciferase gene. The system also altered an endogenous m⁵C site on *MAIGO5* in *A. thaliana*, possibly converting it into the oxidized product 5-hydroxymethylcytosine (hm⁵C). Binding of STTM to target site, although hypothesized to interfere with m⁵C methyltransferase complex, might have led to degradation of non-modified target transcript, suggesting plausible alteration in secondary structure of the m⁵C-modified transcript. The study demonstrates, to my knowledge, the first manipulations on RNA m⁵C by a synthetic system in a highly programmable manner; and an initial failure in adopting an RNA-based system to modify RNA modification which however might have given us insight into the mode of action of an m⁵C site.

Introduction

As early as 1979, DNA m⁵C methylation was linked to regulation of gene expression (Jones & Taylor 1980; McGhee & Ginder 1979). Extensive studies over the years have provided relatively detailed insights about the mechanism and critical impacts of DNA m⁵C in a number of key developmental events such as embryogenesis, X-chromosome inactivation and genomic imprinting (Li, E, Beard & Jaenisch 1993; Mohandas, Sparkes & Shapiro 1981; Razin & Shemer 1995). DNA m⁵C is also well-known as a widespread strategy used by the cell to suppress gene expression in both prokaryotes and eukaryotes, although the DNA methylation landscape, global level and factors involved can differ drastically amongst taxa. For example, in plants, DNA demethylation is carried out through base-excision repair, while mammals likely utilize multi-step conversion of methylated to non-methylated base catalyzed by the DNA

m⁵C dioxygenase TEN-ELEVEN TRANSLOCATION protein family (Ito et al. 2011) (Figure III-1A). Interestingly, quite evolutionarily conserved, a number of enzymes taking part in DNA m⁵C metabolism also play roles in m⁵C methylation of RNA. For example, the DNA m⁵C methyltransferase DNMT2 can install m⁵C on RNA, along with a second class of RNA methyltransferase known as tRNA specific methyltransferase 4 or NOL1/NOP2/SUN domain protein 2 (TRM4/NSUN2). In *D. melanogaster*, the only ortholog of the DNA m⁵C dioxygenase TET family, dTET, instead catalyzes oxidation of RNA m⁵C into hm⁵C, but not DNA m⁵C. Human TET proteins were also reported with m⁵C dioxygenase activities on RNA *in vitro* and *in vivo*, with TET1 showing the highest activity (Fu et al. 2014; He, Chongsheng et al. 2021; Lan et al. 2020; Shen, H et al. 2021) (Figure III-1B). Despite sharing similarities in chemical properties and several enzymes involving its biology with the DNA counterpart, RNA m⁵C is still a relatively new and perplexing frontier.

Understanding of RNA m⁵C methylation has come mostly from studies on the mutations of the enzymes depositing and recognizing it, which often does not provide direct evidence and is poor in specificity due to global changes in the methylation landscape. The lack of specificity hamper confirmation and deeper understanding of RNA m⁵C's functions and mode of actions. Molecular tools that allow targeted manipulations of RNA m⁵C, for example specific removal, would greatly advance our understanding of this "epitranscriptomic" mark, yet have been absent from the field.

A tool that actively removes RNA m⁵C would essentially need to contain a domain capable of converting the methylated base back to conventional cytosine. On DNA, TET1 has been adopted to convert m⁵C into the oxidative product hm⁵C, allowing investigation of DNA m⁵C's functions in a number of studies in both animals and plants (Choudhury et al. 2016; Gallego-Bartolomé et al. 2018; Ji et al. 2018; Liu, XS et al. 2016). Given the lack of a known RNA m⁵C removing enzyme and the potential activities of TET1 on RNA m⁵C (Fu et al. 2014; Lan et al. 2020), TET1 stands out as a domain that could be harnessed for targeted RNA m⁵C-to-hm⁵C conversion, when tethered to a programmable RNA binding domain.

CRISPR-Cas13 is a highly specific and programmable RNA-guided RNA targeting system. Catalytically deactivated versions of Cas13 (dCas13) retain high binding affinity to target RNA and programmability provided by guide RNAs (Abudayyeh, Omar O. et al. 2017; Abudayyeh, Omar O. et al. 2016; Konermann et al. 2018; Smargon et al. 2017). Fusion of several dCas13 proteins from different bacterial species such as dLwaCas13a, dPspCas13b and dRfxCas13d with different RNA modifying domains has enabled successful RNA editing and targeted m⁶A methylation/demethylation in mammalian cells (Abudayyeh, O. O. et al. 2019; Cox et al. 2017; Li, Jiexin et al. 2020; Wilson et al. 2020; Xia et al. 2021), strongly highlighting the potential of dCas13 as RNA binding platform for targeted RNA m⁵C demethylation. In the present study, I tethered dLwaCas13a or dPspCas13b to the human dioxygenase TET1 (hTET1) to create a targeted m⁵C removing system dCas13-hTET1 (Figure III-1), specifically in plants.

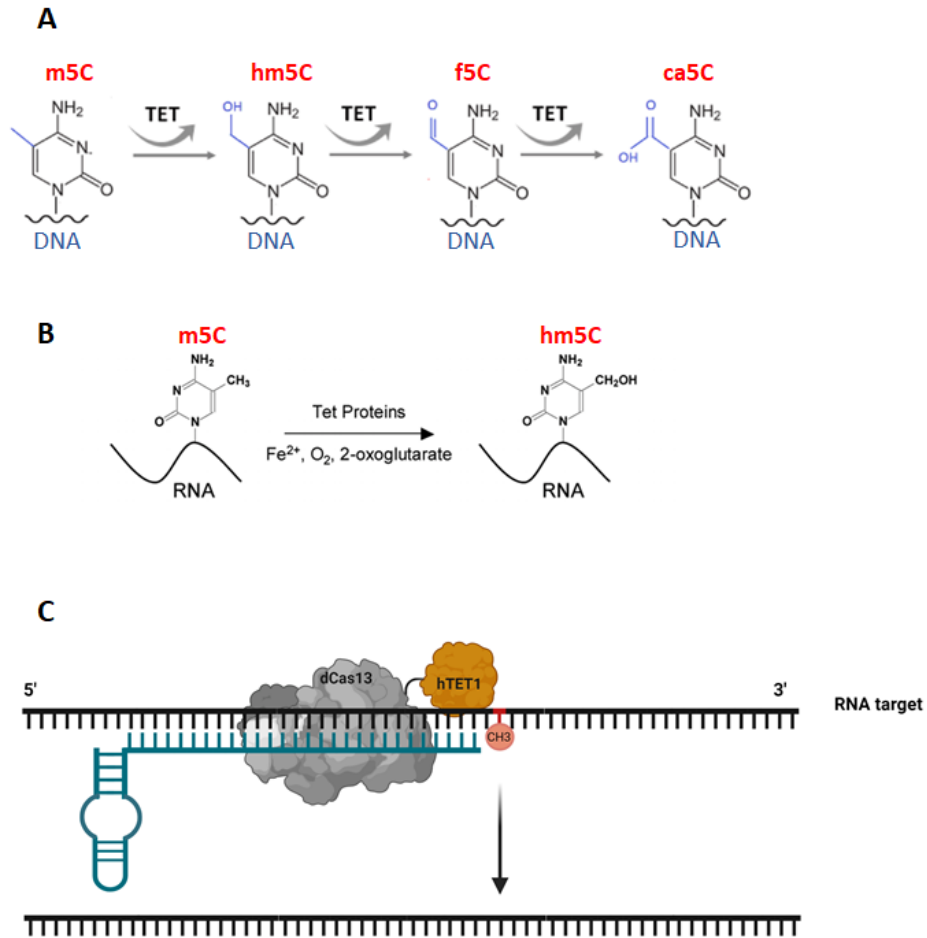


Figure III-1: Harnessing the human DNA dioxygenase TET1 (hTET1) and catalytically deactivated enzyme dCas13 for targeted RNA m⁵C demethylation. A, Serial oxidations catalyzed by hTET1 in DNA (Salomao et al 2019). 5-methylsytosine (m⁵C) is oxidized to cytosine (C) through intermediates 5-hydroxymethylcytosine (hm⁵C), 5-formylcytosine (f⁵C), and 5-carboxylcytosine (ca⁵C). These reactions may occur on RNA (Fu et al. 2014; Shen, Q et al. 2018), especially the first oxidation step (m⁵C to hm⁵C) (B,) was demonstrated *in vitro* (Fu et al 2014). C, hTET1 tethered to RNA-guided RNA binding protein dCas13 potentially can be directed to specific nucleotide(s) and enable oxidative conversion of RNA m⁵C.

In addition to active targeted RNA demethylation, interfering with deposition of a modification can also provide information about its importance, which could be achieved by selective binding of proteins or RNAs to the target site. Here, I explore the potential of Short Tandem Target Mimic (STTM) (Tang, G. et al. 2012), a RNA-based technique that binds and either sequesters or triggers degradation of microRNA targets, in binding to mRNA and interfering with activity of m⁵C methyltransferase(s). STTM itself is derived from Target Mimic (TM), a non-coding RNA of 542 nt containing imperfect binding site, with mismatches and a bulge, to a microRNA and sequesters microRNA away from its mRNA target (Franco-Zorrilla et al. 2007) (Figure III-2A). STTM instead has two perfect binding sites for microRNA, except the bulges, and a partially self-complementary central stem-loop (Figure III-2B). STTM rather triggers degradation of microRNAs in plants (Yan et al. 2012), although there was evidence of its inhibition/sequestration activity in animal cells (Tang, G. et al. 2012). Inspired by the activities of TM and STTM, and the notion that binding of microRNA to mRNA target can induce translation inhibition by altering the conformation of translating ribosomes (Ma, X et al. 2013), I designed and tested two RNA structures based on STTM with respect to their potential to bind to mRNA and interfere with m⁵C deposition by methyltransferases (Figure III-2C). In the two designs, the central stem-loop is partially self-complementary to stabilize the whole structure. Two binding sites of STTM and mutated STTM (mSTTM) either contain bulges (STTM) or no bulges (mSTTM). The design of STTM and/or mSTTM are expected to be stable, binds to mRNA target but does not cause cleavage, and prevent m⁵C methyltransferase(s) from depositing the mark on target (Figure III-2D).

Materials and methods

Plasmid construction

dCas13-(m)TET1: msfGFP-dLwaCas13a and dPspCas13b (4.4 kb and 3.3 kb respectively) gene fragments were amplified from plasmids pC035 and pC0054 (Addgene, Plasmids #91925 and #103870) and cloned into pMDC32 backbone by Gateway cloning to generate pCas13a and pCas13b, respectively. Sequence encoding catalytic domains of (m)hTET1 was amplified from pIRES-hrGFP II-(m)TET1-CD plasmid (Addgene, Plasmid #83568 and #83571) and inserted at 3' end of dCas13 genes by Gibson Assembly (Gibson et al. 2009). For expression of gRNA (including both intrinsic direct repeat (DR) and spacer which base-pairs with target), gene fragments of *AtU6-Bsalx2* or *AtU6-MluI-BclI* were ordered as geneBlocks (IDT) and inserted onto the pCas13-(m)TET1 plasmids. *AtU6-Bsalx2* or *AtU6-MluI-BclI* allows integration of new spacers to be expressed by *AtU6* by either conventional two step digestion-ligation DNA assembly or one step Golden gate cloning (Engler, Kandzia & Marillonnet 2008). Optimized protocol for Golden gate cloning including overnight incubation at 37°C and exclusion of the final 50°C incubation enabled highly reliable insertion of spacers to dCas13-TET1, which was confirmed by PCR of the insert, Sanger sequencing and additional enzyme digest and PCR of sequence flanking Bsal sites for a subset of constructs.

pEmpty and pGRNA: empty vector pEmpty which contains neither of dCas13-hTET1 nor gRNA cassette was generated by HindIII and SpeI double digest of pCas13 plasmid followed by T4 DNA ligation with a 24-nt filler sequence to replace the dCas13 fragment. Similarly, plasmids expressing gRNA only (pGRNA) were derived from respective complete dCas13-TET1 plasmids by removing dCas13-TET1 fragment with HindIII and SpeI double enzyme digest followed by T4 DNA ligation.

STTM and mSTTM: The backbone used to express STTM and mSTTM was a plant binary vector developed in our lab and successfully employed for blocking the function of a tRNA-derived small RNA (Zhao et al, unpublished data). STTM10, mSTTM1 and mSTTM10 sequences were ordered from Integrated DNA Technologies as four oligos (Supplementary Table III-S4), annealed and ligated into the backbone through SpeI and PaeI restriction sites for expression under an ACTIN2 promoter.

Agro-infiltration on *Nicotiana benthamiana*

Plasmids were transformed into *Agrobacterium tumefaciens* USDA by electroporation. USDA cultures of original pGrDL_SPb plasmid (Addgene, Plasmid #83205), m5C sensor reporter plasmid, dCas13-TET1 and control plasmids were incubated at 30°C overnight in Luria-Bertani broth supplemented with 50 ug/mL Kanamycin, 50 ug/mL Rifampicin, 25 uM acetosyringone and 20 mM MES. Cells were harvested and re-suspended in infiltration buffer (1x MS salt, 10 mM MES, 200 µM acetosyringone, 2% sucrose) to an OD of 1 (for reporter plasmid) or 0.8 (for all test plasmids). Each assayed plasmid suspension was mixed with reporter suspension of the same volume. As a result, the final OD of reporter was reduced to 0.5 after mixing with test plasmid, therefore a control suspension of reporter plasmid of OD 0.5 (obtained by mixing with equal volume of infiltration buffer) was included. All suspensions were left in dark for 2 hours before being infiltrated to abaxial side of *N. benthamiana* leaves with 1 mL needle-less syringes.

Dual Luciferase assay

A disk of 3-day post infiltration *N. benthamiana* leave (5mm in diameter) was harvested and snap frozen in liquid nitrogen. Dual Luciferase assay was performed with Dual-Luciferase Reporter Assay System (Promega) as followed: Samples were lyzed with a Tissue Lyser (QIAGEN) and dissolved in 500 uL of Passive Lysis Buffer (Promega), followed by centrifugation at 14000rpm/1 min. 15 uL of supernatant was used as input for Luminometer assay as per instructions by manufacturer on a GloMax Luminometer (Promega). For qualitative figures of chemiluminescence induced by Firefly Luciferase activities, infiltrated leaves were sprayed with 15 mg/mL D-Luciferin sodium salt substrate (Sigma) and subject to imaging with a Chemidoc CCD camera (Bio-rad) immediately. Images were processed with ImageJ.

Arabidopsis transformation and transgenic plant generation

dCas13-TET1, pEmpty, pGRNA or STTM constructs were introduced into *A. thaliana* (Col-0 ecotype) via floral dipping (Clough & Bent 1998). Transformants were selected on 15 ug/uL HygromycinB ½ MS medium (for dCas13 constructs) or on soil with 10ug/mL BASTA (Ammonium Glufosinate) treatment (for STTM constructs). Plants were grown in long day conditions (16-hour light/8-hour darkness) at 21°C.

RT-qPCR

Total RNA was extracted from 4-week old shoot tissues of wild-type, *trm4b-1* or transgenic plants with Spectrum Plant Total RNA extraction kit (Sigma). cDNA was synthesized with Superscript III Reverse transcriptase (Invitrogen) and used as input for quantification with FastStart SYBR Green Master Mix (Roche) on a QuantStudio 7 Flex System (Applied Biosystems). Biological duplicates and technical triplicates were assayed. *TUBULIN 2 (TUB2)* was used as internal control for normalization of transcripts.

BS-amp-seq library construction

Leaf samples of 4-week old transgenic plants were collected for RNA extraction with Spectrum Plant Total RNA extraction kit (Sigma). 1.5 ug total RNA was subject to BS treatment as described previously (David et al. 2017). Briefly, total RNA samples were incubated in Sodium metabisulfite and Hydroquinone for four hours, salts were removed by Micro Bio-spin columns in TRIS (Bio-rad, Cat #7326221) and precipitated with ethanol. BS-treated RNA was used as templates for cDNA synthesis with specific primers for MAG5. The cDNA then underwent the first round of PCR with CS primers and second PCR to add Barcode for Illumina Clustering. All primers for BS-amp-seq library preparation were described previously (David et al. 2017). Each PCR round was performed with four replicates for each amplicon. PCR products were purified with AMPure XP beads (Beckman) as per manufacturer's instructions. Sequencing was performed on a Miseq platform with a Miseq Micro kit (2 × 150 nucleotide paired end).

BS-amp-seq Data analysis

TrimGalore (<https://github.com/FelixKrueger/TrimGalore>) was used to remove adapters from Miseq reads. FastQC and ngsReports (Ward, To & Pederson 2019) were used for quality control of reads. Clean reads were then mapped to a reference (TAIR10_cds_20101214_updated) with meRanT (MeRanTK (Rieder et al. 2015)) in paired-end mode and m⁵C calling was subsequently performed for mapped reads with meRanCall (MeRanTK). A threshold of 1% methylation rate and False discovery rate of 0.01 were used for m⁵C calling.

Results

Design and construction of dCas13-TET1

RNA m⁵C is current a baffling research field and a system for targeted manipulation of this modification for its functional studies is much needed. To this end, I first developed a dCas13-TET1 fusion for active removal of an m⁵C site. The system contains two main components: dCas13-TET1 conjugates with either dLwaCas13a or dPspCas13b, and guide RNA(s) driven by an *AtU6* promoter. dLwaCas13a was derived from study by Abudayyeh, Omar O. et al. (2017) in which the protein was tethered to a monomeric superfolder GFP (msfGFP), enabling subcellular tracking of mRNAs. dPspCas13b was first harnessed for targeted RNA A-to-I editing by Cox et al. (2017) through its fusion with the RNA deaminase ADAR2, and was also successfully used in several other targeted RNA manipulation applications (Abudayyeh, O. O. et al. 2019). The two dCas13 orthologs are the first dCas13 adopted for such applications with high specificity and no reported toxicity as compared to the newer dCas13d ortholog (Buchman et al. 2020; Zhang et al. 2020). dLwaCas13a is about 100 amino acid larger than dPspCas13b, and the added msfGFP domain makes this protein even bigger (approx. 300 amino acid larger than dPspCas13b). However, msfGFP stabilized the dLwaCas13a, in a unclear mechanism (Abudayyeh, Omar O. et al. 2017), and can be used for checking the expression of the protein.

dCas13 presents an excellent RNA binding domain which guides TET1 to an m⁵C target. In order to enhance the specificity of dCas13-TET1, only the catalytic domain of hTET1 (Jin et al. 2014) was tethered to the C-terminus of dCas13 (Figure III-3A) through a three-amino acid Glycine-Serine-Glycine (GSG) linker which provides flexibility for the fusion protein (van Rosmalen, Krom & Merx 2017). Due to reported localization of the m⁵C methyltransferase TRM4B in nucleus in fission yeast (Matsuyama et al. 2006) and its predicted main nuclear localization in *A. thaliana* (Chou & Shen 2010; Hooper et al. 2017; Pierleoni et al. 2006), SV40 nuclear localization signals (NLSs) were added to the design of dCas13-TET1 to promote the demethylation efficiency. Similarly, a second fusion of dCas13b and catalytically inactive mTET1 was generated as a control.

The gRNAs comprising of both Cas13 intrinsic direct repeats (DRs) and spacers matching RNA target sequences for the dCas13-(m)TET1 system were expressed under the Pol III *AfU6* promoter. Hereby, “spacer” is used exclusively to refer to the target-binding sequence on a gRNA of dCas13-(m)TET1.

Both components of dCas13-(m)TET1 were combined on a single vector through several cloning steps (Figure III-3B). I generated two sets of vectors which differ in strategies utilized for integration of new spacers, either by Type II restriction enzymes, *MluI* & *BclI*, or Type IIS restriction enzyme *BsaI*. The latter allows convenient insertion of new spacers by one step Golden gate cloning (Engler, Kandzia & Marillonnet 2008) (Figure III-3B).

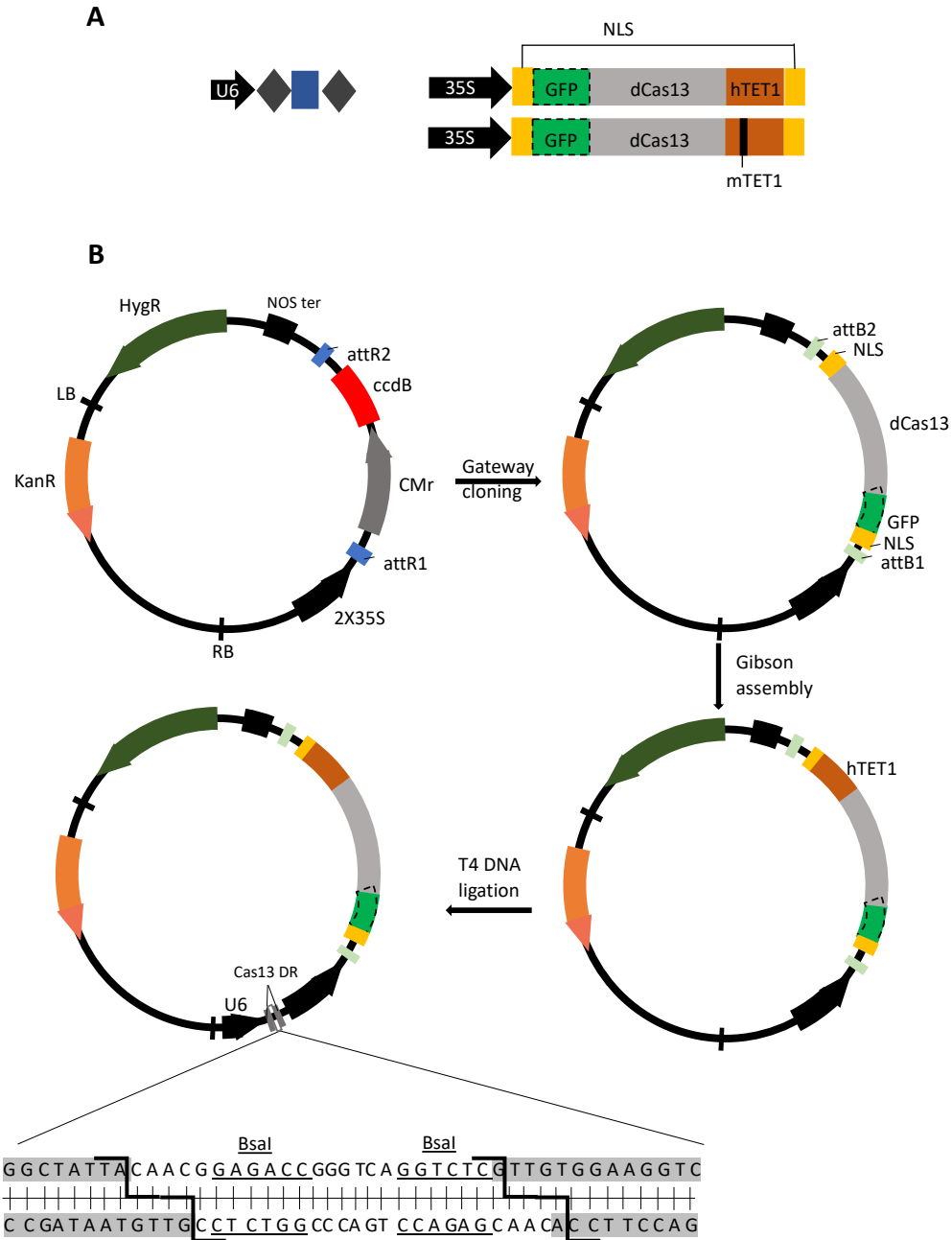


Figure III-3: Design and construction of dCas13-(m)TET1. A, Two components of dCas13-(m)TET1 are gRNA (including both DR - charcoal diamond, and spacer- navy rectangle) driven by *At*U6 promoter, and dCas13-(m)TET1 fusion flanked by SV40 NLSs. GFP domain in dashed box is present in constructs with dLwaCas13a only. B, Flow diagram of dCas13-(m)TET1 construction. New spacers can be cloned into the *Bsal* sites (underlined) by Golden gate cloning. DR, Direct Repeat specific for Cas13.

Characterization of dCas13-TET1 by transient expression in *N. benthamiana*

I utilized the msfGFP domain in dLwaCas13a-TET1 for visualization of the system's subcellular localization and confirmed its nuclear localization (Figure III-4A). However, due to the large size of the construct with dLwaCas13a, increasing data supporting high efficiency of fusion proteins utilizing dPspCas13b as RNA binding domain (Abudayyeh, O. O. et al. 2019; Anderson et al. 2019; Cox et al. 2017; Li, Jiexin et al. 2020; Wilson et al. 2020), and to reduce handling, I selected only the system with dPspCas13b for further experiments.

To assess the efficacy of dCas13b-TET1, I first performed a transient expression assay in *N. benthamiana*. The assay utilized a dual luciferase reporter plasmid previously developed in our lab which contains an m⁵C sensor fragment (Supplementary Information) derived from a transcriptome-wide mapping of m⁵C in *A. thaliana* (Li and Wu et al., unpublished data). Adding of this m⁵C fragment to the 5'UTR of Firefly Luciferase (FLuc) gene in the dual luciferase plasmid pDrDL_SPb (Plasmid #83205, Addgene) significantly enhances the FLuc protein activity when transiently expressed in *N. benthamiana* (Wu et al., unpublished data). I confirmed the observation in an independent experiment (Figure III-4C). Further analyses in our lab demonstrated a correlation between the increased FLuc activity and m⁵C methylation of the added sensor (Wu and Khanduja et al., unpublished data). Therefore, I adopted this reporter plasmid, co-introduced it with the dCas13-TET1 system into *N. benthamiana* (Figure III-4B) and looked for alteration in FLuc activity as an indication of m⁵C removal on the FLuc mRNA by dCas13b-TET1. Spacer targeting an m⁵C site on the sensor (Targeting gRNA 1) was integrated both into dCas13-TET1 and the catalytically inactive dCas13-mTET1 backbone. A second spacer binding toward the end of the FLuc CDS was also introduced into dCas13b-TET1 (Targeting gRNA 2) to test the effect of gRNA binding in a far distance (1.6 kb) (Figure III-4C). A Scramble gRNA and an empty vector (pEmpty) controls were included. Indeed, when the dCas13b-TET1 with either of the two targeting gRNAs were co-infiltrated into *N. benthamiana* with the m⁵C sensor plasmid, a reduction in FLuc activity compared to the m⁵C sensor alone was detected (Figure III-4C,D). In contrast, all the control plasmids with either inactive mTET1, the scrambled gRNA or empty vector did not result in obvious FLuc activity reduction.

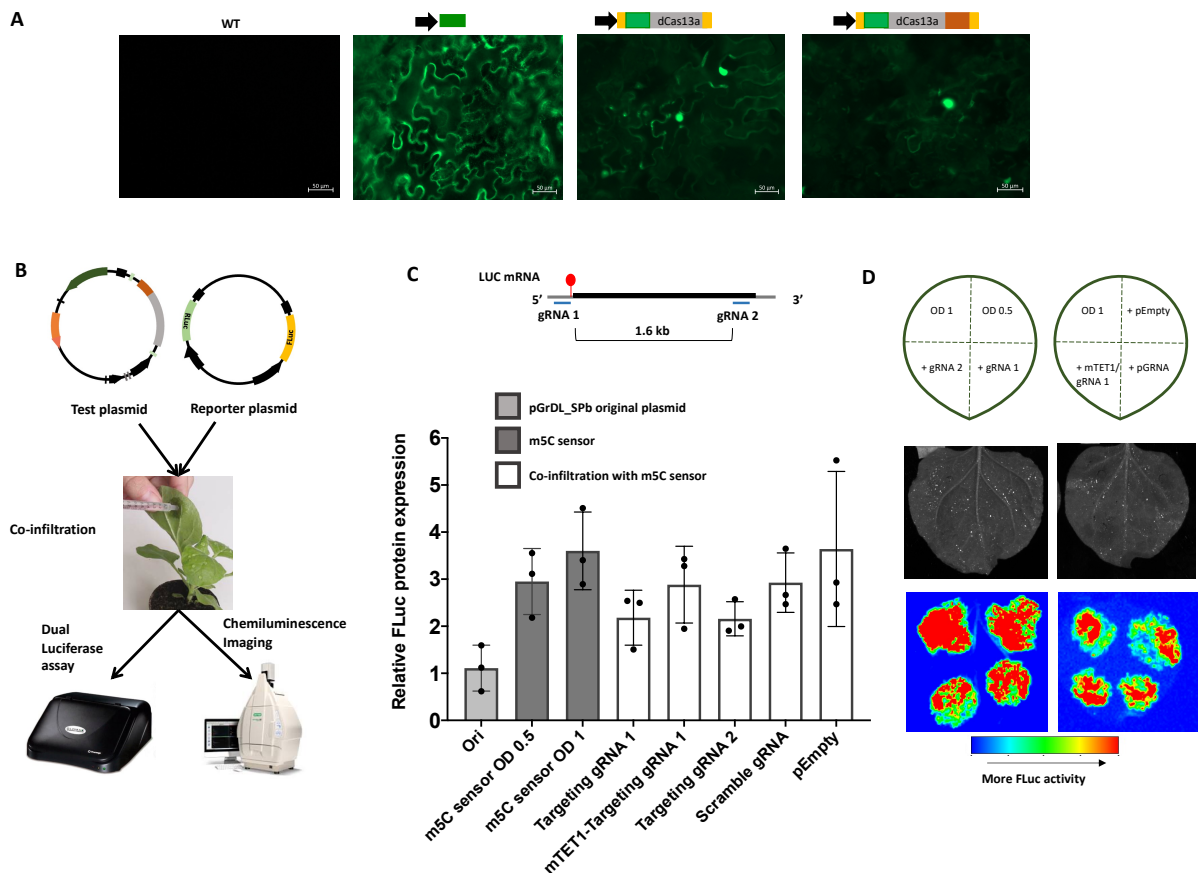


Figure III-4: Characterization of dCas13-TET1 in *N. benthamiana*. A, Nuclear localization of dCas13a and dCas13a-TET1 (3rd and 4th from left) was confirmed by transient expression in *N. benthamiana* and epifluorescence microscopy. msfGFP included in the dLwaCas13a (Abudayyeh, Omar O. et al. 2017) was utilized for visualization. A 35S::GFP transgenic plant (2nd from left) was imaged for comparison. Scale bar = 50 μ m. B, Workflow of co-infiltration and Dual-Luciferase assay for characterization of dCas13b-TET1 in *N. benthamiana*. Original dual luciferase reporter plasmid pGrDL_SPb was modified with insertion of an m⁵C sensor fragment at 5'UTR of the Firefly Luciferase gene (m⁵C sensor). The “m⁵C sensor” reporter plasmid was either co-infiltrated with each of test plasmids (listed in (C)), or infiltrated alone at OD of 0.5 or 1 into abaxial side of *N. benthamiana* leaf. The different ODs accommodated the actual OD of “m⁵C sensor” in each infiltration suspension (0.5) and the sum OD of “m⁵C sensor” and test plasmid when co-infiltrated (0.9) (refer to Methods for more details). 3-day post infiltration leaves were subject to Dual Luciferase assay with a

Luminometer or chemiluminescence imaging with a Chemidoc camera. C, Upper: Spacers design for targeting dCas13b-TET1 to m⁵C sensor conjugated to the Firefly Luciferase reporter gene. Lower: Relative FLuc activity (FLuc/RLuc) determined in Dual-Luciferase assay when the Luciferase reporter plasmid was introduced into *N. benthamiana* alone (steel bar) or with test plasmids (open bars). Ori, pGrDL_SPb original plasmid without m⁵C sensor. D, Qualitative detection of FLuc activity using chemiluminescence imaging. Infiltrated leaves were sprayed with D-Luciferin sodium salt substrate and imaged under a Chemidoc. Upper, schematic of infiltrated samples. Centre, white-light images of infiltrated leaf samples. Lower, chemiluminescence signals of infiltrated leaf samples. OD 1-OD 0.5, m⁵C sensor only at respective ODs. "+", co-infiltration with "m⁵C sensor". pGRNA, plasmid contains gRNA1 but not dCas13-TET1 cassette (Quantitative data for this sample is shown in Supplementary Figure III-S2). Scramble gRNA sample was not included.

m⁵C at C3349 on MAIGO5 (MAG5) as a potential endogenous target for testing of targeted m⁵C demethylation systems

To assess the activity of dCas13b-TET1 on endogenous targets, I first looked for a relatively highly methylated site that would allow reliable evaluation of the system's efficacy. Previously, a transcriptome-wide bisulfite sequencing in *A. thaliana* has revealed a 26-55% methylation at C3349 on *MAG5* mRNA (David et al. 2017). The methylation is tissue-specific and dependent on the *Arabidopsis* methyltransferase TRM4B (David et al., 2017). To gain more insight of the target and to expand the possible ways to use *MAG5* C3349 for monitoring the efficacy of a targeted RNA m⁵C demethylation system, I examined the effect of this m⁵C on *MAG5* mRNA abundance, as m⁵C has been reported to stabilize RNA transcripts (Cui et al. 2017; Warren et al. 2010). However, no effect of losing m⁵C on steady-state *MAG5* transcript abundance was detected (Supplementary Figure II-S1). While it is unclear what this methylation at *MAG5* C3349 does and no phenotypic defect associated with it has been reported *in planta*, high methylation level at this site compared to all other mapped m⁵C sites in *A. thaliana* (David et al 2017) makes it an exceptional target that can be used to assay the efficacy of a targeted RNA m⁵C demethylation system through direct monitoring of m⁵C level.

Efficacy of dCas13b-TET1 on *MAG5* C3349 determined by Bisulfite-amplicon-sequencing

I designed four spacers for dCas13b-TET1 to target C3349 on *MAG5* mRNA. Three spacers bind either zero, six or nine nt 5' to C3349 and were named gRNA0, gRNA6 and gRNA9, respectively. The fourth spacer, gRNA0-m, was derived from gRNA0 with two single-nucleotide deletions (Figure III-5A), aimed to test the impact of mismatches on dCas13-TET1's activity. Complete constructs were transformed into *A. thaliana*. Expression of dCas13b-TET1 mRNA in T₂ transgenic plants was confirmed using RT-qPCR (Supplementary Table III-S1).

To determine the m⁵C abundance at C3349 on *MAG5* mRNA in *MAG5*-targeting dCas13b-TET1 T₂ transgenic plants, Bisulfite-amplicon-sequencing (BS-amp-seq) and m⁵C-RIP-qPCR were planned. BS-amp-seq is derived from BS-RNA-seq and takes advantage of targeted amplification conferred by PCR for enrichment of sequences of interest prior to sequencing (David et al. 2017; Li, Jun et al. 2021). This method is convenient and reliable in identifying highly methylated sites to single nucleotide resolution. However, one limitation of BS-based methods is the inability to discriminate m⁵C and hm⁵C. Reason that hTET1 might further oxidize hm⁵C into 5-formylcytosine (f5C) or 5-carboxylcytosine (ca5C) (DeNizio et al. 2019; Fu et al. 2014) which can be distinguished from m⁵C and hm⁵C by BS-amp-seq, I first examined the occurrence of m⁵C/hm⁵C versus f5C/ca5C/C at C3349 on *MAG5* mRNA in dCas13b-TET1 gRNA0 and gRNA0-m T₂ transgenic plants with BS-amp-seq (Figure III-5B).

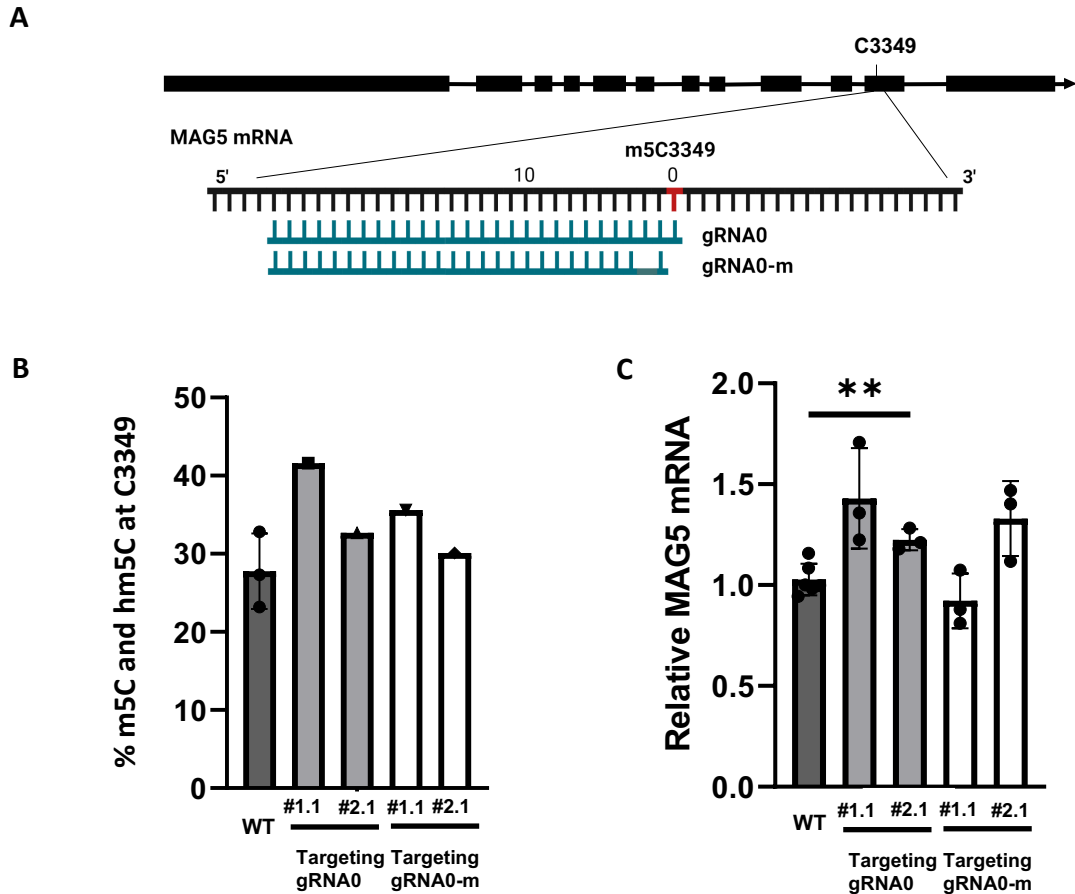


Figure III-5: Impact of stably expressed dCas13b-TET1 targeting *MAG5* C3349.

A, Upper, *MAG5* genomic structure. Black boxes and thin lines represent exons and introns, respectively. Lower, Spacer design to guide dCas13b-TET1 to C3349 on *MAG5* mRNA. Spacers are numbered relative to the methylated cytosine base. gRNA0-m contains two single-nucleotide deletions at position 1 and 3 compared to gRNA0. B, Combined m⁵C and hm⁵C level at *MAG5* C3349 in dCas13b-TET1 gRNA0 and gRNA0-m T₂ transgenic plants detected with BS-amp-seq. Plants of two independent transgenic lines, #1.1 and #2.1, for each construct were analyzed. Each T₂ line shown had one plant replicate however was prepared with four PCR replicates in BS-amp-seq library preparation (refer to Methods for more details). “% m⁵C and hm⁵C at C3349” was determined as percentage of non-converted cytosine in total coverage at the position 3349 on *MAG5*. C, Steady state *MAG5* mRNA abundance measured by RT-qPCR. Technical triplicates were performed. ACT2 was used for normalization. Error bars represent standard deviation of the mean. **, p value < 0.01 by Welch’s t-test.

Surprisingly, using BS-amp-seq, I did not detect reduction but slight to mild increase in m⁵C/hm⁵C level at *MAG5* C3349 in T₂ transgenic plants stably expressing dCas13b-TET1. Furthermore, transcript abundance of *MAG5* mRNA in three out of four transgenic lines tested appeared higher than that of wild-type (Figure III-5C). The results suggest that m⁵C-to-hm⁵C conversion might have occurred and altered mRNA abundance. I sought to confirm the BS-amp-seq results with m⁵C-RIP-qPCR, however could not finish the assay due to the time constraints.

Mutated STTM may cause degradation of non-m⁵C modified mRNA

Along with dCas13-TET1, two RNA designs adapted from the RNA-based technique STTM for binding and sequestering mRNA from being methylated was also examined. STTM10 was designed to cover a 50-nt region surrounding C3349 on *MAG5* mRNA, with the imperfect stem-loop being ten nt 5' of C3349 (Figure III-6A). A second design with no bulges in binding arms was named mutated STTM, or mSTTM. The structure of mSTTM is deemed to be stable thanks to the stem-loop, and bind to mRNA more efficiently than STTM does. Two mSTTM constructs with stem-loop being one or ten nt 5' of C3349 named mSTTM1 and mSTTM10, respectively, were generated (Figure III-6A, Supplementary Figure III-S3). Constructs were transformed into *A. thaliana*. Three independent lines of STTM10 and one line of each of mSTTM1 and mSTTM10 T₁ plants surviving BASTA herbicide selection were subject to BS-amp-seq to examine the change in m⁵C at *MAG5* C3349. However, one line of STTM10 and the mSTTM1 line gave 100% sensitivity to the herbicide in the next generation, another line of STTM10 grew poorly and barely set seeds. Due to the time constraints and presence of plasmid in these plants has not been confirmed, BS-amp-seq results obtained for these three lines were excluded from the main data (Figure III-6B) although within each kind of design (STTM or mSTTM) they showed similar m⁵C levels (Supplementary Figure III-S3). For the lines that still showed BASTA-resistance in T₂ generation, STTM10 exhibited a similar level of m⁵C abundance at *MAG5* C3349 compared to wild-type (Figure III-6B). Interestingly, m⁵C level at *MAG5* C3349 in mSTTM10 increased. I speculate that mSTTM10 might have triggered degradation of non-modified mRNA, causing the overall m⁵C level to rise. Another hypothesis is that binding of mSTTM10 somehow facilitated methyltransferases and enhanced m⁵C

deposition to the site. Unfortunately, confirmation and follow-up experiments could not be undertaken due to time constraints.

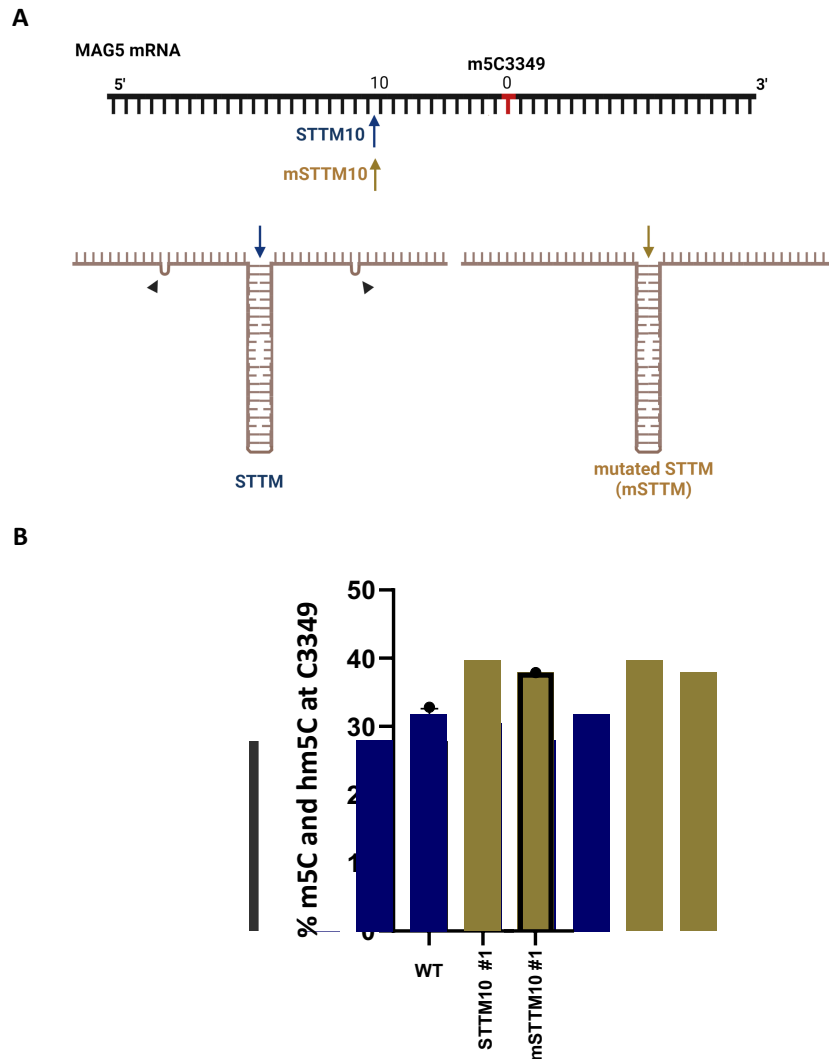


Figure III-6: Testing STTM for targeted prevention of RNA methylation. A, Design of STTM and mutated STTM (mSTTM) constructs for preventing methylation at *MAG5* C3349. STTM10 and mSTTM10 differ by the internal bulges in each binding arm (black arrow heads). Arrows indicate binding site of STTM10 and mSTTM10 to *MAG5* mRNA. B, Combined m⁵C and hm⁵C level at *MAG5* C3349 in STTM10 and mSTTM10 T₁ transgenic plants detected with BS-amp-seq. Each T₁ line shown had one plant replicate however was prepared with four PCR replicates in BS-amp-seq library preparation. The STTM10 line did not show reduction in m⁵C level at C3349 on *MAG5* while slight increase in m⁵C level at this site was observed in the mSTTM10 line. A total of five transgenic lines were assayed, however three lines exhibited 100% sensitivity to herbicide selection in T₂ generation and BS-amp-seq results for these lines are instead shown in Supplementary Figure III-S3.

Discussion

The lack of a system for specific manipulation, especially removal of RNA m⁵C is a big hamper in functional studies of the modification. Here, I offer insights into the potential application of two synthetic systems for targeted alteration of RNA m⁵C, dCas13-TET1 and STTM.

dCas13-TET1

dCas13-TET1 showed promising activity when transiently expressed in *N. benthamiana* to invert the effect of an m⁵C sensor. The high-variation nature of the Dual Luciferase assay prevented more detailed evaluation of the binding effect of dCas13 fusion through dCas13b-mTET1, or the off-target effect of dCas13b-TET1 through the construct with Scramble gRNA. Repeated and follow-up experiments with increased numbers of replicates will be required for more thorough assessment of the effect. In transgenic *A. thaliana*, dCas13b-TET1 altered overall m⁵C/hm⁵C level and the transcript abundance of *MAG5* mRNA. I speculate that a portion of m⁵C had been converted into hm⁵C which altered transcript's turn-over, and that the cell might have tried to compensate the m⁵C loss into hm⁵C with new m⁵C deposition. However, an assay to tease apart m⁵C and hm⁵C such as m⁵C -RIP-seq or direct RNA sequencing will be required to validate this hypothesis.

It is possible that the current design of dCas13-TET1 is not yet optimal. dCas13b-TET1 is designed to localize to the nucleus, which in theory will offer better demethylation efficiency and also ensure that an effect conferred by methylation inside the nucleus, for example on splicing, will not be overlooked. Nevertheless, I appreciate that a cytoplasm-localized system will also need to be examined for valid comparison.

The study presented here also provides more information on the behaviour of dCas13-based systems. gRNA of LwaCas13a was shown to be capable of inducing target degradation in mosquito cell which is independent to the activity of LwaCas13a wild-type enzyme (Tng et al. 2020). Here in plants, I showed that gRNAs of dPspCas13b alone did not lead to reduction in relative FLuc activity when transiently expressed in *N. benthamiana* (Supplementary Figure III-S2A) or reduce *MAG5* mRNA abundance when stably expressed in *A. thaliana* (Supplementary Figure III-S2B,C). It should be noted that in other animals, such gRNA-dependent target degradation effect has not

been reported. The effect observed in mosquito but not in plants or other animals could be due to different model organisms used, or of gRNA design. With respect to the latter possibility, Wang, Q et al. (2019) demonstrated the different effects of gRNAs sharing at least 20 nucleotides (out of 28 nucleotides) on inducing tumor cell death via Cas13's promiscuous RNA degradation activity (Abudayyeh, Omar O. et al. 2016; Cox et al. 2017; Konermann et al. 2018), suggesting that Cas13 gRNAs with subtle changes in design can behave or response differently to cellular factors.

STTM

It is known that expression of transgenes in *A. thaliana* can decrease as generations proceed (Ondrej et al 1999) and can vary amongst plants of the same generation due to a number of mechanisms such as somatic crossing over, RNA and epigenetic silencing or transgene rearrangement (Kohli et al. 2006). This might explain the loss of BASTA-resistance in several of STTM lines in this study. Nevertheless, it is notable that mSTTM10 caused m⁵C level to increase. While it is not clear how mSTTM10 but not STTM10 caused the effect, *MAG5* mRNA secondary structure likely plays an important role. As the first hypothesis, mSTTM10 might have enhanced the affinity and activity of m⁵C methyltransferases to *MAG5* by stabilizing its innate m⁵C-favourable secondary structure. Alternatively, binding of mSTTM10 might have triggered degradation of unmodified transcripts (but not modified ones), leading to the increased overall m⁵C level. This latter hypothesis in turn may imply that m⁵C-modified and non-modified *MAG5* transcripts have different secondary structures, with the unmodified transcripts being more susceptible to mSTTM-triggered degradation. In favour of this hypothesis, the structure of mSTTM with no bulges but the central stem-loop resembles a single binding arm of STTM that is sufficient to trigger degradation of small RNA in plants (Yan et al. 2012). Therefore, while the current design of either STTM10 or mSTTM10 led to interference with m⁵C methyltransferase as planned, the result obtained from mSTTM10 gave information about a possible mechanism that m⁵C methylation on *MAG5* mRNA might use for its effect.

Supplementary data

Supplementary Tables:

Supplementary Table III-S1: Expression of dCas13b-TET1 mRNA in dCas13b-TET1 *MAG5* targeted transgenic plants using RT-qPCR. Primers binding to dCas13b (Supplementary Table III-S2) were used to detect dCas13b-TET1 mRNA. C_t values for three technical replicates of each sample are shown.

Sample	Ct value
WT-1	Undetermined
WT-2	Undetermined
WT-3	Undetermined
gRNA0-1	24.027
gRNA0-2	24.002
gRNA0-3	24.256
gRNA0-m-1	22.693
gRNA0-m-2	22.737
gRNA0-m-3	22.915

Supplementary Table III-S2: Primers used for RT-qPCR in this chapter.

Cas13b_qF	CCCTTCATGATGGCGTAC
Cas13b_qR	CCGACAAAGGCGTGGTG
MAG5_qF	GGTGAAATCAACTCGGAAGGTG
MAG5_qR	GTTGGAGGAGGAGGTAGTGCAG

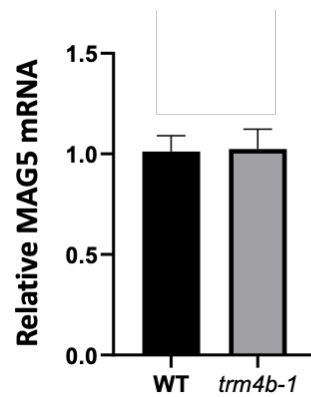
Supplementary Table III-S3: Spacer/gRNA sequences used in this study. Red letters denote overhangs for ligation into respective backbone (via 2x BsaI or MluI/BclI sites)

Transient expression assay in <i>N. benthamiana</i>	
Scramble-F	CAAC GCTAGCTAGCGGCATCATTGACCATACT G
Scramble-R	ACAAC AGTATGGTCAATGATGCCGCTAGCTAGC
Targeting gRNA 2-F	CAAC CCGGTAAGACCTTTCGGTACTTCGTCCA G
Targeting gRNA 2-R	ACAAC TGGACGAAGTACCGAAAGGTCTTACCGG
Targeting gRNA 1-F	CAAC TTTATGATTTTGTGTCTGAAAAATGTTT G
Targeting gRNA 1-R	ACAAC AACATTTTTTCAGACACAAAATCATAAA
<i>A. thaliana</i> transgenic plant	
MAG5A_gRNA_0_F	ACGCGT GGGGATTAGACTACCCCAAAAACGAAGG GGACTAAAACGGGGTTCCACACCTCTTCCACCCATCT TTTTTT
MAG5A_gRNA_0_R	TGATCAAAAAAAGATGGGTGGAAAGAGGTGTGGA ACCCGTTTTAGTCCCCTTCGTTTTTGGGGTAGTCTAAATCCCC

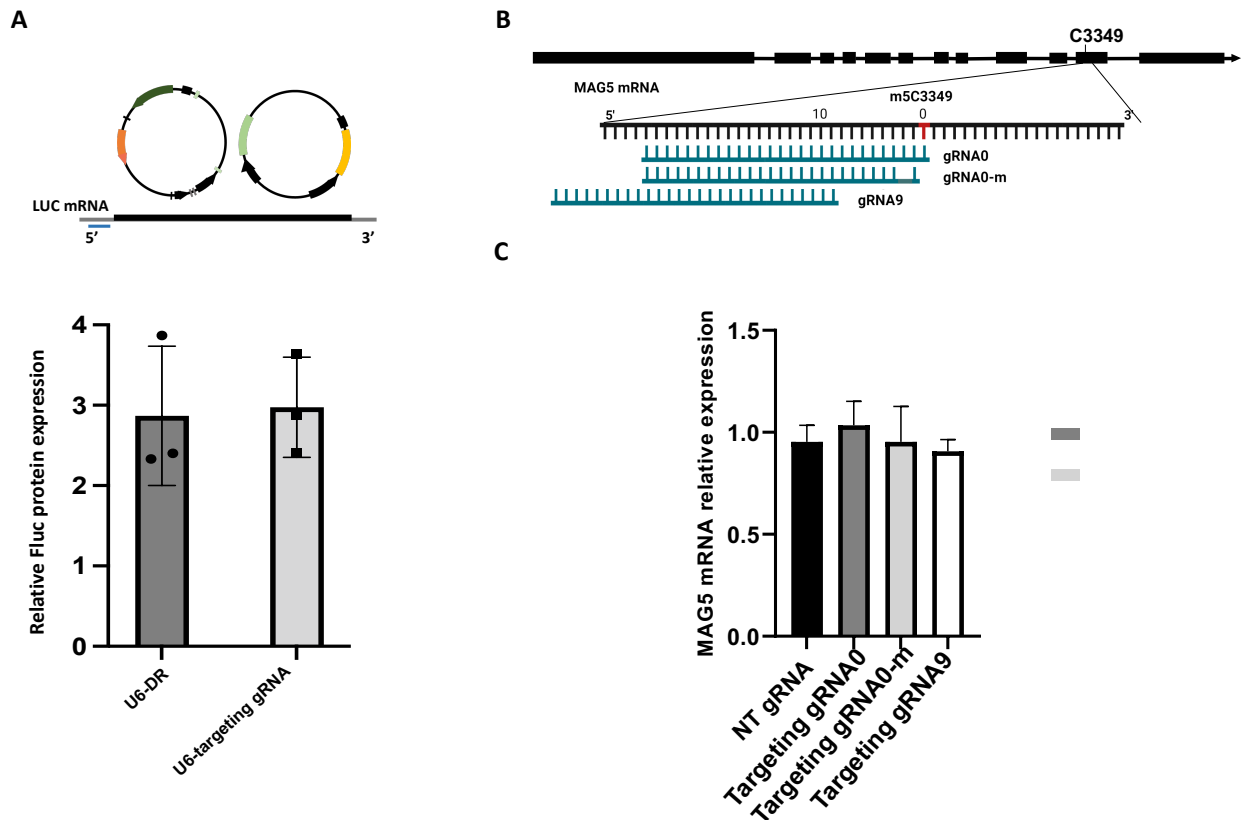
Supplementary Table III-S4: Sequences of STTM and mSTTM. Red letters denote bulges in binding arms, lowercase letters denote stem-loop. Each design was ordered as two fragments (f1 and f2) and anneal together before being cloned into the backbone.

STTM10-f1-F	C TCCTCAGCTGG CTA GGGTCCACA gttgtgtgttatggtctaatttaaat
STTM10-f1-R	aattagaccataacaacaacaacTGTGGAACCC TAG CCAGCTGAGGAGAGCT
STTM10-f2-F	atggtctaaagaagaagaat CCTCTTCCAC CTA CCATCTCTT A
STTM-10-f2-R	CTAGTAAAGAGATGG TAG GTGGAAAGAGGattcttctctttagaccatattta
mSTTM-10-f1-F	C TCCTCAGCTGGGGGTCCACA gttgtgtgttatggtctaatttaaat
mSTTM-10-f1-R	aattagaccataacaacaacaacTGTGGAACCCCCAGCTGAGGAGAGCT
mSTTM-10-f2-F	atggtctaaagaagaagaat CCTCTTCCACCCATCTCTT A
mSTTM-10-f2-R	CTAGTAAAGAGATGGGTGGAAAGAGGattcttctctttagaccatattta
mSTTM-1-f1-F	C AGTGCAGCTTCCTCAGCTGGG gttgtgtgttatggtctaatttaaat
mSTTM-1-f1-R	aattagaccataacaacaacaacCCCAGCTGAGGAAGCTGCACTGAGCT
mSTTM-1-f2-F	atggtctaaagaagaagaat GGTCCACACCTCTTCCACC A
mSTTM-1-f2-R	CTAGTGGTGGAAAGAGGTGTGGAACCattcttctctttagaccatattta

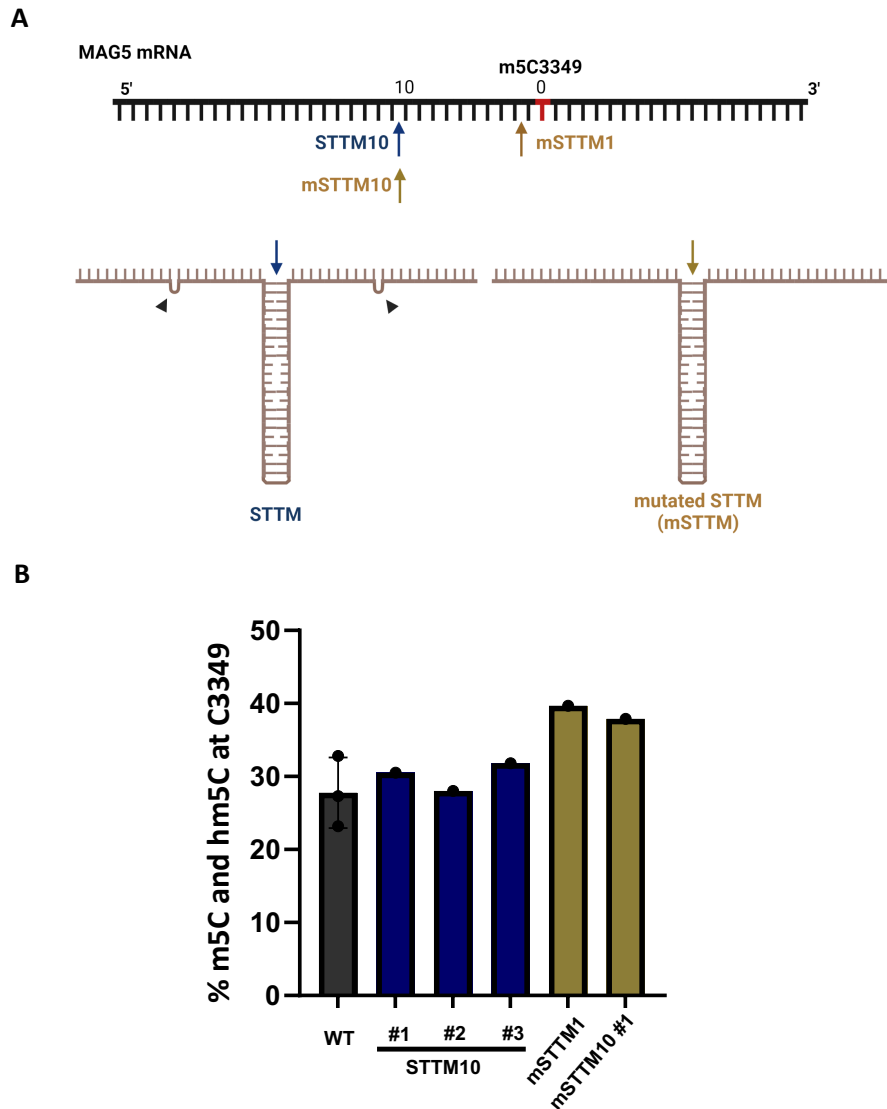
Supplementary Figures:



Supplementary Figure III-S1: *MAG5* mRNA abundance in wild-type *A. thaliana* and *tm4b-1* determined by RT-qPCR. Technical triplicates were performed. Error bars represent standard deviation of mean. *ACT2* was an internal control.



Supplementary Figure III-S2: PspCas13b gRNA alone did not induce target degradation when transiently expressed in *N. benthamiana* (A) or stably expressed in *A. thaliana* (B-C). A, Upper, pGRNA plasmid containing only gRNA but not dCas13-TET1 was co-infiltrated with the “m⁵C sensor” reporter into *N. benthamiana* leaves. Centre, Spacer design for the pGRNA plasmid to target FLuc mRNA. Lower, Relative FLuc activity determined by Dual Luciferase assay for 3-day post infiltration leaves. B, Positioning of spacers for pGRNA to target *MAG5* mRNA in *A. thaliana*. C, *MAG5* mRNA abundance in plants expressing the pGRNA transgenes in (B), measured by RT-qPCR. Biological duplicates and technical triplicates were performed. *ACT2* was an internal control. Error bars represent standard deviation of mean. NT: non-targeting gRNA.



Supplementary Figure III-S3: Testing STTM for targeted prevention of RNA methylation (Additional data for Figure III-6). A, Design of STTM and mutated STTM (mSTTM) constructs for preventing methylation at *MAG5* C3349. STTM and mSTTM differ by the internal bulges in each binding arm (black arrow heads). Arrows indicate binding site of STTM and mSTTM to *MAG5* mRNA. B, Combined m⁵C and hm⁵C level at *MAG5* C3349 in STTM10, mSTTM1 and mSTTM10 T₁ transgenic plants detected with BS-amp-seq. Note that line #3 of STTM10 and the mSTTM1 line showed 100% sensitivity to BASTA selection in T₂ generation and expression of respective STTM or mSTTM in these plants have not been confirmed. Line #2 of STTM10 barely set seeds. Line #1 of STTM10 and mSTTM10 shown in Figure III-6 are also placed here for comparison.

Supplementary Information: Sequence of m⁵C sensor fragment used in transient expression assay (Figure III-4) (Li and Wu et al., unpublished data).
UPPERCASE letters denote m⁵C sites mapped in *A. thaliana*

acattctgatagatacaaaaaaCatttttCagaCaCaaaatCataaaatCttgccttagtagatCaaagttctta

References

- Abudayyeh, OO, Gootenberg, JS, Essletzbichler, P, Han, S, Joung, J, Belanto, JJ, Verdine, V, Cox, DBT, Kellner, MJ, Regev, A, Lander, ES, Voytas, DF, Ting, AY & Zhang, F 2017, 'RNA targeting with CRISPR-Cas13', *Nature*, vol. 550, no. 7675, 2017/10/01, pp. 280-284.
- Abudayyeh, OO, Gootenberg, JS, Franklin, B, Koob, J, Kellner, MJ, Ladha, A, Joung, J, Kirchgatterer, P, Cox, DBT & Zhang, F 2019, 'A cytosine deaminase for programmable single-base RNA editing', *Science*, vol. 365, no. 6451, Jul 26, pp. 382-386.
- Abudayyeh, OO, Gootenberg, JS, Konermann, S, Joung, J, Slaymaker, IM, Cox, DBT, Shmakov, S, Makarova, KS, Semenova, E, Minakhin, L, Severinov, K, Regev, A, Lander, ES, Koonin, EV & Zhang, F 2016, 'C2c2 is a single-component programmable RNA-guided RNA-targeting CRISPR effector', *Science*, vol. 353, no. 6299, p. aaf5573.
- Anderson, KM, Poosala, P, Lindley, SR & Anderson, DM 2019, 'Targeted Cleavage and Polyadenylation of RNA by CRISPR-Cas13', *bioRxiv*, p. 531111.
- Buchman, AB, Brogan, DJ, Sun, R, Yang, T, Hsu, PD & Akbari, OS 2020, 'Programmable RNA Targeting Using CasRx in Flies', *The CRISPR journal*, vol. 3, no. 3, pp. 164-176.
- Chou, K-C & Shen, H-B 2010, 'Plant-mPLoc: A Top-Down Strategy to Augment the Power for Predicting Plant Protein Subcellular Localization', *PLOS ONE*, vol. 5, no. 6, p. e11335.
- Choudhury, SR, Cui, Y, Lubecka, K, Stefanska, B & Irudayaraj, J 2016, 'CRISPR-dCas9 mediated TET1 targeting for selective DNA demethylation at BRCA1 promoter', *Oncotarget*, vol. 7, no. 29, pp. 46545-46556.
- Clough, SJ & Bent, AF 1998, 'Floral dip: a simplified method for Agrobacterium-mediated transformation of *Arabidopsis thaliana*', *Plant J*, vol. 16, no. 6, Dec, pp. 735-743.
- Cox, DBT, Gootenberg, JS, Abudayyeh, OO, Franklin, B, Kellner, MJ, Joung, J & Zhang, F 2017, 'RNA editing with CRISPR-Cas13', *Science*, vol. 358, no. 6366, Nov 24, pp. 1019-1027.
- Cui, X, Liang, Z, Shen, L, Zhang, Q, Bao, S, Geng, Y, Zhang, B, Leo, V, Vardy, LA, Lu, T, Gu, X & Yu, H 2017, '5-Methylcytosine RNA Methylation in *Arabidopsis Thaliana*', *Molecular Plant*, vol. 10, no. 11, pp. 1387-1399.

David, R, Burgess, A, Parker, B, Li, J, Pulsford, K, Sibbritt, T, Preiss, T & Searle, IR 2017, 'Transcriptome-Wide Mapping of RNA 5-Methylcytosine in Arabidopsis mRNAs and Noncoding RNAs', *Plant Cell*, vol. 29, no. 3, Mar, pp. 445-460.

DeNizio, JE, Liu, MY, Leddin, EM, Cisneros, GA & Kohli, RM 2019, 'Selectivity and Promiscuity in TET-Mediated Oxidation of 5-Methylcytosine in DNA and RNA', *Biochemistry*, vol. 58, no. 5, 2019/02/05, pp. 411-421.

Engler, C, Kandzia, R & Marillonnet, S 2008, 'A One Pot, One Step, Precision Cloning Method with High Throughput Capability', *PLOS ONE*, vol. 3, no. 11, p. e3647.

Franco-Zorrilla, JM, Valli, A, Todesco, M, Mateos, I, Puga, MI, Rubio-Somoza, I, Leyva, A, Weigel, D, García, JA & Paz-Ares, J 2007, 'Target mimicry provides a new mechanism for regulation of microRNA activity', *Nature Genetics*, vol. 39, no. 8, 2007/08/01, pp. 1033-1037.

Fu, L, Guerrero, CR, Zhong, N, Amato, NJ, Liu, Y, Liu, S, Cai, Q, Ji, D, Jin, S-G, Niedernhofer, LJ, Pfeifer, GP, Xu, G-L & Wang, Y 2014, 'Tet-Mediated Formation of 5-Hydroxymethylcytosine in RNA', *Journal of the American Chemical Society*, vol. 136, no. 33, 2014/08/20, pp. 11582-11585.

Gallego-Bartolomé, J, Gardiner, J, Liu, W, Papikian, A, Ghoshal, B, Kuo, HY, Zhao, JM-C, Segal, DJ & Jacobsen, SE 2018, 'Targeted DNA demethylation of the Arabidopsis genome using the human TET1 catalytic domain', *Proceedings of the National Academy of Sciences*, vol. 115, no. 9, p. E2125.

Gibson, DG, Young, L, Chuang, R-Y, Venter, JC, Hutchison, CA & Smith, HO 2009, 'Enzymatic assembly of DNA molecules up to several hundred kilobases', *Nature Methods*, vol. 6, no. 5, 2009/05/01, pp. 343-345.

He, C, Bozler, J, Janssen, KA, Wilusz, JE, Garcia, BA, Schorn, AJ & Bonasio, R 2021, 'TET2 chemically modifies tRNAs and regulates tRNA fragment levels', *Nature Structural & Molecular Biology*, vol. 28, no. 1, 2021/01/01, pp. 62-70.

Hooper, CM, Castleden, IR, Tanz, SK, Aryamanesh, N & Millar, AH 2017, 'SUBA4: the interactive data analysis centre for Arabidopsis subcellular protein locations', *Nucleic Acids Res*, vol. 45, no. D1, Jan 4, pp. D1064-d1074.

Ito, S, Shen, L, Dai, Q, Wu, SC, Collins, LB, Swenberg, JA, He, C & Zhang, Y 2011, 'Tet proteins can convert 5-methylcytosine to 5-formylcytosine and 5-carboxylcytosine', *Science*, vol. 333, no. 6047, Sep 2, pp. 1300-1303.

Ji, L, Jordan, WT, Shi, X, Hu, L, He, C & Schmitz, RJ 2018, 'TET-mediated epimutagenesis of the Arabidopsis thaliana methylome', *Nature Communications*, vol. 9, no. 1, pp. 895-895.

Jin, C, Lu, Y, Jelinek, J, Liang, S, Estecio, MR, Barton, MC & Issa, JP 2014, 'TET1 is a maintenance DNA demethylase that prevents methylation spreading in differentiated cells', *Nucleic Acids Res*, vol. 42, no. 11, Jun, pp. 6956-6971.

Jones, PA & Taylor, SM 1980, 'Cellular differentiation, cytidine analogs and DNA methylation', *Cell*, vol. 20, no. 1, May, pp. 85-93.

Kohli, A, Melendi, PG, Abranches, R, Capell, T, Stoger, E & Christou, P 2006, 'The Quest to Understand the Basis and Mechanisms that Control Expression of Introduced Transgenes in Crop Plants', *Plant signaling & behavior*, vol. 1, no. 4, pp. 185-195.

Konermann, S, Lotfy, P, Brideau, NJ, Oki, J, Shokhirev, MN & Hsu, PD 2018, 'Transcriptome Engineering with RNA-Targeting Type VI-D CRISPR Effectors', *Cell*, vol. 173, no. 3, pp. 665-676.e614.

Lan, J, Rajan, N, Bizet, M, Penning, A, Singh, NK, Guallar, D, Calonne, E, Li Greci, A, Bonvin, E, Deplus, R, Hsu, PJ, Nachtergaele, S, Ma, C, Song, R, Fuentes-Iglesias, A, Hassabi, B, Putmans, P, Mies, F, Menschaert, G, Wong, J, Wang, J, Fidalgo, M, Yuan, B & Fuks, F 2020, 'Functional role of Tet-mediated RNA hydroxymethylcytosine in mouse ES cells and during differentiation', *Nature Communications*, vol. 11, no. 1, 2020/10/02, p. 4956.

Li, E, Beard, C & Jaenisch, R 1993, 'Role for DNA methylation in genomic imprinting', *Nature*, vol. 366, no. 6453, 1993/12/01, pp. 362-365.

Li, J, Chen, Z, Chen, F, Xie, G, Ling, Y, Peng, Y, Lin, Y, Luo, N, Chiang, C-M & Wang, H 2020, 'Targeted mRNA demethylation using an engineered dCas13b-ALKBH5 fusion protein', *Nucleic Acids Research*, vol. 48, no. 10, pp. 5684-5694.

Li, J, Wu, X, Do, T, Nguyen, V, Zhao, J, Ng, PQ, Burgess, A, David, R & Searle, IR 2021, 'Quantitative and Single-Nucleotide Resolution Profiling of RNA 5-Methylcytosine', *Methods in molecular biology*, vol. 2298, pp. 135-151.

Liu, XS, Wu, H, Ji, X, Stelzer, Y, Wu, X, Czauderna, S, Shu, J, Dadon, D, Young, RA & Jaenisch, R 2016, 'Editing DNA Methylation in the Mammalian Genome', *Cell*, vol. 167, no. 1, pp. 233-247.e217.

Ma, X, Kim, E-J, Kook, I, Ma, F, Voshall, A, Moriyama, E & Cerutti, H 2013, 'Small interfering RNA-mediated translation repression alters ribosome sensitivity to

inhibition by cycloheximide in *Chlamydomonas reinhardtii*', *The Plant Cell*, vol. 25, no. 3, pp. 985-998.

Matsuyama, A, Arai, R, Yashiroda, Y, Shirai, A, Kamata, A, Sekido, S, Kobayashi, Y, Hashimoto, A, Hamamoto, M, Hiraoka, Y, Horinouchi, S & Yoshida, M 2006, 'ORFeome cloning and global analysis of protein localization in the fission yeast *Schizosaccharomyces pombe*', *Nature Biotechnology*, vol. 24, no. 7, 2006/07/01, pp. 841-847.

McGhee, JD & Ginder, GD 1979, 'Specific DNA methylation sites in the vicinity of the chicken beta-globin genes', *Nature*, vol. 280, no. 5721, Aug 2, pp. 419-420.

Mohandas, T, Sparkes, RS & Shapiro, LJ 1981, 'Reactivation of an inactive human X chromosome: evidence for X inactivation by DNA methylation', *Science*, vol. 211, no. 4480, Jan 23, pp. 393-396.

Pierleoni, A, Martelli, PL, Fariselli, P & Casadio, R 2006, 'BaCellLo: a balanced subcellular localization predictor', *Bioinformatics*, vol. 22, no. 14, pp. e408-e416.

Razin, A & Shemer, R 1995, 'DNA methylation in early development', *Hum Mol Genet*, vol. 4 Spec No, pp. 1751-1755.

Rieder, D, Amort, T, Kugler, E, Lusser, A & Trajanoski, Z 2015, 'meRanTK: methylated RNA analysis ToolKit', *Bioinformatics*, vol. 32, no. 5, pp. 782-785.

Shen, H, Ontiveros, RJ, Owens, MC, Liu, MY, Ghanty, U, Kohli, RM & Liu, KF 2021, 'TET-mediated 5-methylcytosine oxidation in tRNA promotes translation', *Journal of Biological Chemistry*, vol. 296.

Shen, Q, Zhang, Q, Shi, Y, Shi, Q, Jiang, Y, Gu, Y, Li, Z, Li, X, Zhao, K, Wang, C, Li, N & Cao, X 2018, 'Tet2 promotes pathogen infection-induced myelopoiesis through mRNA oxidation', *Nature*, vol. 554, no. 7690, 2018/02/01, pp. 123-127.

Smargon, AA, Cox, DBT, Pyzocha, NK, Zheng, K, Slaymaker, IM, Gootenberg, JS, Abudayyeh, OA, Essletzbichler, P, Shmakov, S, Makarova, KS, Koonin, EV & Zhang, F 2017, 'Cas13b Is a Type VI-B CRISPR-Associated RNA-Guided RNase Differentially Regulated by Accessory Proteins Csx27 and Csx28', *Mol Cell*, vol. 65, no. 4, Feb 16, pp. 618-630.e617.

Tang, G, Yan, J, Gu, Y, Qiao, M, Fan, R, Mao, Y & Tang, X 2012, 'Construction of short tandem target mimic (STTM) to block the functions of plant and animal microRNAs', *Methods*, vol. 58, no. 2, Oct, pp. 118-125.

Tng, PYL, Carabajal Paladino, L, Verkuil, SAN, Purcell, J, Merits, A, Leftwich, PT, Fragkoudis, R, Noad, R & Alphey, L 2020, 'Cas13b-dependent and Cas13b-independent RNA knockdown of viral sequences in mosquito cells following guide RNA expression', *Communications Biology*, vol. 3, no. 1, 2020/07/31, p. 413.

van Rosmalen, M, Krom, M & Merks, M 2017, 'Tuning the Flexibility of Glycine-Serine Linkers To Allow Rational Design of Multidomain Proteins', *Biochemistry*, vol. 56, no. 50, 2017/12/19, pp. 6565-6574.

Wang, Q, Liu, X, Zhou, J, Yang, C, Wang, G, Tan, Y, Wu, Y, Zhang, S, Yi, K & Kang, C 2019, 'The CRISPR-Cas13a Gene-Editing System Induces Collateral Cleavage of RNA in Glioma Cells', *Advanced Science*, vol. 6, no. 20, p. 1901299.

Ward, CM, To, T-H & Pederson, SM 2019, 'ngsReports: a Bioconductor package for managing FastQC reports and other NGS related log files', *Bioinformatics*, vol. 36, no. 8, pp. 2587-2588.

Warren, L, Manos, PD, Ahfeldt, T, Loh, YH, Li, H, Lau, F, Ebina, W, Mandal, PK, Smith, ZD, Meissner, A, Daley, GQ, Brack, AS, Collins, JJ, Cowan, C, Schlaeger, TM & Rossi, DJ 2010, 'Highly efficient reprogramming to pluripotency and directed differentiation of human cells with synthetic modified mRNA', *Cell Stem Cell*, vol. 7, no. 5, Nov 5, pp. 618-630.

Wilson, C, Chen, PJ, Miao, Z & Liu, DR 2020, 'Programmable m⁶A modification of cellular RNAs with a Cas13-directed methyltransferase', *Nature Biotechnology*, vol. 38, no. 12, 2020/12/01, pp. 1431-1440.

Xia, Z, Tang, M, Ma, J, Zhang, H, Gimple, RC, Prager, BC, Tang, H, Sun, C, Liu, F, Lin, P, Mei, Y, Du, R, Rich, JN & Xie, Q 2021, 'Epitranscriptomic editing of the RNA N⁶-methyladenosine modification by dCasRx conjugated methyltransferase and demethylase', *Nucleic Acids Research*, vol. 49, no. 13, pp. 7361-7374.

Yan, J, Gu, Y, Jia, X, Kang, W, Pan, S, Tang, X, Chen, X & Tang, G 2012, 'Effective Small RNA Destruction by the Expression of a Short Tandem Target Mimic in Arabidopsis', *The Plant Cell*, vol. 24, no. 2, pp. 415-427.

Zhang, K, Zhang, Z, Kang, J, Chen, J, Liu, J, Gao, N, Fan, L, Zheng, P, Wang, Y & Sun, J 2020, 'CRISPR/Cas13d-Mediated Microbial RNA Knockdown', *Frontiers in bioengineering and biotechnology*, vol. 8, pp. 856-856.

**Chapter IV: Deciphering RNA 5-methylcytosine in
Arabidopsis thaliana's root development**

Abstract

The importance of plant roots to plant growth and the soil ecosystem has made root development a major focus in plant research. Studies over many decades have gained valuable insights into the molecular network controlling root development but a detailed understanding of all factors influencing root growth remains to be elucidated. The RNA modification 5-methylcytosine (m^5C) has emerged as an additional mediator of root development but the causal m^5C -bearing transcripts and underlying mechanism are poorly understood. In this chapter, I combined different approaches to understand the mechanism of m^5C regulation on *A. thaliana* primary root development. Phenotypical and molecular analyses ruled out a major role for previously described *SHORT HYPOCOTYL 2 (SHY2/IAA3)* and *IAA16* in root growth regulation by RNA m^5C . Mapping of m^5C on these two transcripts further suggested a sparse or spatially and temporally confined methylation. Functional analysis of the only identified m^5C site on *SHY2/IAA3* mRNA did not support its importance *in planta* despite its potential evolutionary conservation found a bioinformatic analysis. Collectively, results in this study contribute to a more comprehensive picture of m^5C regulation in root growth, suggesting a higher complexity of this modification's mode of action that might have not been fully appreciated.

Introduction

Intense research on plant models such as *A. thaliana* over several decades has shed lights on a number of key regulators and underlying mechanisms of root development (Augstein & Carlsbecker 2018; Koevoets et al. 2016; Petricka, Winter & Benfey 2012). Phytohormones such as auxin (Went 1929; Thimann and Went 1934) are among the most important and influential factors, controlling virtually all aspects of root growth. An extensive body of research has developed, highlighting the central role of this hormone in orchestrating diverse pathways to give rise to the root architecture (Leyser 2018; Overvoorde, Fukaki & Beeckman 2010). Auxin exerts its regulatory effects largely via the auxin signaling pathway which deals with transcriptional regulation of genes in accordance with the hormone levels. In brief, presence of auxin triggers degradation of Auxin/Indole-3-Acetic Acid (Aux/IAA) proteins through their interaction with TRANSPORT INHIBITOR

RESPONSE1 (TIR1) and subsequent ubiquitination. In turn, reduced levels of Aux/IAA proteins allow dimerization of AUXIN RESPONSE FACTORS (ARFs) which serve as transcriptional activators for downstream genes directly determining cellular phenotype (Figure IV-1).

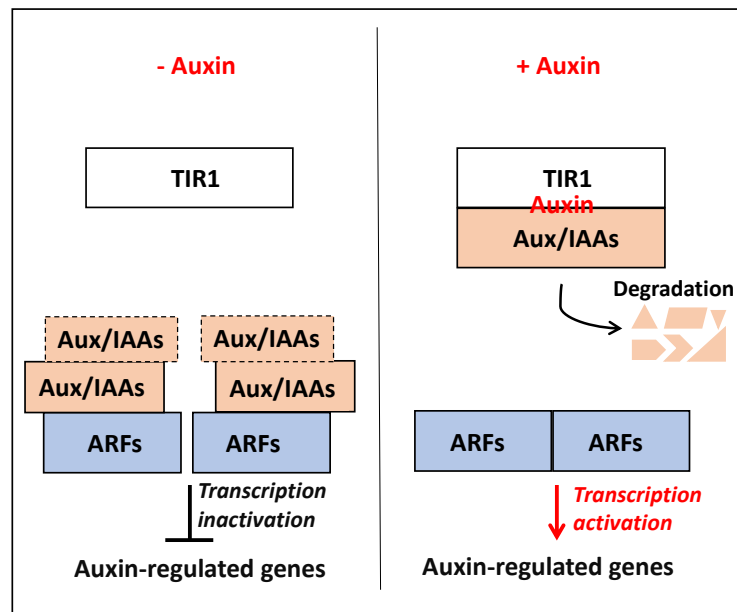


Figure IV-1: Auxin signaling pathway. In the absence of auxin, Aux/IAAs dimerize with one another or with transcription factors ARFs, preventing transcription of downstream genes. In contrast, presence of auxin triggers binding of TIR1 to Aux/IAAs and Aux/IAAs' degradation through ubiquitination. ARFs are allowed to self-dimerize and activate transcription of downstream genes.

In *A. thaliana*, Aux/IAA and ARFs are encoded by 29 and 23 genes respectively. IAAs and ARFs can have redundant functions and their interaction is critical for root growth (Fukaki, Hidehiro, Taniguchi & Tasaka 2006; Lavenus et al. 2013; Qin, He & Huang 2019). Many IAAs were shown to take part in the development of both primary and lateral root, as well as root hair formation and gravitropism. For example, gain-of-function mutants of a number of Aux/IAA proteins including IAA1/AXR5, IAA3/SHY2, IAA12/BDL, IAA14/SLR, IAA18/CRANE, IAA19/MSG2, IAA16 and IAA28 have altered lateral root growth and/or primary root length (Fukaki, H. et al. 2002; Ploense et al.

2009; Rogg, Lasswell & Bartel 2001; Tatematsu et al. 2004; Tian & Reed 1999; Uehara et al. 2008; Yang et al. 2004(Rinaldi et al. 2012)). These gain-of-function mutations often confer the proteins resistance to auxin, which in turn leads to changes in protein, and even transcript level (Tian, Qing, Uhlir & Reed 2002). Temporal and spatial differential expression of IAA and ARFs also contribute to establishing the complex root architecture (Overvoorde, Fukaki & Beeckman 2010). Differential expression of IAA and ARFs is under the control of multiple regulatory layers, with RNA modifications emerging as an important factor that has been largely overlooked.

To date, two RNA modifications N6-methyladenosine (m^6A) and 5-methylcytosine (m^5C) have been linked to root development. While m^6A exhibits a vast involvement in the development of many organs (Arribas-Hernández, Laura et al. 2020; Ruzicka et al. 2017), m^5C thus far appears to show more confined effect on root development. Shorter primary root phenotype was observed in all four reported mutant alleles of the m^5C writer TRM4B (Cui et al. 2017; David et al. 2017). David et al (2017) demonstrated a role for m^5C in root apical meristem cell proliferation through analyzing *trm4b-1* mutant allele. However, their transcriptome-wide Bisulfite-sequencing (BS-RNA-seq) approach failed to detect methylation of specific genes that may have been a direct cause of the root phenotype. In contrast, Cui et al. (2017) utilized an m^5C -RNA immunoprecipitation (m^5C -RIP) approach and found correlations between m^5C loss on two root growth-related transcripts *SHY2/IAA3* and *IAA16*, and the reduced abundance of these transcripts in *trm4b-4* mutant, suggesting a role for them in root growth regulation by m^5C . However, the m^5C -RIP followed by sequencing used in the study could not provide detailed profiling of m^5C site(s) on the transcripts but putative m^5C regions of several hundred bases enriched by immunoprecipitation, hindering confirmation of the modification's functions and further elucidation on its mechanism.

In the present study, I investigate further the molecular mechanisms underlying the connection between m^5C and root development, with a focus on the functional relevance of modification(s) on *SHY2/IAA3* and *IAA16* mRNAs attributed to the shorter primary root phenotype of m^5C -deficient mutants. Root growth assays and transcript quantification using RT-qPCR on four reported *trm4b* mutant alleles and a *SHY2* loss-of-function mutant did not support the key role for *SHY2/IAA3* and *IAA16*

in m⁵C regulation of root growth. Furthermore, massively parallel targeted bisulfite sequencing known as Bisulfite amplicon sequencing (BS-amp-seq) detected m⁵C on *SHY2/IAA3* and *IAA16* at low level and with high variation, suggesting a confined spatial and temporal deposition of the methylation. Although a novel identified methylated site appears conserved in a bioinformatic analysis, a functional study that utilized CRISPR-dCas13-hTET1 (Chapter III) did not support the importance of the site *in planta*. Collectively, the study offers deeper understanding of the methylation profile and functional relevance of m⁵C in *A. thaliana*'s root development.

Materials and methods

Plant materials and growth conditions

Arabidopsis thaliana (Col-0) plants were grown on ½ MS, 1% sucrose medium in long day conditions (16-hour light/8-hour darkness) at 21°C. Characterization of the mutants *trm4b-1* (SAIL_318_G04), and *trm4b-2* (SAIL_667_D03) were described previously (Burgess, David & Searle 2015). *trm4b-3* and *trm4b-4* were obtained from the Arabidopsis Biological Resource Centre. The mutant *shy2-24* in Col-0 background was a gift from Prof. Wolfgang Dröge-Laser, University of Würzburg.

Root assay

Seeds were gas-sterilized (Chlorine) for seven hours and placed on square petri plates (9cmx9cmx2cm) with sterile toothpicks, followed by cold stratification for three days at 4°C. Plates were then moved to a growth chamber and oriented vertically. At least three replicate plates were done for each mutant allele or transgenic line. To rule out the effect of position variation and light-to-light variation, replicates of each line were placed under different lights. Each replicate set includes wild-type and mutant and/or transgenic plants and was put under the same light. Root length was marked after every 24 hours over the course of nine days. At day 9, root images were obtained with an Epson Perfection V700 Photo scanner (Epson) and further processed with ImageJ to determine growth rate over each day.

RT-qPCR

Total RNA was extracted from 9-day old root tissues of wild-type or *trm4b* mutant alleles with Sigma Spectrum Plant Total RNA extraction kit. cDNA was synthesized with Superscript III Reverse transcriptase (Invitrogen) and used as input for quantification with FastStart SYBR Green Master Mix (Roche) on a Quantstudio 7 Flex System. Biological duplicates and technical triplicates were assayed. *TUBULIN 2* (*TUB2*) was used as internal control for normalization of *SHY2/IAA3*, *IAA16* and *ACTIN2* mRNAs.

BS-amp-seq:

1.5 ug total RNA of root and/or shoot tissues of 9-day old wild-type, *trm4b-1* or *trm4b-2* were subject to Bisulfite treatment as described previously (David et al. 2017). Briefly, total RNA samples were incubated in Sodium metabisulfite and Hydroquinone for four hours at 65C. Salts from the reaction were then removed by Microspin columns in Tris (Bio-rad) and RNAs were precipitated with ethanol. BS-treated RNA samples were used as templates for cDNA synthesis with a mixture of primers, each being specific for an amplicon of interest (Supplementary Table IV-S5). Hereon, two approaches were adopted for preparing the BS-amp-seq libraries:

Method A: cDNAs were subject to the first round of PCR for amplification of target fragments. A single PCR reaction was carried out for each amplicon from each biological sample. These PCR products were purified with AMPure XP beads (Beckman Coulter), checked for sizes on a polyacrylamide gel and used as templates for a second PCR with primers containing barcodes for Illumina Sequencing. Products from this second PCR were purified with AMPure XP beads and pooled together for sequencing on a Miseq platform with Miseq Reagent Micro kits (1 x 300 nucleotide single-end).

Method B: Key steps are similar to those of Method A, however, to enhance detectability of low methylated sites, triplicates were performed for the first round of PCR for each amplicon from each biological sample. Products of the triplicates were pooled together and purified with AMPure XP beads. Purified products were then used as templates for the second PCR round. Sequencing was performed on a Miseq with Miseq Reagent Micro kits (2 x 150 nucleotide paired-end)

BS-amp-seq Data analysis

TrimGalore were used to remove adapters from Miseq reads. FastQC and ngsReports (Ward, To & Pederson 2019) were used for quality control of reads and 3' end nucleotides were further removed (TrimGalore) to avoid m⁵C calling bias in downstream analysis. Trimmed reads were then mapped to a reference (TAIR10_cds_20101214_updated) with meRanT (MeRanTK) in single-end (Library I) or paired-end mode (Library II), and m⁵C calling was subsequently performed for mapped reads with meRanCall (MeRanTK). A threshold of 1% methylation rate and False Discovery Rate of 0.01 were used for m⁵C calling.

Conservation analysis of a m⁵C site C348

All *A. thaliana* IAA proteins or IAA3 proteins of all available plant species on NCBI protein database were aligned with Clustal Omega for amino acid conservation analysis. Protein sequence logo (Supplementary Figure IV-S2) was generated with WebLogo (<https://weblogo.berkeley.edu/logo.cgi>, access: 4/8/2021). To assess the conservation of the nucleotide of interest (C348), two additional cytosines with similar contexts ((i) the amino acids they encode are strictly conserved, (ii) they are the third nucleotides of the codons encoding for those amino acids, and (iii) those amino acids can be encoded only by two codons differing by the third nucleotides (C or T)) were analyzed to exclude the effect of species-specific codon bias. Species collections of each of IAA proteins were extracted from NCBI which includes one to three representatives (Accession numbers) of each species whose mRNA sequences for that IAA are available. mRNAs in each species collection were aligned and the percentage of C usage at each of the three sites of interest (C348 and two control sites) was calculated as the number of species using C at that site over the total number of species in that collection. To avoid lineage bias, no more than three species of the same genus was included in each collection. The species collection for each IAA is listed in Appendix. The use of the same collections of species for each protein allows relatively unbiased comparison of base-preferences at the three analyzed sites.

dCas13-TET1 plasmid construction and transgenic plant generation

gRNA spacers were ordered as synthetic oligos of 34-nt from Integrated DNA Technologies (Supplementary Table IV-S6) and ligated into Bsalx2 site in the dCas13-TET1 backbones (Chapter III) by Golden Gate Cloning (Engler, Kandzia & Marillonnet 2008). Successful insertion was monitored with PCR and Sanger sequencing with primers detailed in Supplementary Table IV-S5. Constructs were transformed into *Agrobacterium* USDA cells by electroporation for subsequent plant transformation by floral dipping (Clough & Bent 1998). Transformants were selected on 15 ug/mL Hygromycin B selection medium. 3:1 segregation ratio was used to determine single-insertion event. Heterozygous plants with single insert were carried to the next generation to identify a homozygous line.

Results

SHY2/IAA3 and *IAA16* are not key factors in m⁵C regulation of root development

The importance of m⁵C in root development was linked to the regulation of *SHY2/IAA3* and *IAA16* transcript abundance (Cui et al. 2017). In order to validate the correlation between these transcripts and the short primary root phenotype in m⁵C deficient *trm4b* mutant lines, two experiments were conducted. First, I examined the root phenotype of *shy2-24*, a loss of function mutant with a premature stop codon and significantly reduced level of *SHY2/IAA3* transcript (Tian, Qing, Uhlir & Reed 2002). Previously, it was shown in Landberg ecotype (Ler) that *shy2-24* exhibited significantly poorer root growth compared to wild-type (Tian, Q. & Reed 1999). However, in Columbia background (Col-0), Weiste et al. (2017) demonstrated slightly increased root length of *shy2-24* compared to wild-type at 7-day after germination. Indeed, I observed a consistently better growth rate of *shy2-24* Col-0 than the wild-type Col-0 over the course of nine days, which contrasts with the defective root growth of all of the four *trm4b* mutant alleles when compared to wild-type (Figure IV-2A). *trm4b-1* exhibited the most pronounced phenotype among the four mutant alleles assayed.

Second, root tissues of wild-type, *shy2-24* Col-0 (hereby referred to as *shy2-24*, unless otherwise indicated) and all four *trm4b* mutant alleles were subject to an RT-qPCR for monitoring of *SHY2/IAA3* and *IAA16* transcript abundance. *shy2-24* showed a reduction of around 50% in *SHY2/IAA3* mRNA and unchanged *IAA16* mRNA level compared to wild-type (Figure IV-2B), which is consistent with previously reported data obtained by a gene chip hybridization assay for *shy2-24* Ler (Tian, Qing, Uhlir & Reed 2002). Interestingly, all four *trm4b* mutant alleles had unchanged or even slightly increased level of *SHY2/IAA3* and *IAA16* (Figure IV-2B). The observation was confirmed with a second independent experiment done for the *trm4b-1* mutant (Supplementary Figure IV-S1). Collectively, these data did not support the key link between downregulated *SHY2/IAA3* and *IAA16* transcript abundance and aberrant root development in *trm4b* mutants as previously described, however does not exclude the involvement of these two transcripts.

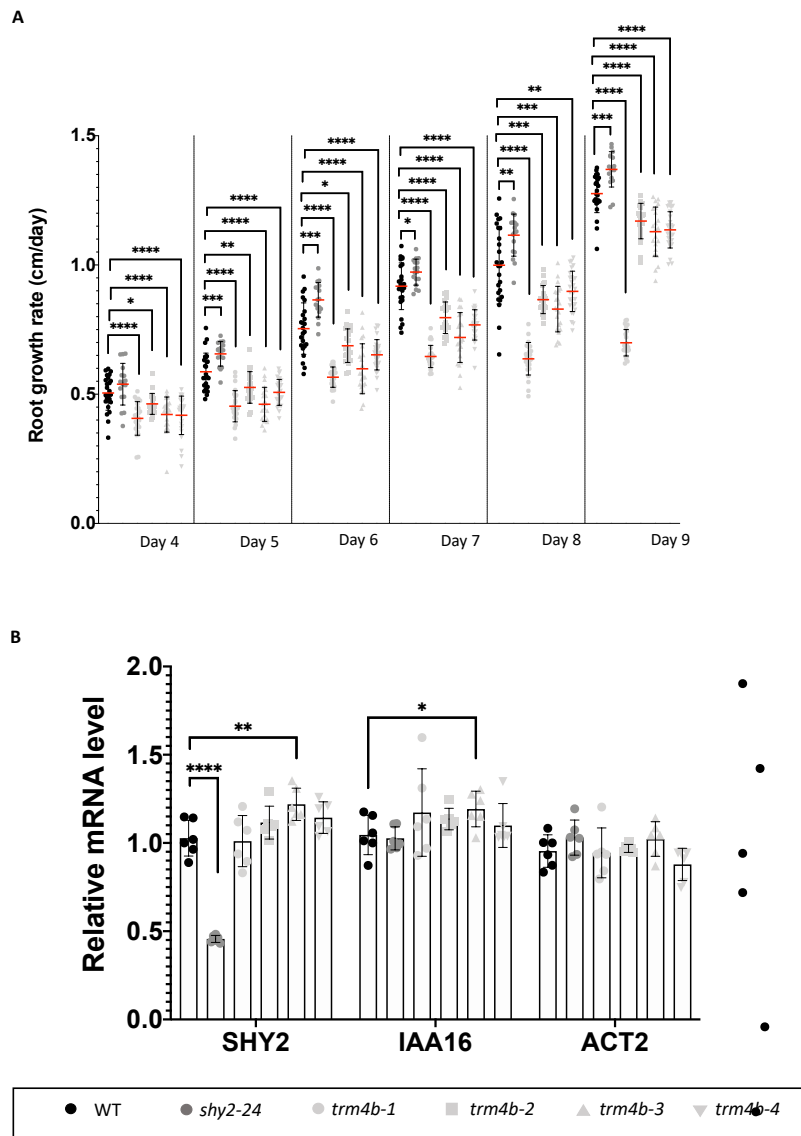


Figure IV-2: Assessing the role of *SHY2/IAA3* and *IAA16* in m5C regulation of root development. A, Root growth rate of *shy2-24* loss-of-function mutant and *trm4b* mutant alleles compared to wild-type. Seeds of each mutant line or wild-type in Col-0 background were plated on ½ MS medium and grown vertically. Three plate replicates with nine plants per plate were done for each line. Root length was marked after each 24 hours. Red lines indicate mean of sample. Error bars indicate standard deviation of mean. B, *SHY2/IAA3* and *IAA16* mRNA level in 9-day old wild-type, *shy2-24* and *trm4b* mutants measured by RT-qPCR. Biological duplicates and technical triplicates were performed. *TUB2* was used as internal control. Error bars represent standard deviation of mean. Welch's t-test, ****: p value <0.0001, **: p value <0.01, *: p value <0.05.

Dynamics of RNA m⁵C methylation on *SHY2/IAA3* and *IAA16* in root tissue

I next sought to verify the methylation status of *SHY2/IAA3* and *IAA16* mRNAs, as well as aimed to detail the methylated sites, to develop a foundation for their functional analysis. David et al. (2017) did not detect m⁵C on *SHY2/IAA3* and *IAA16* in whole-transcriptome BS-RNA-seq while Cui et al. (2017) reported m⁵C peaks of 200-300 nt on these transcripts by m⁵C-RIP-seq. I reasoned that transcriptome-wide RNA-BS-seq might not be sensitive enough to detect lowly methylated sites, so I adopted BS-amp-seq for the putative m⁵C peaks on *SHY2/IAA3* and *IAA16* identified by the m⁵C-RIP-seq. BS-amp-seq takes advantage of PCR to enrich a targeted small fragment (amplicon) of interest before sequencing (David et al. 2017), thus enhancing detection of methylated sites. Two independent libraries were prepared: The first library (library I) was focused on differentiating m⁵C regulating root development by comparing four wild-type root and four shoot tissue samples, along with three *trm4b* root tissue samples. The library I was prepared with a standard BS-amp-seq protocol (Method A) with single PCR reactions for each amplicon in each round. Second library (library II) instead focused on detecting m⁵C methylation in wild-type when compared to *trm4b*, with five replicates prepared for root tissues of each of the two groups. In order to enhance the detectability of lowly methylated sites, in this library II, each amplicon was prepared with triplicates in the first PCR round (Method B).

Reliability of the BS-amp-seq method was confirmed through consistent detection of m⁵C methylation at site C3349 on *MAIGO 5* (David et al. 2017) in all wild-type (30.4-35.1%) and *trm4b-1* samples (1.4-2.5%) in library II (Supplementary Table IV-S4). In both libraries, methylated sites were not detected on *IAA16* with high confidence (less than 1% methylation with coverage >5000 in library I, or with less than 2% methylation with coverage of 50-500 in library II). Methylation was also not detected on *SHY2/IAA3* in all samples of library II, despite sequence coverage of 2000–30,000 fold per amplicon. Notably, in two out of four wild-type root replicates in library I, I found C348 on *SHY2/IAA3* was methylated in 2.7-3.4% of reads (sequence coverage 3187 and 2334, Figure IV-3A, Supplementary Table IV-S1) while no replicates of wild-type shoot or *trm4b* root samples showed m⁵C methylation at this site. Of note, C348 is the summit of the putative m⁵C peak detected by m⁵C-RIP-seq (Figure IV-3B). Together,

the results suggest that C348 is the methylated site involving root growth but its methylation may be meticulously regulated.

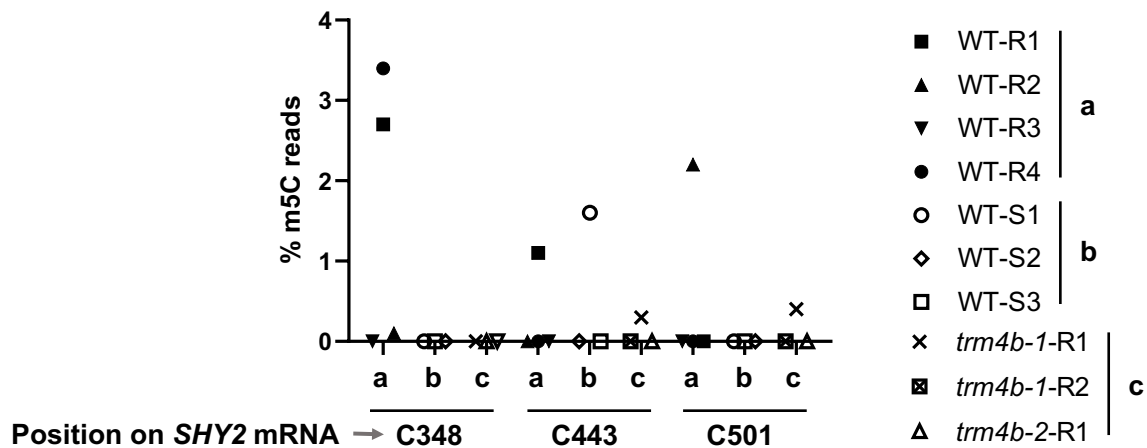


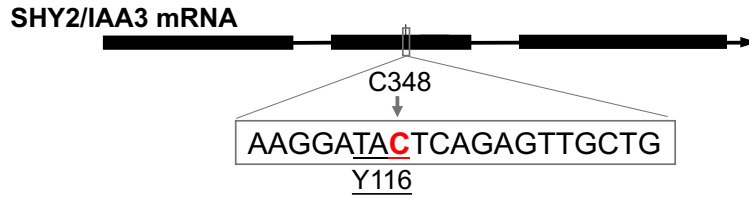
Figure IV-3: Detection of m⁵C sites on *SHY2/IAA3* mRNA using BS-amp-seq (library I). 9-day old wild-type root tissue (WT-R, group a), wild-type shoot tissue (WT-S, group b) and *trm4b* root tissue (*trm4b*-R, group c) were subject to a BS-amp-seq. m⁵C calling was performed using meRanTK package (Rieder et al. 2015) with a calling threshold of 1% and statistical cutoff of FDR ≤0.01. Three high-confidence m⁵C sites identified by meRanTK (C348, C443 and C501) were checked for non-converted cytosine (considered as m⁵C) count and coverage with Integrative Genomics Viewer to determine m⁵C level (% m⁵C reads) at the sites in all biological samples (Note that meRanTK does not call out the site with methylation below calling threshold).

Conservation of C348 on *IAA3* mRNAs

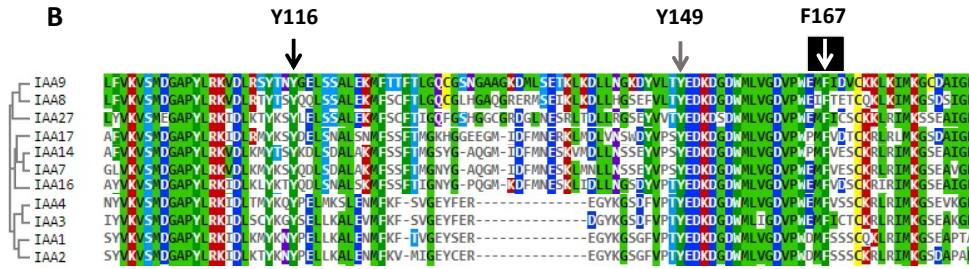
I investigated further the potential role of the novel detected m⁵C site C348 on *SHY2/IAA3*, firstly with a bioinformatic approach. C348 is the third nucleotide of a TAC codon that encodes for tyrosine Y116 on *A. thaliana* *SHY2/IAA3* (*AtSHY2/IAA3*) (Figure IV-4A). In order to assess the conservation of C348 on *SHY2/IAA3*, I sought to compare the

usage of cytosine at this site with two other sites of similar context. The analysis takes advantage of two points: (i) Tyrosine, along with phenylalanine (F) are encoded by only two codons differing by C or T as the third nucleotide (Figure IV-4C); and (ii) Y116, Y149 and F167 of *AtSHY2/IAA3* are strictly conserved amino acids in IAA3 proteins across a number of Pinus, monocots and dicots (Supplementary Figure IV-S2), as well as amongst IAA proteins (Figure IV-4B). It could be expected that if the third nucleotide (C or T) of the codons is not important, the probability to find either of them in any IAA proteins in a random collection of species throughout evolution would be roughly 0.5 (50%), or abide overall codon usage preferences in those species. However, this is not the case for the codon encoding Y116 in *AtSHY2/IAA3*. When analyzing collections (12-81 species each) of Monocot and Dicot species for C usage in codons encoding amino acids corresponding to Y116, Y149 and F167 in *AtSHY2/IAA3* of eleven IAA proteins, I found a bias in using C as the third nucleotide to encode Y116 in the IAA16 clade and IAA3, which is in contrast with a general T bias observed for other IAA proteins as well as for the two control sites Y149 and F167 (Figure IV-4D). This result demonstrates a favour towards using C to encode the tyrosine corresponding to Y116 on *AtSHY2/IAA3* through evolution, and potentially that corresponding nucleotide of IAA16.

A



B



C

Amino acid	Codons
Tyrosine (Y)	TAC TAT
Phenylalanine (F)	TTT TTC

D

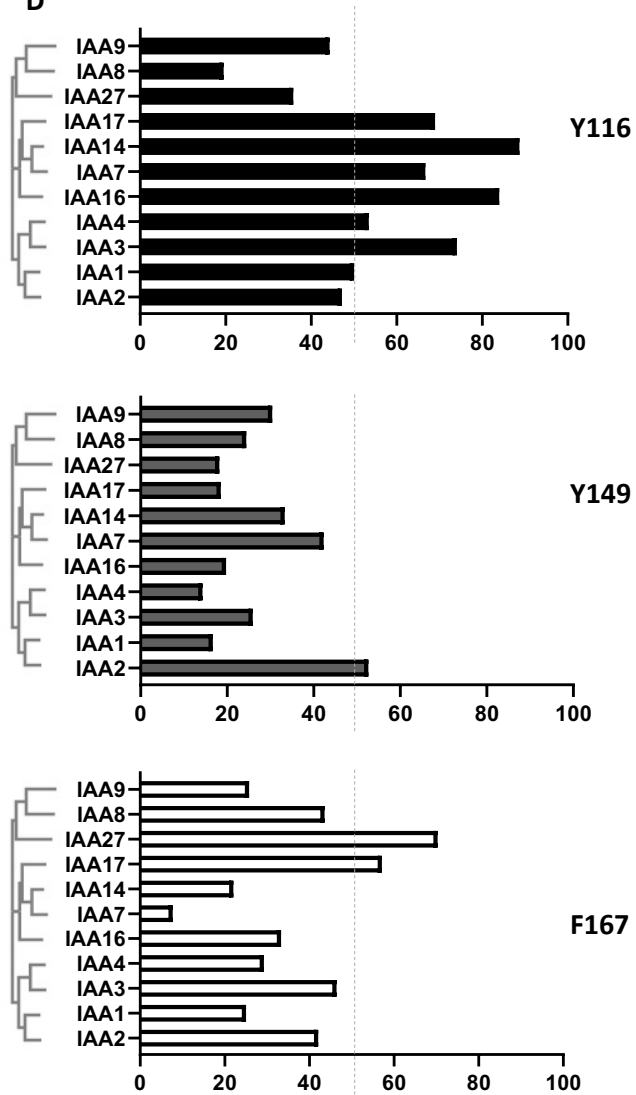


Figure IV-4: Conservation of C348 on *SHY2/IAA3* mRNA. A, Genomic structure of *SHY2/IAA3* with three exons (black boxes) and introns (thin black lines). C348 (red) is the third codon encoding for Y116 (underlined) on exon 2 of *SHY2/IAA3*. B, Multiple sequence alignment of *A. thaliana* IAA proteins. Y116, Y149 and F167 on *SHY2/IAA3* are three highly conserved amino acids (arrowed) across the IAA protein family as well as species of *Pinus*, monocotyledonous and dicotyledonous plants (Supplementary Figure IV-S2). Colour shading was generated in MView tool of Clustal Omega, representing identical amino acids. C, Both Tyrosine and Phenylalanine are encoded by only two codons differing by either C or T as the third nucleotide. D, Usage of C as the third nucleotide in the codons encoding Y116, Y149 and F167 in IAA proteins. Collections of species for each IAA protein were generated and the IAA mRNAs of the species in each collection were aligned and analyzed for the codon they use at sites corresponding to *A. thaliana* Y116, Y149 and F167. Bar charts show percentage of species analyzed using C to encode respective amino acid in each IAA protein. Note that each IAA protein shown has the same collection of species analyzed for all three residues (Y116, Y139 and F167).

Interference to C348 on *SHY2/IAA3* does not cause detectable effect on root growth *in planta*

Lastly, to gain more insight into the potential importance of C348 on *SHY2/IAA3*, I performed functional analysis by directing dCas13-TET1 to C348 on *SHY2/IAA3*. Theoretically, dCas13-TET1 can demonstrate the importance of C348 in two manners: (i) Interfering with m⁵C activity (removes it or prevents its deposition), and/or (ii) interfering with the binding of *SHY2/IAA3* mRNA interacting partners which may not require m⁵C. Four gRNA-spacers were designed to locate dCas13-TET1 to a span of region around C348 on *SHY2/IAA3* (Figure IV-5A, Supplementary Figure IV-S3). Homozygous plants of at least one transgenic line of each spacer were subject to a root assay in which root growth is recorded each day in a course of nine days. Transgenic plants with a scramble spacer (random sequence) or a spacer targeting a different transcript (non-targeting) were used as controls. None of the targeting spacer or control transgenic lines showed significant differential root growth rate from that of wild-type. (Figure IV-5B,C, Supplementary Figure IV-S3).

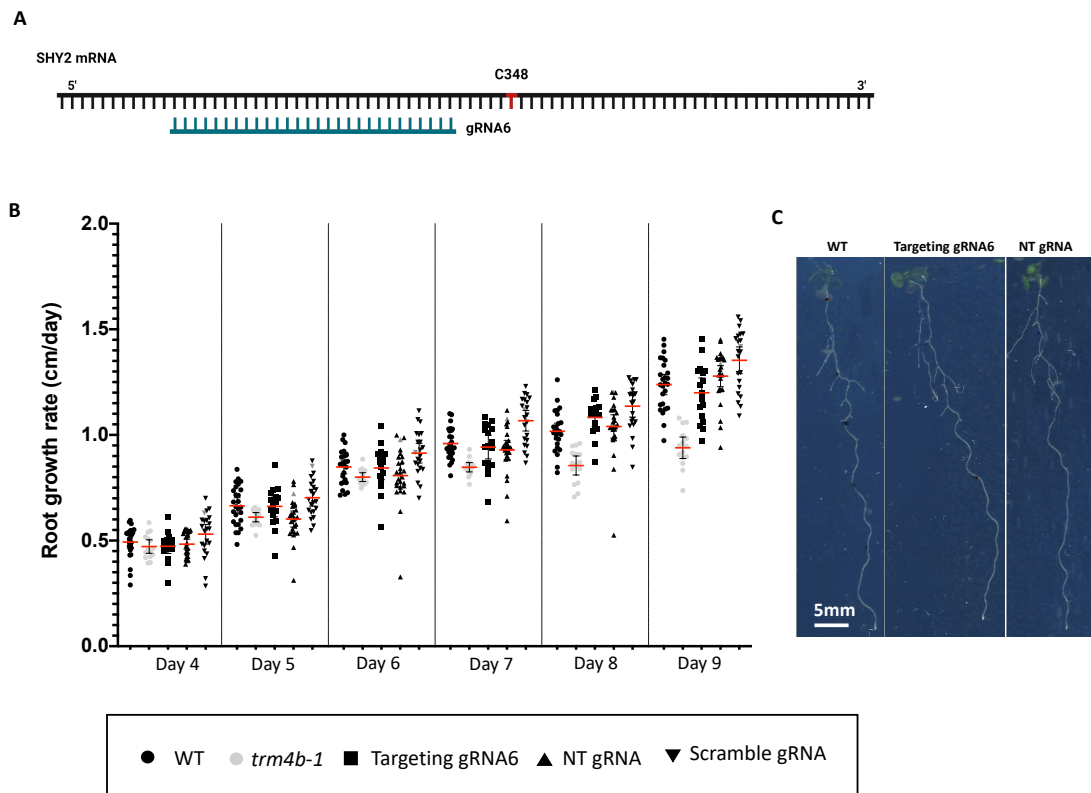


Figure IV-5: Interference of dCas13-TET1 to C348 on *SHY2/IAA3* does not alter root growth in *Arabidopsis*. A, Positioning of spacer gRNA6 for dCas13-TET1 to target C348 on *SHY2/IAA3* mRNA. The number indicates the relative position of 5'-end of the spacer to the target site C348. B, Root growth rate of wild-type, *trm4b-1* and dCas13-TET1 transgenic plants. Homozygous seeds of each construct type were plated on ½ MS medium and grown vertically. Root length was marked every 24 hours. Three plate replicates with nine plants per plate were done for each line. NT, non-targeting. Red lines indicate mean of sample. Error bars indicate standard deviation of the mean. C, Representative root images of 9-day old wild-type and dCas13-TET1 lines with targeting gRNA6 or non-targeting gRNA.

Discussion

Functional relevance of *SHY2/IAA3* and *IAA16* in m⁵C regulation of root development

Despite the correlation reported between RNA m⁵C loss and defective root growth in *A. thaliana*, no solid evidence for the functional relevance of any m⁵C-modified transcripts/targets was provided. While Cui et al (2017) demonstrated a potential role for two m⁵C-bearing transcripts, *SHY2/IAA3* and *IAA16*, in the development of roots, here with more thorough and comprehensive analyses, I provide evidence refuting a strong link between the transcripts along with their m⁵C status, and root development.

Firstly, loss-of-function mutation of *SHY2/IAA3* exhibited distinct root growth profile when compared to m⁵C deficient mutants. Although there are still discrepancies between root phenotypes of *shy2-24* in Ler and Col backgrounds (Tian, Q. & Reed 1999; Weiste et al. 2017), as the *trm4b* mutants used are in Col, phenotype of *shy2-24* Col is considered more reliable when taken into comparison. Secondly, while the shorter primary root phenotype of *trm4b* mutant is pronounced and reproducible, molecular alterations are not. Both differential transcript expression and methylation status of *SHY2/IAA3* and *IAA16* reported previously (Cui et al. 2017) were not reproducible in the present study. The discrepancies may (i) point toward an insignificant role of *SHY2/IAA3* and *IAA16* mRNAs in the regulation of root development by m⁵C methylation; (ii) suggest that m⁵C regulation of root growth is significantly affected by subtle environmental changes which resulted in changing of targets for methylation; or (iii) reflect the meticulous regulation of m⁵C level and associated transcripts in a spatial and temporal manner that caused inconsistent detection when sampling and detecting parameters were slightly changed across laboratories. While the first explanation appears most straightforward, the second and third explanations respectively take into account the possible plasticity and precise regulation of m⁵C, reconciling the conflicting results obtained here and previously described.

It should be noted that while the previously used method, m⁵C-RIP-seq, allows appreciable sensitivity, the technique requires a considerable amount of input RNA (around 200-300 ug compared to 1.5-2 ug of total RNA in BS-amp-seq), implies structural biases, and is poor in reflecting the absolute level of methylation. The low

and variable m⁵C level detected on *SHY2/IAA3* in the BS-amp-seq presented here again supports the idea of spatially- and temporally-confined deposition of the methylation. I propose that to study this issue in a greater detail, examination of different tissue types, at several stages in early root development will be required. In this regard, beside more commonly used methods for m⁵C profiling such as m⁵C-RIP-seq, m⁵C-CLIP-seq or BS-amp-seq, direct RNA sequencing with Nanopore technologies coupled with an adaptive sampling approach, or single-cell RNA-seq could provide valuable information about methylation state of low abundant or lowly methylated transcripts, as well as its spatial and temporal dynamics.

It is significant that an m⁵C candidate site C348 was detected on *SHY2/IAA3* mRNA, and that this site appears conserved through evolution. There exists the possibility that this site confers the plant some advantage in development and therefore is retained to a certain extent. However, as shown through the low reproducibility of *SHY2/IAA3* and *IAA16* transcript abundance and methylation status, as well as no detectable impact of interference to the site *in planta*, the advantage might be overwritable. On the other hand, it is worth noting that little has been investigated experimentally regarding dissociation rate of dCas13 from targets. It is possible that rapid dissociation of the system from bound target leaves the gap for associated machineries to work on *SHY2/IAA3* and for *SHY2/IAA3* to behave itself normally. Additional functional analyses using DNA or RNA base-editors, or prime editor (Abudayyeh, O. O. et al. 2019; Anzalone et al. 2019; Komor et al. 2016) to convert C348 into T at DNA level, or into U at RNA level can provide added evidence for the role of this site.

Other than *SHY2/IAA3* and *IAA16*?

Data presented in this study suggest that m⁵C regulates root development through main targets/factors rather than *SHY2/IAA3* and *IAA16*. There are thousands of m⁵C sites reported in wild-type *A. thaliana* root which are lost in *trm4b* mutants (Cui et al. 2017; David et al. 2017). For example, David et al (2017) showed that C3349 on *MAIGO5 (MAG5)* mRNA is methylated at the rate of 25-26% in 6-day old root tissue. Using 9-day old root tissue, I found a consistent 30.4-35.1% of methylation at this cytosine (Supplementary Table IV-S4), suggesting that changes in methylation level can occur at this site as the roots develop. Given that MAG5 is not known to directly

involve in root development, it could be useful to investigate what role the methylation at this site might play for this organ. Notably, Yang, L et al. (2019) demonstrated that the mobility of an m⁵C-modified transcript *TRANSLATIONALLY CONTROLLED TUMOR PROTEIN 1* which is lost in the double mutant of m⁵C methyltransferases *trm4b trdmt1* promotes root growth, offering an alternative explanation for the mechanism of root development regulation by m⁵C. It should also be noted that TRM4B has other substrates than mRNAs and it is currently unknown how m⁵C on these non-mRNA targets participate in root growth. Clarifying these points will be necessary to better understand the root growth regulation by m⁵C. In addition, as reduction in either m⁶A or m⁵C can cause shorter primary root, whether these two methylations regulate root growth in two independent pathways, their regulations converge, or they cross-talk for a dual-mediator regulation remain an interesting question to be answered.

Additional role for m⁵C?

Beside the shorter primary root and less lateral roots phenotype as previously described (David et al 2017, Cui et al 2017), I noticed a higher density of root hairs in *trm4b-1* mutant, especially towards the root tips (Supplementary Fig IV-S4A). Consistent with the observation, one of the most important regulators in root hair formation TRANSPARENT TESTA GLABRA 1 (Galway et al. 1994; Long & Schiefelbein 2020) exhibits increased mRNA abundance in *trm4b-1* (Supplementary Figure IV-S4B). Therefore, TRM4B might regulate other aspects of root growth that have not been reported.

Supplementary Data

Supplementary Table:

Supplementary Table IV-S1: Methylation found on *SHY2/IAA3* in BS-amp-seq library I. (Supplementary materials for Figure IV-3). m5C sites were called with meranTK with Phred score 30 (Q30) set for base-calling quality, 1% methylation set for methylation calling threshold, and statistical cutoff FDR ≤ 0.01 . C count (m5C) and coverage at sites identified as m5C candidates with meranTK were determined for all samples with IGV (Q20 as used for mapping). WT_R, wild-type root. WT_S, wild-type shoo. *trm4b-1_R*, *trm4b-1* root.

Q30		WT_R1		WT_R2		WT_R4		WT_S1	
SHY2 (AT1G0 4240)	Site	%	C/coverage	%	C/coverage	%	C/coverage	%	C/coverage
	C348	1.5	46/3056	N/A	N/A	2.2	49/2236	N/A	N/A
	C443	1.1	85/8027	N/A	N/A	N/A	N/A	1.4	228/15960
	C501	N/A	N/A	1.6	128/8045	N/A	N/A	N/A	N/A

Q20		C/coverage									
SHY2	Site	WT_R1	WT_R2	WT_R3	WT_R4	WT_S1	WT_S2	WT_S3	<i>trm4b-1_R1</i>	<i>trm4b-1_R2</i>	<i>trm4b-2_R1</i>
	C348	86/3187	1/1747	0/2284	80/2334	1/4673	0/704	0/1252	0/4523	0/2215	0/4974
	C443	91/8071	0/8195	0/2880	1/4526	251/16042	1/7611	1/11563	27/10587	1/9898	1/9758
	C501	1/8049	183/8152	0/2879	1/4553	0/16037	0/7606	2/11558	44/10582	0/9891	0/9756

Supplementary Table IV-S2: Methylation not found on *SHY2/IAA3* in BS-amp-seq library II. C count (m5C) and coverage at C348 and C443 are shown (C/coverage).

		WT					<i>trm4b-1</i>				
SHY2	Site	1	2	3	4	5	1	2	3	4	5
	C348	6/20 787	1/3742	14/12888	42/10872	5/19460	8/17752	8/16484	8/2148	20/117602	3/32444
	C443	32/2 5166	2/5663	5/16174	3/2721	10/27356	10/4676	6/13523	0/3274	46/151341	7/32210

Supplementary Table IV-S3: Codon usage at Y116, Y149 and F167 in IAA proteins of species analyzed (Supplementary materials for Figure IV-4D, Species collections listed in Appendix 3). Y116, Y149 and F167 refer to the positions of these amino acids on *AtSHY2/IAA3*. Codons shown in table are those used in *A. thaliana*. For some IAA proteins, some species were found using both C or T as the third nucleotide to encode the respective amino acid (highlighted in blue). Data is shown as: Codon used in *A. thaliana* – Total number of species use this codon/Total number of species analyzed (*Number of species use both codons with T or C)

	Y116	Y149	F167
IAA1	TAT - 6/12	TAT - 10/12	TTC - 3/12
IAA2	TAC - 17/36	TAC - 20/38	TTC - 16/38
IAA3	TAC - 20/27	TAT - 20/27	TTC - 13/28
IAA4	TAT - 32/58 (*5)	TAT - 52/56 (*4)	TTT - 29/41
IAA27	TAC - 24/67	TAT - 54/66	TTT - 19/64
IAA16	TAC - 68/81 (*4)	TAT - 67/81 (*2)	TTT - 54/81
IAA17	TAC - 20/29	TAT - 22/27	TTC - 16/28
IAA7	TAC - 18/27	TAC - 11/26	TTT - 24/26
IAA14	TAC - 47/53	TAC - 17/51	TTT - 39/50
IAA8	TAT - 33/41	TAT - 31/41	TTT - 22/39
IAA9	TAT - 39/70	TAT - 48/69	TTT - 49/66

Supplementary Table IV-S4: m⁵C level at *MAG5* C3349 in 9-day old *A. thaliana* root tissue determined by BS-amp-seq. Five replicates for wild-type and four replicates for *trm4b-1* are shown. The missing replicate 5 in *trm4b-1* is due to *MAG5* amplicon was not included in this replicate. Given that *trm4b-1* is a null mutant (Burgess et al, 2015), the consistent 1.4-2.5% m⁵C at C3349 but not any other sites on the *MAG5* amplicon in *trm4b-1* suggests that a second m⁵C “writer” can act on this site.

	WT									
MAG5 (AT5G47480)	Coverage					Non-converted cytosines (%)				
	1	2	3	4	5	1	2	3	4	5
	16863	4184	4902	1502	3850	33.3	33.1	34	30.4	35.1

	<i>trm4b-1</i>							
MAG5 (AT5G47480)	Coverage				Non-converted cytosines (%)			
	1	2	3	4	1	2	3	4
	4436	1643	15810	5341	2.1	1.4	1.2	2.5

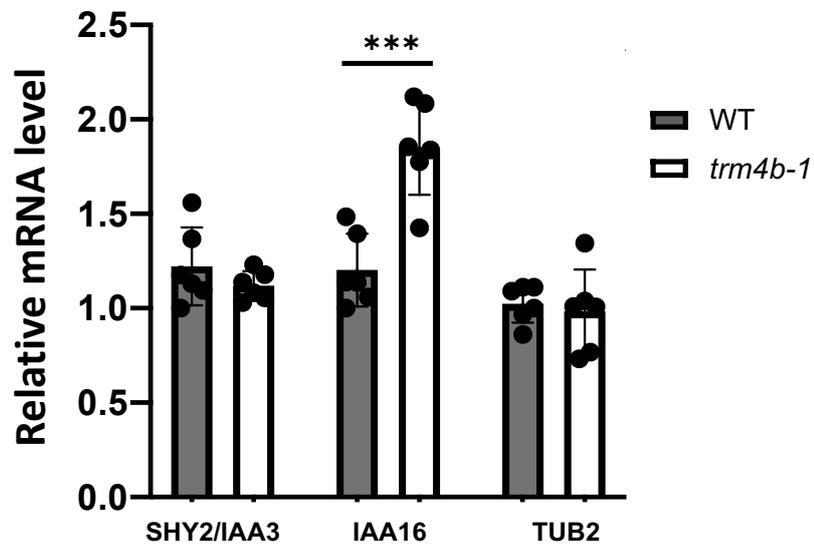
Supplementary Table IV-S5: Primers used in BS-amp-seq. Red letters denote adaptors for library preparation. Lowercase letters denote C or G in the genome converted to T or A *in silico*, respectively.

Primers used in BS-amp-seq	
SHY2_cDNA_1	CTTaAAaATATATCTCATACACCACAaCC
SHY2_cDNA_2	CCCaAaAAACCCaACAACCC
SHY2_cDNA_3	CAAAaTCTaAACCTTTATATCCATCTCTCTC
SHY2_1_F	ACACTGACGACATGGTTCTACA TgTAGGGtTtAGATTGTTGGATGGtAttAG
SHY2_1_R	TAC GGT AGC AGA GAC TTG GTC TCTCTCCCACAaAaAATTTaAACATCACTTCT
SHY2_2_F	ACACTGACGACATGGTTCTACA GAGTTGTTAtAAAGGATAtTtAGAGTTGtTTAAAG
SHY2_2_R	TAC GGT AGC AGA GAC TTG GTC TCTCATACACCACAaCCTAACCTTTaaCTTC
IAA16_cDNA_1	CTaTTCTTaCACTTTTCTAATaCCC
IAA16_cDNA_2	CACaAAATaTCaTCaAaAACTC
IAA16_1_F	ACACTGACGACATGGTTCTACA GTTTAGtTtTTTTAttATAGGtAAtTATGG
IAA16_1_R	TAC GGT AGC AGA GAC TTG GTC TTCCaATTaCTTCTaATCCCTTCATTATTC

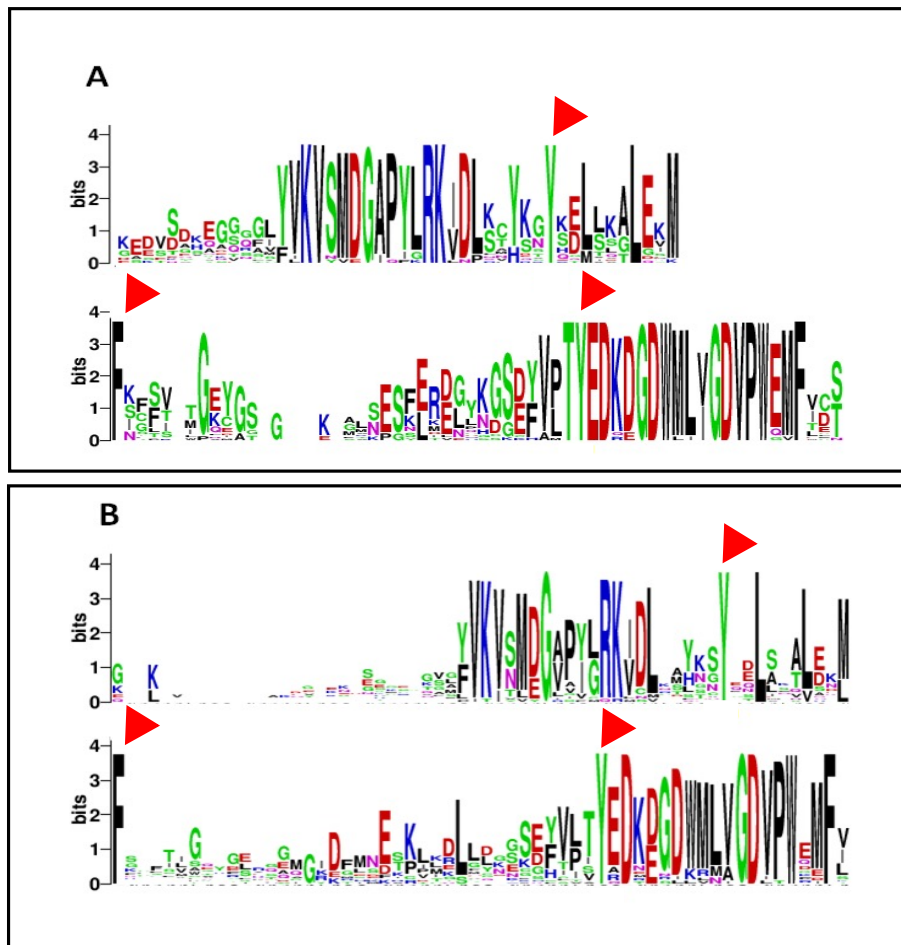
Supplementary Table IV-S6: gRNA spacer sequence for functional analysis using dCas13-TET1. Red letters denote overhangs for ligation into BsaI sites in the vector.

gRNA spacer sequence for functional analysis using dCas13-TET1	
SHY2-gRNA6-F	CAACTTTGTAACAACCTCAGATCTATTTTCCTCG
SHY2-gRNA6-R	ACAACGAGGAAAATAGATCTGAGTTGTTACAAA
SHY2-gRNA9-F	CAACGTAACAACCTCAGATCTATTTTCCTCAAGG
SHY2-gRNA9-R	ACAACCTTGAGGAAAATAGATCTGAGTTGTTAC
SHY2-gRNA15-F	CAACACTCAGATCTATTTTCCTCAAGTATGGTG
SHY2-gRNA15-R	ACAACACCATACTTGAGGAAAATAGATCTGAGT
SHY2-gRNA24'-F	CAACTTCTAAAGCTTTAAGCAACTCTGAGTATG
SHY2-gRNA24'-R	ACAACATACTCAGAGTTGCTTAAAGCTTTAGAA

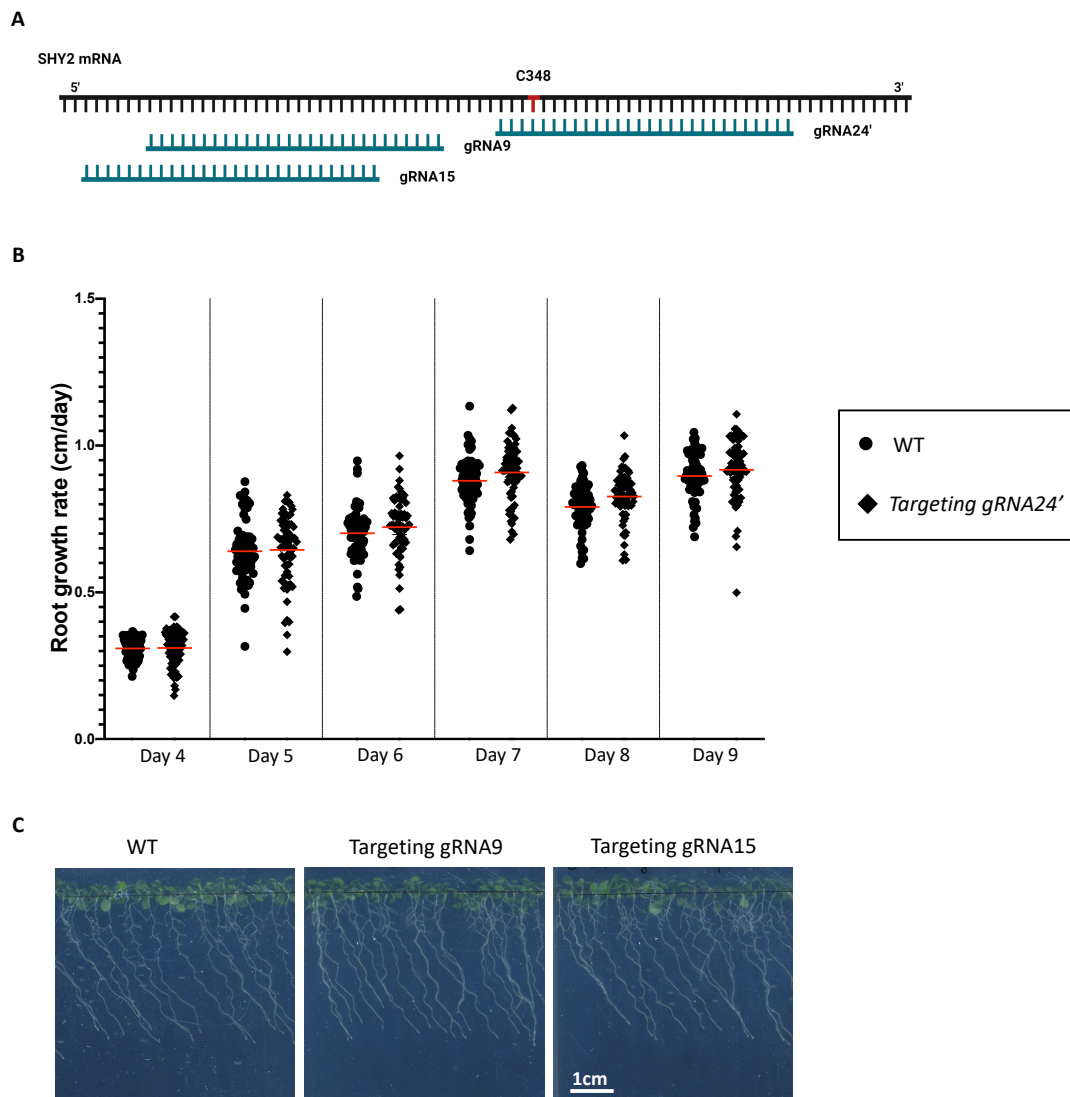
Supplementary Figure:



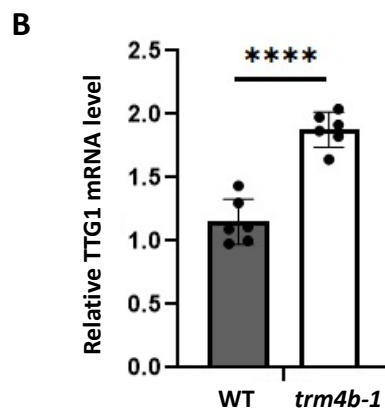
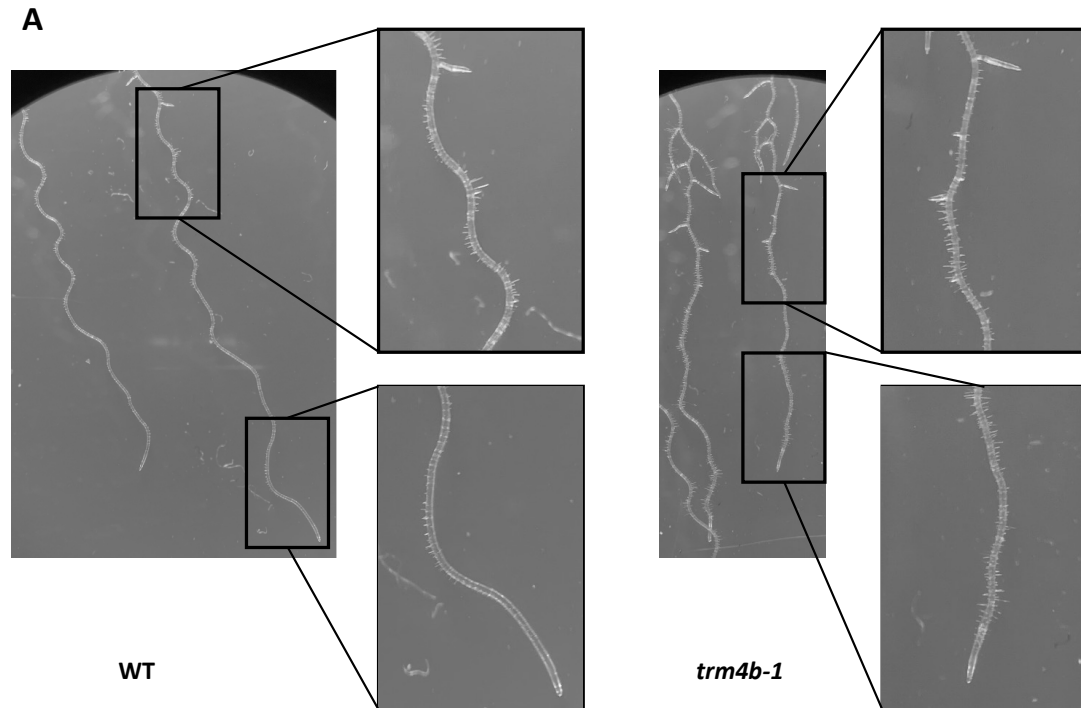
Supplementary Figure IV-S1: Relative transcript abundance of SHY2/IAA3 and IAA16 in wild-type and *trm4b-1* determined by RT-qPCR. This experiment was independent of Figure IV-2. 9-day old root tissues were used. Two biological replicates and three technical triplicates were performed. ACT2 was used as an internal control. Welch's t test, ***: p value < 0.001.



Supplementary Figure IV-S2: Conservation of Y116, Y149 and F167 on *A. thaliana* IAA3. A, Protein sequence logo of multiple sequence alignment for IAA3 across species of Pinus, Monocots and Dicots. B, Protein sequence logo of multiple sequence alignment for all protein in *A. thaliana* IAA family. Tyrosines correspond to Y116 (Upper), Y149 (Lower) and Phenylalanine correspond to F167 (Lower) in *A. thaliana* are indicated with red arrow heads in each panel.



Supplementary Figure IV-S3: Interference of dCas13-TET1 to C348 on SHY2/IAA3 does not alter root growth *in planta* (Supplementary materials for Figure IV-5). A, Positioning of spacers for dCas13-TET1. B-C, Root phenotype of transgenic plants compared to wild-type, illustrated as root growth rate for Targeting gRNA24' (B) or root images at day 9 for gRNA9 and gRNA15 (C). Data in (B) and (C) are generated independently.



Supplementary Figure IV-S4: RNA 5-methylcytosine and root hair production. A, Higher density of root hair observed in m^5C deficient mutant *trm4b-1* under Leica light microscope. The phenotype was observed in six *trm4b-1* plant replicates in two separate plates as opposed to ten wild-type in two separate plates. B, Root hair formation regulator TTG1 showed increased mRNA abundance in *trm4b-1*. Two biological replicates and three technical triplicates were performed. Error bars represent standard deviation of mean. *ACT2* was used as an internal control. Welch's t test, ****: p value < 0.0001

References

Abudayyeh, OO, Gootenberg, JS, Essletzbichler, P, Han, S, Joung, J, Belanto, JJ, Verdine, V, Cox, DBT, Kellner, MJ, Regev, A, Lander, ES, Voytas, DF, Ting, AY & Zhang, F 2017, 'RNA targeting with CRISPR-Cas13', *Nature*, vol. 550, no. 7675, 2017/10/01, pp. 280-284.

Abudayyeh, OO, Gootenberg, JS, Franklin, B, Koob, J, Kellner, MJ, Ladha, A, Joung, J, Kirchgatterer, P, Cox, DBT & Zhang, F 2019, 'A cytosine deaminase for programmable single-base RNA editing', *Science*, vol. 365, no. 6451, Jul 26, pp. 382-386.

Abudayyeh, OO, Gootenberg, JS, Konermann, S, Joung, J, Slaymaker, IM, Cox, DBT, Shmakov, S, Makarova, KS, Semenova, E, Minakhin, L, Severinov, K, Regev, A, Lander, ES, Koonin, EV & Zhang, F 2016, 'C2c2 is a single-component programmable RNA-guided RNA-targeting CRISPR effector', *Science*, vol. 353, no. 6299, p. aaf5573.

Amort, T, Soulière, MF, Wille, A, Jia, X-Y, Fiegl, H, Wörle, H, Micura, R & Lusser, A 2013, 'Long non-coding RNAs as targets for cytosine methylation', *RNA Biology*, vol. 10, no. 6, 2013/06/01, pp. 1002-1008.

Anderson, KM, Poosala, P, Lindley, SR & Anderson, DM 2019, 'Targeted Cleavage and Polyadenylation of RNA by CRISPR-Cas13', *bioRxiv*, p. 531111.

Anzalone, AV, Randolph, PB, Davis, JR, Sousa, AA, Koblan, LW, Levy, JM, Chen, PJ, Wilson, C, Newby, GA, Raguram, A & Liu, DR 2019, 'Search-and-replace genome editing without double-strand breaks or donor DNA', *Nature*, vol. 576, no. 7785, 2019/12/01, pp. 149-157.

Arribas-Hernández, L, Bressendorff, S, Hansen, MH, Poulsen, C, Erdmann, S & Brodersen, P 2018, 'An m(6)A-YTH Module Controls Developmental Timing and Morphogenesis in Arabidopsis', *Plant Cell*, vol. 30, no. 5, May, pp. 952-967.

Arribas-Hernández, L, Simonini, S, Hansen, MH, Paredes, EB, Bressendorff, S, Dong, Y, Østergaard, L & Brodersen, P 2020, 'Recurrent requirement for the m6A-ECT2/ECT3/ECT4 axis in the control of cell proliferation during plant organogenesis', *Development*, vol. 147, no. 14.

Arribas-Hernández, L, Simonini, S, Hansen, MH, Paredes, EB, Bressendorff, S, Dong, Y, Østergaard, L & Brodersen, P 2020, 'Recurrent requirement for the m(6)A-ECT2/ECT3/ECT4 axis in the control of cell proliferation during plant organogenesis', *Development*, vol. 147, no. 14, Jul 24.

Augstein, F & Carlsbecker, A 2018, 'Getting to the Roots: A Developmental Genetic View of Root Anatomy and Function From Arabidopsis to Lycophytes', *Frontiers in Plant Science*, vol. 9, no. 1410, 2018-September-25.

Begik, O, Lucas, MC, Prysycz, LP, Ramirez, JM, Medina, R, Milenkovic, I, Cruciani, S, Liu, H, Vieira, HGS, Sas-Chen, A, Mattick, JS, Schwartz, S & Novoa, EM 2021, 'Quantitative profiling of native RNA modifications and their dynamics using nanopore sequencing', *bioRxiv*, p. 2020.2007.2006.189969.

Blanco, S, Dietmann, S, Flores, JV, Hussain, S, Kutter, C, Humphreys, P, Lukk, M, Lombard, P, Treps, L, Popis, M, Kellner, S, Hölter, SM, Garrett, L, Wurst, W, Becker, L, Klopstock, T, Fuchs, H, Gailus-Durner, V, Hrabě de Angelis, M, Káradóttir, RT, Helm, M, Ule, J, Gleeson, JG, Odom, DT & Frye, M 2014, 'Aberrant methylation of tRNAs links cellular stress to neuro-developmental disorders', *Embo j*, vol. 33, no. 18, Sep 17, pp. 2020-2039.

Blanco, S, Kurowski, A, Nichols, J, Watt, FM, Benitah, SA & Frye, M 2011, 'The RNA–Methyltransferase Misu (NSun2) Poises Epidermal Stem Cells to Differentiate', *PLOS Genetics*, vol. 7, no. 12, p. e1002403.

Bohnsack, MT & Sloan, KE 2018, 'Modifications in small nuclear RNAs and their roles in spliceosome assembly and function', *Biol Chem*, vol. 399, no. 11, Oct 25, pp. 1265-1276.

Bokar, JA, Rath-Shambaugh, ME, Ludwiczak, R, Narayan, P & Rottman, F 1994, 'Characterization and partial purification of mRNA N6-adenosine methyltransferase from HeLa cell nuclei. Internal mRNA methylation requires a multisubunit complex', *J Biol Chem*, vol. 269, no. 26, Jul 1, pp. 17697-17704.

Buchman, AB, Brogan, DJ, Sun, R, Yang, T, Hsu, PD & Akbari, OS 2020, 'Programmable RNA Targeting Using CasRx in Flies', *The CRISPR journal*, vol. 3, no. 3, pp. 164-176.

Bujnicki, JM, Feder, M, Radlinska, M & Blumenthal, RM 2002, 'Structure prediction and phylogenetic analysis of a functionally diverse family of proteins homologous to the MT-A70 subunit of the human mRNA:m(6)A methyltransferase', *J Mol Evol*, vol. 55, no. 4, Oct, pp. 431-444.

Burgess, AL, David, R & Searle, IR 2015, 'Conservation of tRNA and rRNA 5-methylcytosine in the kingdom Plantae', *BMC Plant Biol*, vol. 15, Aug 14, p. 199.

Caplen, NJ, Parrish, S, Imani, F, Fire, A & Morgan, RA 2001, 'Specific inhibition of gene expression by small double-stranded RNAs in invertebrate and vertebrate systems', *Proc Natl Acad Sci U S A*, vol. 98, no. 17, Aug 14, pp. 9742-9747.

Carlile, TM, Rojas-Duran, MF, Zinshteyn, B, Shin, H, Bartoli, KM & Gilbert, WV 2014, 'Pseudouridine profiling reveals regulated mRNA pseudouridylation in yeast and human cells', *Nature*, vol. 515, no. 7525, Nov 6, pp. 143-146.

Chen, K, Lu, Z, Wang, X, Fu, Y, Luo, G-Z, Liu, N, Han, D, Dominissini, D, Dai, Q, Pan, T & He, C 2015, 'High-Resolution N6-Methyladenosine (m6A) Map Using Photo-Crosslinking-Assisted m6A Sequencing', *Angewandte Chemie International Edition*, vol. 54, no. 5, pp. 1587-1590.

Chen, T, Hao, Y-J, Zhang, Y, Li, M-M, Wang, M, Han, W, Wu, Y, Lv, Y, Hao, J, Wang, L, Li, A, Yang, Y, Jin, K-X, Zhao, X, Li, Y, Ping, X-L, Lai, W-Y, Wu, L-G, Jiang, G, Wang, H-L, Sang, L, Wang, X-J, Yang, Y-G & Zhou, Q 2015, 'm⁶A RNA Methylation Is Regulated by MicroRNAs and Promotes Reprogramming to Pluripotency', *Cell Stem Cell*, vol. 16, no. 3, pp. 289-301.

Chou, K-C & Shen, H-B 2010, 'Plant-mPLoc: A Top-Down Strategy to Augment the Power for Predicting Plant Protein Subcellular Localization', *PLOS ONE*, vol. 5, no. 6, p. e11335.

Choudhury, SR, Cui, Y, Lubecka, K, Stefanska, B & Irudayaraj, J 2016, 'CRISPR-dCas9 mediated TET1 targeting for selective DNA demethylation at BRCA1 promoter', *Oncotarget*, vol. 7, no. 29, pp. 46545-46556.

Clough, SJ & Bent, AF 1998, 'Floral dip: a simplified method for Agrobacterium-mediated transformation of *Arabidopsis thaliana*', *Plant J*, vol. 16, no. 6, Dec, pp. 735-743.

Cohn, WE 1960, 'Pseudouridine, a Carbon-Carbon Linked Ribonucleoside in Ribonucleic Acids: Isolation, Structure, and Chemical Characteristics', *Journal of Biological Chemistry*, vol. 235, no. 5, 1960/05/01/, pp. 1488-1498.

Cohn, WE & Volkin, E 1951, 'Nucleoside-5'-Phosphates from Ribonucleic Acid', *Nature*, vol. 167, no. 4247, 1951/03/01, pp. 483-484.

Cong, L, Ran, FA, Cox, D, Lin, S, Barretto, R, Habib, N, Hsu, PD, Wu, X, Jiang, W, Marraffini, LA & Zhang, F 2013, 'Multiplex genome engineering using CRISPR/Cas systems', *Science*, vol. 339, no. 6121, Feb 15, pp. 819-823.

Cox, DBT, Gootenberg, JS, Abudayyeh, OO, Franklin, B, Kellner, MJ, Joung, J & Zhang, F 2017, 'RNA editing with CRISPR-Cas13', *Science*, vol. 358, no. 6366, Nov 24, pp. 1019-1027.

Cui, X, Liang, Z, Shen, L, Zhang, Q, Bao, S, Geng, Y, Zhang, B, Leo, V, Vardy, LA, Lu, T, Gu, X & Yu, H 2017, '5-Methylcytosine RNA Methylation in *Arabidopsis Thaliana*', *Molecular Plant*, vol. 10, no. 11, pp. 1387-1399.

David, R, Burgess, A, Parker, B, Li, J, Pulsford, K, Sibbritt, T, Preiss, T & Searle, IR 2017, 'Transcriptome-Wide Mapping of RNA 5-Methylcytosine in *Arabidopsis* mRNAs and Noncoding RNAs', *Plant Cell*, vol. 29, no. 3, Mar, pp. 445-460.

Delatte, B, Wang, F, Ngoc, LV, Collignon, E, Bonvin, E, Deplus, R, Calonne, E, Hassabi, B, Putmans, P, Awe, S, Wetzel, C, Kreher, J, Soin, R, Creppe, C, Limbach, PA, Gueydan, C, Kruys, V, Brehm, A, Minakhina, S, Defrance, M, Steward, R & Fuks, F 2016, 'RNA biochemistry. Transcriptome-wide distribution and function of RNA hydroxymethylcytosine', *Science*, vol. 351, no. 6270, Jan 15, pp. 282-285.

Delatte, B, Wang, F, Ngoc, LV, Collignon, E, Bonvin, E, Deplus, R, Calonne, E, Hassabi, B, Putmans, P, Awe, S, Wetzel, C, Kreher, J, Soin, R, Creppe, C, Limbach, PA, Gueydan, C, Kruys, V, Brehm, A, Minakhina, S, Defrance, M, Steward, R & Fuks, F 2016, 'Transcriptome-wide distribution and function of RNA hydroxymethylcytosine', *Science*, vol. 351, no. 6270, pp. 282-285.

DeNizio, JE, Liu, MY, Leddin, EM, Cisneros, GA & Kohli, RM 2019, 'Selectivity and Promiscuity in TET-Mediated Oxidation of 5-Methylcytosine in DNA and RNA', *Biochemistry*, vol. 58, no. 5, 2019/02/05, pp. 411-421.

Desrosiers, R, Friderici, K & Rottman, F 1974, 'Identification of Methylated Nucleosides in Messenger RNA from Novikoff Hepatoma Cells', *Proceedings of the National Academy of Sciences*, vol. 71, no. 10, p. 3971.

Dominissini, D, Moshitch-Moshkovitz, S, Schwartz, S, Salmon-Divon, M, Ungar, L, Osenberg, S, Cesarkas, K, Jacob-Hirsch, J, Amariglio, N, Kupiec, M, Sorek, R & Rechavi, G 2012, 'Topology of the human and mouse m6A RNA methylomes revealed by m6A-seq', *Nature*, vol. 485, no. 7397, Apr 29, pp. 201-206.

Dominissini, D, Nachtergaele, S, Moshitch-Moshkovitz, S, Peer, E, Kol, N, Ben-Haim, MS, Dai, Q, Di Segni, A, Salmon-Divon, M, Clark, WC, Zheng, G, Pan, T, Solomon, O, Eyal, E, Hershkovitz, V, Han, D, Doré, LC, Amariglio, N, Rechavi, G & He, C 2016, 'The dynamic N(1)-methyladenosine methylome in eukaryotic messenger RNA', *Nature*, vol. 530, no. 7591, Feb 25, pp. 441-446.

Duan, H-C, Wei, L-H, Zhang, C, Wang, Y, Chen, L, Lu, Z, Chen, PR, He, C & Jia, G 2017, 'ALKBH10B Is an RNA N⁶-Methyladenosine Demethylase Affecting *Arabidopsis* Floral Transition', *The Plant Cell*, vol. 29, no. 12, pp. 2995-3011.

Dubin, DT & Taylor, RH 1975, 'The methylation state of poly A-containing messenger RNA from cultured hamster cells', *Nucleic Acids Res*, vol. 2, no. 10, Oct, pp. 1653-1668.

Dunn, DB 1961, 'The occurrence of 1-methyladenine in ribonucleic acid', *Biochimica et biophysica acta*, vol. 46, no. 1, 1961/01/01/, pp. 198-200.

Ebhardt, HA, Tsang, HH, Dai, DC, Liu, Y, Bostan, B & Fahlman, RP 2009, 'Meta-analysis of small RNA-sequencing errors reveals ubiquitous post-transcriptional RNA modifications', *Nucleic Acids Res*, vol. 37, no. 8, May, pp. 2461-2470.

Edelheit, S, Schwartz, S, Mumbach, MR, Wurtzel, O & Sorek, R 2013, 'Transcriptome-wide mapping of 5-methylcytidine RNA modifications in bacteria, archaea, and yeast reveals m5C within archaeal mRNAs', *PLoS Genet*, vol. 9, no. 6, Jun, p. e1003602.

Elbashir, SM, Harborth, J, Lendeckel, W, Yalcin, A, Weber, K & Tuschl, T 2001, 'Duplexes of 21-nucleotide RNAs mediate RNA interference in cultured mammalian cells', *Nature*, vol. 411, no. 6836, May 24, pp. 494-498.

Engler, C, Kandzia, R & Marillonnet, S 2008, 'A One Pot, One Step, Precision Cloning Method with High Throughput Capability', *PLOS ONE*, vol. 3, no. 11, p. e3647.

Fahiminiya, S, Almurieghi, M, Nawaz, Z, Staffa, A, Lepage, P, Ali, R, Hashim, L, Schwartzentruber, J, Abu Khadija, K, Zaineddin, S, Gamal, H, Majewski, J & Ben-Omran, T 2014, 'Whole exome sequencing unravels disease-causing genes in consanguineous families in Qatar', *Clinical Genetics*, vol. 86, no. 2, pp. 134-141.

Flaherty, SM, Fortes, P, Izaurralde, E, Mattaj, JW & Gilmartin, GM 1997, 'Participation of the nuclear cap binding complex in pre-mRNA 3' processing', *Proc Natl Acad Sci U S A*, vol. 94, no. 22, Oct 28, pp. 11893-11898.

Franco-Zorrilla, JM, Valli, A, Todesco, M, Mateos, I, Puga, MI, Rubio-Somoza, I, Leyva, A, Weigel, D, García, JA & Paz-Ares, J 2007, 'Target mimicry provides a new mechanism for regulation of microRNA activity', *Nature Genetics*, vol. 39, no. 8, 2007/08/01, pp. 1033-1037.

Fu, L, Guerrero, CR, Zhong, N, Amato, NJ, Liu, Y, Liu, S, Cai, Q, Ji, D, Jin, S-G, Niedernhofer, LJ, Pfeifer, GP, Xu, G-L & Wang, Y 2014, 'Tet-Mediated Formation of 5-Hydroxymethylcytosine in RNA', *Journal of the American Chemical Society*, vol. 136, no. 33, 2014/08/20, pp. 11582-11585.

Furuichi, Y, LaFiandra, A & Shatkin, AJ 1977, '5'-Terminal structure and mRNA stability', *Nature*, vol. 266, no. 5599, Mar 17, pp. 235-239.

Gallego-Bartolomé, J, Gardiner, J, Liu, W, Papikian, A, Ghoshal, B, Kuo, HY, Zhao, JM-C, Segal, DJ & Jacobsen, SE 2018, 'Targeted DNA demethylation of the Arabidopsis genome using the human TET1 catalytic domain', *Proceedings of the National Academy of Sciences*, vol. 115, no. 9, p. E2125.

Gallie, DR 1991, 'The cap and poly(A) tail function synergistically to regulate mRNA translational efficiency', *Genes Dev*, vol. 5, no. 11, Nov, pp. 2108-2116.

Galway, ME, Masucci, JD, Lloyd, AM, Walbot, V, Davis, RW & Schiefelbein, JW 1994, 'The TTG Gene Is Required to Specify Epidermal Cell Fate and Cell Patterning in the Arabidopsis Root', *Developmental Biology*, vol. 166, no. 2, 1994/12/01/, pp. 740-754.

Gao, Y, Vasic, R, Song, Y, Teng, R, Liu, C, Gbyli, R, Biancon, G, Nelakanti, R, Lobben, K, Kudo, E, Liu, W, Ardasheva, A, Fu, X, Wang, X, Joshi, P, Lee, V, Dura, B, Viero, G, Iwasaki, A, Fan, R, Xiao, A, Flavell, RA, Li, H-B, Tebaldi, T & Halene, S 2020, 'm⁶A Modification Prevents Formation of Endogenous Double-Stranded RNAs and Deleterious Innate Immune Responses during Hematopoietic Development', *Immunity*, vol. 52, no. 6, pp. 1007-1021.e1008.

Gao, Z, Herrera-Carrillo, E & Berkhout, B 2018, 'Delineation of the Exact Transcription Termination Signal for Type 3 Polymerase III', *Molecular Therapy - Nucleic Acids*, vol. 10, 2018/03/02/, pp. 36-44.

Garcia-Campos, MA, Edelheit, S, Toth, U, Safra, M, Shachar, R, Viukov, S, Winkler, R, Nir, R, Lasman, L, Brandis, A, Hanna, JH, Rossmanith, W & Schwartz, S 2019, 'Deciphering the "m6A Code" via Antibody-Independent Quantitative Profiling', *Cell*, vol. 178, no. 3, 2019/07/25/, pp. 731-747.e716.

Geula, S, Moshitch-Moshkovitz, S, Dominissini, D, Mansour, AA, Kol, N, Salmon-Divon, M, Hershkovitz, V, Peer, E, Mor, N, Manor, YS, Ben-Haim, MS, Eyal, E, Yunger, S, Pinto, Y, Jaitin, DA, Viukov, S, Rais, Y, Krupalnik, V, Chomsky, E, Zerbib, M, Maza, I, Rechavi, Y, Massarwa, R, Hanna, S, Amit, I, Levanon, EY, Amariglio, N, Stern-Ginossar, N, Novershtern, N, Rechavi, G & Hanna, JH 2015, 'Stem cells. m6A mRNA methylation facilitates resolution of naïve pluripotency toward differentiation', *Science*, vol. 347, no. 6225, Feb 27, pp. 1002-1006.

Gibson, DG, Young, L, Chuang, R-Y, Venter, JC, Hutchison, CA & Smith, HO 2009, 'Enzymatic assembly of DNA molecules up to several hundred kilobases', *Nature Methods*, vol. 6, no. 5, 2009/05/01, pp. 343-345.

Goll, MG, Kirpekar, F, Maggert, KA, Yoder, JA, Hsieh, C-L, Zhang, X, Golic, KG, Jacobsen, SE & Bestor, TH 2006, 'Methylation of tRNA^{Asp} by the DNA Methyltransferase Homolog Dnmt2', *Science*, vol. 311, no. 5759, pp. 395-398.

Han, S, Zhao, BS, Myers, SA, Carr, SA, He, C & Ting, AY 2020, 'RNA–protein interaction mapping via MS2- or Cas13-based APEX targeting', *Proceedings of the National Academy of Sciences*, vol. 117, no. 36, p. 22068.

Hausmann, IU, Bodi, Z, Sanchez-Moran, E, Mongan, NP, Archer, N, Fray, RG & Soller, M 2016, 'm6A potentiates Sxl alternative pre-mRNA splicing for robust *Drosophila* sex determination', *Nature*, vol. 540, no. 7632, 2016/12/01, pp. 301-304.

He, C 2010, 'Grand challenge commentary: RNA epigenetics?', *Nat Chem Biol*, vol. 6, no. 12, Dec, pp. 863-865.

He, C, Bozler, J, Janssen, KA, Wilusz, JE, Garcia, BA, Schorn, AJ & Bonasio, R 2021, 'TET2 chemically modifies tRNAs and regulates tRNA fragment levels', *Nature Structural & Molecular Biology*, vol. 28, no. 1, 2021/01/01, pp. 62-70.

Helm, M & Motorin, Y 2017, 'Detecting RNA modifications in the epitranscriptome: predict and validate', *Nature Reviews Genetics*, vol. 18, no. 5, 2017/05/01, pp. 275-291.

Holley, RW, Everett, GA, Madison, JT & Zamir, A 1965, 'NUCLEOTIDE SEQUENCES IN THE YEAST ALANINE TRANSFER RIBONUCLEIC ACID', *J Biol Chem*, vol. 240, May, pp. 2122-2128.

Hongay, CF & Orr-Weaver, TL 2011, 'Drosophila Inducer of MEiosis 4 (IME4) is required for Notch signaling during oogenesis', *Proceedings of the National Academy of Sciences*, vol. 108, no. 36, p. 14855.

Hooper, CM, Castleden, IR, Tanz, SK, Aryamanesh, N & Millar, AH 2017, 'SUBA4: the interactive data analysis centre for *Arabidopsis* subcellular protein locations', *Nucleic Acids Res*, vol. 45, no. D1, Jan 4, pp. D1064-d1074.

Huang, H, Weng, H, Sun, W, Qin, X, Shi, H, Wu, H, Zhao, BS, Mesquita, A, Liu, C, Yuan, CL, Hu, Y-C, Hüttelmaier, S, Skibbe, JR, Su, R, Deng, X, Dong, L, Sun, M, Li, C, Nachtergaele, S, Wang, Y, Hu, C, Ferchen, K, Greis, KD, Jiang, X, Wei, M, Qu, L, Guan, J-L, He, C, Yang, J & Chen, J 2018, 'Recognition of RNA N(6)-methyladenosine by IGF2BP proteins enhances mRNA stability and translation', *Nature cell biology*, vol. 20, no. 3, pp. 285-295.

Huang, T, Chen, W, Liu, J, Gu, N & Zhang, R 2019, 'Genome-wide identification of mRNA 5-methylcytosine in mammals', *Nature Structural & Molecular Biology*, vol. 26, no. 5, 2019/05/01, pp. 380-388.

Huong, TT, Ngoc, LNT & Kang, H 2020, 'Functional Characterization of a Putative RNA Demethylase ALKBH6 in Arabidopsis Growth and Abiotic Stress Responses', *International journal of molecular sciences*, vol. 21, no. 18, p. 6707.

Hussain, S, Sajini, AA, Blanco, S, Dietmann, S, Lombard, P, Sugimoto, Y, Paramor, M, Gleeson, JG, Odom, DT, Ule, J & Frye, M 2013, 'NSun2-mediated cytosine-5 methylation of vault noncoding RNA determines its processing into regulatory small RNAs', *Cell Rep*, vol. 4, no. 2, Jul 25, pp. 255-261.

Ishino, Y, Shinagawa, H, Makino, K, Amemura, M & Nakata, A 1987, 'Nucleotide sequence of the *iap* gene, responsible for alkaline phosphatase isozyme conversion in *Escherichia coli*, and identification of the gene product', *Journal of bacteriology*, vol. 169, no. 12, pp. 5429-5433.

Ito, S, Shen, L, Dai, Q, Wu, SC, Collins, LB, Swenberg, JA, He, C & Zhang, Y 2011, 'Tet proteins can convert 5-methylcytosine to 5-formylcytosine and 5-carboxylcytosine', *Science*, vol. 333, no. 6047, Sep 2, pp. 1300-1303.

Ivashuta, S, Banks, IR, Wiggins, BE, Zhang, Y, Ziegler, TE, Roberts, JK & Heck, GR 2011, 'Regulation of gene expression in plants through miRNA inactivation', *PLOS ONE*, vol. 6, no. 6, p. e21330.

Izaurralde, E, Lewis, J, McGuigan, C, Jankowska, M, Darzynkiewicz, E & Mattaj, JW 1994, 'A nuclear cap binding protein complex involved in pre-mRNA splicing', *Cell*, vol. 78, no. 4, Aug 26, pp. 657-668.

Jackman, JE & Alfonzo, JD 2013, 'Transfer RNA modifications: nature's combinatorial chemistry playground', *Wiley Interdiscip Rev RNA*, vol. 4, no. 1, Jan-Feb, pp. 35-48.

Ji, L, Jordan, WT, Shi, X, Hu, L, He, C & Schmitz, RJ 2018, 'TET-mediated epimutagenesis of the *Arabidopsis thaliana* methylome', *Nature Communications*, vol. 9, no. 1, pp. 895-895.

Jia, G, Fu, Y, Zhao, X, Dai, Q, Zheng, G, Yang, Y, Yi, C, Lindahl, T, Pan, T, Yang, YG & He, C 2011, 'N6-methyladenosine in nuclear RNA is a major substrate of the obesity-associated FTO', *Nat Chem Biol*, vol. 7, no. 12, Oct 16, pp. 885-887.

Jin, C, Lu, Y, Jelinek, J, Liang, S, Estecio, MR, Barton, MC & Issa, JP 2014, 'TET1 is a maintenance DNA demethylase that prevents methylation spreading in differentiated cells', *Nucleic Acids Res*, vol. 42, no. 11, Jun, pp. 6956-6971.

Jinek, M, Chylinski, K, Fonfara, I, Hauer, M, Doudna, JA & Charpentier, E 2012, 'A programmable dual-RNA-guided DNA endonuclease in adaptive bacterial immunity', *Science*, vol. 337, no. 6096, Aug 17, pp. 816-821.

Jones, PA & Taylor, SM 1980, 'Cellular differentiation, cytidine analogs and DNA methylation', *Cell*, vol. 20, no. 1, May, pp. 85-93.

Khoddami, V & Cairns, BR 2013, 'Identification of direct targets and modified bases of RNA cytosine methyltransferases', *Nature Biotechnology*, vol. 31, no. 5, 2013/05/01, pp. 458-464.

Khoddami, V & Cairns, BR 2014, 'Transcriptome-wide target profiling of RNA cytosine methyltransferases using the mechanism-based enrichment procedure Aza-IP', *Nature Protocols*, vol. 9, no. 2, 2014/02/01, pp. 337-361.

Knuckles, P, Lence, T, Haussmann, IU, Jacob, D, Kreim, N, Carl, SH, Masiello, I, Hares, T, Villaseñor, R, Hess, D, Andrade-Navarro, MA, Biggiogera, M, Helm, M, Soller, M, Bühler, M & Roignant, JY 2018, 'Zc3h13/Flacc is required for adenosine methylation by bridging the mRNA-binding factor Rbm15/Spenito to the m(6)A machinery component Wtap/Fl(2)d', *Genes Dev*, vol. 32, no. 5-6, Mar 1, pp. 415-429.

Koevoets, IT, Venema, JH, Elzenga, JTM & Testerink, C 2016, 'Roots Withstanding their Environment: Exploiting Root System Architecture Responses to Abiotic Stress to Improve Crop Tolerance', *Frontiers in Plant Science*, vol. 7, no. 1335, 2016-August-31.

Kohli, A, Melendi, PG, Abranches, R, Capell, T, Stoger, E & Christou, P 2006, 'The Quest to Understand the Basis and Mechanisms that Control Expression of Introduced Transgenes in Crop Plants', *Plant signaling & behavior*, vol. 1, no. 4, pp. 185-195.

Komor, AC, Kim, YB, Packer, MS, Zuris, JA & Liu, DR 2016, 'Programmable editing of a target base in genomic DNA without double-stranded DNA cleavage', *Nature*, vol. 533, no. 7603, May 19, pp. 420-424.

Konermann, S, Lotfy, P, Brideau, NJ, Oki, J, Shokhirev, MN & Hsu, PD 2018, 'Transcriptome Engineering with RNA-Targeting Type VI-D CRISPR Effectors', *Cell*, vol. 173, no. 3, pp. 665-676.e614.

Lan, J, Rajan, N, Bizet, M, Penning, A, Singh, NK, Guallar, D, Calonne, E, Li Greci, A, Bonvin, E, Deplus, R, Hsu, PJ, Nachtergaele, S, Ma, C, Song, R, Fuentes-Iglesias, A, Hassabi, B, Putmans, P, Mies, F, Menschaert, G, Wong, J, Wang, J, Fidalgo, M, Yuan, B & Fuks, F 2020, 'Functional role of Tet-mediated RNA hydroxymethylcytosine in mouse ES cells and during differentiation', *Nature Communications*, vol. 11, no. 1, 2020/10/02, p. 4956.

Lavi, U, Fernandez-Mufioz, R & Darnell, JE, Jr. 1977, 'Content of N-6 methyl adenylic acid in heterogeneous nuclear and messenger RNA of HeLa cells', *Nucleic Acids Research*, vol. 4, no. 1, pp. 63-69.

Legrand, C, Tuorto, F, Hartmann, M, Liebers, R, Jacob, D, Helm, M & Lyko, F 2017, 'Statistically robust methylation calling for whole-transcriptome bisulfite sequencing reveals distinct methylation patterns for mouse RNAs', *Genome research*, vol. 27, no. 9, pp. 1589-1596.

Li, E, Beard, C & Jaenisch, R 1993, 'Role for DNA methylation in genomic imprinting', *Nature*, vol. 366, no. 6453, 1993/12/01, pp. 362-365.

Li, J, Chen, Z, Chen, F, Xie, G, Ling, Y, Peng, Y, Lin, Y, Luo, N, Chiang, C-M & Wang, H 2020, 'Targeted mRNA demethylation using an engineered dCas13b-ALKBH5 fusion protein', *Nucleic Acids Research*, vol. 48, no. 10, pp. 5684-5694.

Li, J, Wu, X, Do, T, Nguyen, V, Zhao, J, Ng, PQ, Burgess, A, David, R & Searle, IR 2021, 'Quantitative and Single-Nucleotide Resolution Profiling of RNA 5-Methylcytosine', *Methods in molecular biology*, vol. 2298, pp. 135-151.

Li, Q, Li, X, Tang, H, Jiang, B, Dou, Y, Gorospe, M & Wang, W 2017, 'NSUN2-Mediated m5C Methylation and METTL3/METTL14-Mediated m6A Methylation Cooperatively Enhance p21 Translation', *Journal of Cellular Biochemistry*, vol. 118, no. 9, pp. 2587-2598.

Li, S & Mason, CE 2014, 'The pivotal regulatory landscape of RNA modifications', *Annu Rev Genomics Hum Genet*, vol. 15, pp. 127-150.

Li, X, Xiong, X, Wang, K, Wang, L, Shu, X, Ma, S & Yi, C 2016, 'Transcriptome-wide mapping reveals reversible and dynamic N1-methyladenosine methylome', *Nature Chemical Biology*, vol. 12, no. 5, 2016/05/01, pp. 311-316.

Li, Y, Wang, X, Li, C, Hu, S, Yu, J & Song, S 2014, 'Transcriptome-wide N6-methyladenosine profiling of rice callus and leaf reveals the presence of tissue-specific competitors involved in selective mRNA modification', *RNA Biology*, vol. 11, no. 9, 2014/09/02, pp. 1180-1188.

Linder, B, Grozhik, AV, Olarerin-George, AO, Meydan, C, Mason, CE & Jaffrey, SR 2015, 'Single-nucleotide-resolution mapping of m6A and m6Am throughout the transcriptome', *Nat Methods*, vol. 12, no. 8, Aug, pp. 767-772.

Liu, B, Merriman, DK, Choi, SH, Schumacher, MA, Plangger, R, Kreutz, C, Horner, SM, Meyer, KD & Al-Hashimi, HM 2018, 'A potentially abundant junctional RNA motif stabilized by m6A and Mg²⁺', *Nature Communications*, vol. 9, no. 1, 2018/07/17, p. 2761.

Liu, F, Clark, W, Luo, G, Wang, X, Fu, Y, Wei, J, Wang, X, Hao, Z, Dai, Q, Zheng, G, Ma, H, Han, D, Evans, M, Klungland, A, Pan, T & He, C 2016, 'ALKBH1-Mediated tRNA Demethylation Regulates Translation', *Cell*, vol. 167, no. 7, Dec 15, p. 1897.

Liu, H, Begik, O, Lucas, MC, Ramirez, JM, Mason, CE, Wiener, D, Schwartz, S, Mattick, JS, Smith, MA & Novoa, EM 2019, 'Accurate detection of m6A RNA modifications in native RNA sequences', *Nature Communications*, vol. 10, no. 1, 2019/09/09, p. 4079.

Liu, J, Yue, Y, Han, D, Wang, X, Fu, Y, Zhang, L, Jia, G, Yu, M, Lu, Z, Deng, X, Dai, Q, Chen, W & He, C 2014, 'A METTL3-METTL14 complex mediates mammalian nuclear RNA N6-adenosine methylation', *Nat Chem Biol*, vol. 10, no. 2, Feb, pp. 93-95.

Liu, N, Dai, Q, Zheng, G, He, C, Parisien, M & Pan, T 2015, 'N(6)-methyladenosine-dependent RNA structural switches regulate RNA-protein interactions', *Nature*, vol. 518, no. 7540, Feb 26, pp. 560-564.

Liu, N, Parisien, M, Dai, Q, Zheng, G, He, C & Pan, T 2013, 'Probing N6-methyladenosine RNA modification status at single nucleotide resolution in mRNA and long noncoding RNA', *RNA (New York, N.Y.)*, vol. 19, no. 12, pp. 1848-1856.

Liu, N, Zhou, KI, Parisien, M, Dai, Q, Diatchenko, L & Pan, T 2017, 'N6-methyladenosine alters RNA structure to regulate binding of a low-complexity protein', *Nucleic Acids Res*, vol. 45, no. 10, Jun 2, pp. 6051-6063.

Liu, X-M, Zhou, J, Mao, Y, Ji, Q & Qian, S-B 2019, 'Programmable RNA N6-methyladenosine editing by CRISPR-Cas9 conjugates', *Nature Chemical Biology*, vol. 15, no. 9, 2019/09/01, pp. 865-871.

Liu, XS, Wu, H, Ji, X, Stelzer, Y, Wu, X, Czauderna, S, Shu, J, Dadon, D, Young, RA & Jaenisch, R 2016, 'Editing DNA Methylation in the Mammalian Genome', *Cell*, vol. 167, no. 1, pp. 233-247.e217.

Long, Y & Schiefelbein, J 2020, 'Novel TTG1 Mutants Modify Root-Hair Pattern Formation in Arabidopsis', *Frontiers in Plant Science*, vol. 11, no. 383, 2020-April-07.

Lorenz, DA, Sathe, S, Einstein, JM & Yeo, GW 2020, 'Direct RNA sequencing enables m(6)A detection in endogenous transcript isoforms at base-specific resolution', *RNA (New York, N.Y.)*, vol. 26, no. 1, pp. 19-28.

Luo, G-Z, MacQueen, A, Zheng, G, Duan, H, Dore, LC, Lu, Z, Liu, J, Chen, K, Jia, G, Bergelson, J & He, C 2014, 'Unique features of the m6A methylome in Arabidopsis thaliana', *Nature Communications*, vol. 5, no. 1, 2014/11/28, p. 5630.

Ma, J, Zhang, L, Chen, S & Liu, H 2021, 'A brief review of RNA modification related database resources', *Methods*, 2021/03/08/.

Ma, X, Kim, E-J, Kook, I, Ma, F, Voshall, A, Moriyama, E & Cerutti, H 2013, 'Small interfering RNA-mediated translation repression alters ribosome sensitivity to inhibition by cycloheximide in *Chlamydomonas reinhardtii*', *The Plant Cell*, vol. 25, no. 3, pp. 985-998.

Manna, S 2015, 'An overview of pentatricopeptide repeat proteins and their applications', *Biochimie*, vol. 113, 2015/06/01/, pp. 93-99.

Martínez-Pérez, M, Aparicio, F, López-Gresa, MP, Bellés, JM, Sánchez-Navarro, JA & Pallás, V 2017, 'Arabidopsis m⁶A demethylase activity modulates viral infection of a plant virus and the m⁶A abundance in its genomic RNAs', *Proceedings of the National Academy of Sciences*, vol. 114, no. 40, p. 10755.

Matsuyama, A, Arai, R, Yashiroda, Y, Shirai, A, Kamata, A, Sekido, S, Kobayashi, Y, Hashimoto, A, Hamamoto, M, Hiraoka, Y, Horinouchi, S & Yoshida, M 2006, 'ORFeome cloning and global analysis of protein localization in the fission yeast *Schizosaccharomyces pombe*', *Nature Biotechnology*, vol. 24, no. 7, 2006/07/01, pp. 841-847.

Mauer, J, Luo, X, Blanjoie, A, Jiao, X, Grozhik, AV, Patil, DP, Linder, B, Pickering, BF, Vasseur, J-J, Chen, Q, Gross, SS, Elemento, O, Debart, F, Kiledjian, M & Jaffrey, SR 2017, 'Reversible methylation of m6Am in the 5' cap controls mRNA stability', *Nature*, vol. 541, no. 7637, 2017/01/01, pp. 371-375.

McGhee, JD & Ginder, GD 1979, 'Specific DNA methylation sites in the vicinity of the chicken beta-globin genes', *Nature*, vol. 280, no. 5721, Aug 2, pp. 419-420.

Mendel, M, Delaney, K, Pandey, RR, Chen, K-M, Wenda, JM, Vågbø, CB, Steiner, FA, Homolka, D & Pillai, RS 2021, 'Splice site m6A methylation prevents binding of U2AF35 to inhibit RNA splicing', *Cell*, vol. 184, no. 12, 2021/06/10/, pp. 3125-3142.e3125.

Meyer, KD 2019, 'DART-seq: an antibody-free method for global m6A detection', *Nature Methods*, vol. 16, no. 12, 2019/12/01, pp. 1275-1280.

Meyer, KD, Saletore, Y, Zumbo, P, Elemento, O, Mason, CE & Jaffrey, SR 2012, 'Comprehensive analysis of mRNA methylation reveals enrichment in 3' UTRs and near stop codons', *Cell*, vol. 149, no. 7, Jun 22, pp. 1635-1646.

Mielecki, D, Zugaj, DŁ, Muszewska, A, Piwowarski, J, Chojnacka, A, Mielecki, M, Nieminuszczy, J, Grynberg, M & Grzesiuk, E 2012, 'Novel AlkB Dioxygenases—Alternative Models for In Silico and In Vivo Studies', *PLOS ONE*, vol. 7, no. 1, p. e30588.

Militello, KT, Chen, LM, Ackerman, SE, Mandarano, AH & Valentine, EL 2014, 'A map of 5-methylcytosine residues in *Trypanosoma brucei* tRNA revealed by sodium bisulfite sequencing', *Molecular and Biochemical Parasitology*, vol. 193, no. 2, 2014/02/01/, pp. 122-126.

Mohandas, T, Sparkes, RS & Shapiro, LJ 1981, 'Reactivation of an inactive human X chromosome: evidence for X inactivation by DNA methylation', *Science*, vol. 211, no. 4480, Jan 23, pp. 393-396.

Parker, MT, Knop, K, Sherwood, AV, Schurch, NJ, Mackinnon, K, Gould, PD, Hall, AJW, Barton, GJ & Simpson, GG 2020, 'Nanopore direct RNA sequencing maps the complexity of *Arabidopsis* mRNA processing and m6A modification', *eLife*, vol. 9, 2020/01/14, p. e49658.

Perry, RP & Kelley, DE 1974, 'Existence of methylated messenger RNA in mouse L cells', *Cell*, vol. 1, no. 1, pp. 37-42.

Pesch, M, Schultheiß, I, Klopffleisch, K, Uhrig, JF, Koegl, M, Clemen, CS, Simon, R, Weidtkamp-Peters, S & Hülskamp, M 2015, 'TRANSPARENT TESTA GLABRA1 and GLABRA1 Compete for Binding to GLABRA3 in *Arabidopsis*', *Plant Physiol*, vol. 168, no. 2, Jun, pp. 584-597.

Petricka, JJ, Winter, CM & Benfey, PN 2012, 'Control of *Arabidopsis* Root Development', *Annual Review of Plant Biology*, vol. 63, no. 1, pp. 563-590.

Pierleoni, A, Martelli, PL, Fariselli, P & Casadio, R 2006, 'BaCellLo: a balanced subcellular localization predictor', *Bioinformatics*, vol. 22, no. 14, pp. e408-e416.

Ping, XL, Sun, BF, Wang, L, Xiao, W, Yang, X, Wang, WJ, Adhikari, S, Shi, Y, Lv, Y, Chen, YS, Zhao, X, Li, A, Yang, Y, Dahal, U, Lou, XM, Liu, X, Huang, J, Yuan, WP, Zhu, XF, Cheng, T, Zhao, YL, Wang, X, Rendtlew Danielsen, JM, Liu, F & Yang, YG 2014, 'Mammalian WTAP is a regulatory subunit of the RNA N6-methyladenosine methyltransferase', *Cell Res*, vol. 24, no. 2, Feb, pp. 177-189.

Pratanwanich, PN, Yao, F, Chen, Y, Koh, CWQ, Wan, YK, Hendra, C, Poon, P, Goh, YT, Yap, PML, Chooi, JY, Chng, WJ, Ng, SB, Thiery, A, Goh, WSS & Göke, J 2021, 'Identification of differential RNA modifications from nanopore direct RNA sequencing with xPore', *Nature Biotechnology*, 2021/07/19.

Qin, Z, Bai, Y & Wu, L 2017, 'Flowering on Time: Multilayered Restrictions on FT in Plants', *Mol Plant*, vol. 10, no. 11, Nov 6, pp. 1365-1367.

Queitsch, C, Sangster, TA & Lindquist, S 2002, 'Hsp90 as a capacitor of phenotypic variation', *Nature*, vol. 417, no. 6889, Jun 6, pp. 618-624.

Razin, A & Shemer, R 1995, 'DNA methylation in early development', *Hum Mol Genet*, vol. 4 Spec No, pp. 1751-1755.

Rieder, D, Amort, T, Kugler, E, Lusser, A & Trajanoski, Z 2015, 'meRanTK: methylated RNA analysis ToolKit', *Bioinformatics*, vol. 32, no. 5, pp. 782-785.

Rinaldi, MA, Liu, J, Enders, TA, Bartel, B & Strader, LC 2012, 'A gain-of-function mutation in IAA16 confers reduced responses to auxin and abscisic acid and impedes plant growth and fertility', *Plant Molecular Biology*, vol. 79, no. 4, 2012/07/01, pp. 359-373.

Rottman, F, Narayan, P, Goodwin, R, Camper, S, Yao, Y, Horowitz, S, Albers, R, Ayers, D, Maroney, P & Nilsen, T 1986, 'Distribution of m6A in mRNA and its Possible Biological Role', in RT Borchardt, CR Creveling & PM Ueland (eds), *Biological Methylation and Drug Design: Experimental and Clinical Role of S-Adenosylmethionine*, Humana Press, Totowa, NJ, pp. 189-200.

Ruzicka, K, Zhang, M, Campilho, A, Bodi, Z, Kashif, M, Saleh, M, Eeckhout, D, El-Showk, S, Li, H, Zhong, S, De Jaeger, G, Mongan, NP, Hejatko, J, Helariutta, Y & Fray, RG 2017, 'Identification of factors required for m(6) A mRNA methylation in Arabidopsis reveals a role for the conserved E3 ubiquitin ligase HAKAI', *New Phytol*, vol. 215, no. 1, Jul, pp. 157-172.

Rytkin, P, Leung, YY, Silverman, IM, Childress, M, Valladares, O, Dragomir, I, Gregory, BD & Wang, LS 2013, 'HAMR: high-throughput annotation of modified ribonucleotides', *Rna*, vol. 19, no. 12, Dec, pp. 1684-1692.

Saletore, Y, Meyer, K, Korlach, J, Vilfan, ID, Jaffrey, S & Mason, CE 2012, 'The birth of the Epitranscriptome: deciphering the function of RNA modifications', *Genome Biology*, vol. 13, no. 10, pp. 175-175.

Schaefer, M, Pollex, T, Hanna, K & Lyko, F 2009, 'RNA cytosine methylation analysis by bisulfite sequencing', *Nucleic Acids Res*, vol. 37, no. 2, Feb, p. e12.

Schibler, U & Perry, RP 1977, 'The 5'-termini of heterogeneous nuclear RNA: a comparison among molecules of different sizes and ages', *Nucleic Acids Res*, vol. 4, no. 12, Dec, pp. 4133-4149.

Schwartz, S, Agarwala, SD, Mumbach, MR, Jovanovic, M, Mertins, P, Shishkin, A, Tabach, Y, Mikkelsen, TS, Satija, R, Ruvkun, G, Carr, SA, Lander, ES, Fink, GR & Regev, A 2013, 'High-resolution mapping reveals a conserved, widespread, dynamic mRNA methylation program in yeast meiosis', *Cell*, vol. 155, no. 6, Dec 5, pp. 1409-1421.

Schwartz, S, Mumbach, MR, Jovanovic, M, Wang, T, Maciag, K, Bushkin, GG, Mertins, P, Ter-Ovanesyan, D, Habib, N, Cacchiarelli, D, Sanjana, NE, Freinkman, E, Pacold, ME, Satija, R, Mikkelsen, TS, Hacohen, N, Zhang, F, Carr, SA, Lander, ES & Regev, A 2014, 'Perturbation of m6A writers reveals two distinct classes of mRNA methylation at internal and 5' sites', *Cell Rep*, vol. 8, no. 1, Jul 10, pp. 284-296.

Scutenaire, J, Deragon, JM, Jean, V, Benhamed, M, Raynaud, C, Favory, JJ, Merret, R & Bousquet-Antonelli, C 2018, 'The YTH Domain Protein ECT2 Is an m(6)A Reader Required for Normal Trichome Branching in Arabidopsis', *Plant Cell*, vol. 30, no. 5, May, pp. 986-1005.

Sednev, MV, Mykhailiuk, V, Choudhury, P, Halang, J, Sloan, KE, Bohnsack, MT & Höbartner, C 2018, 'N(6)-Methyladenosine-Sensitive RNA-Cleaving Deoxyribozymes', *Angew Chem Int Ed Engl*, vol. 57, no. 46, Nov 12, pp. 15117-15121.

Shatkin, AJ 1976, 'Capping of eucaryotic mRNAs', *Cell*, vol. 9, no. 4 pt 2, Dec, pp. 645-653.

Shen, H, Ontiveros, RJ, Owens, MC, Liu, MY, Ghanty, U, Kohli, RM & Liu, KF 2021, 'TET-mediated 5-methylcytosine oxidation in tRNA promotes translation', *Journal of Biological Chemistry*, vol. 296.

Shen, L, Liang, Z, Gu, X, Chen, Y, Teo, Zhi Wei N, Hou, X, Cai, Weiling M, Dedon, Peter C, Liu, L & Yu, H 2016, 'N⁶-Methyladenosine RNA Modification Regulates Shoot Stem Cell Fate in Arabidopsis', *Developmental Cell*, vol. 38, no. 2, pp. 186-200.

Shen, Q, Zhang, Q, Shi, Y, Shi, Q, Jiang, Y, Gu, Y, Li, Z, Li, X, Zhao, K, Wang, C, Li, N & Cao, X 2018, 'Tet2 promotes pathogen infection-induced myelopoiesis through mRNA oxidation', *Nature*, vol. 554, no. 7690, 2018/02/01, pp. 123-127.

Shima, H, Matsumoto, M, Ishigami, Y, Ebina, M, Muto, A, Sato, Y, Kumagai, S, Ochiai, K, Suzuki, T & Igarashi, K 2017, 'S-Adenosylmethionine Synthesis Is Regulated by Selective N(6)-Adenosine Methylation and mRNA Degradation Involving METTL16 and YTHDC1', *Cell Rep*, vol. 21, no. 12, Dec 19, pp. 3354-3363.

Smargon, AA, Cox, DBT, Pyzocha, NK, Zheng, K, Slaymaker, IM, Gootenberg, JS, Abudayyeh, OA, Essletzbichler, P, Shmakov, S, Makarova, KS, Koonin, EV & Zhang, F 2017, 'Cas13b Is a Type VI-B CRISPR-Associated RNA-Guided RNase Differentially

Regulated by Accessory Proteins Csx27 and Csx28', *Mol Cell*, vol. 65, no. 4, Feb 16, pp. 618-630.e617.

Smemo, S, Tena, JJ, Kim, K-H, Gamazon, ER, Sakabe, NJ, Gómez-Marín, C, Aneas, I, Credidio, FL, Sobreira, DR, Wasserman, NF, Lee, JH, Puvion-Randall, V, Tam, D, Shen, M, Son, JE, Vakili, NA, Sung, H-K, Naranjo, S, Acemel, RD, Manzanares, M, Nagy, A, Cox, NJ, Hui, C-C, Gomez-Skarmeta, JL & Nóbrega, MA 2014, 'Obesity-associated variants within FTO form long-range functional connections with IRX3', *Nature*, vol. 507, no. 7492, 2014/03/01, pp. 371-375.

Squires, JE, Patel, HR, Nusch, M, Sibbritt, T, Humphreys, DT, Parker, BJ, Suter, CM & Preiss, T 2012, 'Widespread occurrence of 5-methylcytosine in human coding and non-coding RNA', *Nucleic Acids Res*, vol. 40, no. 11, Jun, pp. 5023-5033.

Su, R, Dong, L, Li, C, Nachtergaele, S, Wunderlich, M, Qing, Y, Deng, X, Wang, Y, Weng, X, Hu, C, Yu, M, Skibbe, J, Dai, Q, Zou, D, Wu, T, Yu, K, Weng, H, Huang, H, Ferchen, K, Qin, X, Zhang, B, Qi, J, Sasaki, AT, Plas, DR, Bradner, JE, Wei, M, Marcucci, G, Jiang, X, Mulloy, JC, Jin, J, He, C & Chen, J 2018, 'R-2HG Exhibits Antitumor Activity by Targeting FTO/m⁶A/MYC/CEBPA Signaling', *Cell*, vol. 172, no. 1, pp. 90-105.e123.

Tang, G & Tang, X 2013, 'Short Tandem Target Mimic: A Long Journey to the Engineered Molecular Landmine for Selective Destruction/Blockage of MicroRNAs in Plants and Animals', *Journal of Genetics and Genomics*, vol. 40, no. 6, 2013/06/20/, pp. 291-296.

Tang, G, Yan, J, Gu, Y, Qiao, M, Fan, R, Mao, Y & Tang, X 2012, 'Construction of short tandem target mimic (STTM) to block the functions of plant and animal microRNAs', *Methods*, vol. 58, no. 2, Oct, pp. 118-125.

Tian, Q & Reed, JW 1999, 'Control of auxin-regulated root development by the Arabidopsis thaliana SHY2/IAA3 gene', *Development*, vol. 126, no. 4, Feb, pp. 711-721.

Tian, Q, Uhlir, NJ & Reed, JW 2002, 'Arabidopsis SHY2/IAA3 inhibits auxin-regulated gene expression', *The Plant Cell*, vol. 14, no. 2, pp. 301-319.

Tng, PYL, Carabajal Paladino, L, Verkuil, SAN, Purcell, J, Merits, A, Leftwich, PT, Fragkoudis, R, Noad, R & Alpey, L 2020, 'Cas13b-dependent and Cas13b-independent RNA knockdown of viral sequences in mosquito cells following guide RNA expression', *Communications Biology*, vol. 3, no. 1, 2020/07/31, p. 413.

Todesco, M, Rubio-Somoza, I, Paz-Ares, J & Weigel, D 2010, 'A collection of target mimics for comprehensive analysis of microRNA function in Arabidopsis thaliana', *PLoS Genet*, vol. 6, no. 7, Jul 22, p. e1001031.

Tuorto, F, Liebers, R, Musch, T, Schaefer, M, Hofmann, S, Kellner, S, Frye, M, Helm, M, Stoecklin, G & Lyko, F 2012, 'RNA cytosine methylation by Dnmt2 and NSun2 promotes tRNA stability and protein synthesis', *Nature Structural & Molecular Biology*, vol. 19, no. 9, 2012/09/01, pp. 900-905.

van den Berg, A, Mols, J & Han, J 2008, 'RISC-target interaction: cleavage and translational suppression', *Biochimica et biophysica acta*, vol. 1779, no. 11, pp. 668-677.

van Rosmalen, M, Krom, M & Merkx, M 2017, 'Tuning the Flexibility of Glycine-Serine Linkers To Allow Rational Design of Multidomain Proteins', *Biochemistry*, vol. 56, no. 50, 2017/12/19, pp. 6565-6574.

Wan, Y, Tang, K, Zhang, D, Xie, S, Zhu, X, Wang, Z & Lang, Z 2015, 'Transcriptome-wide high-throughput deep m6A-seq reveals unique differential m6A methylation patterns between three organs in *Arabidopsis thaliana*', *Genome Biology*, vol. 16, no. 1, 2015/12/14, p. 272.

Wang, M, Ogé, L, Perez-Garcia, M-D, Hamama, L & Sakr, S 2018, 'The PUF Protein Family: Overview on PUF RNA Targets, Biological Functions, and Post Transcriptional Regulation', *International journal of molecular sciences*, vol. 19, no. 2, p. 410.

Wang, Q, Liu, X, Zhou, J, Yang, C, Wang, G, Tan, Y, Wu, Y, Zhang, S, Yi, K & Kang, C 2019, 'The CRISPR-Cas13a Gene-Editing System Induces Collateral Cleavage of RNA in Glioma Cells', *Advanced Science*, vol. 6, no. 20, p. 1901299.

Wang, X, Lu, Z, Gomez, A, Hon, GC, Yue, Y, Han, D, Fu, Y, Parisien, M, Dai, Q, Jia, G, Ren, B, Pan, T & He, C 2014, 'N6-methyladenosine-dependent regulation of messenger RNA stability', *Nature*, vol. 505, no. 7481, 2014/01/01, pp. 117-120.

Wang, X, Zhao, BS, Roundtree, IA, Lu, Z, Han, D, Ma, H, Weng, X, Chen, K, Shi, H & He, C 2015, 'N(6)-methyladenosine Modulates Messenger RNA Translation Efficiency', *Cell*, vol. 161, no. 6, Jun 4, pp. 1388-1399.

Wang, Y, Xiao, Y, Dong, S, Yu, Q & Jia, G 2020, 'Antibody-free enzyme-assisted chemical approach for detection of N6-methyladenosine', *Nature Chemical Biology*, vol. 16, no. 8, 2020/08/01, pp. 896-903.

Wang, Y, Zhang, Z, Sepich-Poore, C, Zhang, L, Xiao, Y & He, C 2021, 'LEAD-m(6) A-seq for Locus-Specific Detection of N(6) -Methyladenosine and Quantification of Differential Methylation', *Angew Chem Int Ed Engl*, vol. 60, no. 2, Jan 11, pp. 873-880.

Ward, CM, To, T-H & Pederson, SM 2019, 'ngsReports: a Bioconductor package for managing FastQC reports and other NGS related log files', *Bioinformatics*, vol. 36, no. 8, pp. 2587-2588.

Warren, L, Manos, PD, Ahfeldt, T, Loh, YH, Li, H, Lau, F, Ebina, W, Mandal, PK, Smith, ZD, Meissner, A, Daley, GQ, Brack, AS, Collins, JJ, Cowan, C, Schlaeger, TM & Rossi, DJ 2010, 'Highly efficient reprogramming to pluripotency and directed differentiation of human cells with synthetic modified mRNA', *Cell Stem Cell*, vol. 7, no. 5, Nov 5, pp. 618-630.

Wei, C-M & Moss, B 1977, 'Nucleotide sequences at the N6-methyladenosine sites of HeLa cell messenger ribonucleic acid', *Biochemistry*, vol. 16, no. 8, 1977/04/19, pp. 1672-1676.

Wei, CM, Gershowitz, A & Moss, B 1976, '5'-Terminal and internal methylated nucleotide sequences in HeLa cell mRNA', *Biochemistry*, vol. 15, no. 2, 1976/01/01, pp. 397-401.

Wei, L-H, Song, P, Wang, Y, Lu, Z, Tang, Q, Yu, Q, Xiao, Y, Zhang, X, Duan, H-C & Jia, G 2018, 'The m6A Reader ECT2 Controls Trichome Morphology by Affecting mRNA Stability in Arabidopsis', *The Plant Cell*, vol. 30, no. 5, pp. 968-985.

Weiste, C, Pedrotti, L, Selvanayagam, J, Muralidhara, P, Fröschel, C, Novák, O, Ljung, K, Hanson, J & Dröge-Laser, W 2017, 'The Arabidopsis bZIP11 transcription factor links low-energy signalling to auxin-mediated control of primary root growth', *PLOS Genetics*, vol. 13, no. 2, p. e1006607.

Wilson, C, Chen, PJ, Miao, Z & Liu, DR 2020, 'Programmable m6A modification of cellular RNAs with a Cas13-directed methyltransferase', *Nature Biotechnology*, vol. 38, no. 12, 2020/12/01, pp. 1431-1440.

Wu, J, Peled-Zehavi, H & Galili, G 2020, 'The m6A reader ECT2 post-transcriptionally regulates proteasome activity in Arabidopsis', *New Phytologist*, vol. 228, no. 1, 2020/10/01, pp. 151-162.

Xia, Z, Tang, M, Ma, J, Zhang, H, Gimple, RC, Prager, BC, Tang, H, Sun, C, Liu, F, Lin, P, Mei, Y, Du, R, Rich, JN & Xie, Q 2021, 'Epitranscriptomic editing of the RNA N6-methyladenosine modification by dCasRx conjugated methyltransferase and demethylase', *Nucleic Acids Research*, vol. 49, no. 13, pp. 7361-7374.

Xiao, W, Adhikari, S, Dahal, U, Chen, Y-S, Hao, Y-J, Sun, B-F, Sun, H-Y, Li, A, Ping, X-L, Lai, W-Y, Wang, X, Ma, H-L, Huang, C-M, Yang, Y, Huang, N, Jiang, G-B, Wang, H-L, Zhou, Q, Wang, X-J, Zhao, Y-L & Yang, Y-G 2016, 'Nuclear m6A Reader YTHDC1 Regulates mRNA Splicing', *Molecular Cell*, vol. 61, no. 4, 2016/02/18/, pp. 507-519.

Xiao, Y, Wang, Y, Tang, Q, Wei, L, Zhang, X & Jia, G 2018, 'An Elongation- and Ligation-Based qPCR Amplification Method for the Radiolabeling-Free Detection of Locus-Specific N(6) -Methyladenosine Modification', *Angew Chem Int Ed Engl*, vol. 57, no. 49, Dec 3, pp. 15995-16000.

Xuan, J-J, Sun, W-J, Lin, P-H, Zhou, K-R, Liu, S, Zheng, L-L, Qu, L-H & Yang, J-H 2017, 'RMBase v2.0: deciphering the map of RNA modifications from epitranscriptome sequencing data', *Nucleic Acids Research*, vol. 46, no. D1, pp. D327-D334.

Yan, J, Gu, Y, Jia, X, Kang, W, Pan, S, Tang, X, Chen, X & Tang, G 2012, 'Effective Small RNA Destruction by the Expression of a Short Tandem Target Mimic in Arabidopsis', *The Plant Cell*, vol. 24, no. 2, pp. 415-427.

Yang, L, Perrera, V, Saplaoura, E, Apelt, F, Bahin, M, Kramdi, A, Olas, J, Mueller-Roeber, B, Sokolowska, E, Zhang, W, Li, R, Pitzalis, N, Heinlein, M, Zhang, S, Genovesio, A, Colot, V & Kragler, F 2019, 'm5C Methylation Guides Systemic Transport of Messenger RNA over Graft Junctions in Plants', *Current Biology*, vol. 29, no. 15, 2019/08/05/, pp. 2465-2476.e2465.

Yang, X, Yang, Y, Sun, B-F, Chen, Y-S, Xu, J-W, Lai, W-Y, Li, A, Wang, X, Bhattarai, DP, Xiao, W, Sun, H-Y, Zhu, Q, Ma, H-L, Adhikari, S, Sun, M, Hao, Y-J, Zhang, B, Huang, C-M, Huang, N, Jiang, G-B, Zhao, Y-L, Wang, H-L, Sun, Y-P & Yang, Y-G 2017, '5-methylcytosine promotes mRNA export — NSUN2 as the methyltransferase and ALYREF as an m5C reader', *Cell Research*, vol. 27, no. 5, 2017/05/01, pp. 606-625.

Yu, H, Pu, Q, Weng, Z, Zhou, X, Li, J, Yang, Y, Luo, W, Guo, Y, Chen, H, Wang, D & Xie, G 2021, 'DNAzyme based three-way junction assay for antibody-free detection of locus-specific N6-methyladenosine modifications', *Biosensors and Bioelectronics*, vol. 194, 2021/12/15/, p. 113625.

Yue, Y, Liu, J, Cui, X, Cao, J, Luo, G, Zhang, Z, Cheng, T, Gao, M, Shu, X, Ma, H, Wang, F, Wang, X, Shen, B, Wang, Y, Feng, X, He, C & Liu, J 2018, 'VIRMA mediates preferential m6A mRNA methylation in 3'UTR and near stop codon and associates with alternative polyadenylation', *Cell Discovery*, vol. 4, no. 1, 2018/02/27, p. 10.

Zaringhalam, M & Papavasiliou, FN 2016, 'Pseudouridylation meets next-generation sequencing', *Methods*, vol. 107, Sep 1, pp. 63-72.

Zhang, K, Zhang, Z, Kang, J, Chen, J, Liu, J, Gao, N, Fan, L, Zheng, P, Wang, Y & Sun, J 2020, 'CRISPR/Cas13d-Mediated Microbial RNA Knockdown', *Frontiers in bioengineering and biotechnology*, vol. 8, pp. 856-856.

Zhao, M, Morohashi, K, Hatlestad, G, Grotewold, E & Lloyd, A 2008, 'The TTG1-bHLH-MYB complex controls trichome cell fate and patterning through direct targeting of regulatory loci', *Development*, vol. 135, no. 11, Jun, pp. 1991-1999.

Zheng, G, Dahl, JA, Niu, Y, Fedorcsak, P, Huang, CM, Li, CJ, Vågbø, CB, Shi, Y, Wang, WL, Song, SH, Lu, Z, Bosmans, RP, Dai, Q, Hao, YJ, Yang, X, Zhao, WM, Tong, WM, Wang, XJ, Bogdan, F, Furu, K, Fu, Y, Jia, G, Zhao, X, Liu, J, Krokan, HE, Klungland, A, Yang, YG & He, C 2013, 'ALKBH5 is a mammalian RNA demethylase that impacts RNA metabolism and mouse fertility', *Mol Cell*, vol. 49, no. 1, Jan 10, pp. 18-29.

Zhong, S, Li, H, Bodi, Z, Button, J, Vespa, L, Herzog, M & Fray, RG 2008, 'MTA is an Arabidopsis messenger RNA adenosine methylase and interacts with a homolog of a sex-specific splicing factor', *The Plant Cell*, vol. 20, no. 5, pp. 1278-1288.

Chapter V: General discussion and Conclusion

General discussion

Targeted manipulations for functional studies of RNA methylations

Tools that allow targeted manipulations of RNA modifications are critical in their functional studies. In this study, I explored the potential use of RNA-guided RNA targeting system CRISPR-dCas13 and RNA-based technique STTM in specific manipulations of RNA m⁶A and m⁵C in *A. thaliana*. dCas13-ALKBH10B led to over-branched trichome phenotype indicative for reduction of m⁶A on *TTG1* mRNA, with reduced m⁶A abundance at one of the targeted sites shown. On the other hand, dCas13-TET1 inverted the effect of m⁵C presence on a Luciferase reporter transcript, pointing towards dCas13-TET1-mediated removal or alteration of the m⁵C.

Interestingly, when dCas13-TET1 was used to target m⁵C site C3349 on the endogenous transcript *MAG5* in *A. thaliana*, it appeared that the m⁵C/hm⁵C level of the site increased. This could be explained as a cellular strategy to increase m⁵C level to compensate the portion that has been converted to hm⁵C by dCas13-TET1. Notably, it was previously shown that in HEK293T cells, binding of dCas13d-mALKBH5 (catalytically inactive ALKBH5) caused slight increase in m⁶A level at a target site compared to when a non-targeting gRNA was used (Xia et al. 2021). The phenomenon could be attributed to alterations of local RNA structure upon binding of the dCas13-mALKBH5 conjugate, making the modified sites more accessible to methyltransferases. Therefore, an alternative hypothesis for the enhanced m⁵C level detected is that the binding of dCas13-TET1 might have changed *MAG5* mRNA secondary structure and promoted m⁵C deposition to site C3349. This could also be the case for mSTTM10, where this mutated STTM structure might have affected *MAG5* conformation and led to an increase in m⁵C level at C3349. On the other hand, it is worth noting that altered RNA secondary structure might not only change the level of modification installed, but could also be a result of methylation (Liu, N. et al. 2015). The observation of increased m⁵C level at *MAG5* C3349 when mSTTM10 was used could also be explained by degradation of non-modified transcripts but not modified ones, which in turn pointed towards different secondary structure of non-modified and m⁵C-modified *MAG5* mRNAs. Therefore, while further experiments are required to clarify the manipulations conferred by the dCas13-“eraser” fusions and mSTTM,

interesting observations have been made and would contribute to the future deciphering of specific RNA modified sites.

In designing system for targeted manipulations of RNA methylation from dCas13, as a relatively new system, there are certain gaps in the current understanding of dCas13's behaviour that should be held on to, such as the kinetics of dCas13 binding to target (dissociation rate from targets), dCas13 and its fusion proteins' turn-over rate and structural difference. These poorly understood features could affect various aspects of translational fusions from dCas13, for example the efficacy, efficiency and specificity. Various applications have also reported slight to marked differences in design of dCas13 fusions, with the most perplexing issue perhaps being the design of gRNA, or in particular the spacer base-pairing with target. Only special feature of a modification, such as prominent occurrence of A-to-I or C-to-U editing on a paired nucleotide allowed more rational design of spacers for targeted RNA editing using dCas13-ADAR2 (Abudayyeh, O. O. et al. 2019; Cox et al. 2017). Other published studies with dCas13 conjugated to m⁶A "writer" and/or "eraser" adopted spacers binding as close as overlapping with modified sites (Xia et al. 2021), to as far as 3 kb from target sites (Li, Jiexin et al. 2020). For each of the strategies, variable modifying efficiency was achieved for different targets. While cellular regulation of specific modified site might have complicated the readouts of a desired edit's efficiency, the observation strongly highlighted the effect of RNA secondary structure for both the accessibility of dCas13 and the catalytic activity of the effector domain. Therefore, biochemical improvements of future dCas13 fusion needs to go along with experimental and computational modelling of an optimal design that takes into account RNA dynamic structure and the fusion protein's configuration. Alternatively, addition of a domain for unwinding of double-stranded regions on RNA, such as a helicase, into dCas13 fusions might be useful in dealing with RNA secondary structure.

It is also worth mentioning that due to the constraint of time and the scope of this study, dCas13-"eraser" fusions were designed and constructed with specific features which could be further investigated or optimized in the future: (i) There could be more effective candidates than hTET1 in removing RNA m⁵C that can be tethered to dCas13. For instance, TET from *D. melanogaster* was reported as an RNA m⁵C dioxygenase (Delatte, Benjamin et al. 2016) and potentially is more active on RNA

than hTET1. (ii) The RNA modifications and their “writers” in this study are reported or suggested to be deposited/function in the nucleus. Therefore, directing dCas13-“eraser” fusions to nucleus likely would help compete with the “writer” proteins and remove the methylations most efficiently. The design also ensures the effects caused by methylation before the transcripts are exported to cytoplasm or other cellular organelles are not overlooked. However, depending on the transcripts and enzymes involved, the localization signal may need amendments to maximize the fusion protein’s activity. (iii) Like most studies with dCas13 fusions, here effector domains were tethered to dCas13’s C terminus. This may or may not affect the fusion protein’s folding and behaviours and will require comparisons to fusion to the N terminus.

While systems with dCas13 have gained certain success in overwriting RNA methylations (this study and others in animals), it remains an open question if an RNA-based structure can serve a similar purpose, that is to bind to mRNA and interfere with RNA methylation deposition. Although my examination of STTM and a derivative structure mSTTM did not gain positive result in RNA methylation interference, given what have been known about the remarkably diverse function and mode of action of different RNA types, more rational designs, high-throughput library screens, or a directed evolution approach might finally lead us to such “RNA-based RNA modification interferer” technique.

Multi-approach functional studies of a modified site – Appreciating discrepancies

There is an undeniable fact that current studies on RNA modifications can feature poorly-overlapping or even conflicting findings, ranging from mapping of modified sites (Saletore et al. 2012; Zaringhalam & Papavasiliou 2016), abundance or even existence of a modification on certain RNA species (Cui et al. 2017; Huang, T et al. 2019), to impacts of a participating enzyme (Hausmann et al. 2016; Hongay & Orr-Weaver 2011). The variations have been attributed to limitations of studying methodologies, techniques, and the presumably highly dynamic regulation of RNA modifications. This notion can be supported with my investigation of root development regulation by m5C (Chapter IV) in which data did not support previously described major roles for *SHY2/IAA3* and *IAA16* in m5C regulation of root development.

In some instances, it is interpretation of data that can make a difference in findings reported. For example, m6A on *TTG1* mRNA was hypothesized to involve trichome patterning through regulating *TTG1* transcript abundance based on the observation that over-branched trichome phenotype in *ect2-1* correlated with reduced mRNA abundance at steady-state, shown through an RT-qPCR, and instability of *TTG1* mRNA, shown through a transcription-inhibition-based RT-qPCR, in the mutant (Wei, L-H et al. 2018). However, RNA-seq in the same study demonstrated a similar abundance of *TTG1* mRNA in wild-type and *ect2-1*. In this study, steady-state *TTG1* mRNA abundance was found not significantly affected by the absence of “reader” protein ECT2 in two biological replicates of *ect2-1* while the trichome phenotype of the mutant remained consistent (Chapter II). Therefore, by somewhat ignoring the discrepancies between their RT-qPCR and RNA-seq data, the authors failed to point out the gap in their model of trichome morphology regulation by m6A, which could be participation of other key factors rather than *TTG1*, or the ability to be overwritten/fine-tuning rather than absolute function of m6A.

The complexity of “epitranscriptomic” regulation requires documentation and more open discussion of seemingly incompatible data. The overall underrepresented number of site-specific functional investigations need to be overcome so that noises in data and interpretation can be cleared out with reproducibility. Along with that, improvements in existing techniques or development of new approaches such as specificity and sensitivity of mapping, tissue-specific investigations or single-cell technologies will be critical resources.

Concluding remark

The exciting discoveries in the field of RNA modifications for the past decade has fuelled explosion of new research and findings in this fast-growing frontier. Mapping of various modifications in different transcriptomes have been valuable, however, substantial works are required to expand the field with not only width but depth. Of these, site-specific functional studies are of utmost importance. By taking small steps, such as verifying previous findings and diving into functional relevance of a specific modified site, RNA modification field can start moving forward firmly and get closer to the establishment of “epitranscriptomics”.

Appendix

Appendix 1: DNA sequences of fusion proteins

Gold = NLS

Black = PspCas13b

Blue = GSG linker

Brown = TET1

NLS-PspCas13b-GSG linker-TET1-NLS

ATGCCCAAAAAGAAGAGGAAAGTGATGAACATCCCCGCTCTGGTGGAAAACCA
GAAGAAGTACTTTGGCACCTACAGCGTGATGGCCATGCTGAACGCTCAGACCG
TGCTGGACCACATCCAGAAGGTGGCCGATATTGAGGGCGAGCAGAACGAGAA
CAACGAGAATCTGTGGTTTCACCCCGTGATGAGCCACCTGTACAACGCCAAGA
ACGGCTACGACAAGCAGCCCGAGAAAACCATGTTTCATCATCGAGCGGCTGCAG
AGCTACTTCCCATTCCCTGAAGATCATGGCCGAGAACCAGAGAGAGTACAGCAA
CGGCAAGTACAAGCAGAACC GCGTGGAAGTGAACAGCAACGACATCTTCGAGG
TGCTGAAGCGCGCCTTCGGCGTGCTGAAGATGTACAGGGACCTGACCAACGCA
TACAAGACCTACGAGGAAAAGCTGAACGACGGCTGCGAGTTCCTGACCAGCAC
AGAGCAACCTCTGAGCGGCATGATCAACA ACTACTACACAGTGGCCCTGCGGA
ACATGAACGAGAGATACGGCTACAAGACAGAGGACCTGGCCTTCATCCAGGAC
AAGCGTTCAAGTTCGTGAAGGACGCCTACGGCAAGAAAAAGTCCCAAGTGAA
TACCGGATTCTTCCTGAGCCTGCAGGACTACAACGGCGACACACAGAAGAAGC
TGCACCTGAGCGGAGTGGGAATCGCCCTGCTGATCTGCCTGTTCCCTGGACAAG
CAGTACATCAACATCTTTCTGAGCAGGCTGCCCATCTTCTCCAGCTACAATGCC
CAGAGCGAGGAACGGCGGATCATCATCAGATCCTTCGGCATCAACAGCATCAA
GCTGCCCAAGGACCGGATCCACAGCGAGAAGTCCAACAAGAGCGTGGCCATG
GATATGCTCAACGAAGTGAAGCGGTGCCCCGACGAGCTGTTCAACAACACTGTC
TGCCGAGAAGCAGTCCCGGTT CAGAATCATCAGCGACGACCACAATGAAGTGC
TGATGAAGCGGAGCAGCGACAGATTCGTGCCTCTGCTGCTGCAGTATATCGAT
TACGGCAAGCTGTTTCGACCACATCAGGTTCCACGTGAACATGGGCAAGCTGAG
ATACCTGCTGAAGGCCGACAAGACCTGCATCGACGGCCAGACCAGAGTCAGAG
TGATCGAGCAGCCCCTGAACGGCTTCGGCAGACTGGAAGAGGCCGAGACAAT
GCGGAAGCAAGAGAACGGCACCTTCGGCAACAGCGGCATCCGGATCAGAGAC
TTCGAGAACATGAAGCGGGACGACGCCAATCCTGCCAACTATCCCTACATCGT
GGACACCTACACACACTACATCCTGGAAAACAACAAGGTTCGAGATGTTTATCAA
CGACAAAGAGGACAGCGCCCCACTGCTGCCCGTGATCGAGGATGATAGATACG
TGGTCAAGACAATCCCCAGCTGCCGGATGAGCACCTGGAAATTCCAGCCATG
GCCTTCCACATGTTTCTGTTTCGGCAGCAAGAAAACCGAGAAGCTGATCGTGGA
CGTGCACAACCGGTACAAGAGACTGTTCCAGGCCATGCAGAAAGAAGAAGTGA
CCGCCGAGAATATCGCCAGCTTCGGAATCGCCGAGAGCGACCTGCCTCAGAA
GATCCTGGATCTGATCAGCGGCAATGCCACGGCAAGGATGTGGACGCCTTCA
TCAGACTGACCGTGGACGACATGCTGACCGACACCGAGCGGAGAATCAAGAGA
TTCAAGGACGACCGGAAGTCCATTCGGAGCGCCGACAACAAGATGGGAAAGAG
AGGCTTCAAGCAGATCTCCACAGGCAAGCTGGCCGACTTCTGGCCAAGGACA
TCGTGCTGTTTCAGCCCAGCGTGAACGATGGCGAGAACAAGATCACCGGCCTG
AACTACCGGATCATGCAGAGCGCCATTGCCGTGTACGATAGCGGCGACGATTA
CGAGGCCAAGCAGCAGTTCAAGCTGATGTTTCGAGAAGGCCCGGCTGATCGGC
AAGGGCACAACAGAGCCTCATCCATTTCTGTACAAGGTGTTTCGCCCGCAGCAT

CCCCGCCAATGCCGTCGAGTTCTACGAGCGCTACCTGATCGAGCGGAAGTTCT
ACCTGACCGGCCTGTCCAACGAGATCAAGAAAGGCAACAGAGTGGATGTGCC
TTCATCCGGCGGGACCAGAACAAGTGGAAAACACCCGCCATGAAGACCCTGGG
CAGAACTCTACAGCGAGGATCTGCCCCGTGGAAGTCCCAGACAGATGTTTCGACA
ATGAGATCAAGTCCCACCTGAAGTCCCTGCCACAGATGGAAGGCATCGACTTC
AACAAATGCCAACGTGACCTATCTGATCGCCGAGTACATGAAGAGAGTGTGGA
CGACGACTTCCAGACCTTCTACCAGTGGAAACCGCAACTACCGGTACATGGACA
TGCTTAAGGGCGAGTACGACAGAAAGGGCTCCCTGCAGCACTGCTTACCAGC
GTGGAAGAGAGAGAAGGCCTCTGGAAAGAGCGGGCCTCCAGAACAGAGCGGT
ACAGAAAGCAGGCCAGCAACAAGATCCGCAGCAACCGGCAGATGAGAAACGC
CAGCAGCGAAGAGATCGAGACAATCCTGGATAAGCGGCTGAGCAACAGCCGG
AACGAGTACCAGAAAAGCGAGAAAAGTATCCGGCGCTACAGAGTGCAGGATGC
CCTGCTGTTTCTGCTGGCCAAAAGACCCTGACCGAACTGGCCGATTTTCGACG
GCGAGAGGTTCAAACCTGAAAGAAATCATGCCCGACGCCGAGAAGGGAATCCTG
AGCGAGATCATGCCCATGAGCTTACCTTCGAGAAAGGCGGGCAAGAAGTACAC
CATCACCAGCGAGGGCATGAAGCTGAAGAACTACGGCGACTTCTTTGTGCTGG
CTAGCGACAAGAGGATCGGCCAACCTGCTGGAACCTCGTGGGCAGCGACATCGT
GTCCAAAGAGGATATCATGGAAGAGTTCAACAAATACGACCAAGTGCAGGCCCG
AGATCAGCTCCATCGTGTTC AACCTGGAAAAGTGGGCCTTCGACACATACCCC
GAGCTGTCTGCCAGAGTGGACCGGGAAGAGAAGGTGGACTTCAAGAGCATCCT
GAAAATCCTGCTGAACAACAAGAACATCAACAAAGAGCAGAGCGACATCCTGC
GGAAGATCCGGAACGCCTTCGATGCAAACAATTACCCCGACAAAGGCGTGGTG
GAAATCAAGGCCCTGCCTGAGATCGCCATGAGCATCAAGAAGGCCTTTGGGGA
GTACGCCATCATGAAGGGAAGCGGGGCTAAAGATTCTGAACTGCCACCTGCA
GCTGTCTTGATCGAGTTATACAAAAGACAAAAGGCCCATATTATACACACCTTG
GGGCAGGACCAAGTGTTGCTGCTGTCAGGGAAATCATGGAGAATAGGTATGGT
CAAAAAGGAAACGCAATAAGGATAGAAATAGTAGTGTACACCGGTAAAGAAGG
GAAAAGCTCTCATGGGTGTCCAATTGCTAAGTGGGTTTTTAAGAAGAAGCAGTGA
TGAAGAAAAAGTTCTTTGTTTGGTCCGGCAGCGTACAGGCCACCACTGTCCAAC
TGCTGTGATGGTGGTGTCTCATCATGGTGTGGGATGGCATCCCTCTTCCAATGG
CCGACCGGCTATACACAGAGCTCACAGAGAATCTAAAGTCATACAATGGGCAC
CCTACCGACAGAAGATGCACCCTCAATGAAAATCGTACCTGTACATGTCAAGGA
ATTGATCCAGAGACTTGTGGAGCTTCATTCTCTTTTGGCTGTTTCATGGAGTATGT
ACTTTAATGGCTGTAAGTTTGGTAGAAGCCCAAGCCCCAGAAGATTTAGAATTG
ATCCAAGCTCTCCCTTACATGAAAAAAACCTTGAAGATAACTTACAGAGTTTGGC
TACACGATTAGCTCCAATTTATAAGCAGTATGCTCCAGTAGCTTACCAAATCAG
GTGGAATATGAAAATGTTGCCCGAGAATGTCGGCTTGGCAGCAAGGAAGGTGCG
TCCCTTCTCTGGGGTCACTGCTTGCCTGGACTTCTGTGCTCATCCCCACAGGG
ACATTCACAACATGAATAATGGAAGCACTGTGGTTTTGTACCTTAACTCGAGAAG
ATAACCGCTCTTTGGGTGTTATTCTCAAGATGAGCAGCTCCATGTGCTACCTC
TTTATAAGCTTTTCAGACACAGATGAGTTTGGCTCCAAGGAAGGAATGGAAGCCA
AGATCAAATCTGGGGCCATCGAGGTCTGGCACCCCGCCGCAAAAAAAGAACG
TGTTTCACTCAGCCTGTTCCCCGTTCTGGAAAGAAGAGGGCTGCGATGATGAC
GGAGGTTCTTGACATAAGATAAGGGCAGTGGAAAAGAAACCTATTCCCCGAAT
CAAGCGGAAGAATAACTCAACAACAACAACAACAGTAAGCCTTCGTCACTGCC
AACCTTAGGGAGTAACACTGAGACCGTGCAACCTGAAGTAAAAAGTGAACCG
AACCCCATTTTTATCTTAAAAAGTTTCAGACAACACTAAAACCTTATTGCTGATGCC
ATCCGCTCCTCACCCAGTGAAAGAGGCATCTCCAGGCTTCTCCTGGTCCCCGA
AGACTGCTTCAGCCACACCAGCTCCACTGAAGAATGACGCAACAGCCTCATGC
GGGTTTTTCAGAAAGAAGCAGCACTCCCCACTGTACGATGCCTTCGGGAAGACT

CAGTGGTGCCAATGCAGCTGCTGCTGATGGCCCTGGCATTTCACAGCTTGGCG
AAGTGGCTCCTCTCCCCACCCTGTCTGCTCCTGTGATGGAGCCCCTCATTAAATT
CTGAGCCTTCCACTGGTGTGACTGAGCCGCTAACGCCTCATCAGCCAAACCAC
CAGCCCTCCTTCCTCACCTCTCCTCAAGACCTTGCCTCTTCTCCAATGGAAGAA
GATGAGCAGCATTCTGAAGCAGATGAGCCTCCATCAGACGAACCCCTATCTGAT
GACCCCTGTACCTGCTGAGGAGAAATTGCCCCACATTGATGAGTATTGGTCA
GACAGTGAGCACATCTTTTTGGATGCAAATATTGGTGGGGTGGCCATCGCACCT
GCTCACGGCTCGGTTTTGATTGAGTGTGCCCGGCGGGAGCTGCACGCTACCAC
TCCTGTTGAGCACCCCAACCGTAATCATCCAACCCGCCTCTCCCTTGTCTTTTA
CCAGCACAAAACCTAAATAAGCCCCAACATGGTTTTGAACTAAACAAGATTAA
GTTTGAGGCTAAAGAAGCTAAGAATAAGAAAATGAAGGCCTCAGAGCAAAAAGA
CCAGGCAGCTAATGAAGGTCCAGAACAGTCCTCTGAAGTAAATGAATTGAACCA
AATTCCTTCTCATAAAGCATTAAACATTAACCCATGACAATGTTGTCACCGTGTCC
CCTTATGCTCTCACACACGTTGCGGGGCCCTATAACCATTGGGTCTGTGAGCTC
CCCAAGAAAAAGCGCAAGGTA

Gold = NLS

Black = PspCas13b

Blue = GSG linker

Cerulean = ALKBH10B

NLS-PspCas13b-GSG linker-ALKBH10B

ATGCCCAAAAAGAAGAGGAAAGTGATGAACATCCCCGCTCTGGTGGAAAACCA
GAAGAAGTACTTTGGCACCTACAGCGTGATGGCCATGCTGAACGCTCAGACCG
TGCTGGACCACATCCAGAAGGTGGCCGATATTGAGGGCGAGCAGAACGAGAA
CAACGAGAATCTGTGGTTTCACCCCGTGATGAGCCACCTGTACAACGCCAAGA
ACGGCTACGACAAGCAGCCCGAGAAAACCATGTTTCATCATCGAGCGGCTGCAG
AGCTACTTCCCATTCCCTGAAGATCATGGCCGAGAACCAGAGAGAGTACAGCAA
CGGCAAGTACAAGCAGAACC GCGTGGAAGTGAACAGCAACGACATCTTCGAGG
TGCTGAAGCGCGCCTTCGGCGTGCTGAAGATGTACAGGGACCTGACCAACGCA
TACAAGACCTACGAGGAAAAGCTGAACGACGGCTGCGAGTTCCTGACCAGCAC
AGAGCAACCTCTGAGCGGCATGATCAACA ACTACTACACAGTGGCCCTGCGGA
ACATGAACGAGAGATACGGCTACAAGACAGAGGACCTGGCCTTCATCCAGGAC
AAGCGTTCAAGTTCGTGAAGGACGCCTACGGCAAGAAAAAGTCCCAAGTGAA
TACCGGATTCTTCCTGAGCCTGCAGGACTACAACGGCGACACACAGAAGAAGC
TGCACCTGAGCGGAGTGGGAATCGCCCTGCTGATCTGCCTGTTCCCTGGACAAG
CAGTACATCAACATCTTTCTGAGCAGGCTGCCCATCTTCTCCAGCTACAATGCC
CAGAGCGAGGAACGGCGGATCATCATCAGATCCTTCGGCATCAACAGCATCAA
GCTGCCCAAGGACCGGATCCACAGCGAGAAGTCCAACAAGAGCGTGGCCATG
GATATGCTCAACGAAGTGAAGCGGTGCCCCGACGAGCTGTTCAACAACACTGTC
TGCCGAGAAGCAGTCCCGTT CAGAATCATCAGCGACGACCACAATGAAGTGC
TGATGAAGCGGAGCAGCGACAGATTCTGCTGCTGCTGCAGTATATCGAT
TACGGCAAGCTGTTTCGACCACATCAGGTTCCACGTGAACATGGGCAAGCTGAG
ATACCTGCTGAAGGCCGACAAGACCTGCATCGACGGCCAGACCAGAGTCAGAG
TGATCGAGCAGCCCCTGAACGGCTTCGGCAGACTGGAAGAGGCCGAGACAAT
GCGGAAGCAAGAGAACGGCACCTTCGGCAACAGCGGCATCCGGATCAGAGAC
TTCGAGAACATGAAGCGGGACGACGCCAATCCTGCCAACTATCCCTACATCGT
GGACACCTACACACACTACATCCTGGAAAACAACAAGGTGAGATGTTTATCAA
CGACAAAGAGGACAGCGCCCCACTGCTGCCCGTGATCGAGGATGATAGATACG
TGGTCAAGACAATCCCCAGCTGCCGGATGAGCACCTGGAAATTCCAGCCATG
GCCTTCCACATGTTTCTGTTTCGGCAGCAAGAAAACCGAGAAGCTGATCGTGGA
CGTGACAAACCGGTACAAGAGACTGTTCCAGGCCATGCAGAAAAGAAGAAGTGA
CCGCCGAGAATATCGCCAGCTTCGGAATCGCCGAGAGCGACCTGCCTCAGAA
GATCCTGGATCTGATCAGCGGCAATGCCACGGCAAGGATGTGGACGCCTTCA
TCAGACTGACCGTGGACGACATGCTGACCGACACCGAGCGGAGAATCAAGAGA
TTCAAGGACGACCGGAAGTCCATTCGGAGCGCCGACAACAAGATGGGAAAGAG
AGGCTTCAAGCAGATCTCCACAGGCAAGCTGGCCGACTTCTGGCCAAGGACA
TCGTGCTGTTTCAGCCCAGCGTGAACGATGGCGAGAACAAGATCACCGGCCTG
AACTACCGGATCATGCAGAGCGCCATTGCCGTGTACGATAGCGGCGACGATTA
CGAGGCCAAGCAGCAGTTCAAGCTGATGTTTCGAGAAGGCCCGGCTGATCGGC
AAGGGCACAACAGAGCCTCATCCATTTCTGTACAAGGTGTTTCGCCCGCAGCAT
CCCCGCCAATGCCGTCGAGTTCTACGAGCGCTACCTGATCGAGCGGAAGTTCT
ACCTGACCGGCCTGTCCAACGAGATCAAGAAAGGCAACAGAGTGGATGTGCC
TTCATCCGGCGGGACCAGAACAAGTGGAAAACACCCGCCATGAAGACCCTGGG

CAGAATCTACAGCGAGGATCTGCCCCGTGGAAGTGCCAGACAGATGTTTCGACA
ATGAGATCAAGTCCCACCTGAAGTCCCTGCCACAGATGGAAGGCATCGACTTC
AACAAATGCCAACGTGACCTATCTGATCGCCGAGTACATGAAGAGAGTGCTGGA
CGACGACTTCCAGACCTTCTACCAGTGGAAACCGCAACTACCGGTACATGGACA
TGCTTAAGGGCGAGTACGACAGAAAGGGCTCCCTGCAGCACTGCTTACCAGC
GTGGAAGAGAGAGAAGGCCTCTGGAAAGAGCGGGCCTCCAGAACAGAGCGGT
ACAGAAAGCAGGCCAGCAACAAGATCCGCAGCAACCGGCAGATGAGAAACGC
CAGCAGCGAAGAGATCGAGACAATCCTGGATAAGCGGCTGAGCAACAGCCGG
AACGAGTACCAGAAAAGCGAGAAAGTGATCCGGCGCTACAGAGTGCAGGATGC
CCTGCTGTTTCTGCTGGCCAAAAAGACCCTGACCGAACTGGCCGATTTTCGACG
GCGAGAGGTTCAAACCTGAAAGAAATCATGCCCGACGCCGAGAAGGGAATCCTG
AGCGAGATCATGCCCATGAGCTTACCTTCGAGAAAGGCGGCAAGAAGTACAC
CATCACCAGCGAGGGCATGAAGCTGAAGAACTACGGCGACTTCTTTGTGCTGG
CTAGCGACAAGAGGATCGGCAACCTGCTGGAAGTCTGTTGGCAGCGACATCGT
GTCCAAAGAGGATATCATGGAAGAGTTCAACAAATACGACCAGTGCAGGCCCG
AGATCAGCTCCATCGTGTTC AACCTGGAAAAGTGGGCCTTCGACACATACCCC
GAGCTGTCTGCCAGAGTGGACCGGGAAGAGAAGGTGGACTTCAAGAGCATCCT
GAAAATCCTGCTGAACAACAAGAACATCAACAAAGAGCAGAGCGACATCCTGC
GGAAGATCCGGAACGCCCTTCGATGCAAACAATTACCCCGACAAAGGCGTGGTG
GAAATCAAGGCCCTGCCTGAGATCGCCATGAGCATCAAGAAGGCCTTTGGGGA
GTACGCCATCATGAAG**GGAAGCGGG**GAGAGTGTCAATTGATCACTTTGTCACAT
GGAGACTCATCCCAGAATACAAGAGACCTAACGGCTGTGTCATCAACTTCTTTG
AAGAGGGTGAATACTCACAGCCTTTCCTCAAACCACCTCACTTAGAACAACCAA
TCTCCACTCTTGTCTCTCTGAATCAACAATGGCCTATGGACGCATTCTCTCAA
GTGACAACGAAGGCAACTTCAGAGGACCTTTGACACTCTCTCTCAAACAAGGAT
CTTTGTTGGTGATGAGAGGGAACAGTGCAGACATGGCAAGACATGTAATGTGT
CCATCACAAAACAAAAGAGTAAGCATCACATTCTTTCGTATTCGACCTGACACAT
ATCATAACCATTCAACAACCCAACAGTCCTCGCAACGACGGTGTGTCATGACAATGT
GGCAACCCTACCAAATGACACCAACTCCATTCCCTCAATGGTTATGATCATTCAAT
TGACATGATGCCAAAACCTTGGAGTCCTACGTCCTCCAATGGTCATGATGGCACC
ACCACCGGTTCAACCAATGATATTACCAAGTCCCAATGTGATGGGAACCGGTG
GTGGTACCGGTGTTTTCTTACCATGGGCCTCTGTTAATAGCTCAAGAAAACATG
TGAAGCATTTGCCTCCACGCGCGCAGAAGAAGCGATTACTTCCGCTTCTCCT
GCTGCTTCTTCTTCTCCAGCTGGAGGATCCACCTCTGAGCCTGTGATCACTGTA
GGTTAA

Appendix 2: Sequence of gRNA arrays (Chapter II)

Blue = AtU6

Red = DR

Black = SPACER

Sequence of “3’UTR gRNA array”:

AtU6-DR-(SPACER-DR)₄

```
AGAAATCTCAA AATTCCGGCAGAACAATTTTGAATCTCGATCCGTAGAAACGAG
ACGGTCATTGTTTTAGTTCCACCACGATTATATTTGAAATTTACGTGAGTGTGAG
TGAGACTTGCATAAGAAAATAAAAATCTTTAGTTGGGAAAAAATTCAATAATATAAA
TGGGCTTGAGAAGGAAGCGAGGGATAGGCCTTTTTCTAAAATAGGCCCATTTAA
GCTATTAACAATCTTCAA AAGTACCACAGCGCTTAGGTAAAGAAAGCAGCTGAG
TTTATATATGGTTAGAGACGAAGTAGTGATTGGGACGCGT GTTGTGGAAGGTCC
AGTTTTGAGGGGCTATTACAACCTAAAATCCTTATTGATCACTTCACATCGTTGT
GGAAGGTCCAGTTTTGAGGGGCTATTACAACTTACAATCAGATAGATACAGAGT
CATTGGTTGTGGAAGGTCCAGTTTTGAGGGGCTATTACAACAAATGAATTCAGT
TTTAGTTACAATCAGGTTGTGGAAGGTCCAGTTTTGAGGGGCTATTACAACACA
CAACATAAGATAATAGTATCATTGGTTGTGGAAGGTCCAGTTTTGAGGGGCTA
TTACAACTTTTTT
```

Sequence of “all-gRNA array”:

AtU6-DR-(SPACER-DR)₆

```
AGAAATCTCAA AATTCCGGCAGAACAATTTTGAATCTCGATCCGTAGAAACGAG
ACGGTCATTGTTTTAGTTCCACCACGATTATATTTGAAATTTACGTGAGTGTGAG
TGAGACTTGCATAAGAAAATAAAAATCTTTAGTTGGGAAAAAATTCAATAATATAAA
TGGGCTTGAGAAGGAAGCGAGGGATAGGCCTTTTTCTAAAATAGGCCCATTTAA
GCTATTAACAATCTTCAA AAGTACCACAGCGCTTAGGTAAAGAAAGCAGCTGAG
TTTATATATGGTTAGAGACGAAGTAGTGATTGGGACGCGT GTTGTGGAAGGTCC
AGTTTTGAGGGGCTATTACAACCTAAAATCCTTATTGATCACTTCACATCGTTGT
GGAAGGTCCAGTTTTGAGGGGCTATTACAACTTACAATCAGATAGATACAGAGT
CATTGGTTGTGGAAGGTCCAGTTTTGAGGGGCTATTACAACAAATGAATTCAGT
TTTAGTTACAATCAGGTTGTGGAAGGTCCAGTTTTGAGGGGCTATTACAACACA
CAACATAAGATAATAGTATCATTGGTTGTGGAAGGTCCAGTTTTGAGGGGCTA
TTACAACGGTCAGTGTCAGTCGGATTTTTCAAGAGGTTGTGGAAGGTCCAGTTT
TGAGGGGCTATTACAACATCTGGATAACGAATCTGGAGCTGAATTGTTGTGGA
GGTCCAGTTTTGAGGGGCTATTACAACTTTTTT
```

Appendix 3: Collections of species used for conservation analysis of C348 on SHY2/IAA3 (Chapter IV)

IAA1:

HF583022.1 *Schiedea hookeri*
HF583021.1 *Schiedea menziesii*
HF583020.1 *Schiedea mannii*
HF583019.1 *Schiedea kealiae*
HF583018.1 *Schiedea ligustrina*
HF583017.1 *Schiedea salicaria*
HF583016.1 *Schiedea spergulina*
HF583015.1 *Schiedea globosa*
HF583014.1 *Schiedea membranacea*
HF583013.1 *Schiedea adamantis*
HF583012.1 *Schiedea kaalae*
AJ251791.1 *Oryza sativa*
NM_117536.4 *Arabidopsis thaliana*
AJ575098.1 *Triticum aestivum*
HM487597.1 *Arabidopsis thaliana* ecotype Tsu-1
HM487596.1 *Arabidopsis thaliana* ecotype Ts-1
HM487595.1 *Arabidopsis thaliana* ecotype Tamm-2
HM487594.1 *Arabidopsis thaliana* ecotype RRS-10
HM487593.1 *Arabidopsis thaliana* ecotype Rrs-7
HM487592.1 *Arabidopsis thaliana* ecotype NFA-8
HM487591.1 *Arabidopsis thaliana* ecotype Lov-5
HM487590.1 *Arabidopsis thaliana* ecotype LER-1
HM487589.1 *Arabidopsis thaliana* ecotype GOT-7
HM487588.1 *Arabidopsis thaliana* ecotype Est-1
HM487587.1 *Arabidopsis thaliana* ecotype Cvi-0
HM487586.1 *Arabidopsis thaliana* ecotype Br-0
HM487585.1 *Arabidopsis thaliana* ecotype Bor-4
KR076511.1 *Boehmeria nivea*

KC632528.1 *Pyrus pyrifolia*
L15448.1 *Arabidopsis thaliana*
GU348523.2 *Arabidopsis thaliana* ecotype Shakdara
GU348522.2 *Arabidopsis thaliana* ecotype Fei-0
GU348521.2 *Arabidopsis thaliana* ecotype C24
GU348520.2 *Arabidopsis thaliana* ecotype Bur-0
GU348519.2 *Arabidopsis thaliana* ecotype Bay-0
HM122439.1 *Malus x domestica*
HM165183.1 *Catharanthus roseus*
AY556421.1 *Elaeis guineensis*
AY289600.1 *Pinus taeda*
AF373100.1 *Populus tremula x Populus tremuloides*
AJ563599.2 *Oryza sativa Indica Group*

IAA2:

AF022013.1 *Solanum lycopersicum (Lycopersicon esculentum)*
DQ900820.1 *Cestrum elegans*
MK738001.1 *Diospyros kaki*
MG198855.1 *Betula platyphylla*
JN379432.1 *Solanum lycopersicum (Lycopersicon esculentum)*
NM_001279113.2 *Solanum lycopersicum (Lycopersicon esculentum)*
AF027157.1 *Arabidopsis thaliana*
NM_113203.5 *Arabidopsis thaliana*
HM487610.1 *Arabidopsis thaliana* ecotype Tsu-1
HM487609.1 *Arabidopsis thaliana* ecotype Ts-1
HM487608.1 *Arabidopsis thaliana* ecotype Tamm-2
HM487607.1 *Arabidopsis thaliana* ecotype RRS-10
HM487606.1 *Arabidopsis thaliana* ecotype Rrs-7
HM487605.1 *Arabidopsis thaliana* ecotype NFA-8
HM487604.1 *Arabidopsis thaliana* ecotype Lov-5
HM487603.1 *Arabidopsis thaliana* ecotype LER-1
HM487602.1 *Arabidopsis thaliana* ecotype GOT-7

HM487601.1 *Arabidopsis thaliana* ecotype Est-1
HM487600.1 *Arabidopsis thaliana* ecotype Cvi-0
HM487599.1 *Arabidopsis thaliana* ecotype Br-0
HM487598.1 *Arabidopsis thaliana* ecotype Bor-4
NM_001293866.1 *Malus domestica*
NM_001338609.1 *Arabidopsis thaliana*
EU170472.1 *Eucommia ulmoides*
GU594248.1 *Solanum nigrum* clone 105
KR076512.1 *Boehmeria nivea*
NM_001288102.1 *Solanum tuberosum*
L15449.1 *Arabidopsis thaliana*
GU348528.2 *Arabidopsis thaliana* ecotype Shakdara
GU348527.2 *Arabidopsis thaliana* ecotype Fei-0
GU348526.2 *Arabidopsis thaliana* ecotype C24
GU348525.2 *Arabidopsis thaliana* ecotype Bur-0
GU348524.2 *Arabidopsis thaliana* ecotype Bay-0
HM122443.1 *Malus x domestica*
AY289601.1 *Pinus taeda*
EF053504.1 *Solanum tuberosum*
AJ306825.1 *Populus tremula x Populus tremuloides*
XM_010324706.3 PREDICTED: *Solanum lycopersicum*
KR349178.1 *Pinus massoniana*
XM_024309463.2 PREDICTED: *Rosa chinensis*
XM_020318018.2 PREDICTED: *Aegilops tauschii* subsp. *strangulata*
XM_024771831.2 PREDICTED: *Medicago truncatula*
XM_010049666.3 PREDICTED: *Eucalyptus grandis*
XM_033291407.1 PREDICTED: *Brassica rapa*
XM_009146994.3 PREDICTED: *Brassica rapa*
XM_033288345.1 PREDICTED: *Brassica rapa*
XM_009110097.3 PREDICTED: *Brassica rapa*
XM_012222006.3 PREDICTED: *Jatropha curcas*
XM_020372539.2 PREDICTED: *Cajanus cajan*

XM_020833666.2 PREDICTED: *Dendrobium catenatum*
XM_015717611.2 PREDICTED: *Ricinus communis*
XM_002965368.2 PREDICTED: *Selaginella moellendorffii*
XM_024589569.1 PREDICTED: *Populus trichocarpa*
XM_024589568.1 PREDICTED: *Populus trichocarpa*
XM_024603235.1 PREDICTED: *Populus trichocarpa*
XM_010232266.3 PREDICTED: *Brachypodium distachyon*
XM_006406038.2 PREDICTED: *Eutrema salsugineum*
XM_006298617.2 PREDICTED: *Capsella rubella*
XM_004968405.3 PREDICTED: *Setaria italica*
XM_022707190.1 PREDICTED: *Brassica napus*
XM_013807294.2 PREDICTED: *Brassica napus*
XM_013857323.2 PREDICTED: *Brassica napus*
XM_002457156.2 PREDICTED: *Sorghum bicolor*
XM_021455159.1 PREDICTED: *Sorghum bicolor*
XM_021455158.1 PREDICTED: *Sorghum bicolor*
XM_002885496.2 PREDICTED: *Arabidopsis lyrata subsp. lyrata*
XM_020556087.1 PREDICTED: *Prunus persica*
XM_007223342.2 PREDICTED: *Prunus persica*
XM_010468300.2 PREDICTED: *Camelina sativa*
XM_010468298.2 PREDICTED: *Camelina sativa*
XM_010468301.2 PREDICTED: *Camelina sativa*
XM_019247288.1 PREDICTED: *Beta vulgaris subsp. vulgaris*
XM_010667579.2 PREDICTED: *Beta vulgaris subsp. vulgaris*
XM_010667580.1 PREDICTED: *Beta vulgaris subsp. vulgaris*
XM_010649983.2 PREDICTED: *Vitis vinifera*
XM_002277762.4 PREDICTED: *Vitis vinifera*
XM_009411096.2 PREDICTED: *Musa acuminata subsp. malaccensis*
XM_009411095.2 PREDICTED: *Musa acuminata subsp. malaccensis*
XM_007012113.2 PREDICTED: *Theobroma cacao*
XM_013783043.1 PREDICTED: *Brassica oleracea var. oleracea*
XM_013770110.1 PREDICTED: *Brassica oleracea var. Oleracea*

IAA3:

AK227549.1 *Arabidopsis thaliana*
HM487636.1 *Arabidopsis thaliana* ecotype Tsu-1
HM487635.1 *Arabidopsis thaliana* ecotype Ts-1
HM487634.1 *Arabidopsis thaliana* ecotype Tamm-2
HM487633.1 *Arabidopsis thaliana* ecotype RRS-10
HM487632.1 *Arabidopsis thaliana* ecotype Rrs-7
HM487631.1 *Arabidopsis thaliana* ecotype NFA-8
HM487630.1 *Arabidopsis thaliana* ecotype Lov-5
HM487629.1 *Arabidopsis thaliana* ecotype LER-1
HM487628.1 *Arabidopsis thaliana* ecotype GOT-7
HM487627.1 *Arabidopsis thaliana* ecotype Est-1
HM487626.1 *Arabidopsis thaliana* ecotype Cvi-0
HM487625.1 *Arabidopsis thaliana* ecotype Br-0
HM487624.1 *Arabidopsis thaliana* ecotype Bor-4
GU348536.2 *Arabidopsis thaliana* ecotype C24
L15450.1 *Arabidopsis thaliana*
GU348535.2 *Arabidopsis thaliana* ecotype Bur-0
GU348538.1 *Arabidopsis thaliana* ecotype Shakdara
GU348537.1 *Arabidopsis thaliana* ecotype Fei-0
GU348534.1 *Arabidopsis thaliana* ecotype Bay-0
XM_009115734.3 PREDICTED: *Brassica rapa*
DQ900822.1 *Cestrum elegans*
AF022015.1 *Solanum lycopersicum* (*Lycopersicon esculentum*)
KC477278.1 *Populus tomentosa*
MT270133.1 *Galium aparine*
MG198857.1 *Betula platyphylla*
JN379434.1 *Solanum lycopersicum* (*Lycopersicon esculentum*)
NM_001279327.1 *Solanum lycopersicum* (*Lycopersicon esculentum*)
MG189377.1 *Malus domestica*
GQ386948.1 *Solanum tuberosum*

KR076514.1 *Boehmeria nivea*
 AY289603.1 *Pinus taeda*
 DQ115325.1 *Solanum lycopersicum (Lycopersicon esculentum)*
 AM943976.1 *Populus alba*
 AJ306827.1 *Populus tremula x Populus tremuloides*
 XM_041143795.1 PREDICTED: *Juglans microcarpa x Juglans regia*
 XM_016865653.2 PREDICTED: *Gossypium hirsutum*
 XM_016865652.2 PREDICTED: *Gossypium hirsutum*
 XM_016873596.2 PREDICTED: *Gossypium hirsutum*
 XM_006593924.4 PREDICTED: *Glycine max*
 XM_024330631.2 PREDICTED: *Rosa chinensis*
 XM_013611519.3 PREDICTED: *Medicago truncatula*
 XM_008802095.4 PREDICTED: *Phoenix dactylifera*
 XM_008802094.4 PREDICTED: *Phoenix dactylifera*
 XM_026807529.2 PREDICTED: *Phoenix dactylifera*
 XM_026807528.2 PREDICTED: *Phoenix dactylifera*
 XM_038847178.1 PREDICTED: *Tripterygium wilfordii*
 XM_012214368.3 PREDICTED: *Jatropha curcas*
 XM_020543086.3 PREDICTED: *Zea mays*
 XM_020543084.3 PREDICTED: *Zea mays*
 XM_020543083.3 PREDICTED: *Zea mays*
 XM_020543082.3 PREDICTED: *Zea mays*
 XM_020543081.3 PREDICTED: *Zea mays*
 XM_008675721.4 PREDICTED: *Zea mays*
 XM_020543087.2 PREDICTED: *Zea mays*
 XM_020543085.2 PREDICTED: *Zea mays*
 XM_035069112.1 PREDICTED: *Populus alba*
 XM_034373245.1 PREDICTED: *Prunus dulcis*
 XM_004134055.3 PREDICTED: *Cucumis sativus*
 XM_004139186.3 PREDICTED: *Cucumis sativus*
 XM_031117479.1 PREDICTED: *Quercus lobata*
 XM_029273245.1 PREDICTED: *Cajanus cajan*

XM_010911141.3 PREDICTED: *Elaeis guineensis*
XM_010911134.3 PREDICTED: *Elaeis guineensis*
XM_020833844.2 PREDICTED: *Dendrobium catenatum*
XM_020848885.2 PREDICTED: *Dendrobium catenatum*
XM_020848884.2 PREDICTED: *Dendrobium catenatum*
XM_015215652.2 PREDICTED: *Solanum pennellii*
XM_027477727.1 PREDICTED: *Abrus precatorius*
XM_004497955.3 PREDICTED: *Cicer arietinum*
XM_015774120.2 PREDICTED: *Oryza sativa*
XM_002516978.3 PREDICTED: *Ricinus communis*
XM_002320217.2 PREDICTED: *Populus trichocarpa*
XM_010232494.3 PREDICTED: *Brachypodium distachyon*
XM_003567452.4 PREDICTED: *Brachypodium distachyon*
XM_010103991.2 PREDICTED: *Morus notabilis*
XM_006403143.2 PREDICTED: *Eutrema salsugineum*
XM_010089457.2 PREDICTED: *Morus notabilis*
XM_010088826.2 PREDICTED: *Morus notabilis*
XM_024162922.1 PREDICTED: *Morus notabilis*
XM_006281105.2 PREDICTED: *Capsella rubella*
XM_022827024.1 PREDICTED: *Setaria italica*
XM_004967581.4 PREDICTED: *Setaria italica*
XM_013806290.2 PREDICTED: *Brassica napus*
XM_022692695.1 PREDICTED: *Brassica napus*
XM_022291559.1 PREDICTED: *Momordica charantia*
XM_021966396.1 PREDICTED: *Prunus avium*
XM_021457703.1 PREDICTED: *Sorghum bicolor*
XM_002455440.2 PREDICTED: *Sorghum bicolor*
XM_016085127.2 PREDICTED: *Arachis duranensis*
XM_021015385.1 PREDICTED: *Arabidopsis lyrata subsp. lyrata*
XM_006838806.3 PREDICTED: *Amborella trichopoda*
XM_007226200.2 PREDICTED: *Prunus persica*
XM_020399433.1 PREDICTED: *Asparagus officinalis*

XM_020230192.1 *PREDICTED: Ananas comosus*
 XM_020230191.1 *PREDICTED: Ananas comosus*
 KU573103.1 *Populus tomentosa clone Ptom.001G177400*
 XM_019398066.1 *PREDICTED: Nicotiana attenuata*
 XM_010483534.2 *PREDICTED: Camelina sativa*
 XM_010676554.2 *PREDICTED: Beta vulgaris subsp. vulgaris*
 XM_010695821.2 *PREDICTED: Beta vulgaris subsp. vulgaris*
 XM_010443693.1 *PREDICTED: Camelina sativa*
 XM_002281109.4 *PREDICTED: Vitis vinifera*
 XM_018596772.1 *PREDICTED: Raphanus sativus*
 XM_007030506.2 *PREDICTED: Theobroma cacao*
 XM_007034891.2 *PREDICTED: Theobroma cacao*
 XM_006355988.2 *PREDICTED: Solanum tuberosum*
 XM_013751135.1 *PREDICTED: Brassica oleracea var. oleracea*
 XM_004288378.2 *PREDICTED: Fragaria vesca subsp. Vesca*

IAA4:

AK227549.1 *Arabidopsis thaliana*
 HM487636.1 *Arabidopsis thaliana ecotype Tsu-1*
 HM487635.1 *Arabidopsis thaliana ecotype Ts-1*
 HM487634.1 *Arabidopsis thaliana ecotype Tamm-2*
 HM487633.1 *Arabidopsis thaliana ecotype RRS-10*
 HM487632.1 *Arabidopsis thaliana ecotype Rrs-7*
 HM487631.1 *Arabidopsis thaliana ecotype NFA-8*
 HM487630.1 *Arabidopsis thaliana ecotype Lov-5*
 HM487629.1 *Arabidopsis thaliana ecotype LER-1*
 HM487628.1 *Arabidopsis thaliana ecotype GOT-7*
 HM487627.1 *Arabidopsis thaliana ecotype Est-1*
 HM487626.1 *Arabidopsis thaliana ecotype Cvi-0*
 HM487625.1 *Arabidopsis thaliana ecotype Br-0*
 HM487624.1 *Arabidopsis thaliana ecotype Bor-4*
 GU348536.2 *Arabidopsis thaliana ecotype C24*

L15450.1 *Arabidopsis thaliana*
 GU348535.2 *Arabidopsis thaliana* ecotype Bur-0
 GU348538.1 *Arabidopsis thaliana* ecotype Shakdara
 GU348537.1 *Arabidopsis thaliana* ecotype Fei-0
 GU348534.1 *Arabidopsis thaliana* ecotype Bay-0
 XM_009115734.3 PREDICTED: *Brassica rapa*
 DQ900822.1 *Cestrum elegans*
 AF022015.1 *Solanum lycopersicum* (*Lycopersicon esculentum*)
 KC477278.1 *Populus tomentosa*
 MT270133.1 *Galium aparine*
 MG198857.1 *Betula platyphylla*
 JN379434.1 *Solanum lycopersicum* (*Lycopersicon esculentum*)
 NM_001279327.1 *Solanum lycopersicum* (*Lycopersicon esculentum*)
 MG189377.1 *Malus domestica*
 GQ386948.1 *Solanum tuberosum*
 KR076514.1 *Boehmeria nivea*
 AY289603.1 *Pinus taeda*
 DQ115325.1 *Solanum lycopersicum* (*Lycopersicon esculentum*)
 AM943976.1 *Populus alba*
 AJ306827.1 *Populus tremula* x *Populus tremuloides*
 XM_041143795.1 PREDICTED: *Juglans microcarpa* x *Juglans regia*
 XM_016865653.2 PREDICTED: *Gossypium hirsutum*
 XM_016865652.2 PREDICTED: *Gossypium hirsutum*
 XM_016873596.2 PREDICTED: *Gossypium hirsutum*
 XM_006593924.4 PREDICTED: *Glycine max*
 XM_024330631.2 PREDICTED: *Rosa chinensis*
 XM_013611519.3 PREDICTED: *Medicago truncatula*
 XM_008802095.4 PREDICTED: *Phoenix dactylifera*
 XM_008802094.4 PREDICTED: *Phoenix dactylifera*
 XM_026807529.2 PREDICTED: *Phoenix dactylifera*
 XM_026807528.2 PREDICTED: *Phoenix dactylifera*
 XM_038847178.1 PREDICTED: *Tripterygium wilfordii*

XM_012214368.3 PREDICTED: *Jatropha curcas*
XM_020543086.3 PREDICTED: *Zea mays*
XM_020543084.3 PREDICTED: *Zea mays*
XM_020543083.3 PREDICTED: *Zea mays*
XM_020543082.3 PREDICTED: *Zea mays*
XM_020543081.3 PREDICTED: *Zea mays*
XM_008675721.4 PREDICTED: *Zea mays*
XM_020543087.2 PREDICTED: *Zea mays*
XM_020543085.2 PREDICTED: *Zea mays*
XM_035069112.1 PREDICTED: *Populus alba*
XM_034373245.1 PREDICTED: *Prunus dulcis*
XM_004134055.3 PREDICTED: *Cucumis sativus*
XM_004139186.3 PREDICTED: *Cucumis sativus*
XM_031117479.1 PREDICTED: *Quercus lobata*
XM_029273245.1 PREDICTED: *Cajanus cajan*
XM_010911141.3 PREDICTED: *Elaeis guineensis*
XM_010911134.3 PREDICTED: *Elaeis guineensis*
XM_020833844.2 PREDICTED: *Dendrobium catenatum*
XM_020848885.2 PREDICTED: *Dendrobium catenatum*
XM_020848884.2 PREDICTED: *Dendrobium catenatum*
XM_015215652.2 PREDICTED: *Solanum pennellii*
XM_027477727.1 PREDICTED: *Abrus precatorius*
XM_004497955.3 PREDICTED: *Cicer arietinum*
XM_015774120.2 PREDICTED: *Oryza sativa*
XM_002516978.3 PREDICTED: *Ricinus communis*
XM_002320217.2 PREDICTED: *Populus trichocarpa*
XM_010232494.3 PREDICTED: *Brachypodium distachyon*
XM_003567452.4 PREDICTED: *Brachypodium distachyon*
XM_010103991.2 PREDICTED: *Morus notabilis*
XM_006403143.2 PREDICTED: *Eutrema salsugineum*
XM_010089457.2 PREDICTED: *Morus notabilis*
XM_010088826.2 PREDICTED: *Morus notabilis*

XM_024162922.1 *PREDICTED: Morus notabilis*
 XM_006281105.2 *PREDICTED: Capsella rubella*
 XM_022827024.1 *PREDICTED: Setaria italica*
 XM_004967581.4 *PREDICTED: Setaria italica*
 XM_013806290.2 *PREDICTED: Brassica napus*
 XM_022692695.1 *PREDICTED: Brassica napus*
 XM_022291559.1 *PREDICTED: Momordica charantia*
 XM_021966396.1 *PREDICTED: Prunus avium*
 XM_021457703.1 *PREDICTED: Sorghum bicolor*
 XM_002455440.2 *PREDICTED: Sorghum bicolor*
 XM_016085127.2 *PREDICTED: Arachis duranensis*
 XM_021015385.1 *PREDICTED: Arabidopsis lyrata subsp. lyrata*
 XM_006838806.3 *PREDICTED: Amborella trichopoda*
 XM_007226200.2 *PREDICTED: Prunus persica*
 XM_020399433.1 *PREDICTED: Asparagus officinalis*
 XM_020230192.1 *PREDICTED: Ananas comosus*
 XM_020230191.1 *PREDICTED: Ananas comosus*
 KU573103.1 *Populus tomentosa clone Ptom.001G177400*
 XM_019398066.1 *PREDICTED: Nicotiana attenuata*
 XM_010483534.2 *PREDICTED: Camelina sativa*
 XM_010676554.2 *PREDICTED: Beta vulgaris subsp. vulgaris*
 XM_010695821.2 *PREDICTED: Beta vulgaris subsp. vulgaris*
 XM_010443693.1 *PREDICTED: Camelina sativa*
 XM_002281109.4 *PREDICTED: Vitis vinifera*
 XM_018596772.1 *PREDICTED: Raphanus sativus*
 XM_007030506.2 *PREDICTED: Theobroma cacao*
 XM_007034891.2 *PREDICTED: Theobroma cacao*
 XM_006355988.2 *PREDICTED: Solanum tuberosum*
 XM_013751135.1 *PREDICTED: Brassica oleracea var. oleracea*
 XM_004288378.2 *PREDICTED: Fragaria vesca subsp. vesca*